



The Abdus Salam
International Centre for Theoretical Physics



1944-12

**Joint ICTP-IAEA Workshop on Nuclear Reaction Data for Advanced
Reactor Technologies**

19 - 30 May 2008

**Sensitivity and Uncertainty Analysis for the Neutronic Design of Advanced Nuclear
Systems.**

G. Palmiotti
*Idaho National Lab.
Idaho Falls
USA*



Sensitivity and Uncertainty Analysis for the Neutronic Design of Advanced Nuclear Systems

G. Palmiotti

Joint ICTP-IAEA Workshop on Nuclear
Reaction Data for Advanced Reactor
Technologies

Trieste - Italy, 26 - 27 May 2008

Background

- In general, the uncertainty analysis performed using current covariance data shows that the present integral parameters uncertainties resulting from the assumed uncertainties on nuclear data are probably acceptable in the early phases of design feasibility studies.
- However, in the successive phase of preliminary conceptual designs and in later design phases of selected reactor and fuel cycle concepts, there is the need for improved data and methods, in order to reduce margins, both for economic and safety reasons.
- It is then important to define as soon as possible priority issues, i.e. which are the nuclear data (isotope, reaction type, energy range) that need improvement, in order to quantify target accuracies and to select a strategy to meet the requirements needed (e.g. by some selected new differential measurements and by the use of integral experiments).

Background

- The ultimate goal is a design that has as low as possible uncertainties.
- There are two main sources of uncertainties: input data, and modeling
 - Example of input physical data: cross sections, fabrication data, etc.
 - Modeling uncertainties: coming from approximations made in the computational methodology used in the design process.
- High-fidelity simulation can provide a major benefit if it can reduce to the smallest amount the impact of uncertainties coming from the modeling of the physical processes.
- A scientific based approach can allow a reliable propagation of uncertainties and a correct evaluation of the impact of the uncertainty coming from the input data.

Sample of Target Reactor Performance (Fast Reactor)

Parameter	Current Uncertainty ^{a)}				Targeted Uncertainty	
	Input data origin (a priori)	Input data origin ^{b)} (av. exper.)	Modeling origin	Total		
Neutronics ^{c)}						
Core						
Multiplication factor, K_{eff} ($\Delta k/k$)	1%	0.2%	0.5%	0.5%	0.3%	
Power peak	1%	1%	3%	3%	2%	
Power distribution ^{d)}	1%	1%	6%	6%	3%	
Conversion ratio (absolute value in %)	5%	5%	2%	5%	2%	
Control rod worth: Element	5%	4%	6%	7%	5%	
Control rod worth: Total	5%	4%	4%	5%	2%	
Burnup reactivity swing ($\Delta k/k$)	0.7%	0.5%	0.5%	0.7%	0.3%	

Sample of Target Reactor Performance (Fast Reactor)

Parameter	Current Uncertainty ^{a)}				Targeted Uncertainty	
	Input data origin (a priori)	Input data origin ^{b)} (av. exper.)	Modeling origin	Total		
Neutronics ^{c)}						
Core						
Reactivity coefficients: total	7%	5%	15%	15%	7%	
Reactivity coefficients: component	20%	10%	20%	20%	10%	
Fast flux for damage	7%	6%	3%	7%	3%	
Kinetics parameters	10%	10%	5%	10%	5%	
Local nuclide densities: Major	5%	4%	3%	5%	2%	
Local nuclide densities: Minor	30%	20%	10%	20%	10%	
Fuel decay heat at shutdown	10%	10%	3%	10%	5%	

Sample of Target Reactor Performance (Fast Reactor)

Parameter	Current Uncertainty ^{a)}				Targeted Uncertainty	
	Input data origin (a priori)	Input data origin ^{b)} (av. exper.)	Modeling origin	Total		
Neutronics ^{c)}						
Shielding						
Out of Core Coolant Activation	70%	70%	70%	100%	50	
Shield Dimensioning (Total Flux)	70%	40%	30%	50%	20%	
Structural Damage Out of Core (Total Flux)	40%	40%	30%	50%	20%	

Sample of Target Reactor Performance (Fast Reactor)

Parameter	Current Uncertainty ^{a)}				Targeted Uncertainty	
	Input data origin (a priori)	Input data origin ^{b)} (av. exper.)	Modeling origin	Total		
Neutronics ^{c)}						
Fuel Cycle						
Neutron Dose at Fuel Fabrication	15%	15%	15%	20%	10%	
Decay Heat of Spent Fuel at Repository	50%	50%	15%	50%	20%	
Radiotoxicity at repository	50%	50%	15%	50%	20%	

Background

- Sensitivity and uncertainty analyses are the main instruments for dealing with the sometimes scarce knowledge of the input parameters used in simulation tools.
- Sensitivity coefficients are the key quantities that have to be evaluated. They are determined and assembled, using different methodologies, in a way that when multiplied by the variation of the corresponding input parameter they will quantify the impact on the targeted quantities whose sensitivity is referred to.
- Sensitivity coefficients can be used for different objectives:
 - uncertainty estimates,
 - design optimization,
 - determination of target accuracy requirements,
 - adjustment of input parameters,
 - evaluations of the representativity of an experiment with respect to a reference design configuration.

Uncertainty Evaluation

- In uncertainty assessment, the sensitivity coefficients are multiplied by the uncertainties of the input parameters in order to obtain the uncertainty of the targeted parameter of interest.
- The origin and quality of the uncertainties of the input parameters can be different and vary quite a lot:
 - In some cases, they are provided by the expert judgment of qualified designer.
 - In some other cases more useful information is available, for instance from experimental values, and they are cast in more rigorous formalism (e.g. covariance matrix for neutron cross sections, where correlations in energy and among the different input parameters, like reactions and isotopes, are also provided).

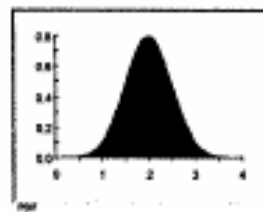
$$\Delta R^2 = S_R^+ D S_R$$

where ΔR is the uncertainty, S_R are the sensitivity coefficients arrays, and D is the covariance matrix.

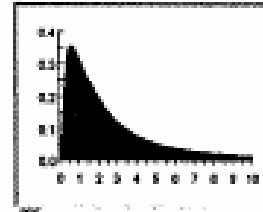
Uncertainty Evaluation (cont.)

- Uncertainty evaluation can be performed also without the help of sensitivity coefficients. Uncertainties on input parameters can be propagated either using a stochastic approach (Monte Carlo methods type) or by some regression techniques.
- In the case of the Monte Carlo methodology, several runs of the same problems are performed with different random input values, taken within the range of the specified uncertainty and associated distribution law, and then at the end the final results are statistically combined in order to determine the average value and the associated standard deviation.

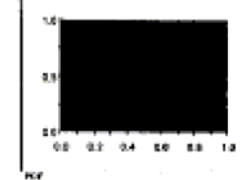
Normal Distribution



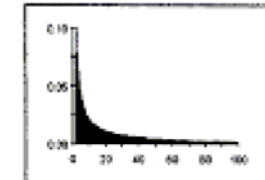
Log-Normal Distribution



Uniform Distribution



Log-Uniform Distribution



- Smarter sampling techniques (e.g. Latin Hypercube) for Monte Carlo simulations are developed in order to minimize the total number of direct calculations.



Idaho National Laboratory

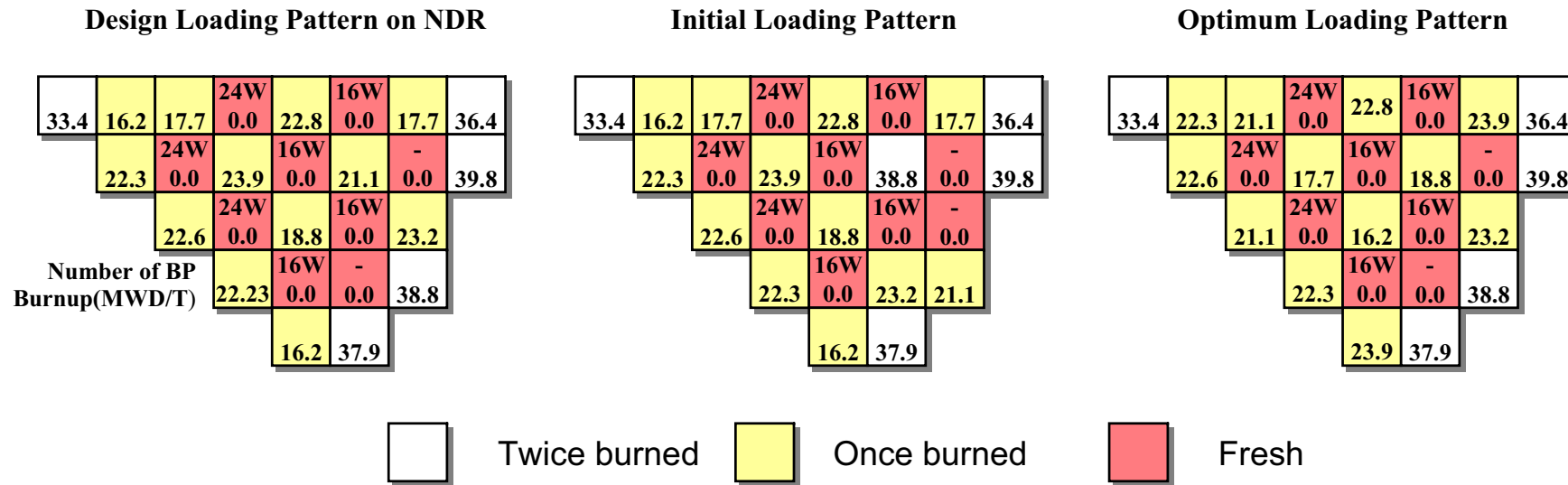
Design Optimization

- Design optimization can take advantage of sensitivity coefficients by using them in optimization algorithms.
- The main problem in this case is related to the fact that in most cases the sensitivity coefficients are calculated with linear approximation: they need to be determined repeatedly to take into account the nonlinear effects.
- There is also the problem of taking into account multi-physics effects.
- Sensitivity coefficients are evaluated only relative to one field (e.g. neutronics or thermal-hydraulics).



Idaho National Laboratory

Comparison of ALPSMAP-generated Loading Patterns with Actual Design (courtesy of T. K. Kim)



	Initial LP	Optimum LP	NDR
EOC SB ¹⁾	1 ppm	134 ppm	121 ppm
PPPF ²⁾	1.481	1.522	1.486
CPU time ³⁾	-	11708sec	-

1) EOC Burnup = 16400 MWD/T

2) Design limitation = 1.527

3) Computer = IBMPC with Pentium-II Processor



Idaho National Laboratory

Current Methodologies

- There are two main methodologies developed for sensitivity and uncertainty analysis:
 - the forward (direct) calculation method
 - the adjoint method
- The forward approach is preferable when there are few input parameters that can vary and many output parameters of interest.
- The adjoint methodology is preferable when there are a limited number of object parameters and a very large number of input parameters that are uncertain.

Forward Methods

- Stochastic (probabilistic with Monte Carlo method) has some drawbacks:
 - ❖ large number of direct calculations
 - ❖ only uncertainty can be evaluated and sensitivity coefficients cannot be directly obtained
- The method has been widely used in other fields than nuclear, and it is very popular for waste repository assessments (e. g. GOLDSIM)
- Automatic differentiation:
 - ❖ codes are directly modified in order to evaluate derivatives, through direct calculations, for all input parameters that are deemed to vary
 - ❖ it can be very computational intensive
 - ❖ it requires direct intervention within the code
 - ❖ Software exists that directly modifies a code to add automatic differentiation if the used language of programming is FORTRAN or C

Adjoint Methods

- The adjoint methodologies are based on the perturbation theory originally developed in the quantum mechanics field.
- Classical perturbation theory that makes use of the adjoint function (also called importance), has been widely used in neutronics to calculate the variation of the fundamental eigenvalue.
- For the generalized perturbation theory (GPT) a generalized importance is calculated for each output parameter of interest by solving an inhomogeneous adjoint neutron transport equation that contains a source term depending on a specific output parameter.



Idaho National Laboratory

Adjoint Methods

- The adjoint methodology type of approach has been extended to other fields including nuclide depletion calculations where the adjoint solution of the Bateman equation is used, and Depletion Perturbation Theory (DPT) calculates the importance functions for the coupled neutron and nuclide field.
- Oblow and others have extended the adjoint methodology to the thermal-hydraulics field. Cacuci, Park, and Gandini have developed adjoint methodologies for time-dependent transient problems for application to safety analysis or reactor operation optimization.
- Automatic differentiation tools employing the so-called reverse mode are able to compute a discrete adjoint; in practice, the reverse mode requires more user intervention than forward sensitivity computations.



Idaho National Laboratory

Adjoint Methods

- The main drawback of the adjoint methodology is related to the number of adjoint functions that have to be calculated if there is a large number of objective parameters. In many cases, the memory requirements for the adjoint method are significant, as many intermediate states must be recorded. Also inconvenient is the fact that the adjoint solution has to be coded directly inside of the code.
- Among the existing codes that are widely used, mostly in neutronics, we can list: VARI3D and its DPT version at ANL, the sensitivity capability of FORMOSA system (mainly for thermal reactor applications) at the North Carolina State University, the TSUNAMI (limited only to K_{eff}) and FORSS system at ORNL, the sensitivity and uncertainty modules that are part of the European fast reactor code system ERANOS.



Idaho National Laboratory

Historical Notes

- The perturbation theory has been introduced in reactor physics in the 50' and one can find a classical presentation in the Weinberg and Wigner book. This is the perturbation theory applied to the k_{eff} of the critical reactor and L. N. Usachev gave a comprehensive development in an article published at the Geneva conference of 1955.
- It is interesting to note that the perturbation theory applied to reactor makes use of a definition of a function (the adjoint flux), that has a specific physical meaning if one is dealing with a non-conservative system as in the case of a nuclear reactor. This physical interpretation of the adjoint flux has been the focus of extensive studies, during the 60', in particular by J. Lewins.
- The perturbation theory, mostly developed and applied for reactivity coefficient studies, was readily used for an application, sensitivity studies, that had a spectacular development in the 70' and 80'. This development was made possible by a generalization of the perturbation theory (thanks again to Usachev), that deals with the general problem of a variation of any kind of a neutron flux functional. Usachev derived an explicit formulation that relates the functional variation to any change of the Boltzmann operator.



Idaho National Laboratory

Historical Notes

- This development, and its further generalization by Gandini, to the case of any kind of linear and bilinear functional of the real and adjoint flux, opened a new territory for the perturbation theory. It was now possible to relate explicitly the variation of any type of integral parameter (multiplication factor, reaction rates, reactivity coefficients, source values, etc.) to any kind of change of the operator that characterizes the system.
- The application of the generalized perturbation theory to real life problems lead to new interesting developments that allowed to clarify specific characteristics of the new theory with implications for the computation of the generalized importance functions introduced by the theory.
- Starting from the early 70' the generalized perturbation methods, which were essentially developed and used in Europe, became popular also in the rest of the world and in particular with new developments in several U. S. laboratories, ANL and ORNL, and in Japan.

Historical Notes

- The perturbation methods, and their main application in the field of sensitivity analysis, have been used mostly in their first order formulation. Actually, as for any perturbation theory, the power of the method is particularly evident when one considers small perturbations (for instance for cross-sections σ) that therefore induce little changes of the functions (e. g. the neutron flux φ), that characterize the system, and for whom one can neglect the second order product (for instance $\delta\sigma\delta\varphi$). However, there have been theoretical developments that take into accounts higher order effects without losing all the advantages typical of the first order formulations.
- Among the theoretical developments after the 70' that had significant practical impact, one has to mention the extension of the perturbation theory to the nuclide field that allows to study the burn up due to irradiation in the reactor at the first order, and to higher orders. Subsequently a new formulation, the “Equivalent Generalized Perturbation Theory” EGPT, allowed to treat in a very simple and efficient way the perturbation and sensitivity analyses for reactivity coefficients.
- Among the most recent development it is worth to mention those related to the ADS (Accelerator Driven System) case with functionals that allow to calculate the sensitivity of the source importance (φ^*) and the inhomogeneous reactivity.
- Finally, one should remind that, besides the neutronic field, there have been several studies for extending the perturbation theory developed for reactor physics to other domains (thermal-hydraulics, safety, etc.) with very interesting theoretical developments.



Theory

Homogeneous and inhomogeneous Boltzmann equations:

$$A\Phi = \frac{F\Phi}{K_{eff}} \quad (1) \quad A * \Phi^* = \frac{F * \Phi^*}{K_{eff}} \quad (2) \quad A\Phi_s = F\Phi_s + S \quad (3)$$

Where in multigroup notation:

$$A_g = \Omega \Delta \psi_g + \sigma_t \psi_g - \sum_g \sigma_{g \rightarrow g'} \Phi_{g'} \quad (4)$$

$$F_g = \chi_g \sum_{g'} \nu \sigma_f^{g'} \Phi_{g'} \quad (5)$$

Theory

$$\Phi = \int \psi d\Omega \quad (6)$$

The inhomogeneous multiplication factor is defined as:

$$k_s = \frac{\langle F\Phi_s \rangle}{\langle A\Phi_s \rangle} \quad (7)$$

$$S_m = \frac{S}{1 - k_s} \quad (8)$$

The inhomogeneous reactivity is defined as:

$$\rho_s = 1 - \frac{1}{k_s} = \frac{\langle F\Phi_s \rangle - \langle A\Phi_s \rangle}{\langle F\Phi_s \rangle} = -\frac{\langle S \rangle}{\langle F\Phi_s \rangle} \quad (9)$$



Idaho National Laboratory

Theory

Classical Perturbation Theory

We consider the perturbed equation:

$$A' \Phi' = \frac{F' \Phi'}{K'_{eff}} \quad (10)$$

Multiplying Eq. (2) by Φ' and Eq. (10) by Φ^* and then subtracting, we obtain:

$$\delta\rho = \frac{1}{k'} - \frac{1}{k} = \frac{\langle \Phi^*, (\partial A - \partial F) \Phi' \rangle}{\langle \Phi^*, \frac{1}{k'} F' \Phi' \rangle} \quad (11)$$

For the first order approximation we consider $\Phi' \approx \Phi$

Theory

Sensitivity Coefficients

The variations of any integral parameter Q due to variations of cross sections σ can be expressed using perturbation theories to evaluate sensitivity coefficients S :

$$\delta Q/Q = \sum_j S_j \frac{\delta \sigma_j}{\sigma_j} \quad (12)$$

where the sensitivity coefficients S_j are formally given by:

$$S_j = \frac{\partial Q}{\partial \sigma_j} \cdot \frac{\sigma_j}{Q} \quad (13)$$

For the Classical Perturbation Theory this gives:

$$S_j = \frac{\partial K}{\partial \sigma_j} \cdot \frac{\sigma_j}{K} \quad (14)$$

Theory

In the case of the Generalized Importance Theory (GPT), for practical purposes, in the expression of any integral parameter Q , the explicit dependence from some cross-sections (e.g. σ_i^e) and the implicit dependence from some other cross-sections (e.g. σ_j^{im}) are kept separated:

$$\begin{aligned} \sigma_i^e \\ \sigma_j^{im} \end{aligned}$$

$$Q = f(\sigma_j^{im}, \sigma_i^e) \quad (15)$$

As an example, we consider a reaction rate:

$$R = \langle \underline{\sigma}^e, \underline{\Phi} \rangle \quad (16)$$

In Eq. (16), $\underline{\sigma}^e$ can be an energy dependent detector cross-section, R is “explicitly” dependent on the $\underline{\sigma}^e$ and “implicitly” dependent on the cross-sections which characterize the system, described by the flux $\underline{\Phi}$. In other terms, R depends on the system cross-sections via $\underline{\Phi}$.



Theory

Equation (12) can be rewritten as follows:

$$\delta Q / Q = \sum_j S_j \frac{\delta \sigma_j^{im}}{\sigma_j^{im}} + \left(\frac{\partial Q}{\partial \sigma^e} \cdot \frac{\sigma^e}{Q} \right) \cdot \frac{\delta \sigma^e}{\sigma^e} \quad (17)$$

where we have the hypothesis of an explicit dependence of Q on only one σ^e . If we drop the index “ im ”:

$$\delta Q / Q = \sum_j S_j \frac{\delta \sigma_j}{\sigma_j} + \left(\frac{\partial Q}{\partial \sigma^e} \cdot \frac{\sigma^e}{Q} \right) \cdot \frac{\delta \sigma^e}{\sigma^e} = I + D \quad (18)$$

where the term I is generally called “indirect” effect, and the term D is called “direct” effect. While the direct effects can be obtained with explicit expressions of the derivatives of Q , the indirect effect (i.e. the sensitivity coefficients S), can be obtained with perturbation expression, most frequently at the first order.

Theory

For a reaction rate in a source driven system:

$$R_s = \langle \sigma_f \Phi_s \rangle \quad (19)$$

Sensitivity coefficients are calculated using GPT (Generalized Importance Theory). :

$$\frac{\sigma}{\langle \sigma_f \Phi_s \rangle} \frac{d\langle \sigma_f \Phi_s \rangle}{d\sigma} = \sigma \left\{ \frac{\left\langle \left(\frac{\partial \sigma_f}{\partial \sigma} \right) \Phi_s \right\rangle}{\langle \sigma_f \Phi_s \rangle} - \left\langle \tilde{\Psi}^*, \left(\frac{\partial A}{\partial \sigma} - \frac{\partial F}{\partial \sigma} \right) \Phi_s \right\rangle \right\} \quad (20)$$

Theory

The Generalized Importance Function Ψ^* satisfies the equation:

$$(A^* - F^*)\tilde{\Psi}^* = \frac{\partial R_s}{\partial \Phi_s} = \sigma_f(r, E) \quad (21)$$

Using Eq. (3) and Eq. (21) we can establish the principle of conservation of importance:

$$R_s = \langle \sigma_f \Phi_s \rangle = \langle S \tilde{\Psi}^* \rangle \quad (22)$$

When a perturbation is made:

$$A' \Phi'_s = F' \Phi'_s + S \quad (23)$$

Theory

We can calculate the variation of the integral parameter for the indirect effect as:

$$\delta R_S = R'_S - R_S = \langle \tilde{\Psi}^*, (\partial A - \partial F) \Phi' \rangle \quad (24)$$

In the case of a reaction rate ratio:

$$I_S = \frac{\langle \sigma_f \Phi_1 \rangle}{\langle \sigma_f \Phi_2 \rangle} \quad (25)$$

The adjoint importance satisfies the following equation:

$$(A^* - F^*) \tilde{\Psi}^* = \frac{\sigma_f(r, E)}{\langle \sigma_f \Phi_1 \rangle} - \frac{\sigma_f(r, E)}{\langle \sigma_f \Phi_2 \rangle} \quad (26)$$

Theory

For a critical system, only reaction rate ratio can be calculated, otherwise there is no solution to the generalized importance equation. The source has to be orthogonal to the direct flux and give no contribution to the total balance:

$$\left(A^* - \frac{F^*}{K} \right) \tilde{\Psi}^* = \frac{\sigma_f(r, E)}{\langle \sigma_f \Phi_1 \rangle} - \frac{\sigma_f(r, E)}{\langle \sigma_f \Phi_2 \rangle} \quad (27)$$

If we, for instance, consider the power peak, this parameter can be expressed as the ratio:

$$R = \frac{\langle \Sigma_p \Phi \rangle_{MAX}}{\langle \Sigma_p \Phi \rangle_{Reactor}} = \frac{I_1}{I_2} \quad (28)$$

with Σ_p the power cross-section, essentially represented by $E_f \cdot \Sigma_f$,
where E_f is the average energy released per fission.



Theory

The direct effect sensitivity coefficient for Σ_p are (numerator and denominator) defined as:

$$S_j = \frac{\partial I_1}{\partial \Sigma_p} \cdot \frac{\Sigma_p}{I_1} - \frac{\partial I_2}{\partial \Sigma_p} \cdot \frac{\Sigma_p}{I_2} \quad (28)$$

The indirect sensitivity coefficients are defined as:

$$S_j = \left\langle \Psi^*, \sigma_j \Phi \right\rangle \quad (29)$$

and Ψ^* is the importance function solution of:

$$\left(A^* - \frac{F^*}{K} \right) \tilde{\Psi}^* = \frac{\Sigma_p(r, E)_{Max}}{I_1} - \frac{\Sigma_p(r, E)_{Reactor}}{I_2} \quad (30)$$

Theory

Sensitivity Coefficients : The Case of Reactivity Coefficients (EGPT)

For the Equivalent Generalized Perturbation Theory the integral parameter is defined as:

$$I_s = \frac{1}{k'} - \frac{1}{k} = \frac{\langle \Phi^*, (\partial A - \partial F) \Phi' \rangle}{\langle \Phi^*, \frac{1}{k'} F' \Phi' \rangle} \quad (31)$$

Where $(\partial A - \partial F)$ characterizes the reactivity coefficient and the sensitivity coefficients are calculated using the fact that changing the order of the derivatives does not change the results:

$$\frac{\sigma}{I_s} \frac{dI_s}{d\sigma} = \frac{\langle \Phi'^*, (\partial A' - \partial F') \Phi' \rangle}{\langle \Phi'^*, \frac{1}{k'} F' \Phi' \rangle} - \frac{\langle \Phi^*, (\partial A - \partial F) \Phi \rangle}{\langle \Phi^*, \frac{1}{k} F \Phi \rangle} \quad (32)$$

Theory

A reactivity coefficient (like the Doppler effect) can be expressed as a variation of the reactivity of the unperturbed system (characterized by a value K of the multiplication factor, a Boltzmann operator M, a flux Φ and an adjoint flux Φ^*) :

$$\Delta\rho = \left(1 - \frac{1}{K_p}\right) - \left(1 - \frac{1}{K}\right) = \frac{1}{K} - \frac{1}{K_p} \quad (33)$$

where K_p corresponds to a variation of the Boltzmann operator such that :

$$\begin{aligned} M &\rightarrow M_p \left(= M + \delta M_p\right) & \Phi &\rightarrow \Phi_p \left(= \Phi + \delta \Phi_p\right) \\ \underline{\Phi}^* &\rightarrow \underline{\Phi}_p^* \left(= \underline{\Phi}^* + \delta \underline{\Phi}_p^*\right) & K &\rightarrow K_p \left(= K + \delta K_p\right) \end{aligned} \quad (34)$$

The sensitivity coefficients (at first order) for $\Delta\rho$ to variations of the σ_j are given as :

$$S_j^{RO} = \frac{\partial(\Delta\rho)}{\partial\sigma_j} \cdot \frac{\sigma_j}{\Delta\rho} = \left\{ \frac{1}{I_f^p} \langle \underline{\Phi}_p^*, \sigma_j \underline{\Phi}_p \rangle - \frac{1}{I_f} \langle \underline{\Phi}^*, \sigma_j \underline{\Phi} \rangle \right\} \quad (35)$$

where $I_f = \langle \underline{\Phi}^*, F \underline{\Phi} \rangle$ and $I_f^p = \langle \underline{\Phi}_p^*, F \underline{\Phi}_p \rangle$



Idaho National Laboratory

Theory

The external source importance is defined as:

$$\phi^* = \frac{\bar{s}^*}{\bar{\chi}^*} = \frac{\langle \Phi^*, S \rangle}{\langle S \rangle} \left/ \frac{\int dr [\Phi^* \chi] [\Sigma_f \Phi_s]}{\langle \Sigma_f \Phi_s \rangle} \right. \quad (36)$$

For the sensitivity analysis we introduce the function:

$$G = I_S - \langle \Psi^*, (A - F)\Phi_s - S \rangle - \langle \Psi, \left(A^* - \frac{1}{k} F^* \right) \Phi^* \rangle \quad (37)$$

Requiring this function to be stationary with respect to the variations of Φ_s and Φ^* leads to the equations for the direct and adjoint importance functions:



Idaho National Laboratory

Theory

$$(A^* - F^*)\tilde{\Psi}^* = \frac{1}{I_s} \frac{\partial I_s}{\partial \Phi_s} = - \frac{[\Phi^* \chi] \Sigma_f(r, E)}{\int dr [\Phi^* \chi] [\Sigma_f \Phi_s]} + \frac{\Sigma_f(r, E)}{\langle \Sigma_f \Phi_s \rangle} \quad (38)$$

$$\left(A - \frac{1}{k} F\right)\tilde{\Psi} = \frac{1}{I_s} \frac{\partial I_s}{\partial \Phi^*} = \frac{S(r, E)}{\langle \Phi^* S \rangle} - \frac{[\Sigma_f \Phi_s] \chi(r, E)}{\int dr [\Phi^* \chi] [\Sigma_f \Phi_s]} \quad (39)$$

The sensitivity coefficients for the source importance are calculated as:

$$\frac{\sigma}{I_s} \frac{dI_s}{d\sigma} = \frac{\sigma}{I_s} \left\{ \frac{\partial I_s}{\partial \sigma} - \left\langle \tilde{\Psi}^*, \left(\frac{\partial A}{\partial \sigma} - \frac{\partial F}{\partial \sigma} \right) \Phi_s - \frac{\partial S}{\partial \sigma} \right\rangle - \left\langle \tilde{\Psi}, \left(\frac{\partial A}{\partial \sigma} - \frac{1}{k} \frac{\partial F}{\partial \sigma} \right) \Phi^* \right\rangle \right\} \quad (40)$$

Theory

The generalized importance for the inhomogeneous reactivity is calculated as:

$$(A^* - F^*)\tilde{\Psi}^* = \frac{1}{I_s} \frac{\partial I_s}{\partial \Phi_s} = - \frac{S(r, E)}{\Phi_s(r, E) \langle S \rangle} + \frac{[\nu \Sigma_f \Phi_s(r)] \chi(r, E)}{\Phi_s(r, E) \langle F \Phi_s \rangle} \quad (41)$$

Sensitivity coefficients are calculated as:

$$\frac{\sigma}{I_s} \frac{dI_s}{d\sigma} = \frac{\sigma}{I_s} \left\{ \frac{\rho_s \langle \partial \nu \Sigma_f \Phi_s \rangle}{\langle F \Phi_s \rangle} - \left\langle \tilde{\Psi}^*, \left(\frac{\partial A}{\partial \sigma} - \frac{\partial F}{\partial \sigma} \right) \Phi_s \right\rangle \right\} \quad (42)$$

Theory

Sensitivity Coefficients : The Case of Nuclide Transmutation (i.e. nuclide densities at end of irradiation)

The generic nuclide K transmutation during irradiation can be represented as the nuclide density variation between time t_0 and t_F . If we denote n_F^K the “final” density, the appropriate sensitivity coefficients are given by :

$$S_j^K = \frac{\partial n_F^K}{\partial \sigma_j} \cdot \frac{\sigma_j}{n_F^K} = \frac{1}{n_F^K} \int_{t_0}^{t_F} \underline{n}^* \sigma_j \underline{n} \ dt \quad (43)$$

where the time dependent equations to obtain \underline{n}^* and \underline{n} are the classical Bateman equation and its adjoint equation, with appropriate boundary conditions:

$$\frac{dn_k(t)}{dt} = \sum_{j=1}^{K-1} C_{kj} n_j(t) - C_{kk} n_k(t) \quad (44)$$



Idaho National Laboratory

Theory

Sensitivity Coefficients : The Case of the Reactivity Loss during Irradiation, $\Delta\rho^{cycle}$

At first order:

$$\Delta\rho^{cycle} = \sum_K \Delta n^K \rho_K \quad \Delta n^K = n_F^K - n_0^K \quad (45)$$

and ρ_K is the reactivity per unit mass associated to the isotope K.

The related sensitivity coefficients associated to the variation of a σ_j , are given by :

$$S_j^{cycle} = \frac{\sigma_j}{\Delta\rho^{cycle}} \frac{\partial \Delta\rho^{cycle}}{\partial \sigma_j} = \frac{\sigma_j}{\Delta\rho^{cycle}} \left(\sum_K \frac{\partial n^K}{\partial \sigma_j} \cdot \rho_K + \sum_K \Delta n_K \frac{\partial \rho_K}{\partial \sigma_j} \right) \quad (46)$$

or:

$$S_j^{cycle} = \frac{\sigma_j}{\Delta\rho^{cycle}} \frac{\partial \Delta\rho^{cycle}}{\partial \sigma_j} = \frac{\sigma_j}{\Delta\rho^{cycle}} \left(\sum_K \frac{\partial n^K}{\partial \sigma_j} \cdot \rho_K + \sum_K \Delta n_K \frac{\partial \rho_K}{\partial \sigma_j} \right) \quad (47)$$



Idaho National Laboratory

Target Accuracy Assessments

- Target accuracy assessments are the inverse problem of the uncertainty evaluation.
- In order to establish priorities and target accuracies on data uncertainty reduction, a formal approach can be adopted by defining target accuracy on design parameter and finding out required accuracy on data.
- The unknown uncertainty data requirements can be obtained by solving a minimization problem where the sensitivity coefficients in conjunction with the existing constraints provide the needed quantities to find the solutions:

$$\sum_i \lambda_i / d_i^2 = \min \quad i = 1 \dots I \quad (48)$$

$$\sum_i S_{ni}^2 d_i^2 < Q_n^T \quad n = 1 \dots N \quad (49)$$

where d_i are the uncertainties to be found, S_{ni} are the sensitivity coefficients for the integral parameter Q_n , Q^T are the target accuracies on the N integral parameters, and λ_i are cost parameters.

Representativity

- A further use of sensitivity coefficients is, in conjunction with a covariance matrix, a representativity analysis of proposed or existing experiments.
- The calculation of correlations among the design and experiments allow to determine how representative is the latter of the former, and consequently, to optimize the experiments and to reduce their numbers.

$$r_{RE} = \frac{(S_R^+ D S_E)}{[(S_R^+ D S_R)(S_E^+ D S_E)]^{1/2}} \quad (50)$$

- Formally one can reduce the estimated uncertainty on a design parameter by a quantity that represents the knowledge gained by performing the experiment:

$$\Delta R_1^2 = \Delta R_0^2 (1 - r_{RE}^2) \quad (51)$$

Representativity

If more than one experiment is available, the Eq. (50) can be generalized. In the case of two experiments, characterized by sensitivity matrices S_{E1} and S_{E2} the following expression:

$$\Delta R_0'^2 = \Delta R_0^2 \left[1 - \frac{1}{1 - r_{12}^2} (r_{R1} - r_{R2})^2 - \frac{2}{1 + r_{12}} r_{R1} r_{R2} \right] \quad (52)$$

$$r_{12} = \frac{(S_{E1}^+ D S_{E2})}{[(S_{E1}^+ D S_{E1})(S_{E2}^+ D S_{E2})]^{1/2}} \quad (53)$$

$$r_{R1} = \frac{(S_R^+ D S_{E1})}{[(S_R^+ D S_R)(S_{E1}^+ D S_{E1})]^{1/2}} \quad (54)$$

$$r_{R2} = \frac{(S_R^+ D S_{E2})}{[(S_R^+ D S_R)(S_{E2}^+ D S_{E2})]^{1/2}} \quad (55)$$



Idaho National Laboratory

Adjustments

- Sensitivity coefficients are also used in input parameter adjustments, where the coefficients are used within a fitting methodology (e.g. least square fit, Lagrange multipliers with most likelihood function, etc.) in order to reduce the discrepancies between measured and calculational results.
- The resulting adjusted input parameters can be subsequently used, sometimes in conjunction with bias factors, to obtain calculational results to which a reduced uncertainty will be associated.
- If we define: $y_j = (\sigma_j^{\text{adj}} - \sigma_j) / \sigma_j$ and $y_{Q_i}^{\text{exp}} = (Q_i^{\text{exp}} - Q_i) / Q_i$, the y_j are given by:

$$\bar{y} = \left(S^T D_Q^{-1} S + D^{-1} \right)^{-1} S^T D_Q^{-1} \bar{y}_Q^{\text{exp}} \quad (56)$$

where D_Q is the covariance matrix of the experiments, D the covariance matrix of the cross sections and S is the sensitivity matrix. It will also result an adjusted covariance matrix for the nuclear data:

$$(D^{\text{adj}})^{-1} = D^{-1} + S^T D_Q^{-1} S \quad (57)$$



Idaho National Laboratory

ERANOS Sensitivity Capabilities

- 1, 2, and 3D adjoint capability for calculation of adjoint flux and generalized importance function.
- Calculation of source term for functionals linear in the real or adjoint flux (e. g. reaction rate, reaction rate ratio, power density, etc.)
- Elimination of fundamental mode contamination, higher eigenfunctions calculation.
- Perturbation components, sensitivity coefficients in diffusion and transport theory for any possible change of cross sections, fission spectra, nuclide densities, or macroscopic variation.
- Sensitivity coefficients to bilinear functionals (e. g. reactivity coefficients, β_{eff}) using equivalent generalized perturbation theory.

ERANOS Sensitivity Capabilities (cont.)

- Direct and indirect effects calculations.
- Inhomogeneous solutions for ADS (ϕ^* , inhomogeneous reactivity).
- Representativity factors between reference design and experiments.
- Special treatment of positive and negative source for S_n transport calculations.
- Time dependent perturbation theory in the nuclide evolution field for burn up and fuel cycle calculations (neutron sources, decay heat in the repository, radiotoxicity, etc.).
- Target accuracy assessment in connection with optimization code.

MUSE Experiment

- The MUSE3 experiments consisted of inserting a standard commercial (d,t) 14 MeV neutron generator, loaded inside a standard MASURCA subassembly, at the core center of different subcritical configurations, the tritium target being located at the core midplane. These subcritical configurations are loaded with UO_2 - PuO_2 fuel (Pu enrichment $\approx 25\%$) with sodium coolant. The core height was 60 cm and the fuel radius ranged from 45 to 51 cm depending on reactivity. The 14 MeV neutron emission was isotropic, with an emission level of $3 \cdot 10^8$ n/s in the continuous mode and 10^5 n/ μ s in the pulsed situation. The neutrons of spontaneous fissions or (α,n) reactions origin create an inherent source in the subcritical core and induce an initial power.



Idaho National Laboratory

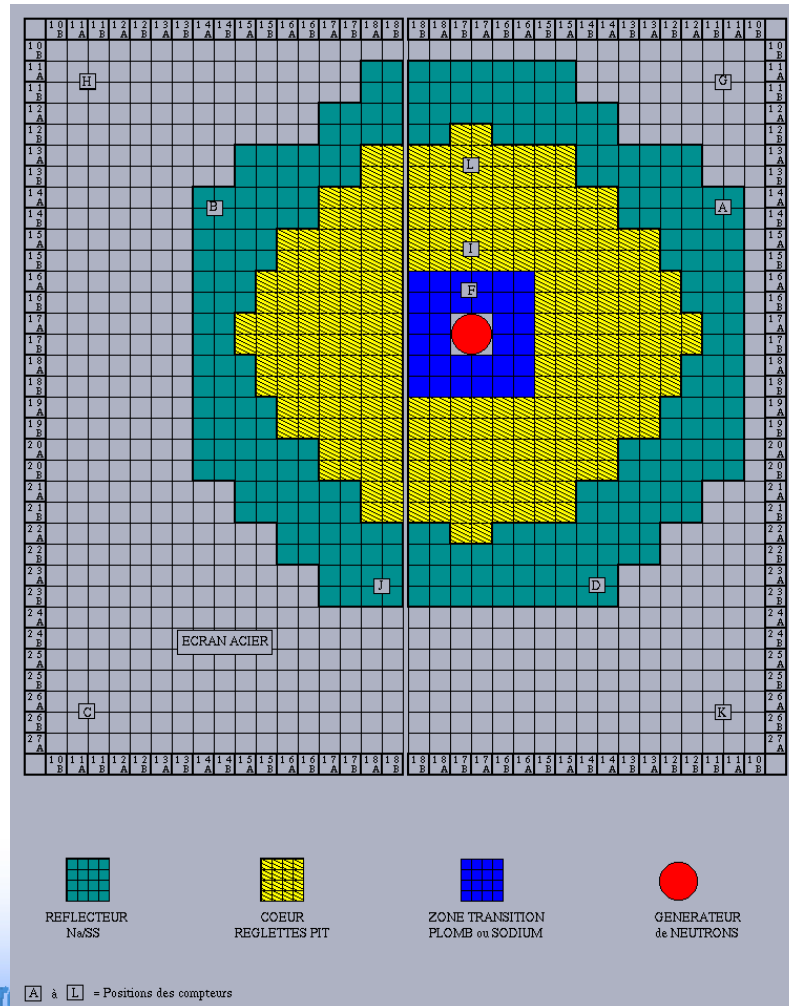
MUSE Experiment

- The MUSE3 experiments started with a critical reference followed by three subcritical configurations called SC1, SC2 and SC3 of about -500, -1000 and -1500 pcm ($1\text{pcm}=0.001\%$ of $\Delta k/k$) respectively, which were obtained by unloading peripheral MASURCA subassemblies from the critical reference. Some measurements were performed with the generator wrapped in a 1 mm thick cadmium layer, to prevent the neutrons moderated by the generator's light materials from entering the core. In a later phase, the neutron generator was surrounded successively by sodium and pure lead buffers of about 12 cm radius, to simulate the diffusing properties of a spallation source and to modify the importance of the 14 MeV neutrons emitted by the generator. In these two configurations, a subcriticality level of about - 4500 pcm was obtained by adjusting the external fuel loading



Idaho National Laboratory

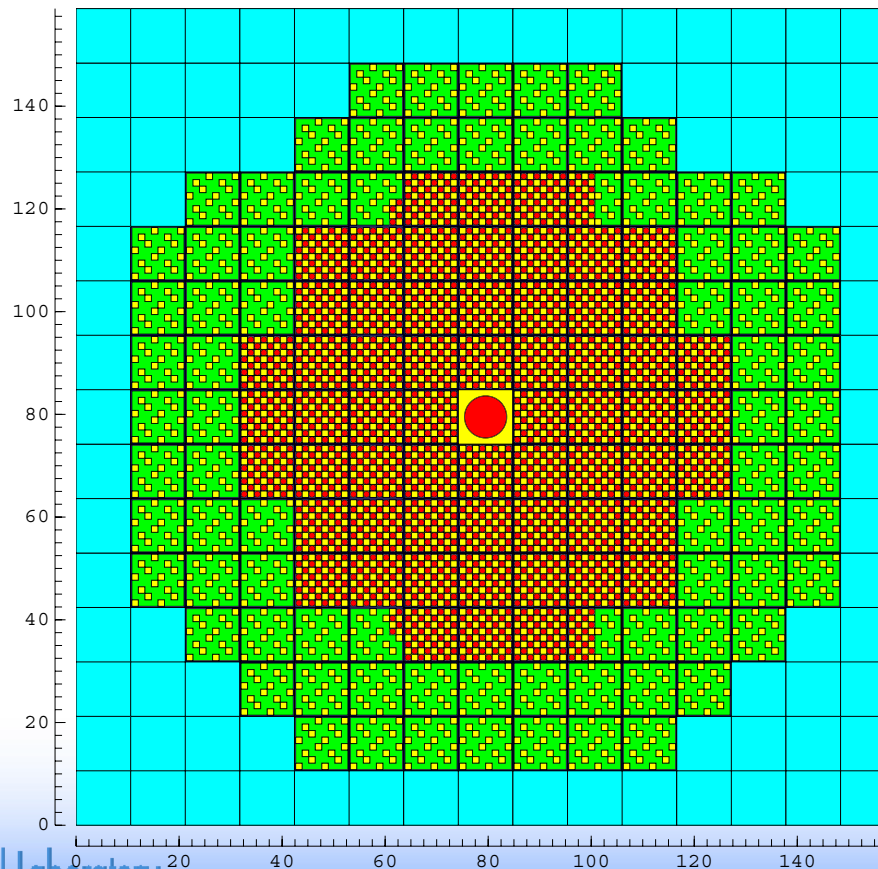
The MUSE Experiment



Idaho National Laboratory

The MUSE Experiment

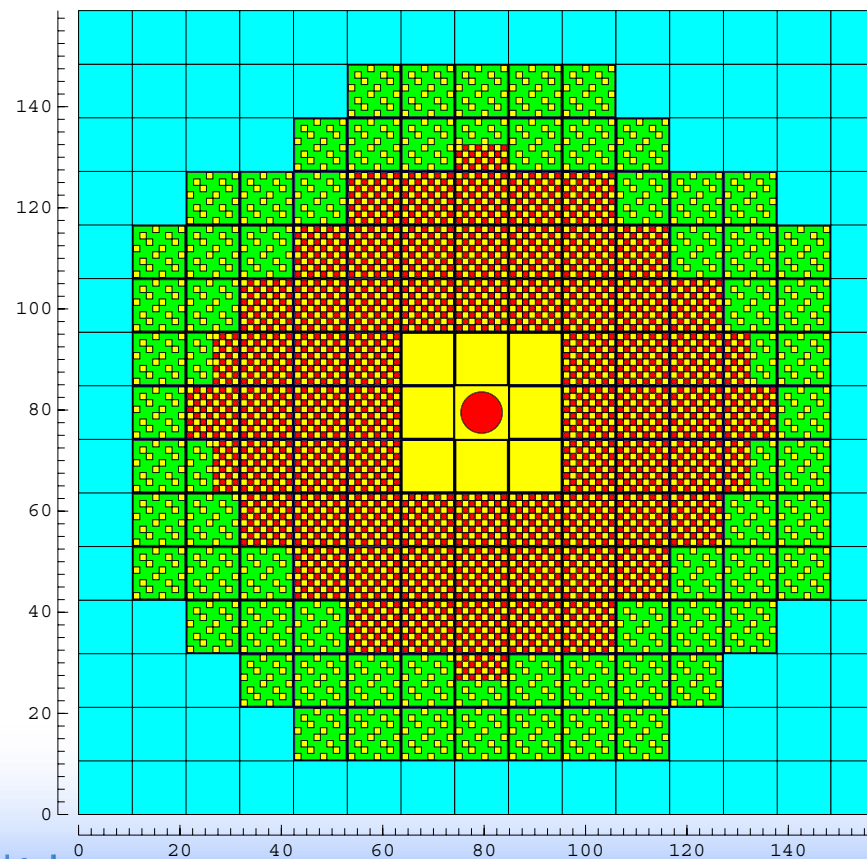
Monte Carlo model for the reference configuration



Idaho National Laboratory

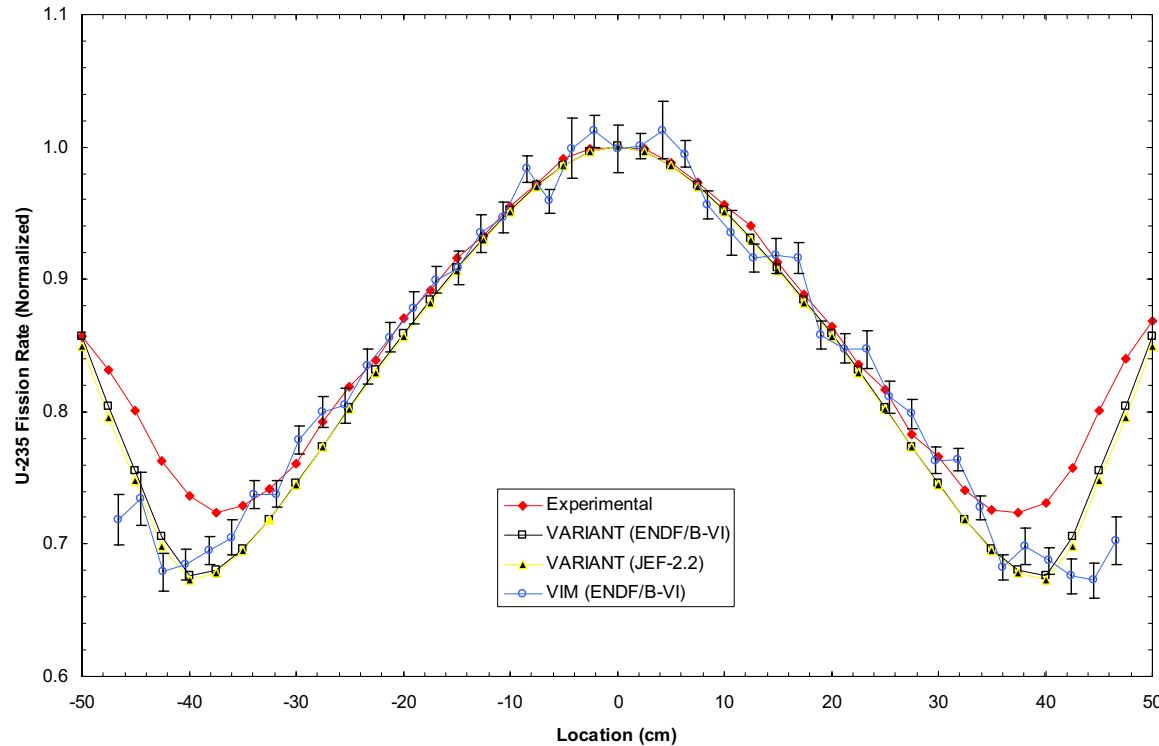
The MUSE Experiment

Monte Carlo model for the buffer configuration



Idaho National Laboratory

The MUSE Experiment



Fission rate radial distribution



Idaho National Laboratory

MUSE Experiment

Reactivity level comparison between experiment and calculations

Experimental Configuration	Measured Experimental Reactivity	Monte Carlo Calculations ENDF/B-VI	Deterministic Transport ENDF/B-VI	Deterministic Transport JEF2.2
Reference	-112 ± 60	$+666 \pm 23$	+1342	+327
Subcritical level 3	-1579 ± 90	-812 ± 30	-50	-1053
Subcritical with Pb buffer	-5687 ± 120	-4564 ± 28	-4268	-5398
Subcritical with Na buffer	-5893 ± 120	-4977 ± 26	-4232	-5270

MUSE Experiment

Perturbation breakdown of isotopes and components
of the reactivity (expressed in p.c.m)
difference between JEF2.2 and ENDF/B-VI

ISOTOPE	Perturbation Components					
	Capture	Fission	Elastic	Inelastic	$N \rightarrow 2N$	SUM
U^{238}	134	11	- 56	- 369	110	- 170
Pu^{239}	- 290	- 9	57	- 37	10	- 269
Pu^{240}	- 188	- 19	18	- 9	2	- 196
Am^{241}	- 102	15	- 3	3	-	- 87
Fe^{56}	35	-	- 91	- 47	3	- 100
O^{16}	2	-	- 129	-	-	- 127



Idaho National Laboratory

Representativity of MUSE

- Accelerator Driven Systems differ from the MUSE3 experiments essentially by three factors: the external source: (spallation for the first one, fusion source for the second}; coolant and fuel compositions; size.
- We will use the correlation methodology in order to quantify how relevant the MUSE3 experiments are with respect to actual ADS designs. A 100 MWth and 1500 MWth concepts will be considered in these calculations.



Idaho National Laboratory

Representativity of MUSE

- The 100 MWth option is designed with a liquid metal coolant (lead-bismuth) and is representative of a demonstration plant where, at first, the fuel will be $\text{UO}_2\text{-PuO}_2$ and where gradually more and more actinides with advanced fuel will be introduced . The $\text{UO}_2\text{-PuO}_2$ fuel has a Pu fuel fraction of less than 40% and gives a K_{eff} of about 0.97. The spallation source is produced by a 600 MeV proton beam on a lead-bismuth target.



Idaho National Laboratory

Representativity of MUSE

Representativity between MUSE-3 and a 100 MWth Pb-Bi ADS

	k _{eff}		ϕ^*	
	JEF2.2	ERALIB1	JEF2.2	ERALIB1
Total Uncertainty [%] on the Experiment : MUSE3 Pb	1.64	0.22	6.48	6.42
Total Uncertainty [%] on the Reactor : Hybrid System	1.64	0.47	0.78	0.65
Representativity Factor	0.95161	0.74529	0.89830	0.97818
Reduced Uncertainty [%] on the Reactor	0.15	0.21	0.15	0.03
CALCULATED VALUES FOR THE HYBRID SYSTEM : $\phi^* = 0.815$ $K_{eff} = 0.96363$				

Representativity of MUSE

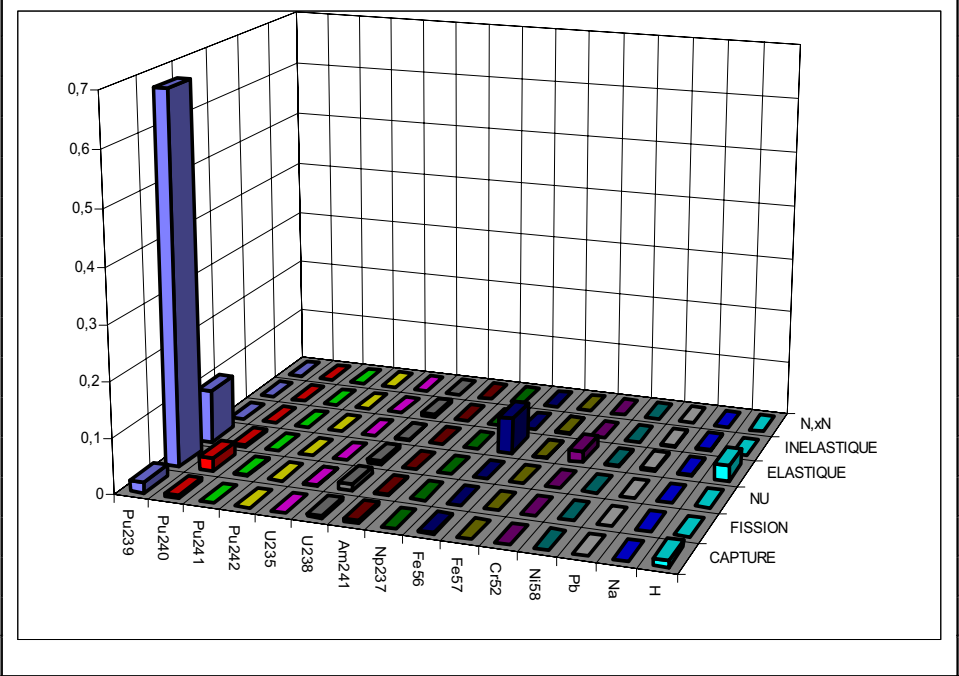
The calculated uncertainties for k_{eff} and φ^* of the Hybrid System using the JEF2.2 and ERALIB1 dispersion matrix show that for the k_{eff} parameter using the unadjusted library JEF2.2 the uncertainty profiles are dominated by the contribution due to the Pu239 cross sections so that in this case the representativity of the MUSE3 experiment is important. When using the ERALIB1 adjusted library, the absolute value of the uncertainty is dominated by the contribution due to the unadjusted lead cross sections, and the uncertainty profiles of the two parameters change: the representativity between the two systems decreases sharply. For the φ^* , in both cases, JEF2.2 and ERALIB1, the Pu239 does not play any role. The two uncertainty profiles are dominated by the contribution due to the lead cross sections increasing the representativity factor.



Idaho National Laboratory

The MUSE Experiment

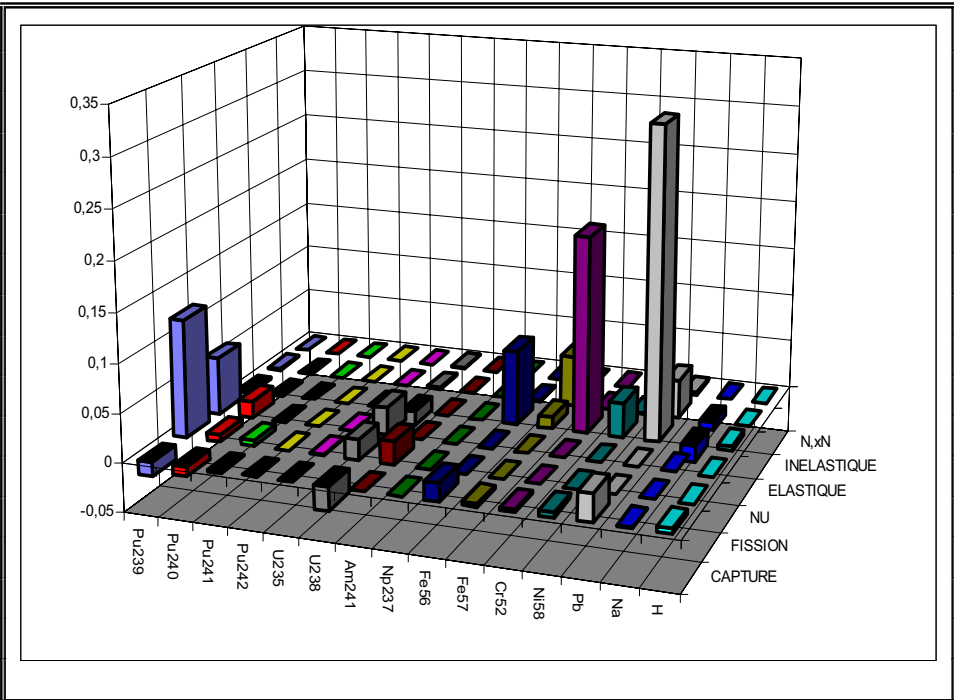
Isotope	σ_{cap}	σ_{fiss}	ν	σ_{el}	σ_{inel}	$\sigma_{n,2n}$	Total
Pu239	2.3E-1	1.4E+0	5.2E-1	1.4E-2	2.3E-2	8.8E-4	1.5E+0
Pu240	1.2E-1	2.6E-1	9.0E-2	8.0E-3	8.3E-3	3.1E-4	3.0E-1
Pu241	1.6E-2	7.9E-2	1.5E-2	6.3E-4	7.6E-4	2.7E-4	8.2E-2
Pu242	3.6E-3	6.9E-3	2.4E-3	3.1E-4	3.5E-4	3.0E-5	8.2E-3
U235	3.1E-3	3.2E-2	2.9E-3	2.5E-4	2.1E-4	1.8E-5	3.2E-2
U238	1.1E-1	1.7E-1	1.3E-1	3.5E-2	1.1E-1	5.8E-3	2.7E-1
Am241	1.2E-1	5.8E-2	2.0E-2	2.7E-4	2.8E-3	0.0E+0	1.3E-1
Np237	3.7E-8	3.2E-9	1.2E-9	1.3E-10	1.1E-10	0.0E+0	3.7E-8
Fe56	7.7E-2	0.0E+0	0.0E+0	4.3E-1	4.0E-2	0.0E+0	4.4E-1
Fe57	1.1E-2	0.0E+0	0.0E+0	2.2E-2	4.6E-2	0.0E+0	5.2E-2
Cr52	2.1E-2	0.0E+0	0.0E+0	2.3E-1	5.0E-3	0.0E+0	2.3E-1
Ni58	3.5E-2	0.0E+0	0.0E+0	7.2E-2	4.6E-3	0.0E+0	8.0E-2
Pb	3.4E-2	0.0E+0	0.0E+0	1.1E-1	4.0E-2	1.1E-2	1.3E-1
Na	7.3E-3	0.0E+0	0.0E+0	8.1E-2	8.8E-2	0.0E+0	1.2E-1
H	1.8E-1	0.0E+0	0.0E+0	2.8E-1	0.0E+0	0.0E+0	3.3E-1
Total	3.7E-1	1.4E+0	5.5E-1	5.8E-1	1.6E-1	1.3E-2	1.7E+0



Keff Uncertainties (%) in the MUSE3 Pb Configuration - JEF2

The MUSE Experiment

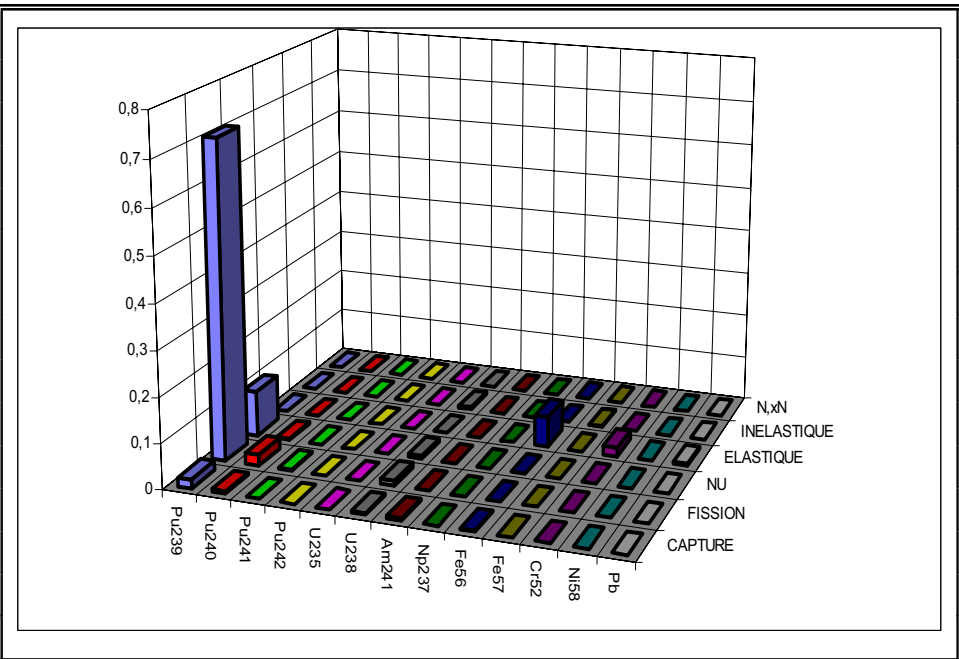
Isotope	σ_{cap}	σ_{fiss}	ν	σ_{el}	σ_{inel}	$\sigma_{n,2n}$	Total
Pu239	2.4E-2i	7.0E-2	4.9E-2	8.7E-3i	7.8E-3	1.7E-3	8.2E-2
Pu240	2.0E-2i	1.7E-2	2.7E-2	6.7E-3i	1.7E-3i	8.0E-4	2.4E-2
Pu241	7.2E-3i	1.6E-2	4.9E-3i	7.9E-4i	6.9E-4	2.7E-4	1.3E-2
Pu242	3.6E-3i	3.0E-3	1.7E-3	3.1E-4	3.4E-4	0.0E+0	9.5E-4i
U235	2.3E-3i	6.9E-3	1.6E-3	1.1E-3i	1.3E-3	3.1E-4	6.7E-3
U238	3.1E-2i	2.9E-2	3.4E-2	2.4E-2i	8.7E-3	5.0E-3	2.3E-2
Am241	0.0E+0	3.1E-2	0.0E+0	0.0E+0	0.0E+0	0.0E+0	3.1E-2
Np237	3.7E-8	3.2E-9	1.2E-9	1.3E-10	1.1E-10	0.0E+0	3.7E-8
Fe56	2.7E-2	0.0E+0	0.0E+0	5.5E-2	5.4E-3	0.0E+0	6.2E-2
Fe57	1.1E-2	0.0E+0	0.0E+0	2.2E-2	4.6E-2	0.0E+0	5.2E-2
Cr52	1.1E-2	0.0E+0	0.0E+0	9.0E-2	3.8E-3	0.0E+0	9.1E-2
Ni58	1.4E-2	0.0E+0	0.0E+0	3.8E-2	2.7E-3	0.0E+0	4.0E-2
Pb	3.4E-2	0.0E+0	0.0E+0	1.1E-1	4.0E-2	1.1E-2	1.3E-1
Na	5.7E-3	0.0E+0	0.0E+0	2.5E-2i	1.8E-2i	0.0E+0	3.1E-2i
H	1.4E-2	0.0E+0	0.0E+0	1.3E-2	0.0E+0	0.0E+0	2.0E-2
Total	2.3E-2	8.5E-2	6.5E-2	1.6E-1	5.9E-2	1.2E-2	2.0E-1



Keff Uncertainties (%) in the MUSE3 Pb Configuration - ERALIB1

Representativity of MUSE

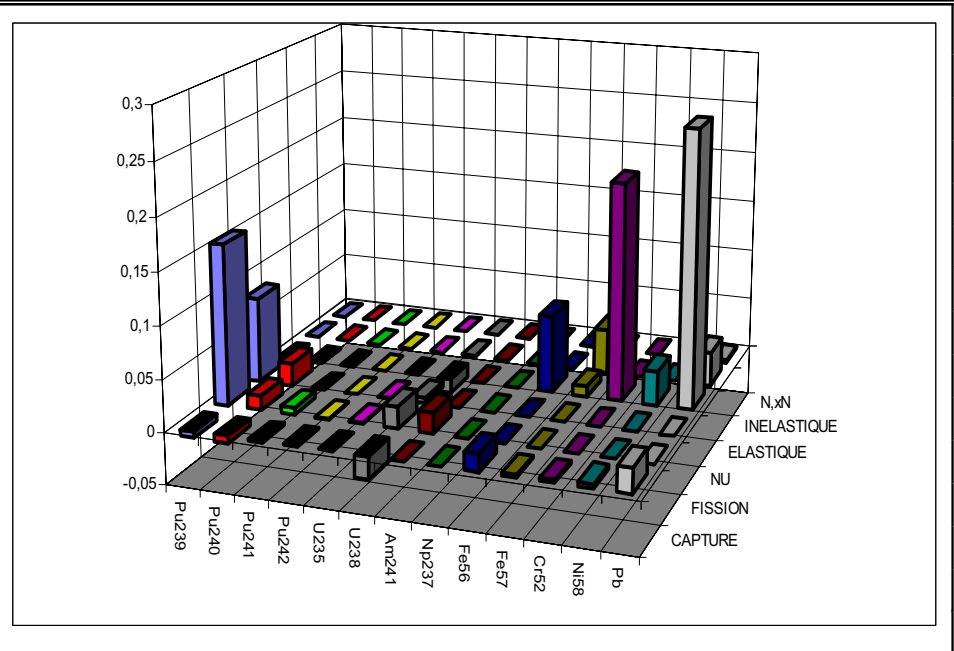
Isotope	σ_{cap}	σ_{fiss}	ν	σ_{el}	σ_{inel}	$\sigma_{n,2n}$	Total
Pu239	1.8E-1	1.2E+0	4.4E-1	7.2E-3	2.0E-2	4.0E-4	1.3E+0
Pu240	1.9E-1	4.4E-1	1.4E-1	8.0E-3	1.3E-2	3.3E-4	5.0E-1
Pu241	1.1E-1	5.6E-1	9.7E-2	2.7E-3	4.6E-3	9.4E-4	5.8E-1
Pu242	4.8E-2	9.7E-2	3.2E-2	2.6E-3	4.1E-3	2.7E-4	1.1E-1
U235	2.2E-3	2.7E-2	2.2E-3	1.2E-4	1.9E-4	8.1E-6	2.7E-2
U238	1.2E-1	1.2E-1	1.0E-1	2.2E-2	8.8E-2	3.5E-3	2.2E-1
Am241	9.9E-2	4.4E-2	1.5E-2	1.4E-4	2.2E-3	0.0E+0	1.1E-1
Np237	8.7E-17	4.5E-17	1.7E-17	2.1E-19	3.3E-18	0.0E+0	9.9E-17
Fe56	9.6E-2	0.0E+0	0.0E+0	3.8E-1	9.5E-2	0.0E+0	4.0E-1
Fe57	1.4E-2	0.0E+0	0.0E+0	1.7E-2	9.2E-2	0.0E+0	9.5E-2
Cr52	1.3E-2	0.0E+0	0.0E+0	1.1E-1	6.0E-3	0.0E+0	1.1E-1
Ni58	9.1E-4	0.0E+0	0.0E+0	1.1E-3	1.8E-4	0.0E+0	1.5E-3
Pb	3.2E-2	0.0E+0	0.0E+0	3.7E-1	1.4E-1	3.8E-2	4.0E-1
Total	3.4E-1	1.4E+0	4.8E-1	5.4E-1	2.1E-1	3.8E-2	1.6E+0



Keff Uncertainties (%) in the 100 MWth Hybrid System - JEF2

Representativity of MUSE

Isotope	σ_{cap}	σ_{fiss}	ν	σ_{el}	σ_{inel}	$\sigma_{n,2n}$	Total
Pu239	3.5E-2i	1.4E-1	2.7E-2	7.0E-3i	1.3E-2i	1.0E-3	1.4E-1
Pu240	1.8E-2i	5.9E-2	6.5E-2	9.8E-3i	7.9E-3	6.6E-4	8.6E-2
Pu241	2.9E-2	1.3E-1	7.9E-2	1.3E-3i	4.5E-3	9.2E-4	1.6E-1
Pu242	1.0E-2	2.5E-2	3.0E-2	2.6E-3	4.1E-3	0.0E+0	4.1E-2
U235	3.0E-3i	1.2E-2	3.2E-3	1.0E-3i	1.5E-3	2.5E-4	1.2E-2
U238	5.2E-2i	2.7E-2	3.9E-2i	2.7E-2i	3.0E-2i	3.0E-3	7.2E-2i
Am241	0.0E+0	2.5E-2	0.0E+0	0.0E+0	0.0E+0	0.0E+0	2.5E-2
Np237	8.7E-17	4.5E-17	1.7E-17	2.1E-19	3.3E-18	0.0E+0	9.9E-17
Fe56	5.7E-2	0.0E+0	0.0E+0	5.4E-2	3.0E-2	0.0E+0	8.4E-2
Fe57	1.4E-2	0.0E+0	0.0E+0	1.7E-2	9.2E-2	0.0E+0	9.5E-2
Cr52	7.0E-3	0.0E+0	0.0E+0	2.9E-2i	2.3E-3i	0.0E+0	2.9E-2i
Ni58	3.3E-3i	0.0E+0	0.0E+0	5.2E-3i	1.1E-3i	0.0E+0	6.2E-3i
Pb	3.2E-2	0.0E+0	0.0E+0	3.7E-1	1.4E-1	3.8E-2	4.0E-1
Total	3.5E-2	2.1E-1	1.0E-1	3.7E-1	1.6E-1	3.8E-2	4.7E-1

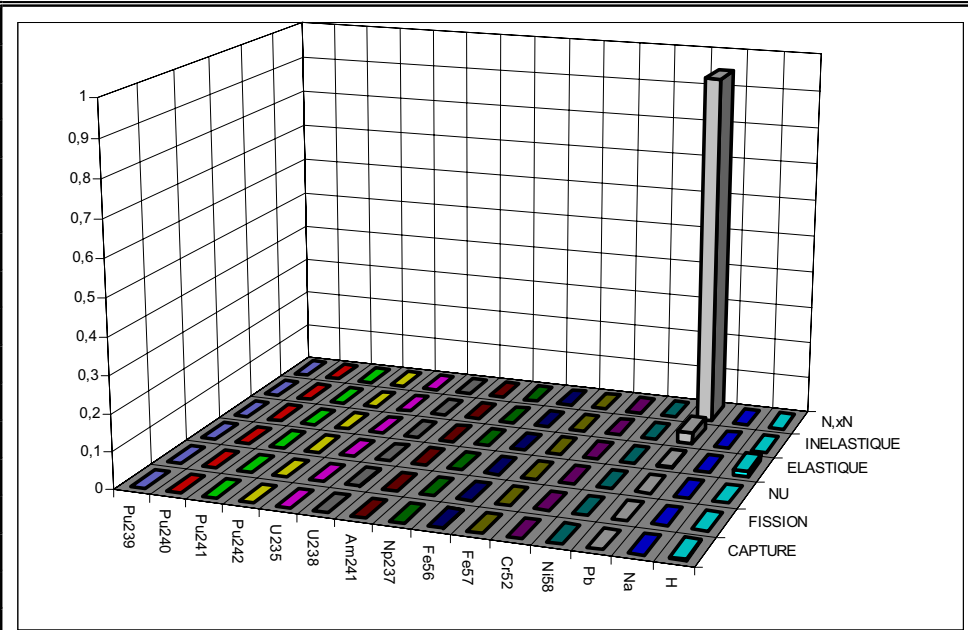


Keff Uncertainties (%) in the 100 MWth Hybrid System - ERALIB1



The MUSE Experiment

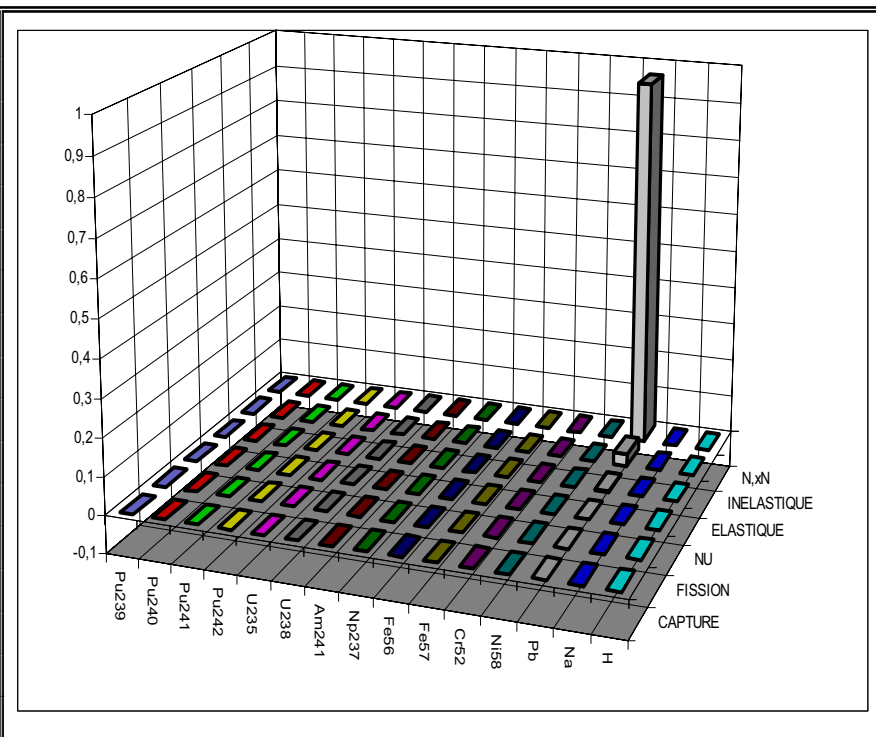
Isotope	σ_{cap}	σ_{fiss}	ν	σ_{el}	σ_{inel}	$\sigma_{n,2n}$	Total
Pu239	5.3E-2	1.1E-1	2.2E-2	4.7E-3	9.4E-3	6.4E-3	1.2E-1
Pu240	2.3E-2	2.5E-2	6.6E-3	2.5E-3	3.7E-3	3.4E-3	3.5E-2
Pu241	2.4E-3	6.4E-3	1.1E-3	2.1E-4	3.0E-4	1.8E-4	6.9E-3
Pu242	9.2E-4	7.6E-4	2.2E-4	9.8E-5	1.4E-4	3.0E-4	1.3E-3
U235	7.0E-4	4.0E-3	1.9E-4	8.1E-5	9.2E-5	6.2E-5	4.1E-3
U238	1.4E-2	8.9E-2	2.3E-2	1.2E-2	4.0E-2	4.9E-2	1.1E-1
Am241	2.9E-2	2.0E-2	6.6E-3	9.2E-5	1.1E-3	0.0E+0	3.6E-2
Np237	3.8E-8	7.2E-9	2.8E-9	3.1E-11	3.7E-10	0.0E+0	3.9E-8
Fe56	1.5E-1	0.0E+0	0.0E+0	8.3E-2	9.6E-2	0.0E+0	2.0E-1
Fe57	3.0E-3	0.0E+0	0.0E+0	3.5E-3	3.4E-2	0.0E+0	3.4E-2
Cr52	2.8E-2	0.0E+0	0.0E+0	2.5E-2	1.7E-1	0.0E+0	1.8E-1
Ni58	3.7E-2	0.0E+0	0.0E+0	1.7E-2	2.5E-2	0.0E+0	4.8E-2
Pb	7.4E-2	0.0E+0	0.0E+0	2.2E-1	1.1E+0	6.3E+0	6.4E+0
Na	4.3E-2	0.0E+0	0.0E+0	2.1E-2	5.5E-2	0.0E+0	7.3E-2
H	3.8E-1	0.0E+0	0.0E+0	8.2E-1	0.0E+0	0.0E+0	9.0E-1
Total	4.3E-1	1.4E-1	3.3E-2	8.5E-1	1.2E+0	6.3E+0	6.5E+0



ϕ^* Uncertainties (%) in the MUSE3 Pb Configuration with Generator ON -
JEF2

The MUSE Experiment

Isotope	σ_{cap}	σ_{fiss}	ν	σ_{el}	σ_{inel}	$\sigma_{n,2n}$	Total
Pu239	2.1E-2	3.9E-2	1.5E-2	5.9E-3	9.4E-3	8.1E-3i	4.7E-2
Pu240	1.2E-2	1.4E-2	4.3E-3	3.1E-3	3.7E-3	5.5E-3i	1.9E-2
Pu241	2.5E-3i	3.2E-3	1.2E-3i	3.1E-4	2.8E-4	1.8E-4	1.6E-3
Pu242	1.4E-3	2.8E-4	2.1E-4	9.7E-5	1.4E-4	0.0E+0	1.5E-3
U235	3.8E-4	5.3E-3	8.7E-4	4.4E-4	4.7E-4	1.4E-3i	5.3E-3
U238	8.6E-3	6.3E-2	2.3E-2	1.8E-3	9.0E-3i	4.8E-2	8.2E-2
Am241	0.0E+0	7.4E-3	0.0E+0	0.0E+0	0.0E+0	0.0E+0	7.4E-3
Np237	3.8E-8	7.2E-9	2.8E-9	3.1E-11	3.7E-10	0.0E+0	3.9E-8
Fe56	1.5E-1	0.0E+0	0.0E+0	2.2E-2	4.4E-2	0.0E+0	1.5E-1
Fe57	3.0E-3	0.0E+0	0.0E+0	3.5E-3	3.4E-2	0.0E+0	3.4E-2
Cr52	2.7E-2	0.0E+0	0.0E+0	2.0E-2	1.6E-1	0.0E+0	1.6E-1
Ni58	3.4E-2	0.0E+0	0.0E+0	1.4E-2	2.0E-2	0.0E+0	4.2E-2
Pb	7.4E-2	0.0E+0	0.0E+0	2.2E-1	1.1E+0	6.3E+0	6.4E+0
Na	4.3E-2	0.0E+0	0.0E+0	1.1E-2	3.6E-2	0.0E+0	5.7E-2
H	2.9E-2	0.0E+0	0.0E+0	4.2E-2	0.0E+0	0.0E+0	5.2E-2
Total	1.8E-1	7.6E-2	2.7E-2	2.3E-1	1.2E+0	6.3E+0	6.4E+0

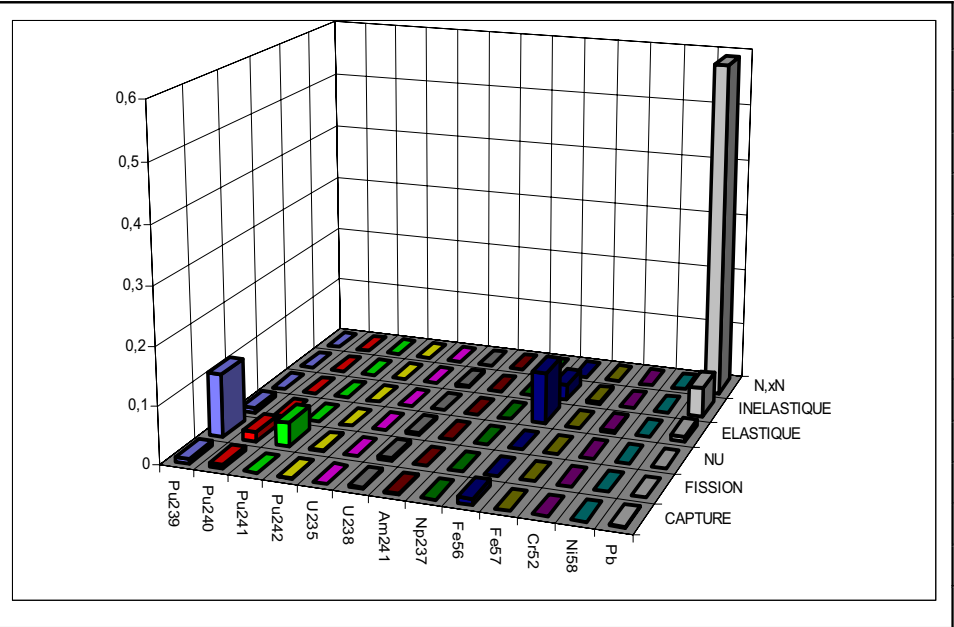


ϕ^* Uncertainties (%) in the MUSE3 Pb Configuration with Generator ON – ERALIB1



Representativity of MUSE

Isotope	σ_{cap}	σ_{fiss}	ν	σ_{el}	σ_{inel}	$\sigma_{n,2n}$	Total
Pu239	7.3E-2	2.6E-1	7.2E-2	3.9E-3	6.3E-3	4.1E-4	2.8E-1
Pu240	6.4E-2	1.0E-1	2.6E-2	4.5E-3	5.5E-3	5.8E-4	1.2E-1
Pu241	2.6E-2	1.6E-1	1.6E-2	1.6E-3	2.0E-3	2.3E-4	1.6E-1
Pu242	1.6E-2	2.6E-2	8.3E-3	1.5E-3	2.0E-3	4.5E-4	3.2E-2
U235	8.4E-4	6.8E-3	3.6E-4	6.5E-5	5.7E-5	6.2E-6	6.9E-3
U238	4.4E-2	5.7E-2	4.6E-2	1.2E-2	4.2E-2	4.0E-3	9.6E-2
Am241	3.5E-2	1.8E-2	6.0E-3	7.3E-5	1.0E-3	0.0E+0	3.9E-2
Np237	3.5E-17	1.3E-17	5.0E-18	1.2E-19	1.5E-18	0.0E+0	3.8E-17
Fe56	8.0E-2	0.0E+0	0.0E+0	2.4E-1	1.3E-1	0.0E+0	2.8E-1
Fe57	1.1E-2	0.0E+0	0.0E+0	7.5E-3	4.0E-2	0.0E+0	4.2E-2
Cr52	1.0E-2	0.0E+0	0.0E+0	4.1E-2	2.6E-2	0.0E+0	4.9E-2
Ni58	7.1E-4	0.0E+0	0.0E+0	7.5E-4	2.3E-4	0.0E+0	1.1E-3
Pb	3.2E-2	0.0E+0	0.0E+0	7.7E-2	1.8E-1	6.0E-1	6.3E-1
Total	1.5E-1	3.3E-1	9.2E-2	2.5E-1	2.3E-1	6.0E-1	7.9E-1

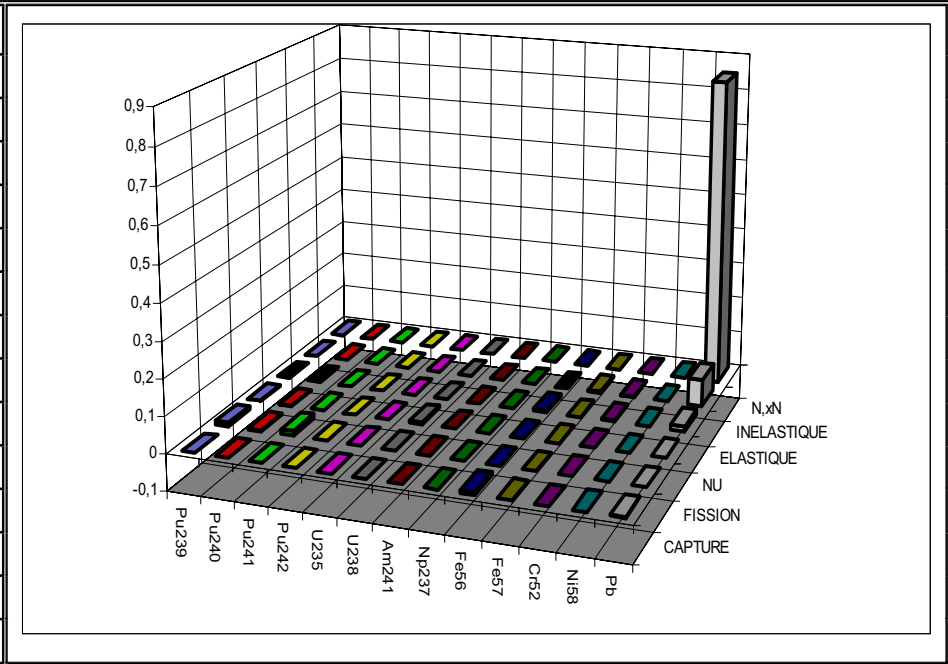


ϕ^* Uncertainties (%) in the 100 MWth Hybrid System - JEF2



Representativity of MUSE

Isotope	σ_{cap}	σ_{fiss}	ν	σ_{el}	σ_{inel}	$\sigma_{n,2n}$	Total
Pu239	4.2E-3	6.7E-2	3.3E-2	5.2E-3i	7.7E-3	1.2E-3i	7.5E-2
Pu240	2.4E-2	3.3E-2	1.2E-2	7.2E-3i	6.2E-3	1.2E-3i	4.2E-2
Pu241	2.0E-2	7.6E-2	1.5E-2	5.1E-4	1.9E-3	2.2E-4	8.0E-2
Pu242	8.2E-3	6.9E-3	8.0E-3	1.5E-3	1.9E-3	0.0E+0	1.4E-2
U235	7.5E-4i	4.5E-3	2.5E-3	1.7E-4i	4.4E-4i	2.0E-4i	5.1E-3
U238	9.6E-3	1.1E-2	4.4E-2	9.1E-3	1.1E-2	4.2E-3	4.9E-2
Am241	0.0E+0	8.6E-3	0.0E+0	0.0E+0	0.0E+0	0.0E+0	8.6E-3
Np237	3.5E-17	1.3E-17	5.0E-18	1.2E-19	1.5E-18	0.0E+0	3.8E-17
Fe56	5.8E-2	0.0E+0	0.0E+0	5.1E-2	2.3E-2i	0.0E+0	7.4E-2
Fe57	1.1E-2	0.0E+0	0.0E+0	7.5E-3	4.0E-2	0.0E+0	4.2E-2
Cr52	8.3E-3	0.0E+0	0.0E+0	3.9E-2	2.2E-2	0.0E+0	4.6E-2
Ni58	1.1E-3i	0.0E+0	0.0E+0	4.6E-4i	4.5E-4	0.0E+0	1.1E-3i
Pb	3.2E-2	0.0E+0	0.0E+0	7.7E-2	1.8E-1	6.0E-1	6.3E-1
Total	7.6E-2	1.1E-1	5.9E-2	1.0E-1	1.8E-1	6.0E-1	6.5E-1



ϕ^* Uncertainties (%) in the 100 MWth Hybrid System - ERALIB1

Representativity of MUSE

- The 1500 MWth ADS has a gas (helium) coolant and is representative of a typical ADS to be introduced in the existing nuclear park in order to reduce waste. The fuel is a “Pu + MA double strata”, that is coming from a Fast Reactor where it has been recycled several times. In the double strata approach, ADS are associated with PWR's and FR's, in order to reduce the amount of waste requiring disposal (in fact some residual losses exist in the reprocessing plants). The target and buffer are both made of liquid lead-bismuth.



Idaho National Laboratory

Representativity of MUSE

Representativity between MUSE-3 and a 1500 MWth Gas-Cooled ADS

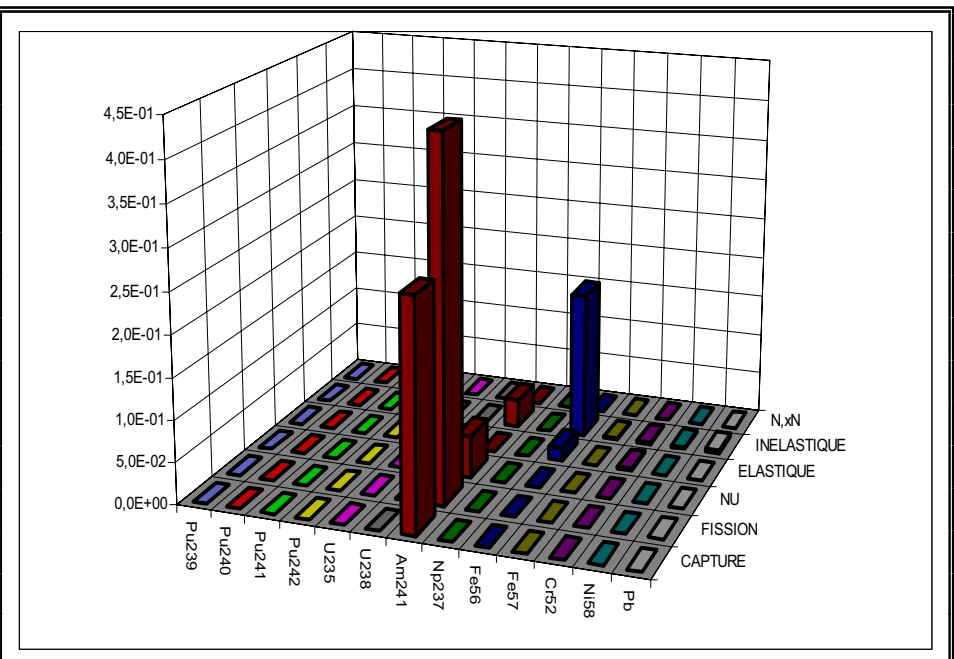
	k _{eff}		ϕ^*	
	JEF2.2	ERALIB1	JEF2.2	ERALIB1
Total Uncertainty [%] on the Experiment : MUSE3 Pb	1.64	0.22	6.48	6.42
Total Uncertainty [%] on the Reactor : Hybrid System	1.73	0.70	1.72	1.57
Representativity Factor	0.10927	0.22208	0.63409	0.16870
Reduced Uncertainty [%] on the Reactor	1.71	0.66	1.03	1.53
CALCULATED VALUES FOR THE HYBRID SYSTEM : $\phi^* = 1.01$ $K_{eff} = 0.95408$				

Representativity of MUSE

For the ϕ^* parameter, one can observe that using the unadjusted library JEF2.2 the uncertainty profiles are dominated by the contribution due to the Pu239 cross sections so that in this case the correlation between the parameters analysed remains relatively high. When using the ERALIB1 adjusted library, the uncertainties profiles of the two parameters change: the correlation between the two systems decreases sharply. For the parameter K_{eff} in the two cases the uncertainty profiles make the correlation factor quite small (the 1500 MWth system is dominated by the uncertainty on Am241). One can conclude that MUSE3 is not representative of a commercial ADS of this type. This conclusion shows that although MUSE experiment brings a large contribution to the understanding of ADS systems, caution should be given to the different aspects of the measured values for transferring to the ADS neutronic characteristics.

Representativity of MUSE

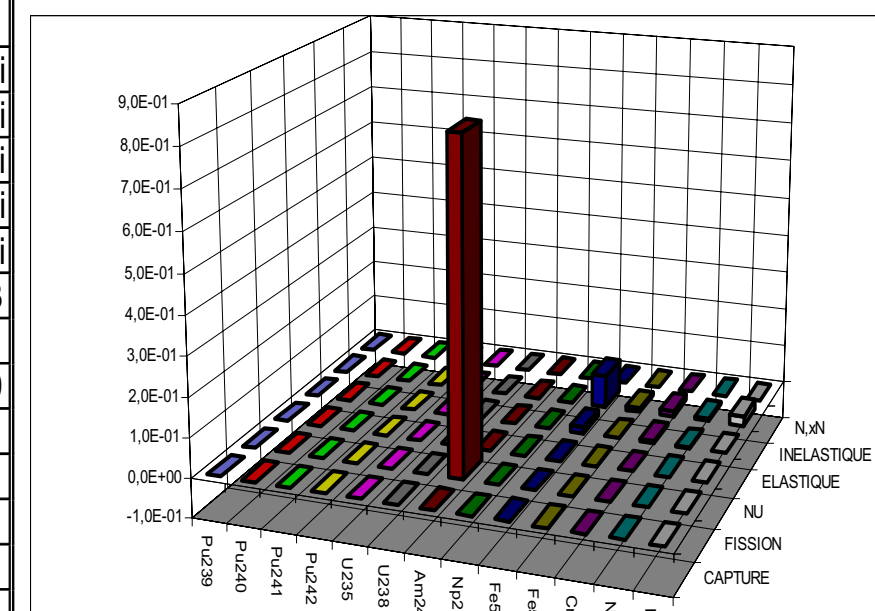
Isotope	σ_{cap}	σ_{fiss}	ν	σ_{el}	σ_{inel}	$\sigma_{n,2n}$	Total
Pu239	1,6E-17	2,6E-16	8,0E-17	1,2E-18	2,7E-17	2,1E-20	2,8E-16
Pu240	1,5E-17	9,8E-17	3,1E-17	1,6E-18	1,7E-17	1,0E-20	1,0E-16
Pu241	1,0E-17	1,1E-16	1,8E-17	5,2E-19	5,6E-18	5,3E-20	1,1E-16
Pu242	4,1E-18	2,1E-17	6,8E-18	5,1E-19	4,8E-18	8,5E-21	2,3E-17
U235	3,5E-20	2,5E-18	7,4E-20	3,7E-21	4,9E-20	0,0E+0	2,5E-18
U238	5,4E-21	5,0E-19	1,2E-20	1,7E-21	4,6E-20	5,3E-23	5,0E-19
Am241	9,1E-3	1,1E-2	3,9E-3	2,4E-5	3,2E-3	0,0E+0	1,5E-2
Np237	3,2E-19	4,6E-19	1,7E-19	1,7E-21	1,9E-19	0,0E+0	6,2E-19
Fe56	3,7E-4	0,0E+0	0,0E+0	2,1E-3	7,3E-3	0,0E+0	7,6E-3
Fe57	4,5E-5	0,0E+0	0,0E+0	1,1E-4	6,8E-4	0,0E+0	6,9E-4
Cr52	1,1E-4	0,0E+0	0,0E+0	8,6E-4	9,0E-4	0,0E+0	1,2E-3
Ni58	3,8E-4	0,0E+0	0,0E+0	1,5E-4	8,5E-4	0,0E+0	9,5E-4
Pb	4,7E-5	0,0E+0	0,0E+0	2,2E-4	1,1E-3	9,0E-6	1,1E-3
Total	9,1E-3	1,1E-2	3,9E-3	2,3E-3	8,2E-3	9,0E-6	1,7E-2



Keff Uncertainties (%) in the 1500 MWth Hybrid System – JEF2

Representativity of MUSE

Isotope	σ_{cap}	σ_{fiss}	ν	σ_{el}	σ_{inel}	$\sigma_{n,2n}$	Total
Pu239	1,3E-11i	1,3E-10i	5,9E-11i	4,1E-12	1,2E-11	8,0E-13i	1,5E-10i
Pu240	1,0E-11i	4,6E-11i	3,4E-11i	3,6E-12	1,4E-11i	5,3E-13i	6,0E-11i
Pu241	3,0E-18	3,3E-11i	1,4E-17	3,7E-19i	5,4E-18	5,2E-20	3,3E-11i
Pu242	5,1E-16	2,6E-11i	6,5E-18	5,0E-19	4,7E-18	0,0E+0	2,6E-11i
U235	3,3E-13i	4,3E-12i	2,1E-12i	3,9E-13	1,7E-12i	6,7E-14i	5,0E-12i
U238	4,7E-13	1,1E-12i	1,1E-12	3,7E-13	6,3E-13	3,6E-16i	9,2E-13
Am241	0,0E+0	6,4E-3	0,0E+0	0,0E+0	0,0E+0	0,0E+0	6,4E-3
Np237	3,2E-19	4,6E-19	1,7E-19	1,7E-21	1,9E-19	0,0E+0	6,2E-19
Fe56	2,6E-4	0,0E+0	0,0E+0	8,4E-4	2,0E-3	0,0E+0	2,2E-3
Fe57	4,5E-5	0,0E+0	0,0E+0	1,1E-4	6,8E-4	0,0E+0	6,9E-4
Cr52	8,1E-5	0,0E+0	0,0E+0	5,3E-4	8,2E-4	0,0E+0	9,8E-4
Ni58	2,7E-4	0,0E+0	0,0E+0	1,6E-4	5,8E-4	0,0E+0	6,7E-4
Pb	4,7E-5	0,0E+0	0,0E+0	2,2E-4	1,1E-3	9,0E-6	1,1E-3
Total	3,9E-4	6,4E-3	6,8E-11i	1,0E-3	2,6E-3	9,0E-6	7,0E-3

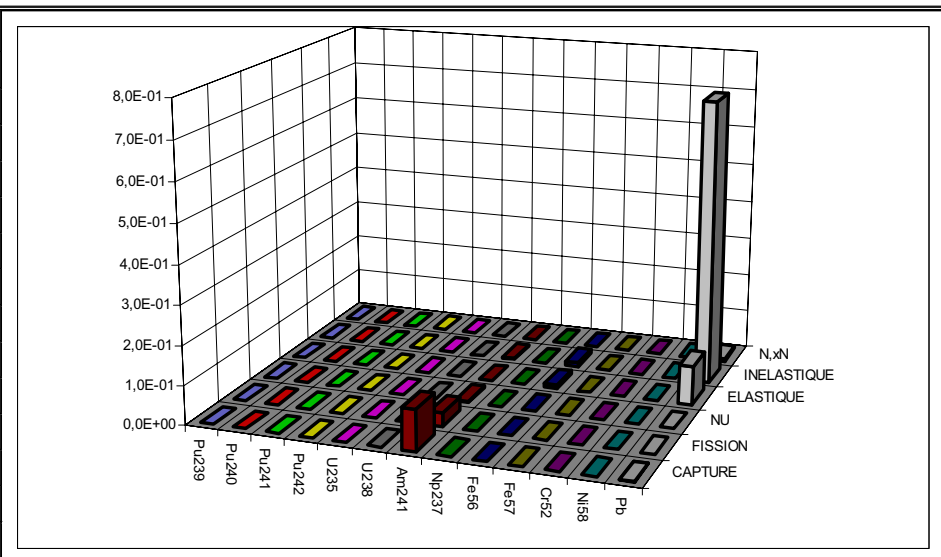


Keff Uncertainties (%) in the 1500 MWth Hybrid System – ERALIB1



Representativity of MUSE

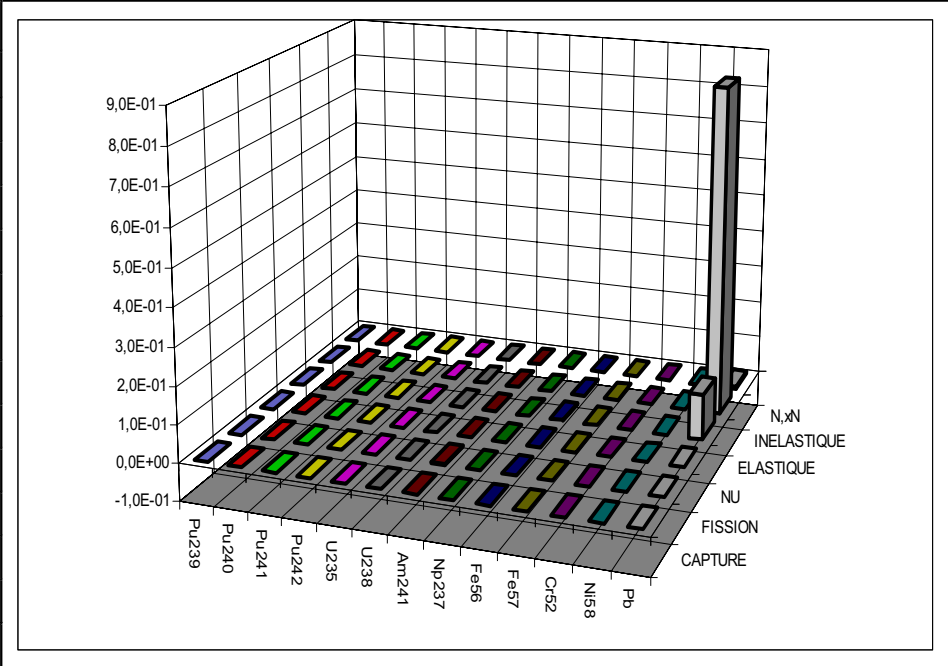
Isotope	σ_{cap}	σ_{fiss}	ν	σ_{el}	σ_{inel}	$\sigma_{n,2n}$	Total
Pu239	9,3E-18	1,3E-16	3,7E-17	2,7E-18	4,6E-18	5,3E-20	1,4E-16
Pu240	8,5E-18	3,4E-17	7,9E-18	3,0E-18	2,6E-18	6,0E-20	3,7E-17
Pu241	4,6E-18	6,4E-17	8,3E-18	1,0E-18	9,9E-19	5,5E-20	6,4E-17
Pu242	2,1E-18	6,1E-18	1,4E-18	9,6E-19	8,6E-19	4,6E-20	6,8E-18
U235	2,0E-20	1,4E-18	3,5E-20	8,1E-21	1,0E-20	1,8E-22	1,4E-18
U238	2,9E-21	1,4E-19	1,6E-21	4,2E-21	1,2E-20	1,9E-22	1,4E-19
Am241	5,6E-3	3,2E-3	1,1E-3	6,4E-5	9,3E-4	0,0E+0	6,6E-3
Np237	1,9E-19	1,7E-19	6,0E-20	3,7E-21	5,4E-20	0,0E+0	2,7E-19
Fe56	2,6E-4	0,0E+0	0,0E+0	1,6E-3	1,8E-3	0,0E+0	2,4E-3
Fe57	2,2E-5	0,0E+0	0,0E+0	5,3E-5	3,9E-4	0,0E+0	4,0E-4
Cr52	4,9E-5	0,0E+0	0,0E+0	4,2E-4	3,4E-4	0,0E+0	5,4E-4
Ni58	8,3E-5	0,0E+0	0,0E+0	1,8E-4	1,4E-4	0,0E+0	2,5E-4
Pb	3,4E-4	0,0E+0	0,0E+0	5,4E-3	1,5E-2	1,4E-3	1,6E-2
Total	5,6E-3	3,2E-3	1,1E-3	5,7E-3	1,5E-2	1,4E-3	1,7E-2



$\phi * \text{Uncertainties (\%)} \text{ in the 1500 MWth Hybrid System – JEF2}$

Representativity of MUSE

Isotope	σ_{cap}	σ_{fiss}	ν	σ_{el}	σ_{inel}	$\sigma_{n,2n}$	Total
Pu239	5,2E-12i	4,5E-11i	2,6E-11i	4,1E-12	3,6E-12i	1,0E-12i	5,2E-11i
Pu240	4,5E-12i	1,5E-11i	1,1E-11i	2,8E-12	1,3E-12i	1,0E-12i	1,8E-11i
Pu241	5,3E-19i	1,6E-11i	7,2E-18	1,0E-18	9,5E-19	5,4E-20	1,6E-11i
Pu242	2,8E-16	3,9E-12i	1,3E-18	9,5E-19	8,5E-19	0,0E+0	3,9E-12i
U235	2,1E-13i	1,6E-12i	9,8E-13i	3,2E-13	1,9E-13i	9,7E-14i	1,9E-12i
U238	2,3E-13	1,0E-13i	1,2E-13i	2,8E-13	1,6E-13	5,8E-16i	3,6E-13
Am241	0,0E+0	9,1E-4	0,0E+0	0,0E+0	0,0E+0	0,0E+0	9,1E-4
Np237	1,9E-19	1,7E-19	6,0E-20	3,7E-21	5,4E-20	0,0E+0	2,7E-19
Fe56	2,3E-4	0,0E+0	0,0E+0	5,4E-4	1,9E-4	0,0E+0	6,2E-4
Fe57	2,2E-5	0,0E+0	0,0E+0	5,3E-5	3,9E-4	0,0E+0	4,0E-4
Cr52	4,3E-5	0,0E+0	0,0E+0	3,4E-4	3,2E-4	0,0E+0	4,7E-4
Ni58	7,4E-5	0,0E+0	0,0E+0	1,4E-4	9,5E-5	0,0E+0	1,8E-4
Pb	3,4E-4	0,0E+0	0,0E+0	5,4E-3	1,5E-2	1,4E-3	1,6E-2
Total	4,2E-4	9,1E-4	2,8E-11i	5,5E-3	1,5E-2	1,4E-3	1,6E-2



$\phi * \text{Uncertainties (\%)} \text{ in the 1500 MWth Hybrid System –ERALIB1}$

Representativity Studies

Sensitivity coefficients are calculated on:

- K_{eff}
- $^{238}\text{U } \sigma_f / ^{239}\text{Pu } \sigma_f$ at core center
- $\eta = v \sum_f / \sum_a$ (being representative of the adjoint)
- β_{eff} (if available)
- $^{238}\text{U } \sigma_f$ slope close to reflector or blanket
- $^{239}\text{Pu } \sigma_f$ slope close to reflector or blanket
- Control rod reactivity (if available)
- Coolant void reactivity (if available)

Selected Experiments

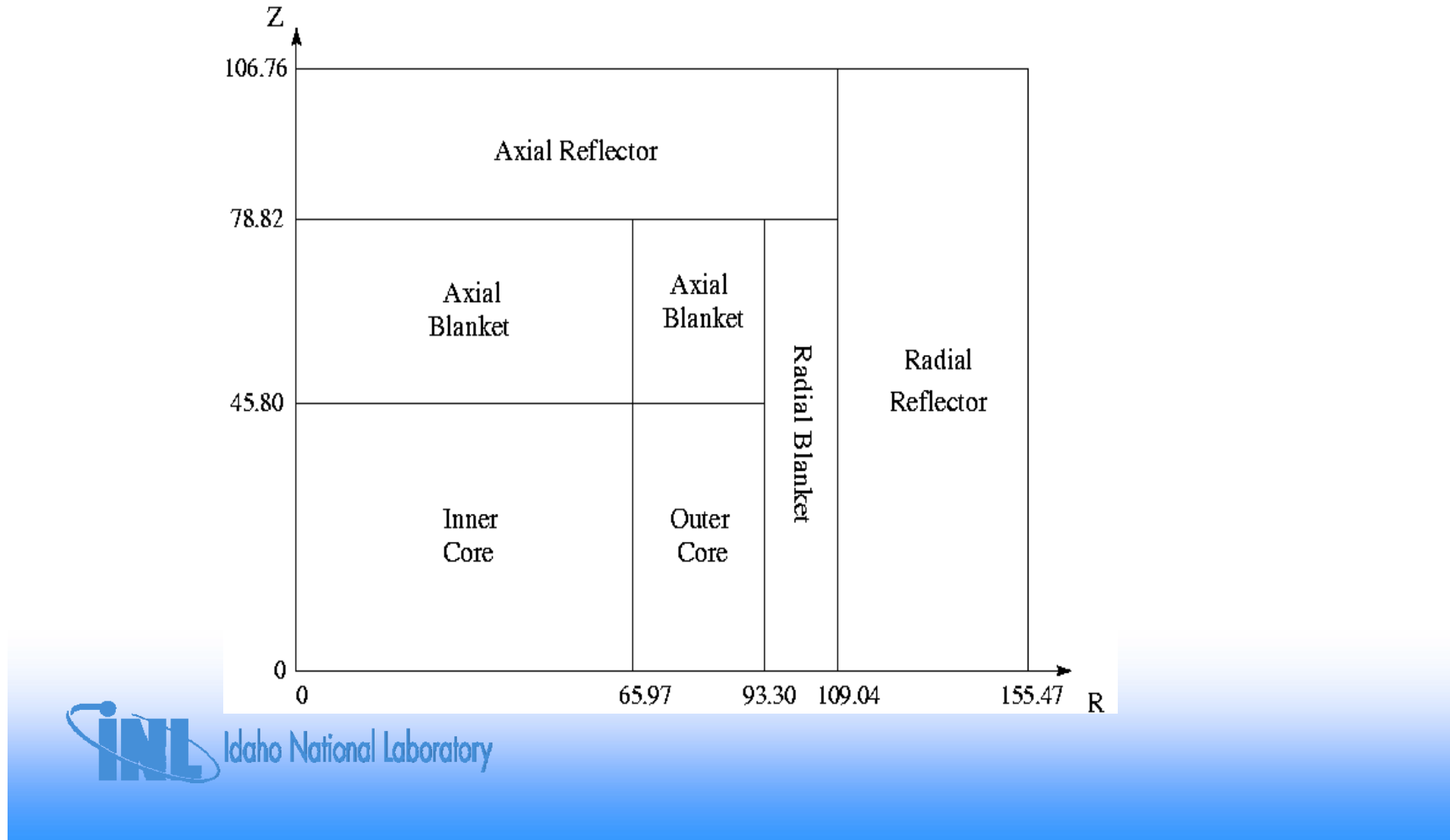
- ZPPR-2, ZPPR-3, ZPPR-9, and ZPPR-10 as representative of large size sodium cooled fast reactor (EFR)
- ZPPR-15 for the small size sodium cooled fast transmuter reactor (SFR)
- ZPR3-48, -53, -54, 55, ZPR9-28, -31 for the gas cooled fast reactor (GCFR)



Idaho National Laboratory

ZPPR-15

The ZPPR-15A experiment was performed to support the DOE innovative design initiatives in August 1985. The assembly is based on sodium cooled, metallic fueled, homogeneous, two-enrichment-zone core of about 330MWe size. With respect to the ZPPR-15A, the EFR has a bigger size and an oxide fuel loading; the SFR has a comparable size, metallic fuel, but a larger amount of minor actinides. and, additionally, the SFR has no blanket.



Idaho National Laboratory

ZPPR-15

Representativity

	R = EFR E = ZPPR- 15A	R = SFR E = ZPPR- 15A	R = EFR E = ZPPR- 15A	R = SFR E = ZPPR- 15A
Integral Parameter	K_{eff}	K_{eff}	$\frac{\langle \sigma_{f,U8} \Phi \rangle_{\text{pos1}}}{\langle \sigma_{f,Pu9} \Phi \rangle_{\text{pos1}}}$	$\frac{\langle \sigma_{f,U8} \Phi \rangle_{\text{pos1}}}{\langle \sigma_{f,Pu9} \Phi \rangle_{\text{pos1}}}$
Absolute Value in R:	1.108481	1.052802	0.025	0.025
Absolute Value in E:	.986312	.986312	0.020	0.020
Total Uncertainty in R:	1.02	1.10	4.84	4.75
Total Uncertainty in E:	1.42	1.42	7.36	7.37
Representativity factor:	0.931	0.613	0.235	0.148
Reduced Uncertainty in R:	0.37	0.87	4.71	4.69



Idaho National Laboratory

ZPPR-15 Representativity

	R = EFR E = ZPPR- 15A	R = SFR E = ZPPR- 15A	R = EFR E = ZPPR- 15A	R = SFR E = ZPPR- 15A
Integral Parameter	Void coefficient $(\rho_{\text{void}} - \rho_{\text{ref}})$	Void coefficient $(\rho_{\text{void}} - \rho_{\text{ref}})$	$\frac{\langle \sigma_{f,U8} \Phi \rangle_{\text{pos2}}}{\langle \sigma_{f,U8} \Phi \rangle_{\text{pos3}}}$	$\frac{\langle \sigma_{f,U8} \Phi \rangle_{\text{pos2}}}{\langle \sigma_{f,U8} \Phi \rangle_{\text{pos3}}}$
Absolute Value in R:	1934.5 pcm	1831 pcm	3.139	3.043
Absolute Value in E:	1652.9 pcm	1652.9 pcm	4.196	4.196
Total Uncertainty in R:	8.40	17.75	3.81	5.46
Total Uncertainty in E:	20.43	20.43	4.12	4.12
Representativity factor:	0.685	0.566	0.932	0.928
Reduced Uncertainty in R:	6.12	14.64	1.38	2.03

ZPPR-15 Representativity

	R = EFR E = ZPPR- 15A	R = SFR E = ZPPR- 15A	R = EFR E = ZPPR- 15A	R = SFR E = ZPPR- 15A
Integral Parameter	$\frac{\langle v\Sigma_f \Phi \rangle}{\langle \Sigma_a \Phi \rangle}$	$\frac{\langle v\Sigma_f \Phi \rangle}{\langle \Sigma_a \Phi \rangle}$	$\frac{\langle \sigma_{f,Pu9} \Phi \rangle_{pos2}}{\langle \sigma_{f,Pu9} \Phi \rangle_{pos3}}$	$\frac{\langle \sigma_{f,Pu9} \Phi \rangle_{pos2}}{\langle \sigma_{f,Pu9} \Phi \rangle_{pos3}}$
Absolute Value in R:	2.94	3.03	0.586	0.045
Absolute Value in E:	2.92	2.92	0.579	0.579
Total Uncertainty in R:	0.04	0.05	1.43	2.59
Total Uncertainty in E:	0.03	0.03	2.02	2.02
Representativity factor:	0.856	0.696	0.836	0.853
Reduced Uncertainty in R:	0.02	0.04	0.78	1.35



ZPPR-15 Representativity

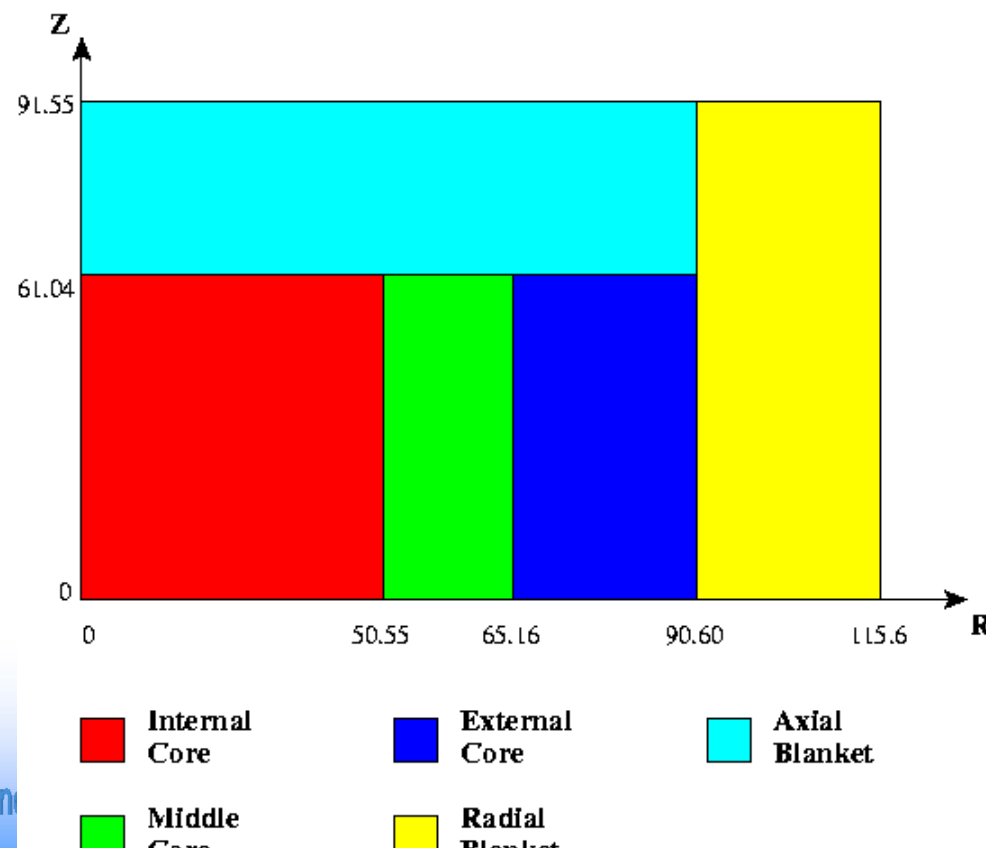
	$R = EFR$ $E = ZPPR-15A$	$R = SFR$ $E = ZPPR-15A$
Integral Parameter	β_{eff}	β_{eff}
Absolute Value in R:	206.2 pcm	207.5 pcm
Absolute Value in E:	213.6 pcm	213.6 pcm
Total Uncertainty in R:	0.70	0.64
Total Uncertainty in E:	0.67	0.67
Representativity factor:	0.950	0.593
Reduced Uncertainty in R:	0.22	0.51



Idaho National Laboratory

ZPR-9

The ZPR-9 Phase I Assembly is the first in a series of critical assemblies designed to provide a reference set of reactor physics measurements in support of a 300MWe GFR Demonstration Plant designed by General Atomic. The Phase I Assembly was the first complete mockup of a GFR core ever built. This assembly was a uniform, single composition core with loading that matched the average enrichment (17.3%) and coolant volume fraction (53%) of the GFR Demonstration Plant. The ZPR-9 Phase I Assembly experiment went critical on April 3, 1975 and the experimental program was completed on June 25, 1975. With respect to the ZPR-9, the GFR core has a bigger size (24000 l compared to 3140 l), but has no blanket. The GFR has a 5% minor actinides loading, while the ZPR-9 contains no minor actinides



ZPR-9 Representativity

	R = GFR E = ZPR-9	R = GFR E = ZPR-9	R = GFR E = ZPR-9
Integral Parameter	K_{eff}	β_{eff}	$\frac{\langle \sigma_{f,U8} \Phi \rangle_{\text{pos2}}}{\langle \sigma_{f,U8} \Phi \rangle_{\text{pos3}}}$
Absolute Value in R:	1.01045	191 pcm	2.061
Absolute Value in E:	0.99749	222 pcm	2.125
Total Uncertainty in R:	1.20	0.90	1.98
Total Uncertainty in E:	1.24	0.58	2.19
Representativity factor:	0.693	0.677	0.146
Reduced Uncertainty in R:	0.86	0.66	1.96
Integral Parameter	$\frac{\langle v \Sigma_f \Phi \rangle}{\langle \Sigma_a \Phi \rangle}$	$\frac{\langle \sigma_{f,U8} \Phi \rangle_{\text{pos1}}}{\langle \sigma_{f,Pu9} \Phi \rangle_{\text{pos1}}}$	$\frac{\langle \sigma_{f,Pu9} \Phi \rangle_{\text{pos2}}}{\langle \sigma_{f,Pu9} \Phi \rangle_{\text{pos3}}}$
Absolute Value in R:	2.94	0.028	0.777
Absolute Value in E:	2.93	0.030	1.353
Total Uncertainty in R:	0.05	7.58	3.12
Total Uncertainty in E:	0.02	6.59	0.41
Representativity factor:	0.653	0.914	0.08
Reduced Uncertainty in R:	0.04	3.08	3.11

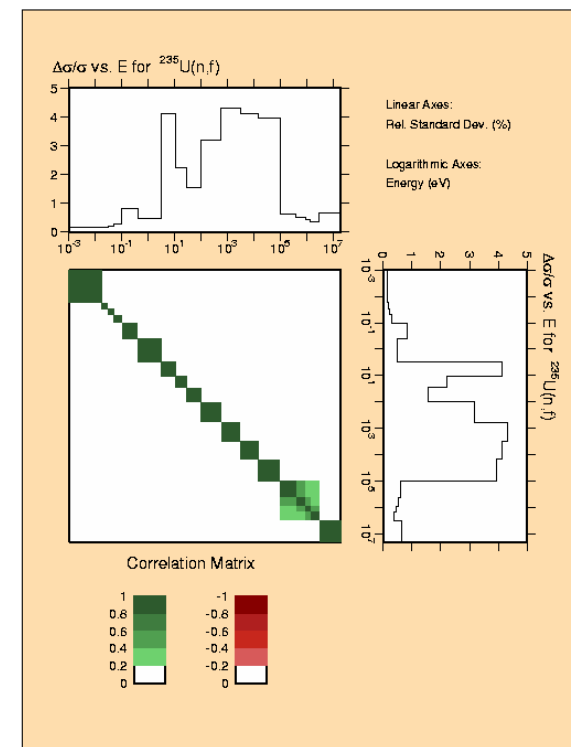
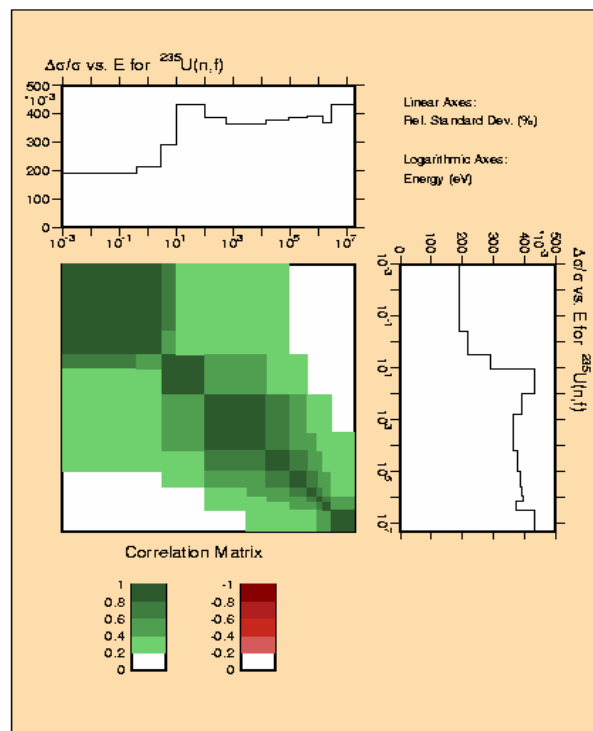
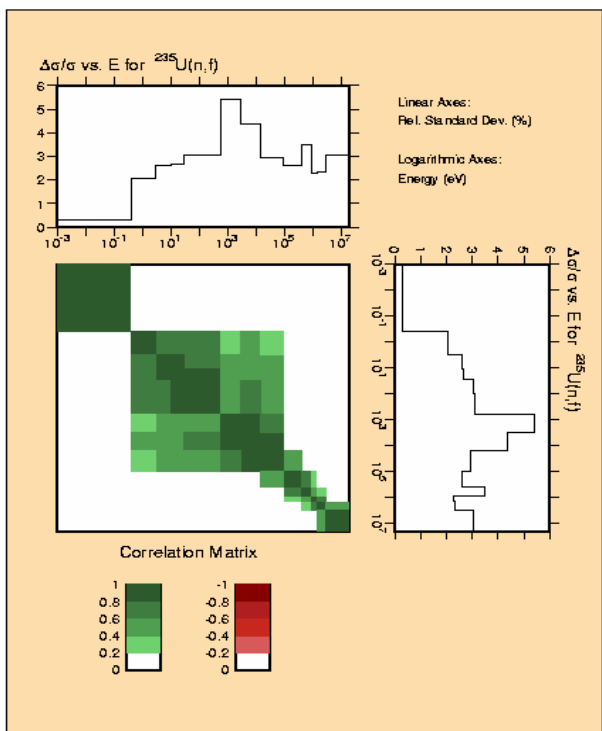


Idaho National Laboratory

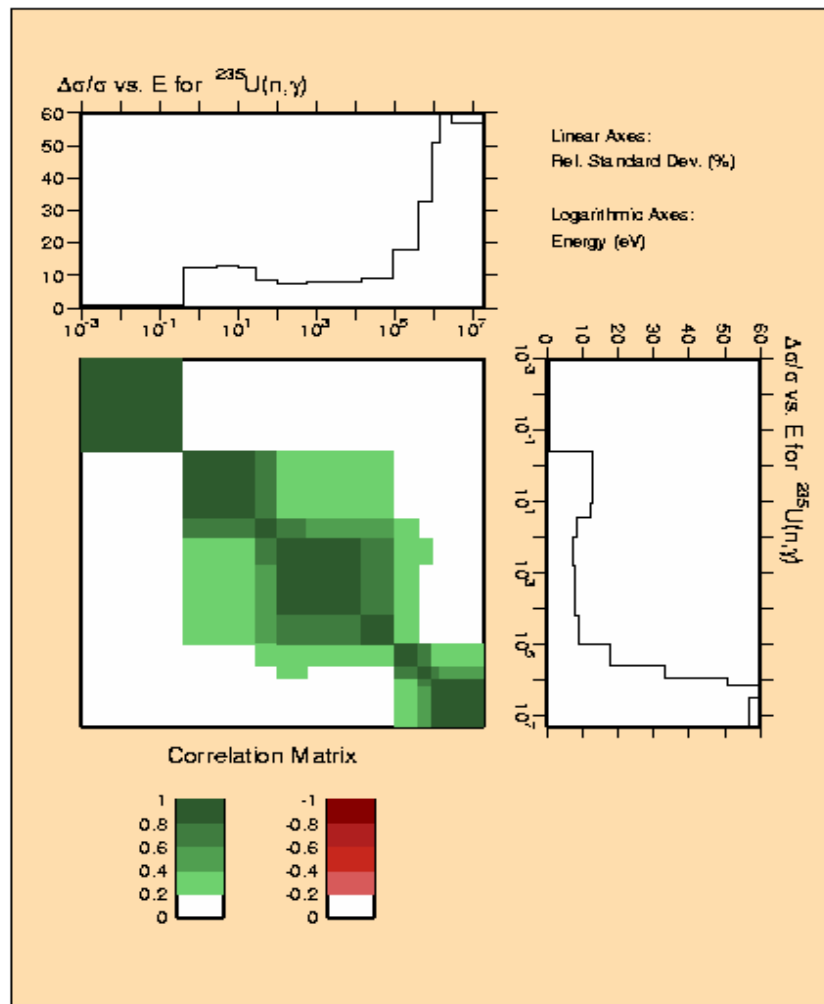
Covariance Data

- Covariance data have been scarce in the past. The first comprehensive effort was done for ENDF/B-IV at the end of the 70' and a code, PUFF, was written for processing this type of information
- After that no major effort was made until the 90' when scattered data were provided for few isotopes and reaction rates for different files (dosimetry, fusion, JEFF, ENDF)
- The Japanese were the only one that made a consistent and coherent issue for their files JENDL 3.2 and 3.3, but many very uncertainty low values for some important isotopes (U and Pu) have been questioned by the evaluator community
- In any case many questions are still open:
 - how good quality are these values?
 - are they scientifically based?
 - are they consistent with the basic data on the files?

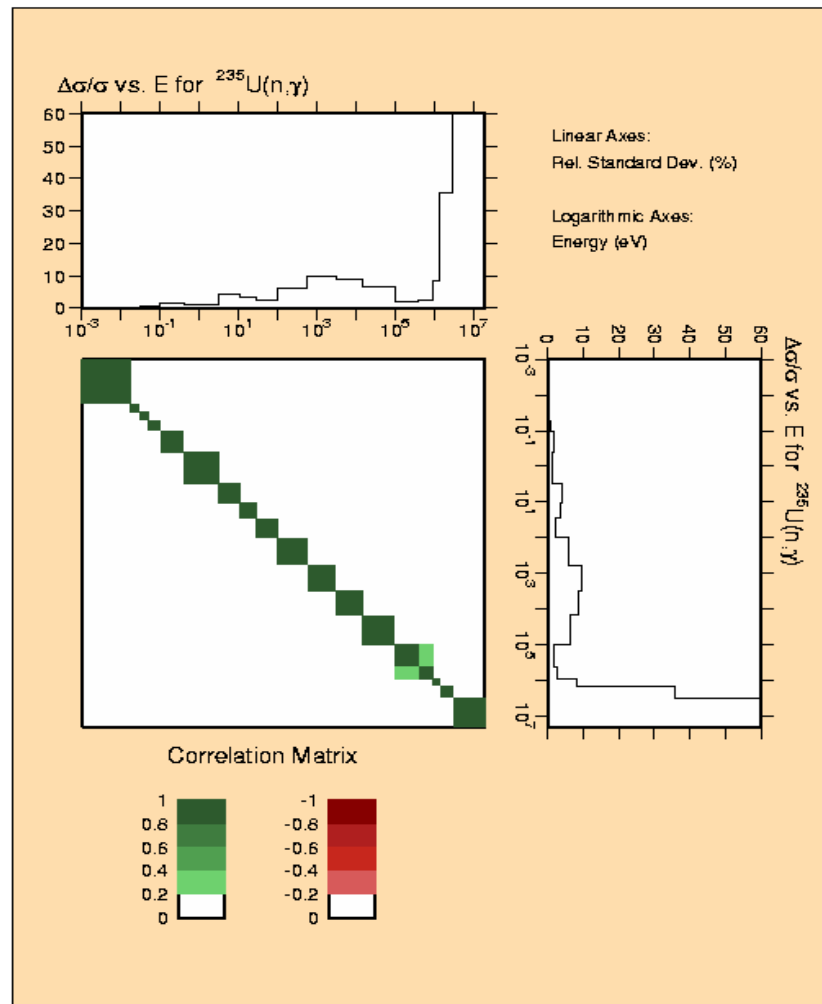
U-235(n,f)



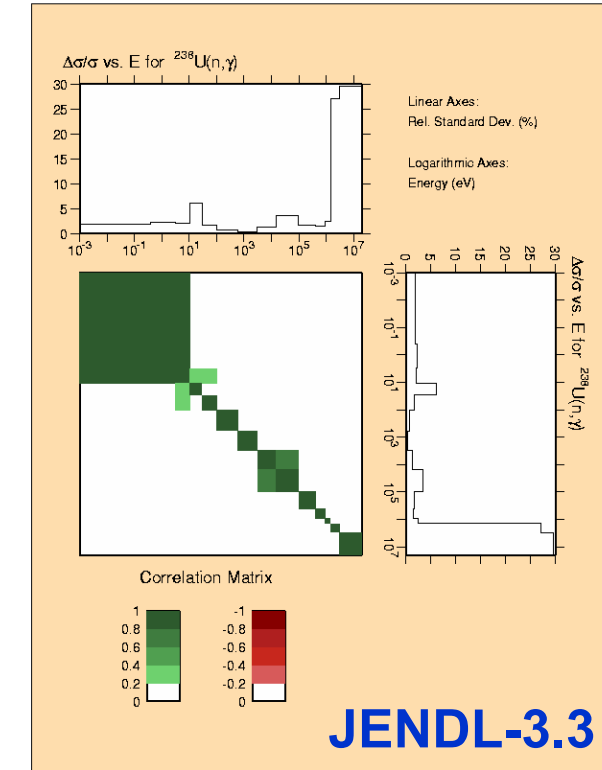
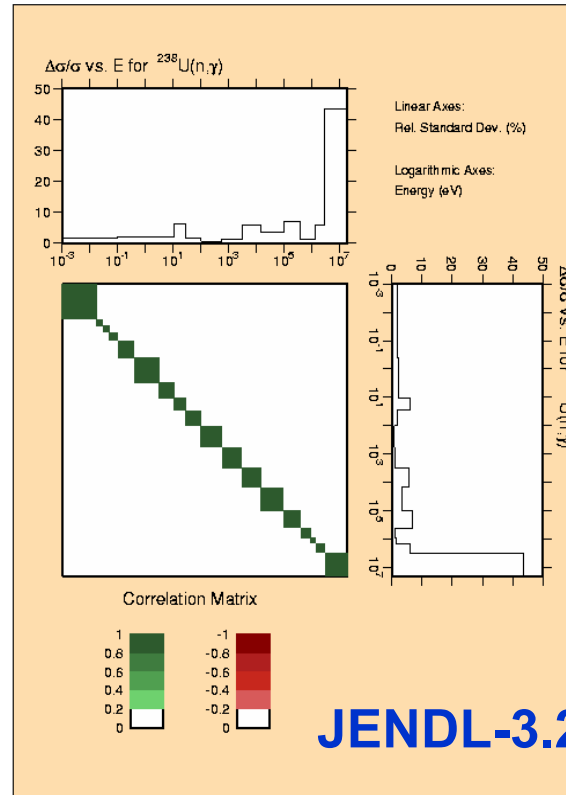
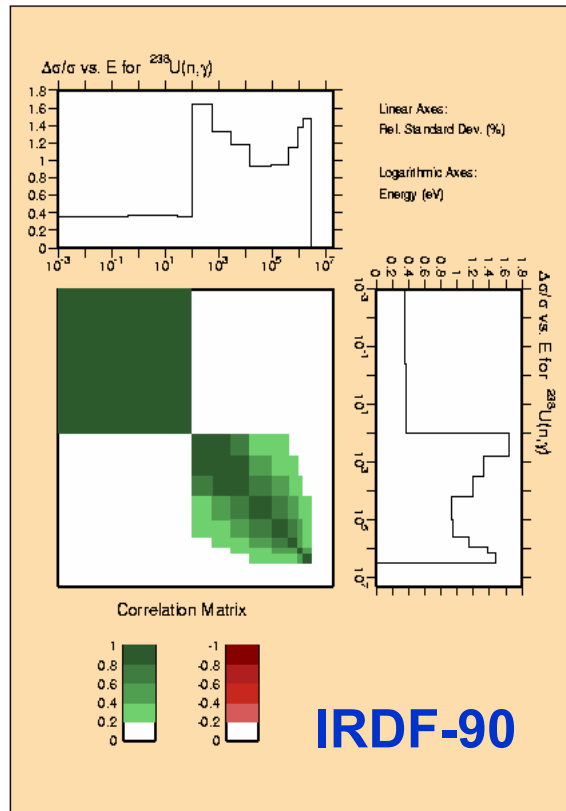
U-235(n,γ)



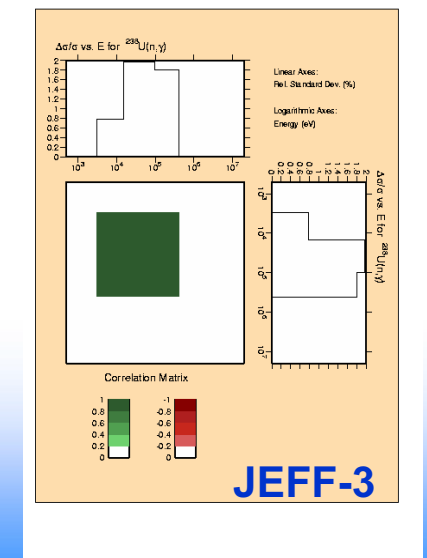
JEF-2.2 (=ENDF/B-V)



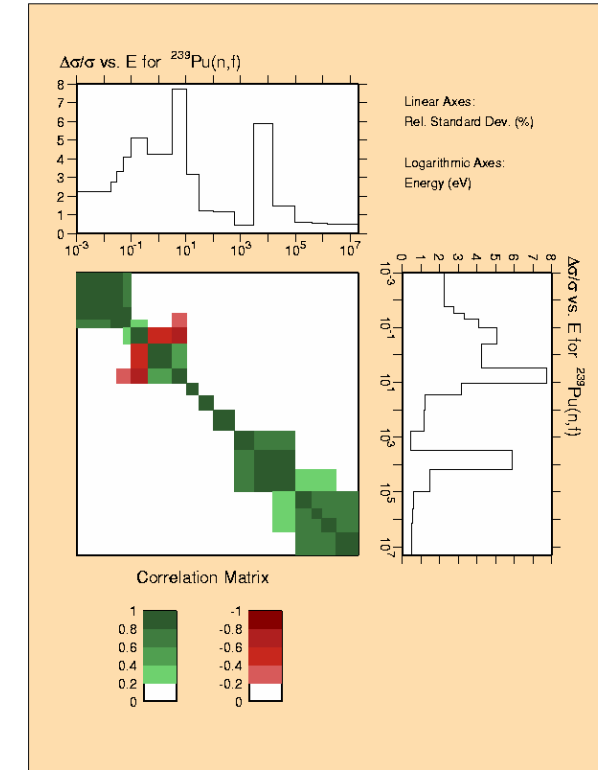
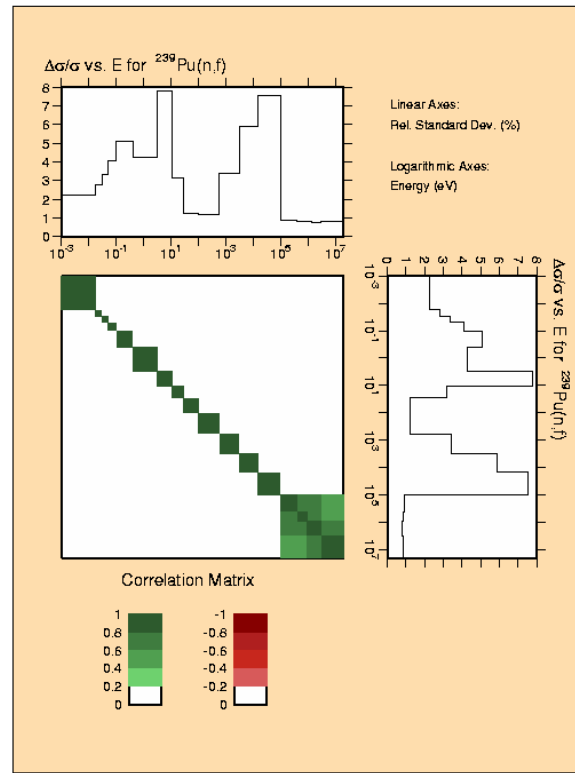
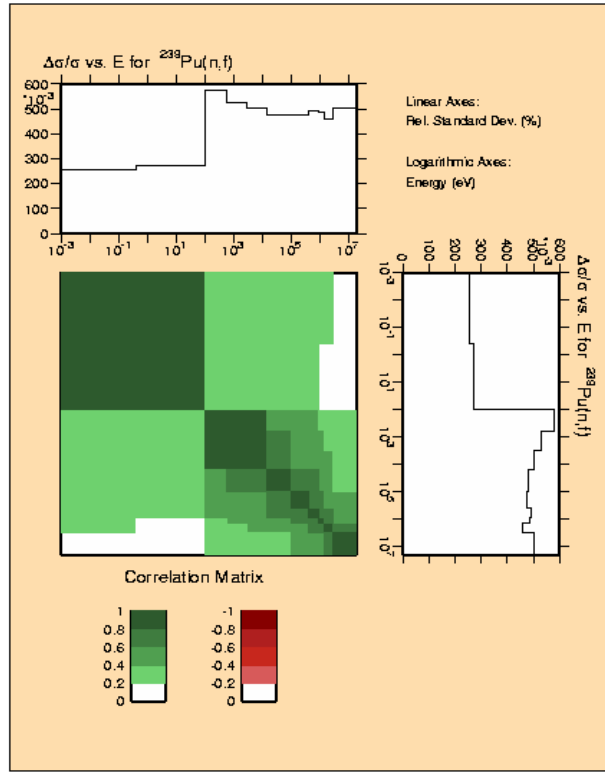
JENDL-3.2



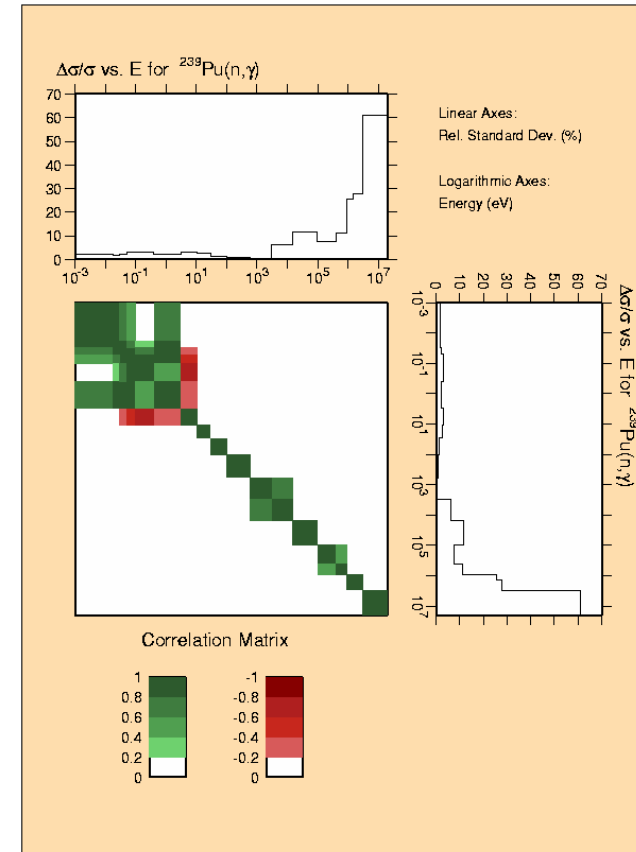
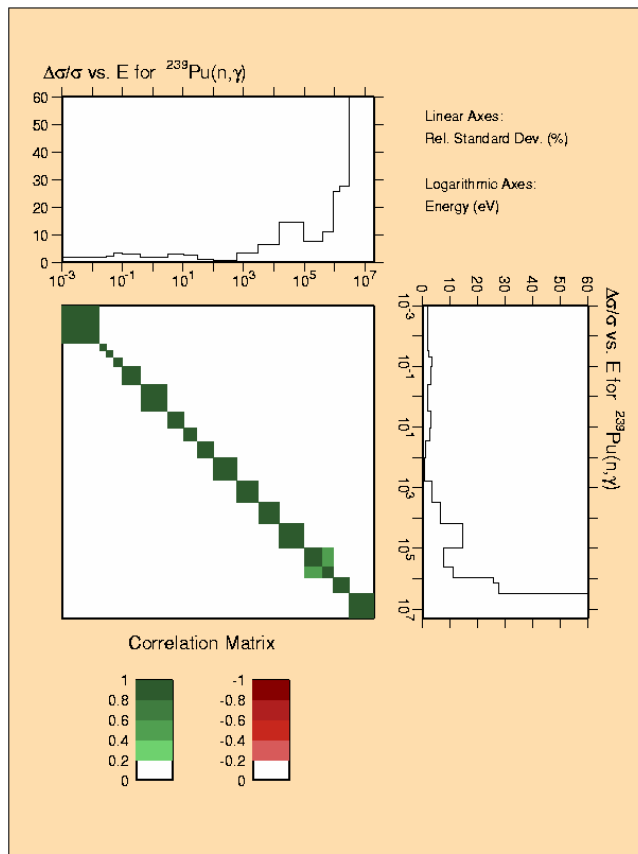
U-238(n, γ)



Pu-239(n,f)



Pu-239(n,γ)



JENDL-3.2

JENDL-3.3



“Home made” covariance Matrix (ANL)

- We started by taking into account the results of clean integral experiment analysis, in particular irradiated sample/fuel analysis, which gave valuable information on capture and some ($n,2n$) cross-sections, and fission rate measurements in critical assemblies
- The uncertainty values, are given by “energy band”, consistent with multigroup energy structures used for deterministic calculations both of thermal and fast reactors
- 15 energy groups have been selected between 20 MeV and $E(\text{thermal})$. Two extra groups have been added between 150MeV and 20MeV for ADS applications
- The uncertainty values are given only for neutron cross-section data of actinides and structural materials. Fission products related uncertainties have not been considered in this study
- The covariance matrix diagonal values have been estimated on the performance of the most recent JEF files in the analysis of a large set of integral experiments in different spectra. However, it was observed that the performance obtained using ENDF/B files was not substantially different. Therefore, the covariance matrix can be applied to both files

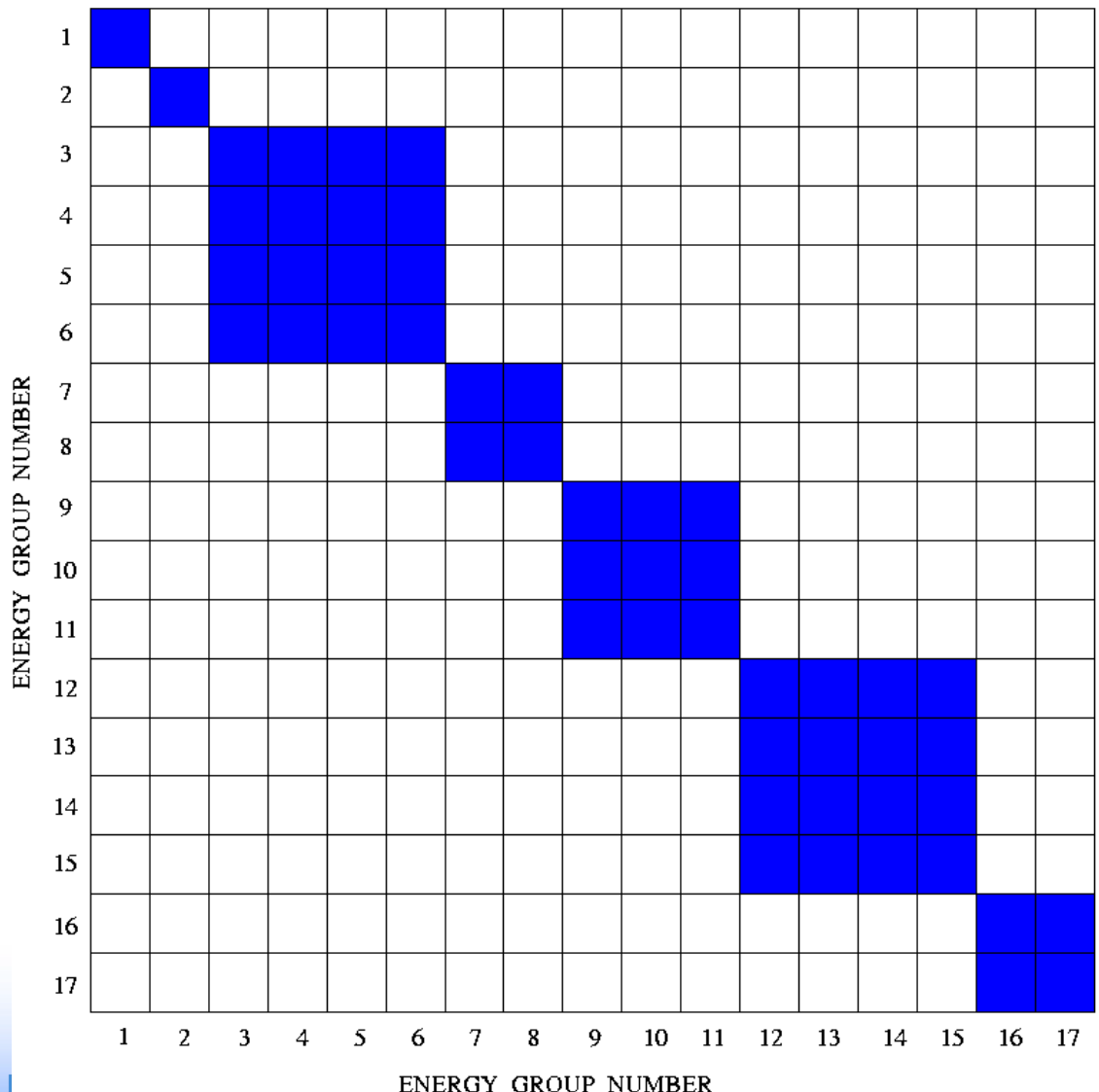
“Home made” covariance Matrix (ANL)

“User oriented” covariance matrix, mostly from “educated” guesses using information from integral experiments

- At first, only “diagonal” values of the full covariance matrices have been derived. Their use implies to neglect all type of correlation (in energy, between different isotopes, among reactions, etc.) and, consequently, to underestimate uncertainties.
- Partial energy correlations. Initial guess (a very “crude” guess) can be to use the same correlations for all isotopes and reactions, under the form of full energy correlation in 5 energy bands.
- The idea is to single out:
 - 1) the region above the threshold of fertile isotope fission cross-sections, and of many inelastic cross-sections, up to 20 MeV
 - 2) the region of the continuum down to the upper unresolved resonance energy limit,
 - 3) the unresolved resonance energy region,
 - 4) the resolved resonance region,
 - 5) the thermal range.

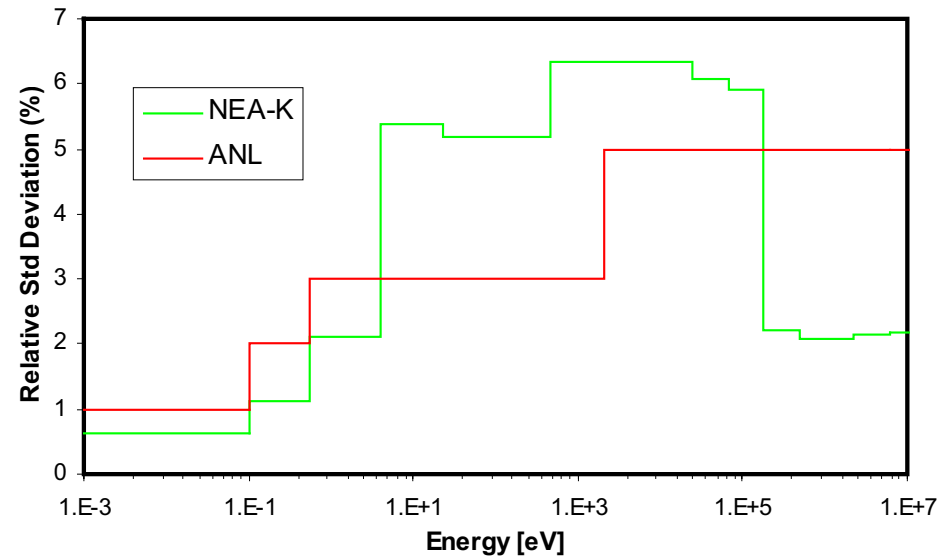


Energy group structure and proposed partial energy correlation.

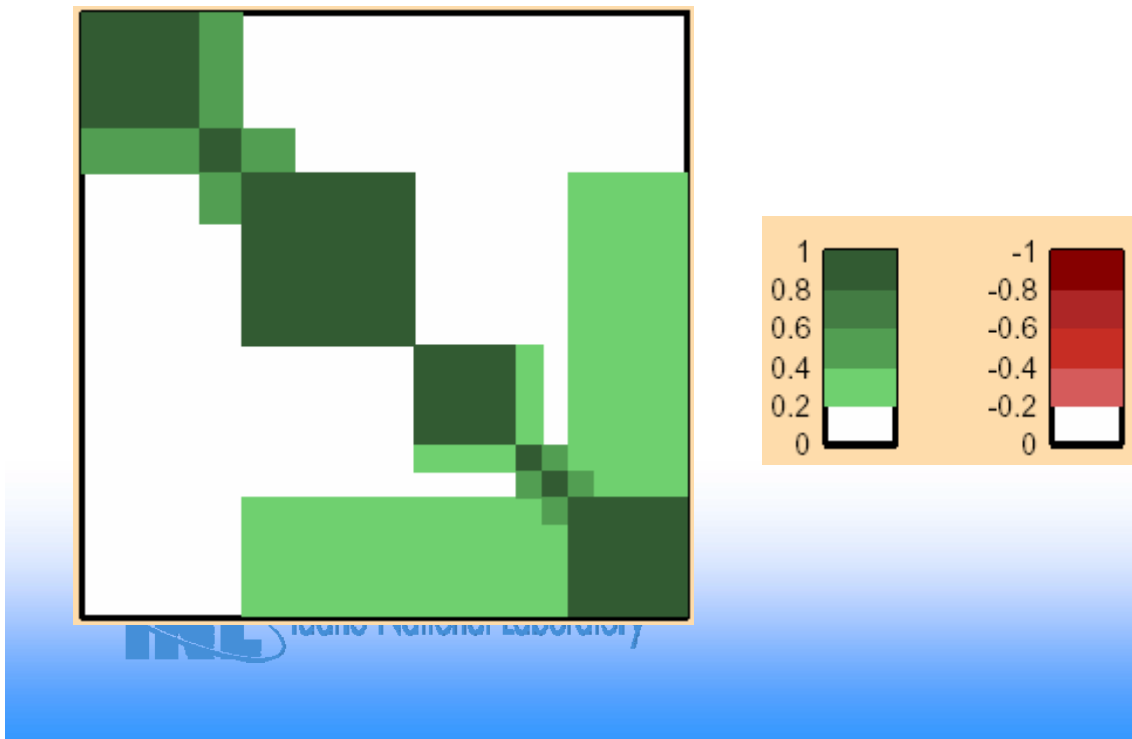


Energy Group	MeV
1	1.50000E+2
2	5.51820E+1
3	1.96403E+1
4	6.06531E+0
5	2.23130E+0
6	1.35335E+0
7	4.97871E-1
8	1.83156E-1
9	6.73795E-2
10	2.47875E-2
11	9.11882E-3
12	2.03468E-3
13	4.53999E-4
14	2.26033E-5
15	4.00000E-6
16	5.40000E-7
17	1.00000E-7

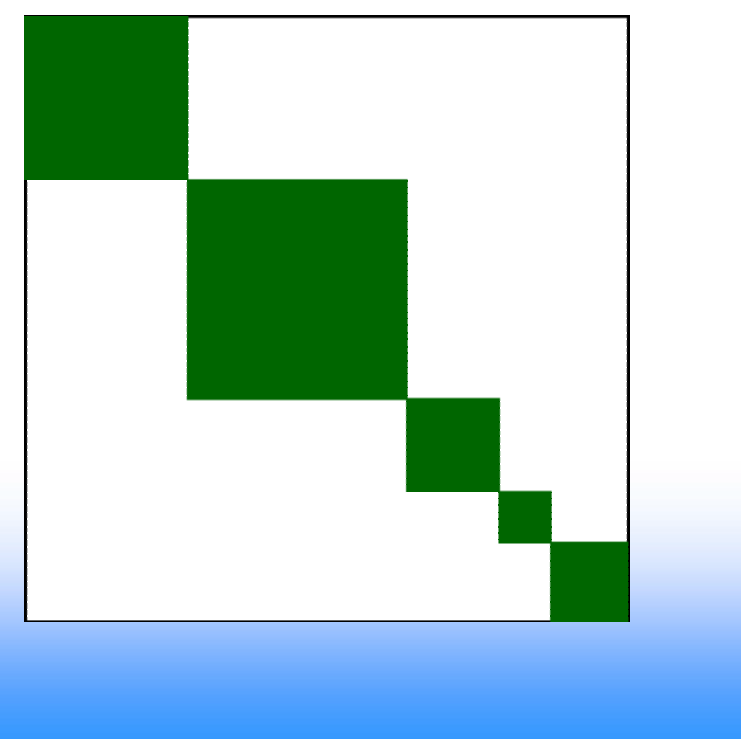
Pu239(n,f)



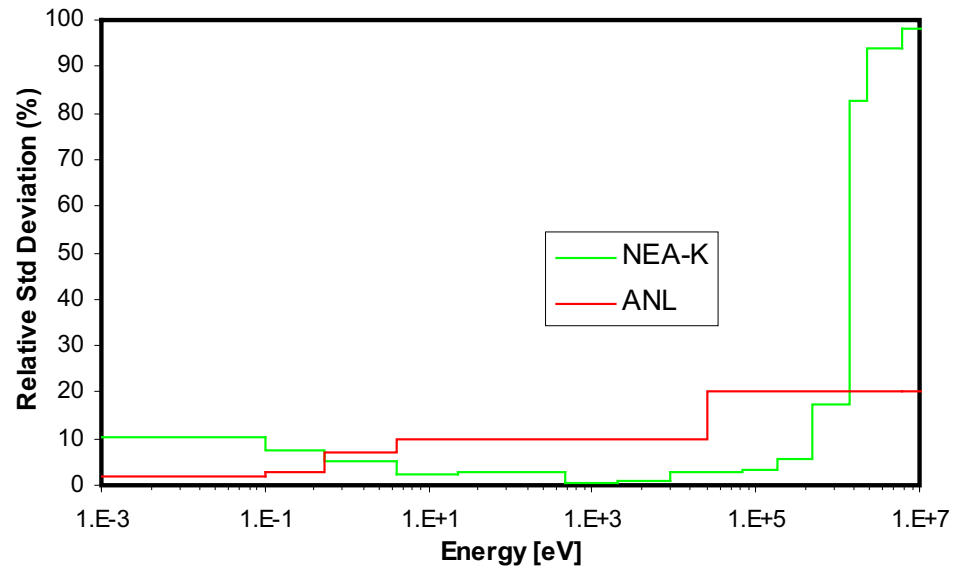
NEA-K Corr. Matrix



ANL Corr. Matrix

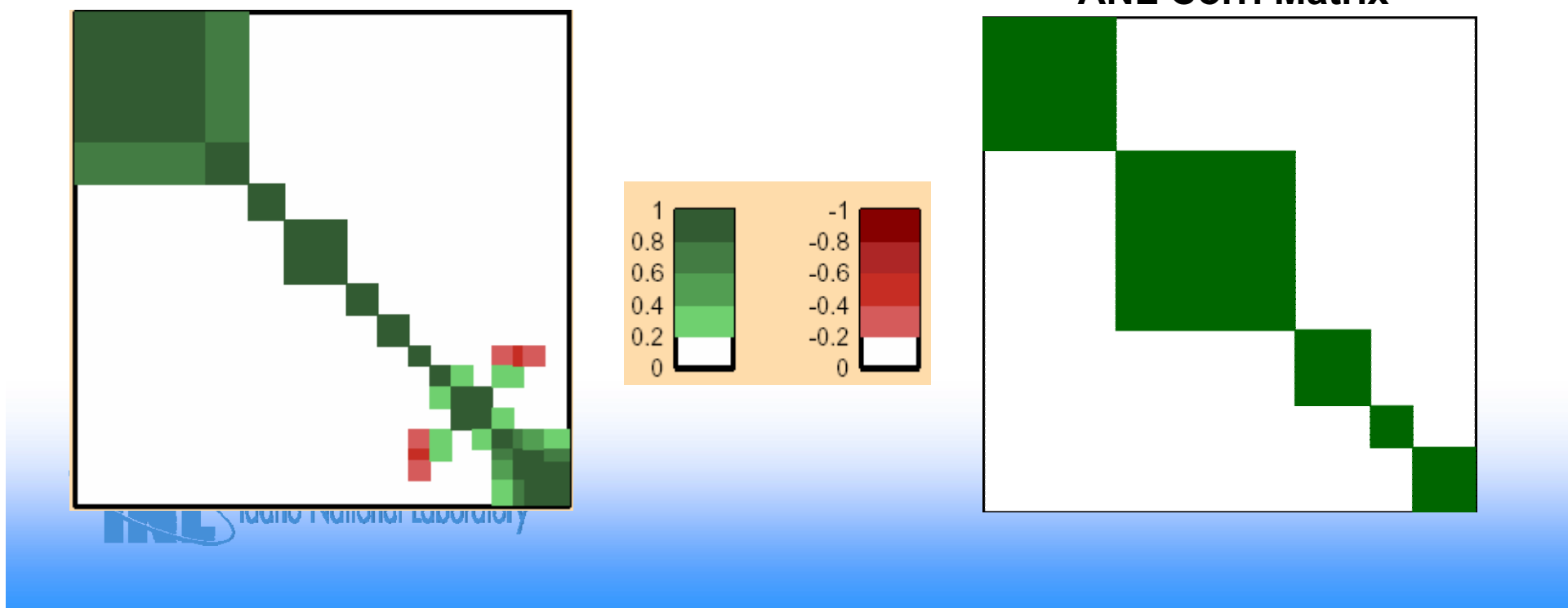


Pu240(n,γ)

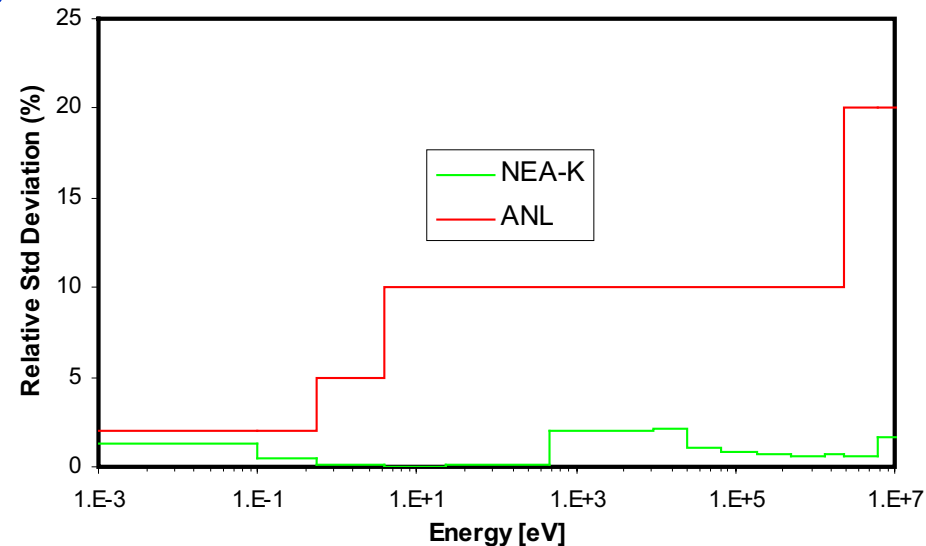


NEA-K Corr. Matrix

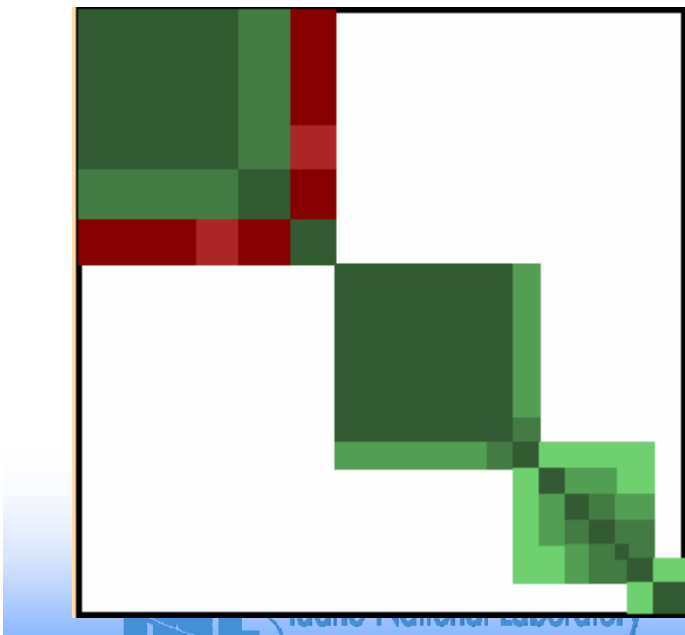
ANL Corr. Matrix



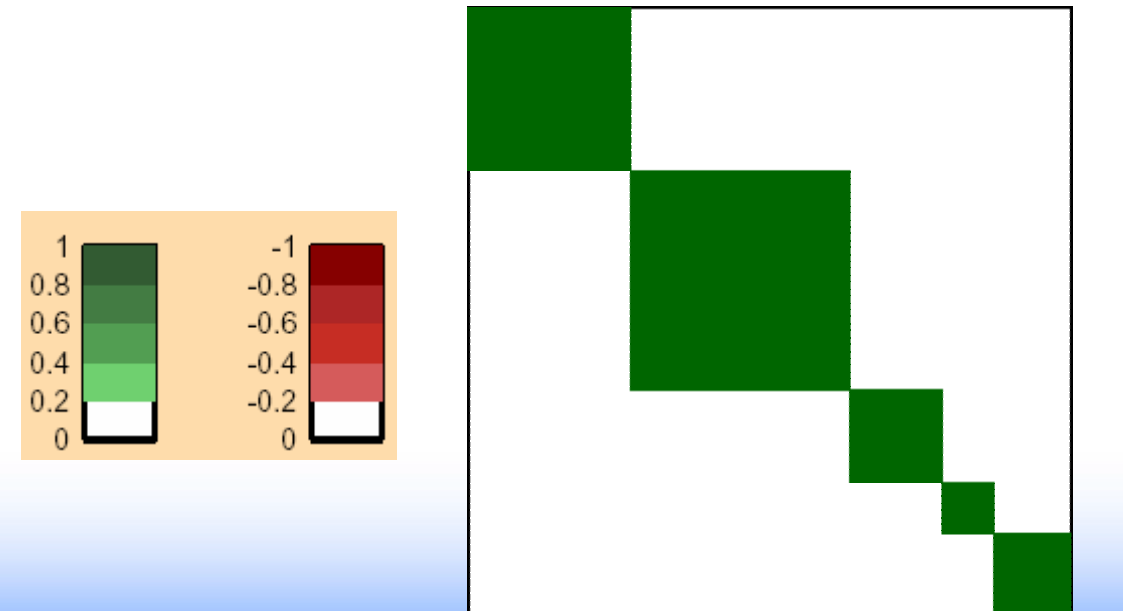
Pu-241(n,f)



NEA-K Corr. Matrix



ANL Corr. Matrix



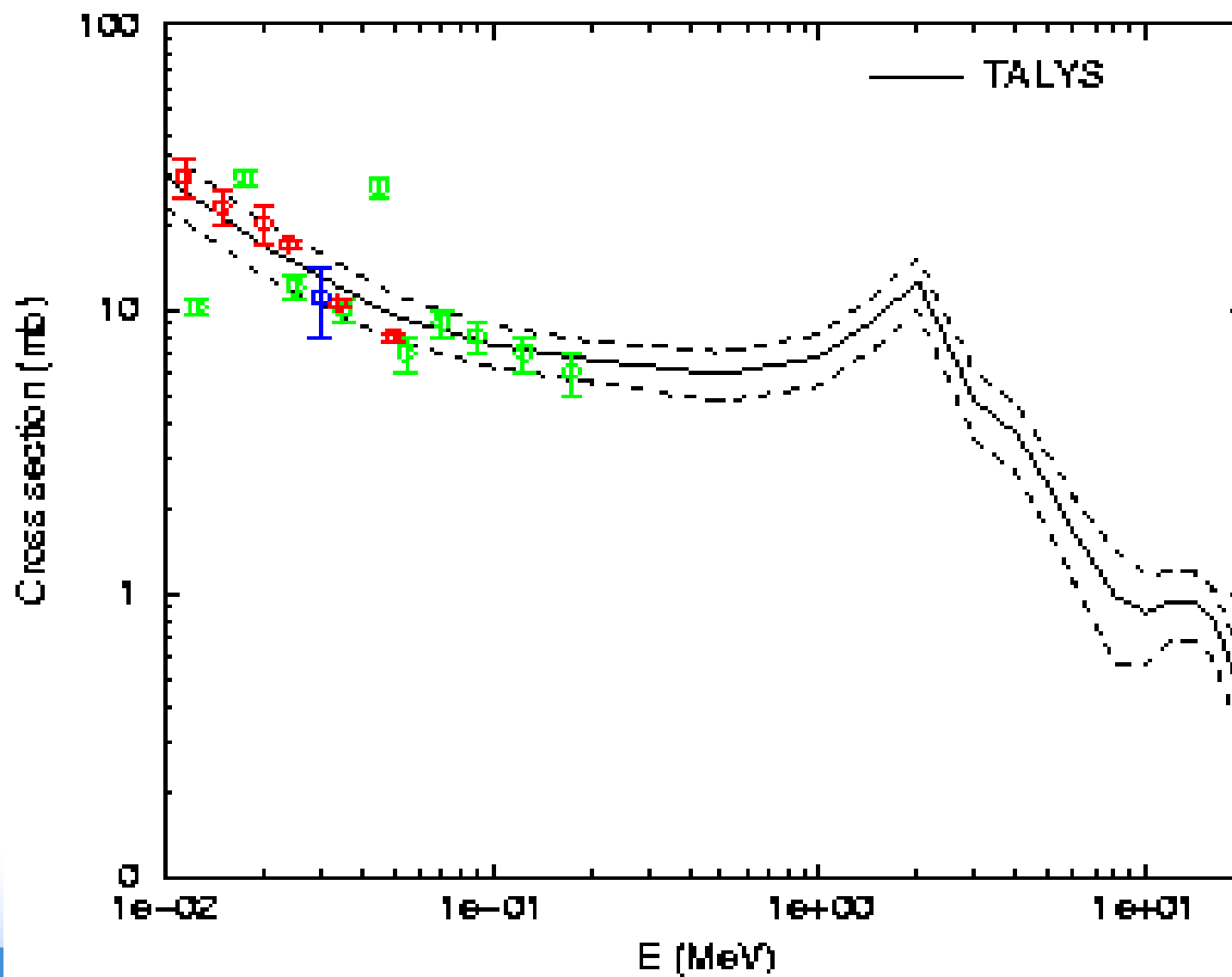
However, nuclear physicists can provide much better, scientifically based, covariance data:

- **Needed: Systematical approach to provide covariance data with evaluated nuclear data files.**
- **Close interplay between experiments and nuclear models needed.**
- A powerful approach : Propagate model parameter uncertainties to cross section uncertainties with Monte Carlo
- **Random sampling of model parameters**
- **Full covariance file produced.**
- **Requirement 1: Parameter uncertainties and correlations should be physical**
- **Requirement 2: Produced uncertainties and correlations need to be credible, when compared with experimental covariances.**



And here an example of recent results.....
Idaho National Laboratory

$^{90}\text{Zr}(\text{n},\gamma)$



BOLNA Covariance Matrix

Preliminary cross section covariances have been developed for a NEA- WPEC Subgroup at **BNL** for 45 out of 52 requested materials:

- **36 isotopes** (^{16}O , ^{19}F , ^{23}Na , ^{27}Al , ^{28}Si , ^{52}Cr , $^{56;57}\text{Fe}$, ^{58}Ni , $^{90;91;92;94}\text{Zr}$, $^{166;167;168;170}\text{Er}$, $^{206;207;208}\text{Pb}$, ^{209}Bi , $^{233;234;236}\text{U}$, ^{237}Np , $^{238;240;241;242}\text{Pu}$, $^{241;242m;243}\text{Am}$, $^{242;243;244;245}\text{Cm}$) were evaluated using the **BNL-LANL** methodology, based on the ENDF/B-VII.0 library, the Atlas of Neutron resonances, the nuclear model code **EMPIRE** and the Bayesian code Kalman
- **6 isotopes** ($^{155; 156; 157; 158; 160}\text{Gd}$ and ^{232}Th) were taken from ENDF/BVII.0; and
- **3 isotopes** (^1H , ^{238}U and ^{239}Pu) were taken from JENDL-3.3.

LANL has evaluated the covariance matrices for U235, U238 and Pu239, in the fast energy region

To complete these data, at **ORNL** resonance-parameter covariance evaluations were done for ^{235}U , ^{238}U , and ^{239}Pu with the computer code **SAMMY**

Finally, covariance data files for Pb isotopes have been produced at **NRG** by a purely stochastic approach



BOLNA Covariance Matrix

All the available **BNL** data have been used:

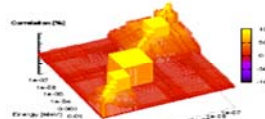
Preliminary Cross Section and ν -bar
Covariances for WPEC Subgroup 26

by

D. Rochman, M. Herman, P. Obložinský
and S. F. Mughabghab

January 2007

Report prepared for WPEC Subgroup 26
"Nuclear Data Needs for Advanced Reactor Systems"
Proposed by P.J. Finck, coordinated by M. Salvatores



National Nuclear Data Center
BNL Report: BNL-77407-2007-IR

- except the U-235, U-238 and Pu-239 data, which have been taken from the combined **LANL/ORNL** evaluation,
- and the Pb isotope data, taken from the **NRG** evaluation.
- Missing data have been taken from the **ANL** estimated covariance data

Energy correlations have been used, but practically no reaction cross-correlations



BOLNA Diagonal Values

Gr	E [MeV]	U235						U238					
		ν	σ_f	σ_{inel}	σ_{el}	σ_{capt}	$\sigma_{n,2n}$	ν	σ_f	σ_{inel}	σ_{el}	σ_{capt}	$\sigma_{n,2n}$
1	19.6	0.89	0.5	21.73	9.6	61.13	20.35	1.26	0.57	29.28	13.3	21.41	5.32
2	6.07	0.69	0.47	6.79	4.15	36.99	8.86	1.17	0.55	19.75	14.5	13.5	0
3	2.23	0.56	0.48	6.41	4.54	19.14	0	1.34	0.6	20.58	18.7	6.05	0
4	1.35	0.55	0.46	7.55	3.56	16.1	0	1.3	2.91	11.56	5.35	2.27	0
5	4.98e-1	0.61	0.5	11.32	2.87	22.13	0	2	5.26	4.19	1.92	1.41	0
6	1.83e-1	0.66	0.53	15.01	2.38	30.64	0	2	5.14	10.96	2.12	1.67	0
7	6.74e-2	0.66	0.5	14.72	2.63	32.89	0	2	5.14	11.12	3.76	1.64	0
8	2.48e-2	0.66	0.58	50	3.24	34.03	0	2	50.31	0	1.52	9.43	0
9	9.12e-3	0.66	3.18	48.48	5.16	33.92	0	2	214.62	0	0.67	3.11	0
10	2.03e-3	0.66	0.77	0	2.07	4.56	0	2	9.69	0	0.72	2.1	0
11	4.54e-4	0.66	0.44	0	1.33	0.63	0	2	2.38	0	2.39	1.71	0
12	2.26e-5	0.69	0.62	0	1.52	0.65	0	2	5.82	0	5.97	1.03	0
13	4.00e-6	0.69	0.4	0	1.78	1.36	0	2	51.89	0	0.82	2.45	0
14	5.40e-7	0.71	0.3	0	3.42	1.55	0	2	55.19	0	0.92	1.66	0
15	1.00e-7	0.71	0.25	0	4.9	1.73	0	2	55.42	0	0.94	1.64	0

BOLNA Diagonal Values

		Np237						Pu239					
Gr	E [MeV]	v	σ_f	σ_{inel}	σ_{el}	σ_{capt}	$\sigma_{n,2n}$	v	σ_f	σ_{inel}	σ_{el}	σ_{capt}	$\sigma_{n,2n}$
1	19.6	1.94	5.58	42.85	2.39	41.47	9.51	0.5	0.63	23.06	6.94	37.08	8.53
2	6.07	2.19	7.9	6.54	3.7	36.48	0	0.17	0.69	22.18	9.36	37.8	4.34
3	2.23	1.47	7.63	22.35	4.12	17.62	0	0.17	0.89	19	10.3	26.56	0
4	1.35	0.66	5.82	28.6	3.62	10.34	0	0.12	0.64	29.01	10.29	18.18	0
5	4.98e-1	0.6	5.79	44.99	3.47	5.79	0	0.19	0.68	34.01	5.66	11.55	0
6	1.83e-1	0.6	5.79	54.97	4.07	2.08	0	0.54	0.85	46.06	3.98	9.04	0
7	6.74e-2	0.6	5.79	36.27	4.37	6.66	0	0.58	0.72	40.04	2.37	10.12	0
8	2.48e-2	0.6	5.79	0	4.48	5.25	0	0.58	0.96	28.52	2.16	7.39	0
9	9.12e-3	0.6	5.79	0	3.93	5.25	0	0.65	0.62	8.64	4.04	15.46	0
10	2.03e-3	0.6	5.77	0	2.44	5.54	0	0.2	1.2	0	0.74	1.39	0
11	4.54e-4	0.6	7.54	0	2.41	1.7	0	0.2	1.24	0	1.2	1.25	0
12	2.26e-5	0.6	4.64	0	2.31	0.55	0	0.2	0.47	0	0.24	0.61	0
13	4.00e-6	0.6	5.58	0	2.23	0.7	0	0.2	1.43	0	0.3	1.22	0
14	5.40e-7	0.6	14.74	0	2.18	2.41	0	0.2	0.88	0	0.44	1.36	0
15	1.00e-7	0.6	4.55	0	2.03	1.55	0	0.2	1.11	0	0.68	1.6	0

BOLNA Diagonal Values

		Pu240						Pu241					
Gr	E [MeV]	v	σ_f	σ_{inel}	σ_{el}	σ_{capt}	$\sigma_{n,2n}$	v	σ_f	σ_{inel}	σ_{el}	σ_{capt}	$\sigma_{n,2n}$
1	19.6	1.09	9.56	37.11	2.34	52.16	54.09	0.45	24.09	25.15	4.45	55.39	39.68
2	6.07	2.65	4.8	9.65	5.19	32.47	0	0.27	14.16	19.47	3.74	54.1	33.43
3	2.23	2.69	5.65	10.09	5.42	19.74	0	0.27	21.26	18.38	4.39	38.41	0
4	1.35	3.74	5.82	7.79	4.76	16.28	0	0.28	16.62	19.78	5.38	31.66	0
5	4.98e-1	4.81	3.91	9.78	5.53	14.29	0	0.29	13.54	20.92	5.16	20.51	0
6	1.83e-1	4.81	5.7	42.55	5.76	13.79	0	0.29	19.87	30.09	4.69	11.29	0
7	6.74e-2	4.81	7.45	48.58	5.8	11.31	0	0.29	8.74	37.51	3.92	4.43	0
8	2.48e-2	4.81	7.45	0	5.05	10.21	0	0.29	11.29	0	9.14	7.79	0
9	9.12e-3	4.81	8.01	0	2.08	4.35	0	0.29	10.44	0	9.29	7.73	0
10	2.03e-3	4.81	21.62	0	1.26	1.47	0	0.29	12.68	0	10.96	7.74	0
11	4.54e-4	4.81	4.72	0	1.64	1.63	0	0.29	19.38	0	10.87	7.43	0
12	2.26e-5	4.81	8.91	0	3.25	5.5	0	0.29	4.21	0	10.66	8.38	0
13	4.00e-6	4.81	1.22	0	0.48	0.44	0	0.29	26.83	0	11.49	6.37	0
14	5.40e-7	4.81	29.76	0	4.58	3.23	0	0.29	2.94	0	9.91	6.84	0
15	1.00e-7	4.81	48.46	0	5.64	4.79	0	0.29	3.27	0	11.32	3.59	0

BOLNA Diagonal Values

		Am241						Am242m					
Gr	E [MeV]	v	σ_f	σ_{inel}	σ_{el}	σ_{capt}	$\sigma_{n,2n}$	v	σ_f	σ_{inel}	σ_{el}	σ_{capt}	$\sigma_{n,2n}$
1	19.6	1.88	12.74	55.29	3.51	28.83	10.03	10.43	21.37	55.82	8.36	84.91	31.77
2	6.07	1.98	11.67	15.2	3.77	15.38	0	0.91	23.36	17.32	12.05	63.01	37.23
3	2.23	1.91	9.81	29.63	5.12	9.16	0	0.66	19.7	23.84	11.15	43.35	0
4	1.35	0.98	8.25	24.45	4.52	6.9	0	0.68	16.51	26.47	12.06	39.41	0
5	4.98e-1	1	8.29	23.03	5.5	5.29	0	0.7	16.57	27.1	13.66	29	0
6	1.83e-1	1	8.29	48.53	5.2	6.79	0	0.7	16.57	33.65	13.91	19.39	0
7	6.74e-2	1	7.39	51.78	4.81	7.96	0	0.7	14.43	31.15	12.76	18.01	0
8	2.48e-2	1	13.71	0	11.54	6.85	0	0.7	11.8	50	18.89	19.17	0
9	9.12e-3	1	13.51	0	12.35	6.66	0	0.7	12.36	0	19.36	20.23	0
10	2.03e-3	1	13.41	0	9.7	6.59	0	0.7	12.2	0	19.42	20.08	0
11	4.54e-4	1	8.08	0	14.53	3.67	0	0.7	10.39	0	16.68	11.39	0
12	2.26e-5	1	5.15	0	14.03	1.82	0	0.7	10.38	0	19.95	13.25	0
13	4.00e-6	1	6.72	0	14.2	5.54	0	0.7	7	0	20.61	13.57	0
14	5.40e-7	1	8.93	0	13.81	1.26	0	0.7	8.83	0	17.64	19.87	0
15	1.00e-7	1	3.02	0	13.03	1.8	0	0.7	8.06	0	21.78	19.6	0

BOLNA Diagonal Values

Am243								Cm244							
Gr	E [MeV]	v	σ_f	σ_{inel}	σ_{el}	σ_{capt}	$\sigma_{n,2n}$	v	σ_f	σ_{inel}	σ_{el}	σ_{capt}	$\sigma_{n,2n}$		
1	19.6	1.88	14.44	61.97	7.51	60.42	26.63	10.55	17.86	38.26	10.5	89.19	40.91		
2	6.07	1.98	11.03	17.87	4.64	41.5	0	11.08	31.25	22.67	10.2	53.78	0		
3	2.23	1.91	5.97	35.3	7.49	21.66	0	10.68	43.8	15.1	5.56	36.49	0		
4	1.35	1.09	9.18	42.15	4.11	14.18	0	5.5	50.01	18.18	10.7	20.8	0		
5	4.98e-1	1.2	9.62	40.98	5.9	8.92	0	5.6	36.53	29.09	9.33	22.54	0		
6	1.83e-1	1.2	9.62	79.53	7.84	6.6	0	5.6	47.56	63.31	8.38	17.71	0		
7	6.74e-2	1.2	7.12	80.77	4.41	4.57	0	5.6	26.26	59.72	9.21	17.43	0		
8	2.48e-2	1.2	13.79	0	9.13	6.77	0	5.6	19.03	0	14.9	19.32	0		
9	9.12e-3	1.2	13.54	0	9.6	6.64	0	5.6	11.92	0	14.0	12.14	0		
10	2.03e-3	1.2	13.41	0	7.68	6.58	0	5.6	5.27	0	7.72	4.47	0		
11	4.54e-4	1.2	9.64	0	8.96	2.31	0	5.6	5.7	0	3.61	4.6	0		
12	2.26e-5	1.2	5.95	0	8.22	1.74	0	5.6	17.09	0	7.75	6.64	0		
13	4.00e-6	1.2	4.81	0	7	3.43	0	5.6	21.99	0	6.62	11.79	0		
14	5.40e-7	1.2	2.25	0	12.4	3.75	0	5.6	26.4	0	6.16	12.16	0		
15	1.00e-7	1.2	2.12	0	11.4	3.58	0	5.6	27.18	0	6.12	12.51	0		

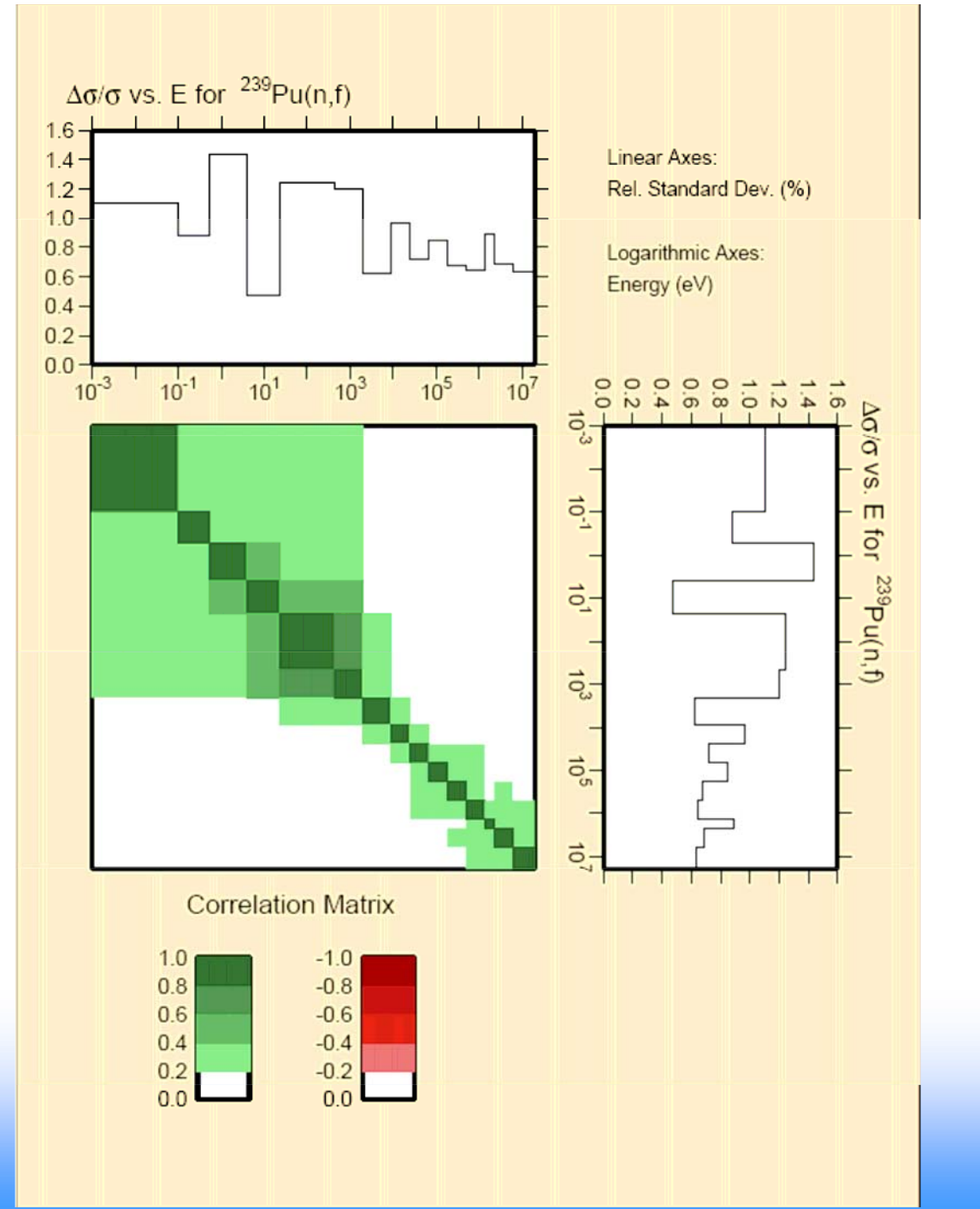
BOLNA Diagonal Values

		Pb207				Bi				Fe56				Zr90			
Gr	E [MeV]	σ_{inel}	σ_{el}	σ_{capt}	$\sigma_{n,2n}$												
1	19.6	17.01	4	61.28	5.69	5.25	0.83	47.58	9.39	12.97	4.61	46.24	7.05	11.32	0.44	46.36	6.74
2	6.07	4.98	5.81	24.25	0	2.44	1.02	27.74	0	7.23	8.14	31.69	0	17.96	0.92	18.59	0
3	2.23	13.77	4.43	21.56	0	34.07	2.06	17.56	0	25.4	5.89	23.48	0	18.52	3.96	9.14	0
4	1.35	11.31	4.78	19.46	0	41.77	4.59	11.35	0	16.12	0.64	7.43	0	50	3.39	6.26	0
5	4.98e-1	0	2.44	16.41	0	0	2.22	8.32	0	0	1.71	4.02	0	0	2.77	5.16	0
6	1.83e-1	0	3.73	15.94	0	0	1.8	8.79	0	0	2.08	10.77	0	0	2.02	3.13	0
7	6.74e-2	0	6.35	15.96	0	0	1.88	6.05	0	0	2.05	13.19	0	0	3.09	5.2	0
8	2.48e-2	0	8.85	15.05	0	0	2.41	3.85	0	0	4.6	8.81	0	0	4.43	7.89	0
9	9.12e-3	0	12	14.27	0	0	1.82	0.71	0	0	3.98	8.56	0	0	5.93	6.96	0
10	2.03e-3	0	16.6	20.01	0	0	1.93	0.43	0	0	4.16	11.23	0	0	6.83	10.55	0
11	4.54e-4	0	10.69	8.6	0	0	1.85	1.47	0	0	4.28	11.25	0	0	6.73	5.95	0
12	2.26e-5	0	0	0	0	0	1.82	1.82	0	0	4.31	11.25	0	0	6.7	2.75	0
13	4.00e-6	0	0	0	0	0	1.8	1.86	0	0	4.31	11.25	0	0	6.7	2.56	0
14	5.40e-7	0	0	0	0	0	1.8	1.87	0	0	4.31	11.25	0	0	6.7	2.53	0

BOLNA Diagonal Values

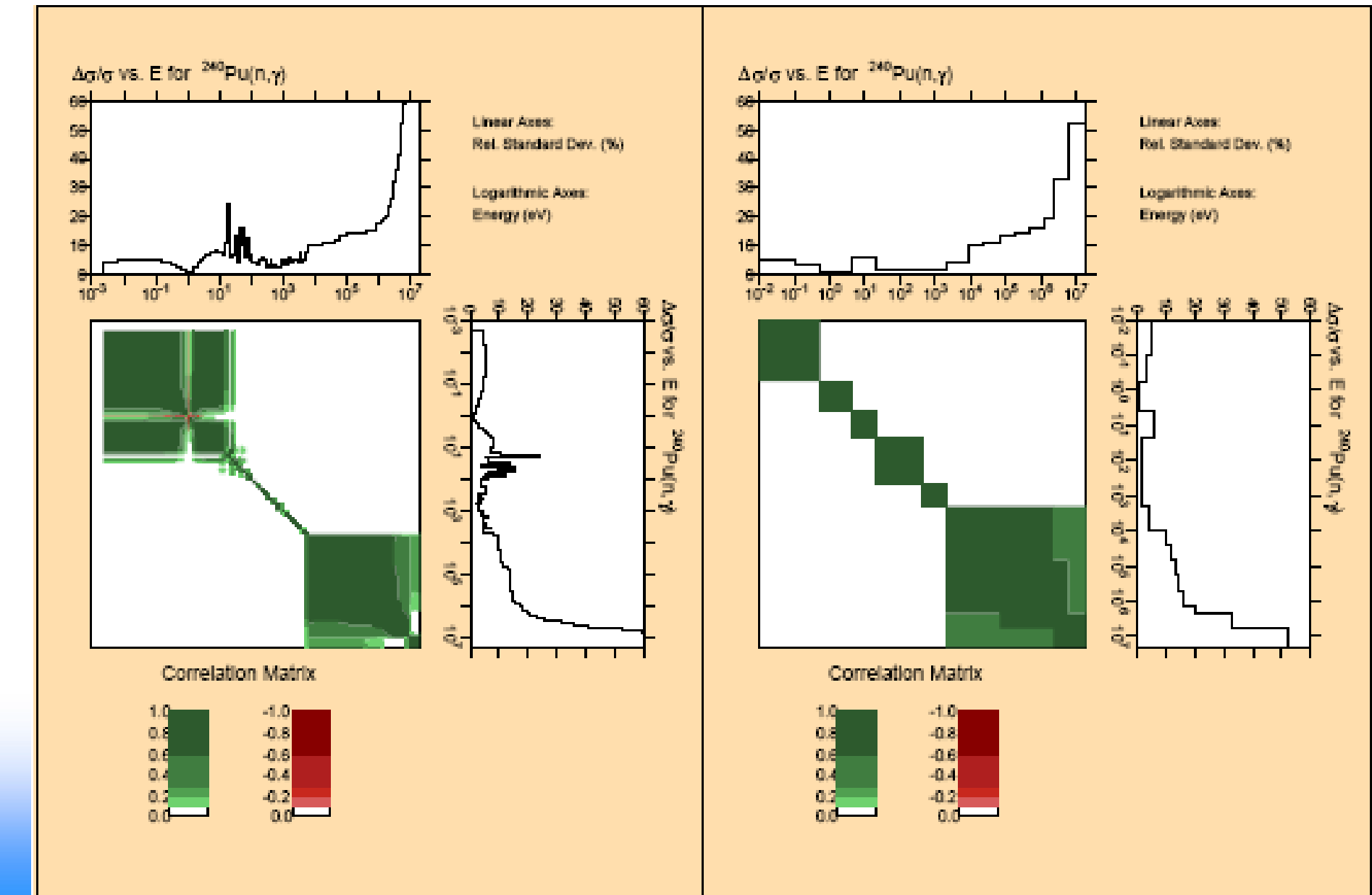
Si					O					Na				
Gr	E [MeV]	σ_{inel}	σ_{el}	σ_{capt}	$\sigma_{n,2n}$	σ_{inel}	σ_{el}	σ_{capt}	$\sigma_{n,2n}$	σ_{inel}	σ_{el}	σ_{capt}	$\sigma_{n,2n}$	
1	19.6	21.38	0.69	52.87	50	100	84.6	100	100	18.79	1.8	46.44	11.07	
2	6.07	13.54	2.77	11.12	0	0	54.9	100	0	8.87	4.62	24.33	0	
3	2.23	50	1.66	10.07	0	0	12.1	100	0	12.56	3.72	1.7	0	
4	1.35	0	1.43	6.77	0	0	1.43	100	0	28	3.01	7.44	0	
5	4.98e-1	0	1.08	3.86	0	0	1.68	81.81	0	50	3.31	6.81	0	
6	1.83e-1	0	2.97	5.65	0	0	1.68	69.63	0	0	3.25	23.59	0	
7	6.74e-2	0	4.3	11.19	0	0	2.36	47.27	0	0	2.38	6.79	0	
8	2.48e-2	0	4.18	8.93	0	0	2.35	28.21	0	0	2.87	6.63	0	
9	9.12e-3	0	3.62	8.71	0	0	2.24	12.1	0	0	3.23	1.18	0	
10	2.03e-3	0	3.23	5.12	0	0	2.23	9.36	0	0	4.93	2.28	0	
11	4.54e-4	0	3.03	3.57	0	0	2.22	10.42	0	0	4.76	2.3	0	
12	2.26e-5	0	2.97	3.25	0	0	2.22	11.29	0	0	4.73	2.29	0	
13	4.00e-6	0	2.97	3.23	0	0	2.23	10.62	0	0	4.71	2.29	0	
14	5.40e-7	0	2.97	3.22	0	0	2.23	11.03	0	0	4.7	2.29	0	
15	1.00e-7	0	2.9	2.96	0	0	2	8	0	0	4.59	2.07	0	

15 Groups BOLNA Covariance Matrix for the Pu239 (n,f)

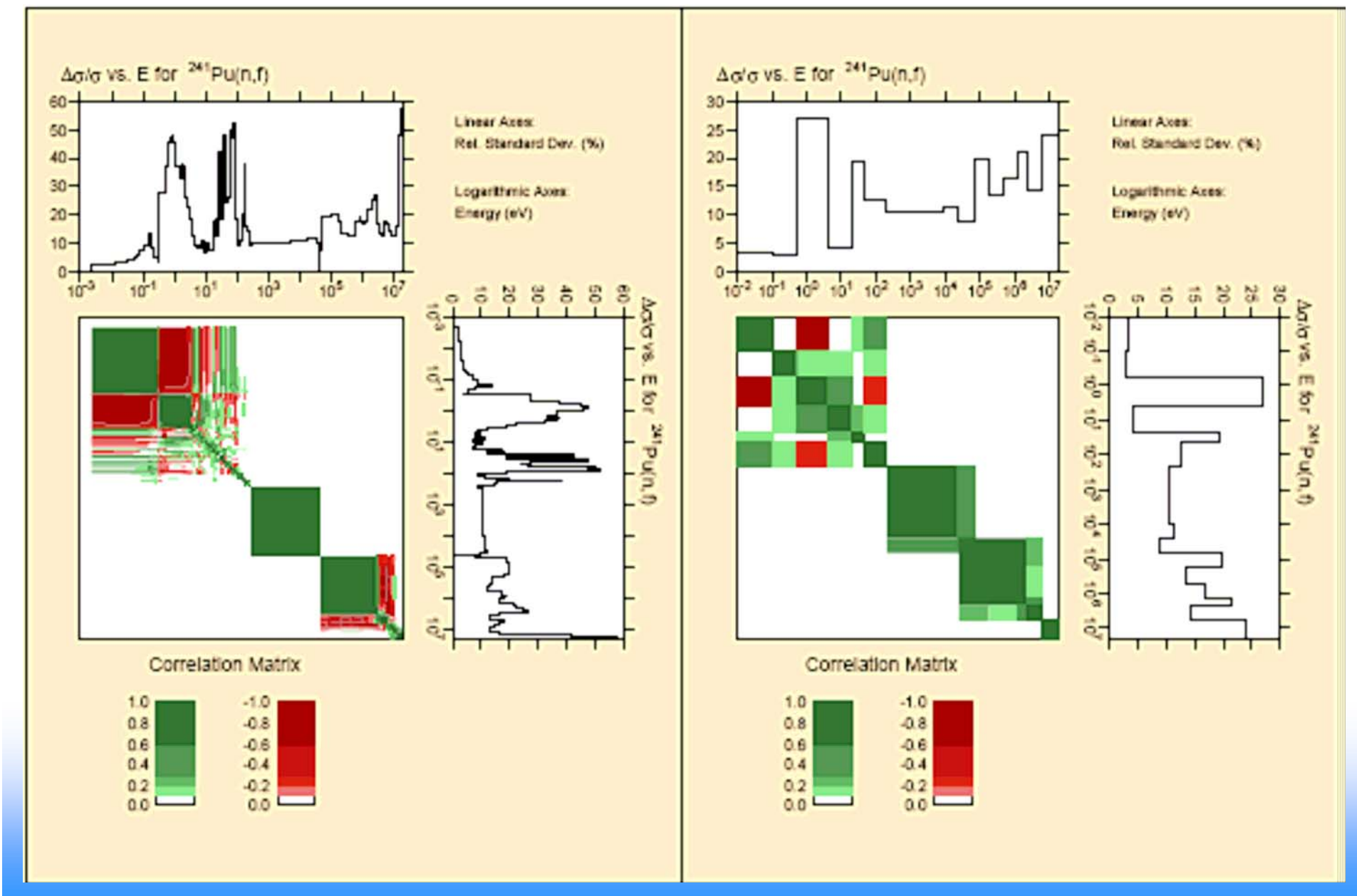


Idaho National Laboratory

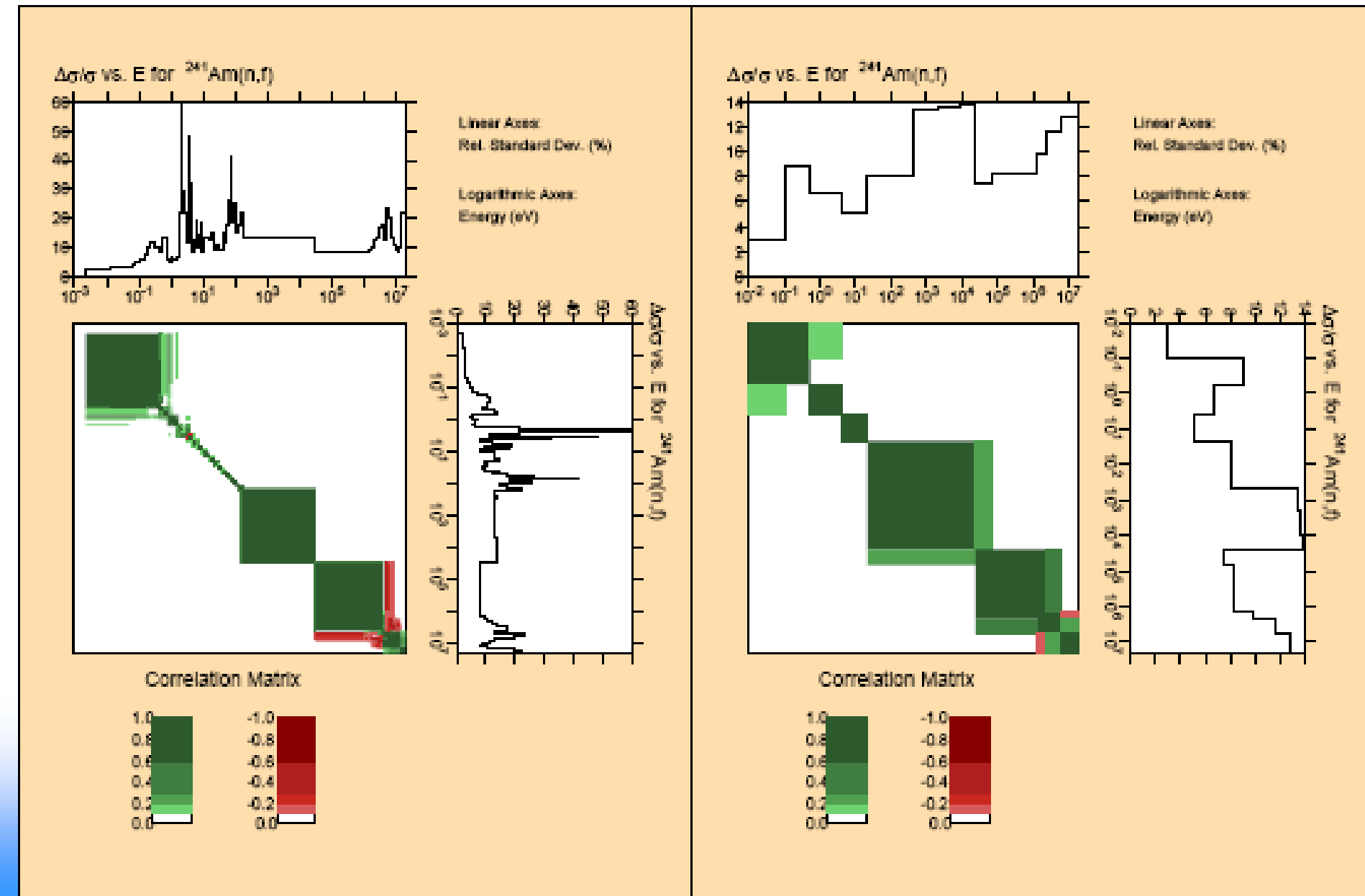
BOLNA Covariance Matrix in 187 (Left) and 15 (Right) Groups for the Pu-240(n, γ) Reaction



BOLNA Covariance Matrix in 187 (Left) and 15 (Right) Groups for the Pu-241(n,f) Reaction

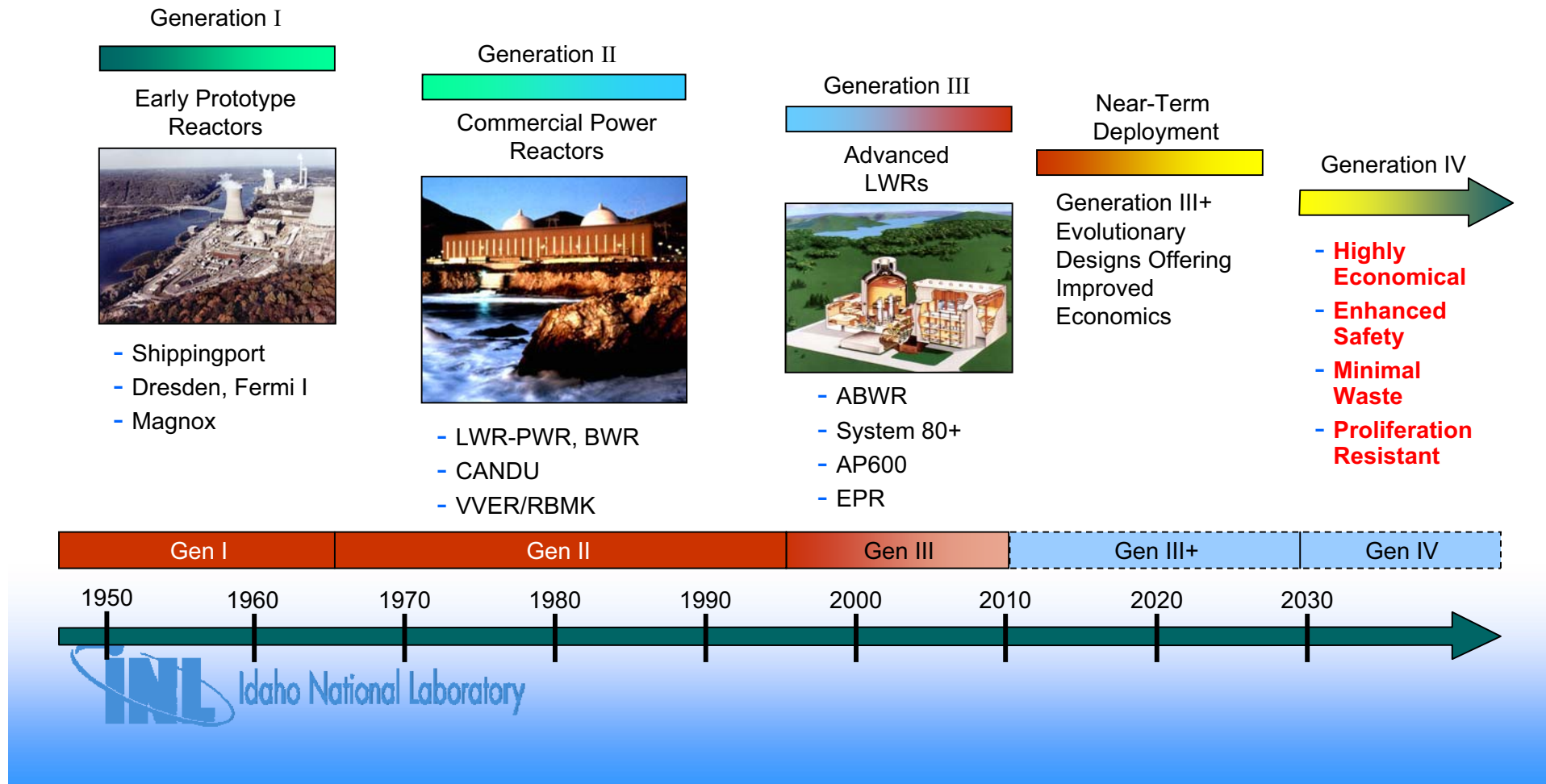


BOLNA Covariance Matrix in 187 (Left) and 15 (Right) Groups for the Am-241(n,f) Reaction



Sensitivity and uncertainty analysis: the case of GENERATION IV and Innovative Fuel Cycles

Nuclear energy systems deployable no later than 2030 in both developed and developing countries, for generation of electricity and other energy products



The Role of Nuclear Data and impact of uncertainties in Developing Future Generation Nuclear Energy

Some examples related to:

- Extended Burnups for LWR's
- Very High Temperature Reactors
- Fast Reactors: GFR, SFR, LFR
- Fuel Cycle Performance
- Accelerator Driven Systems



Idaho National Laboratory

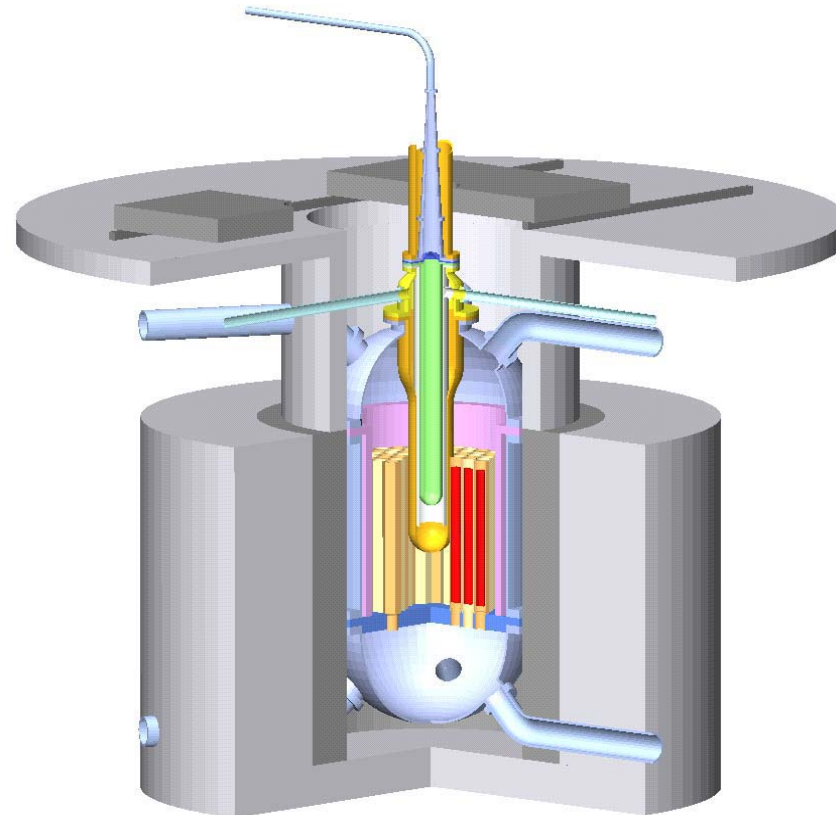
Features of the Investigated Fast Systems

System	Coolant	Fuel Type	TRU/(U+TRU)	MA/(U+TRU)	Power [MW _{th}]
ABTR	Na	Metal	0.162	~ 0	250
SFR	Na	Metal	0.605	0.106	840
EFR	Na	MOX	0.237	0.012	3600
GFR	He	Carbide	0.217	0.050	2400
LFR	Pb	Metal	0.233	0.024	900
ADS	LBE	Nitride	1.000	0.680	380



Idaho National Laboratory

Uncertainty Evaluation and Target Accuracy Requirements for an Accelerator Driven System



An alternative burner
Fuel is fertile free



Idaho National Laboratory

ISSUES

- *Nuclear data uncertainties and their impact on a very wide range of ADS integral parameters have been assessed in order to consolidate preliminary design studies.*
- *The availability of very general tools for sensitivity and uncertainty analysis together with new variance-covariance matrix data, produced in a joint effort under the auspices of the OECD-NEA makes that endeavor particularly significant.*
- *We discuss major results of interest for a fast neutron ADS, (loaded with a Minor Actinide dominated fuel and potentially U-free) and point out the most important fields and data types, where priority improvements are required.*



Idaho National Laboratory

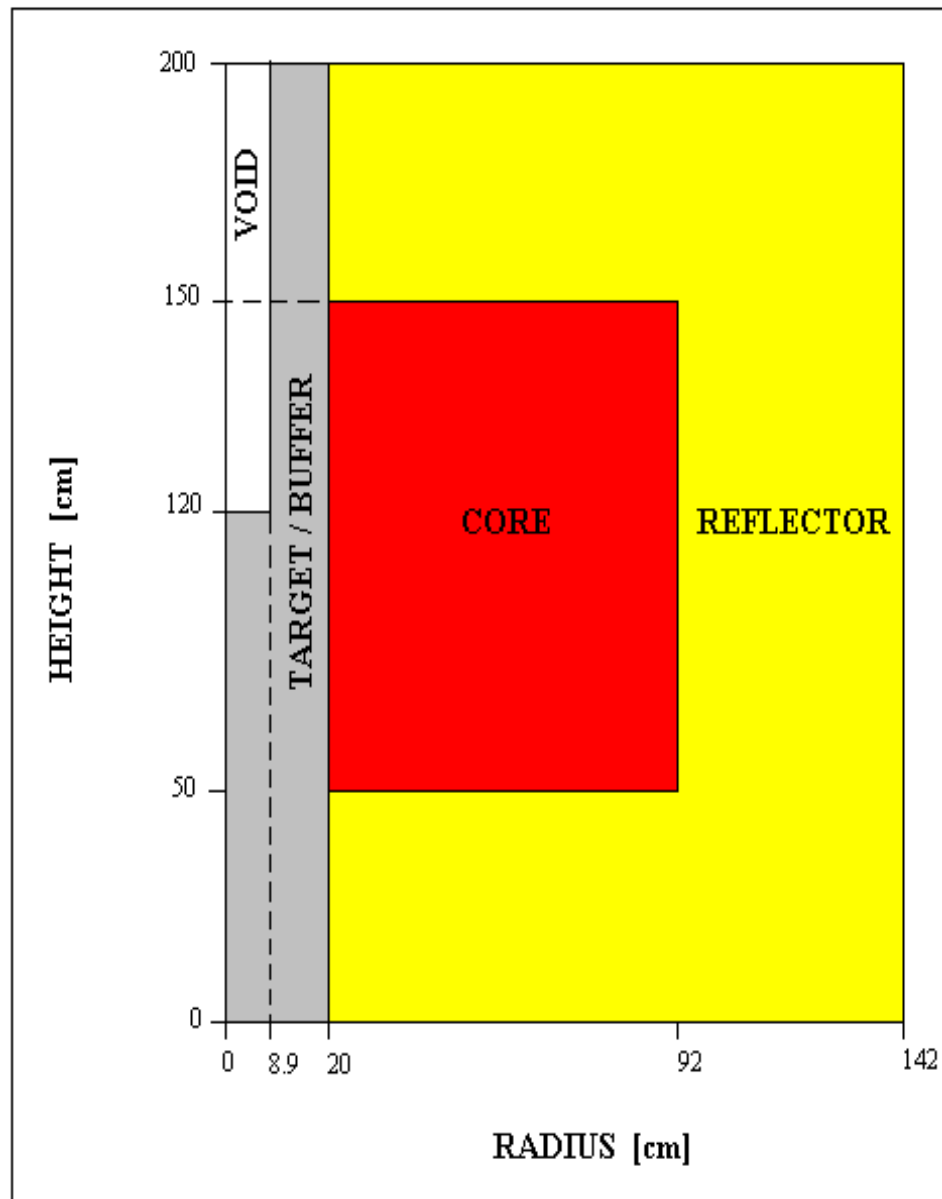
REFERENCE CALCULATIONS

- The chosen ADS system had some general features (e.g., the mass ratio between plutonium and MA, the americium-to-curium ratio, etc.) that are representative of the class of MA transmutes with a fast neutron spectrum and a uranium-free fuel.
- The target and the coolant material of the core are the Pb-Bi eutectic.
- This model is very close to the sub-critical core, which has been analyzed in the framework of an international OECD-NEA benchmark



Idaho National Laboratory

ADS System Geometry and Fuel Composition



Fuel			
Isotope	Compositions [10^{24} at./cm 3]	Isotope	Compositions [10^{24} at./cm 3]
Np237	4.377E-04	Fe58	4.386E-05
Pu238	4.226E-05	Cr50	1.128E-04
Pu239	5.051E-04	Cr52	2.096E-03
Pu240	2.321E-04	Cr53	2.328E-04
Pu241	1.232E-04	Cr54	5.682E-05
Pu242	9.102E-05	Ni58	6.451E-05
Am241	8.084E-04	Ni60	2.384E-05
Am242m	1.089E-05	Ni61	1.015E-06
Am243	5.827E-04	Ni62	3.173E-06
Cm242	4.079E-08	Ni64	7.792E-07
Cm243	3.326E-06	Mo	1.163E-04
Cm244	2.371E-04	Mn	1.114E-04
Cm245	3.164E-05	Pb	6.360E-03
Cm246	5.355E-07	Bi	7.865E-03
Zr	7.477E-03	W182	6.984E-06
N15	1.058E-02	W183	3.770E-06
Fe54	9.759E-04	W184	8.045E-06
Fe56	1.488E-02	W186	7.439E-06
Fe57	3.507E-04		



Idaho National Laboratory

Sensitivity coefficients (in a 17 energy group structure) have been calculated with the CEA ERANOS code system for all the ADS parameters potentially most sensitive to nuclear data uncertainties:

- Multiplication factor,
- Power peak,
- Burn-up $\Delta k/k$,
- Coolant void reactivity coefficient,
- Doppler reactivity coefficient,
- Nuclide density at end of cycle (transmutation potential),
- Ratio φ^* of the average external source importance to average fission neutron importance,
- Max dpa, Max He and Max H production and
- Maximum value of the ratio (He production)/dpa

SELECTED RESULTS

	k_{eff}	Peak Power	Void reactivity	Burnup reactivity
Pu238	0.25	1.8	0.5	40.9
Pu239	0.20	1.5	0.8	5.4
Pu240	0.23	1.7	0.5	2.3
Pu241	1.05	7.6	2.0	21.4
Pu242	0.17	1.2	0.5	3.1
Np237	0.37	2.7	1.2	2.7
Am241	0.97	7.0	4.1	9.1
Am242m	0.14	1.0	0.3	17.8
Am243	0.63	4.9	2.2	5.8
Cm242	0.0	0.0	0.0	25.7
Cm244	1.9	13.7	3.5	34.1
Cm245	1.05	7.6	1.6	26.7
Fe56	0.93	7.2	5.5	1.1
Pb	0.09	0.5	4.0	0.4
Bi209	0.31	2.2	12.1	0.5
Total	2.94	21.4	15.5	77.5

Uncertainties (%) on ADS Parameters. Breakdown by Isotope Contribution



Idaho National Laboratory

	ϕ^*	(n,p)	(n, α)/DPA
Pu238	0.2	2.0	1.5
Pu239	0.2	1.7	1.3
Pu240	0.1	1.9	1.4
Pu241	0.8	8.6	6.3
Pu242	0.1	1.4	1.0
Np237	0.2	3.0	2.2
Am241	0.5	7.8	5.7
Am242m	0.1	1.2	0.9
Am243	0.4	5.0	4.2
Cm244	0.9	15.8	11.3
Cm245	0.8	8.6	6.3
Fe56	0.3	8.1	6.3
Pb	0.3	2.4	3.4
Bi209	0.9	3.9	4.3
Total	1.9	24.5	18.5

**Uncertainties (%) on ADS High Energy Parameters.
Breakdown by Isotope Contribution**



Idaho National Laboratory

	σ_{capt}	σ_{fiss}	ν	σ_{inel}	Total
Pu238	0.02	0.21	0.13	0.01	0.25
Pu239	0.10	0.12	0.06	0.11	0.20
Pu240	0.08	0.16	0.14	0.03	0.23
Pu241	0.07	1.04	0.04	0.02	1.05
Pu242	0.06	0.15	0.03	0.02	0.17
Np237	0.18	0.29	0.06	0.13	0.37
Am241	0.46	0.83	0.16	0.16	0.97
Am243	0.29	0.35	0.09	0.43	0.63
Cm242	0.00	0.00	0.00	0.00	0.00
Cm243	0.00	0.12	0.01	0.00	0.12
Cm244	0.11	1.90	0.36	0.04	1.94
Cm245	0.01	1.04	0.13	0.01	1.05
Fe56	0.05	0.00	0.00	0.93	0.93
Bi209	0.02	0.00	0.00	0.31	0.31
Total	0.61	2.61	0.47	1.10	2.94



Uncertainties (%) Breakdown by Isotope and Reaction Type

Gr.	Energy	Cm244 σ_{fiss}	Cm245 σ_{fiss}
1	19.6 MeV	0.1	0.0
2	6.07 MeV	0.6	0.2
3	2.23 MeV	0.8	0.2
4	1.35 MeV	1.5	0.5
5	498 keV	0.5	0.5
6	183 keV	0.3	0.6
7	67.4 keV	0.2	0.4
8	24.8 keV	0.0	0.1
9	9.12 keV	0.0	0.1
10	2.03 keV	0.0	0.1
11-15	454 eV-thermal	0.0	0.0
Total		1.9	1.0



**Energy Breakdown of k_{eff} Selected Uncertainties
Components (%)**

	σ_{capt}	σ_{fiss}	ν	Total
Pu238	2.6	30.2	18.3	35.4
Pu241	0.9	10.6	0.3	10.6
Am241	2.8	8.0	1.6	8.8
Am242m	0.6	12.8	1.0	12.9
Am243	1.4	2.7	0.7	5.0
Cm242	1.3	23.0	5.3	23.6
Cm244	2.1	28.5	5.2	29.1
Cm245	0.1	11.9	1.8	12.0
Total	5.2	52.5	20.0	56.6

**Burnup Uncertainties Contributions (%). Breakdown
by Isotope and Reaction Type**



Idaho National Laboratory

	σ_{capt}	σ_{fiss}	σ_{inel}	Total
Pu241	0.6	7.6	0.1	7.6
Np237	1.4	2.1	1.0	2.7
Am241	3.6	5.8	1.2	7.0
Am243	2.3	2.4	3.5	4.9
Cm244	0.9	13.4	0.3	13.7
Cm245	0.1	7.6	0.1	7.6
Fe56	0.4	0.0	7.2	7.2
Bi209	0.2	0.0	2.2	2.2
Total	4.8	18.6	8.6	21.4

Peak Power Uncertainties (%) Breakdown by Isotope and Reaction Type



Idaho National Laboratory

	σ_{capt}	σ_{fiss}	σ_{el}	σ_{inel}	Total
Pu241	0.1	2.0	0.0	0.1	2.0
Am241	2.1	3.3	0.1	0.7	4.1
Am243	1.3	1.6	0.1	0.6	2.2
Cm244	0.5	3.2	0.0	0.2	3.5
Fe56	0.4	0.0	1.0	5.4	5.5
Pb	1.5	0.0	2.8	2.3	4.0
Bi209	0.7	0.0	1.6	12.0	12.1
Total	3.3	5.6	3.5	13.5	15.5

Void Reactivity Uncertainties (%) Breakdown by Isotope and Reaction Type



	σ_{capt}	σ_{fiss}	ν	σ_{inel}	$\sigma_{n,2n}$	Total
Pu241	0.5	6.3	0.2	0.1	0.0	6.3
Np237	1.1	1.7	0.3	0.9	0.0	2.2
Am241	2.8	4.8	0.9	1.1	0.0	5.7
Am243	1.8	2.0	0.5	3.2	0.0	4.2
Cm244	0.7	11.1	2.1	0.3	0.0	11.3
Cm245	0.0	6.2	0.8	0.1	0.0	6.3
Fe56	0.2	0.0	0.0	6.3	0.0	6.3
Pb	0.5	0.0	0.0	3.2	1.2	3.4
Bi209	0.2	0.0	0.0	3.0	3.2	4.3
Total	3.8	15.4	2.8	8.5	3.4	18.6

Max(n,α)/DPA Uncertainties (%) Breakdown by Isotope
and Reaction Type



Idaho National Laboratory

ADS SELECTED RESULTS: SUMMARY

- Pu-241 and some of the higher Pu isotopes contribute to the uncertainties, while the Pu-239 contribution is always very small, in agreement with what was already pointed out in a recent study.
- However, the major contributions are due to MA data and in particular to Cm-244 data uncertainties. Am-241, Am-243, Cm-245 give also some noteworthy contributions.
- The role of fission cross-section uncertainties is remarkable for most parameters. In fact, uncertainties in the fission cross-sections have both an effect on reactivity and an effect in the hardness of the spectrum. This last effect can be seen both on the Power Peak and on the Max He/dpa ratios.
- As for structural materials, Fe-56 and Bi-209 show not negligible effects.
- There is relatively small impact of (n,2n) cross-sections, due to the low values of uncertainty in the present variance-covariance data (~10%)
- Fe-56 inelastic cross-section has a significant impact on the void reactivity coefficient.



Target Accuracy Assessments

- Target accuracy assessments are the inverse problem of the uncertainty evaluation.
- In order to establish priorities and target accuracies on data uncertainty reduction, a formal approach can be adopted by defining target accuracy on design parameter and finding out required accuracy on data.
- The unknown uncertainty data requirements can be obtained by solving a minimization problem where the sensitivity coefficients in conjunction with the existing constraints provide the needed quantities to find the solutions:

$$\sum_i \lambda_i / d_i^2 = \min \quad i = 1 \dots I \quad (48)$$

$$\sum_i S_{ni}^2 d_i^2 < Q_n^T \quad n = 1 \dots N \quad (49)$$

where d_i are the uncertainties to be found, S_{ni} are the sensitivity coefficients for the integral parameter Q_n , Q^T are the target accuracies on the N integral parameters, and λ_i are cost parameters.

In the case of an ADS, any preliminary design should require accuracies of the following order of magnitude:

- multiplication factor: ~1% $\Delta k/k$
- power peak: ~5%
- void reactivity coefficient: ~10%
- reactivity due to burn-up: max uncertainty ~1% $\Delta k/k$

These target accuracies are needed to fix preliminary required performances of the accelerator (e.g. required range of proton current) and to determine the required subcritical level for the safety case.

If these values are introduced as « design target accuracies » in the procedure outlined previously, required target accuracies on the nuclear data can be obtained.

Some selected significant results are shown in the next slide



Isotope	Cross Section	Energy	BOLNA Uncertainty (%)	Required Accuracy (%)
Am241	σ_{cap}	1.35 - 0.498 MeV	6.9	7.5
		498 - 183 keV	5.3	5.5
		183 - 67.4 keV	6.8	5.1
		67.4 - 24.8 keV	8.0	5.9
		24.8 - 9.12 keV	6.8	6.3
		9.12 - 2.03 keV	6.7	6.9
	σ_{fiss}	6.07 - 2.23 MeV	11.7	5.6
		2.23 - 1.35 MeV	9.8	4.6
		1.35 – 0.498 MeV	8.2	3.9
Cm244	σ_{fiss}	6.07 - 2.23 MeV	31.2	10.0
		2.23 - 1.35 MeV	43.8	8.5
		1.35 – 0.498 MeV	50.0	5.0
Cm245	σ_{fiss}	498 - 183 keV	37.2	9.7
		183 - 67.4 keV	47.4	9.6
Fe56	σ_{inel}	1.35 – 0.498 keV	16.1	4.9

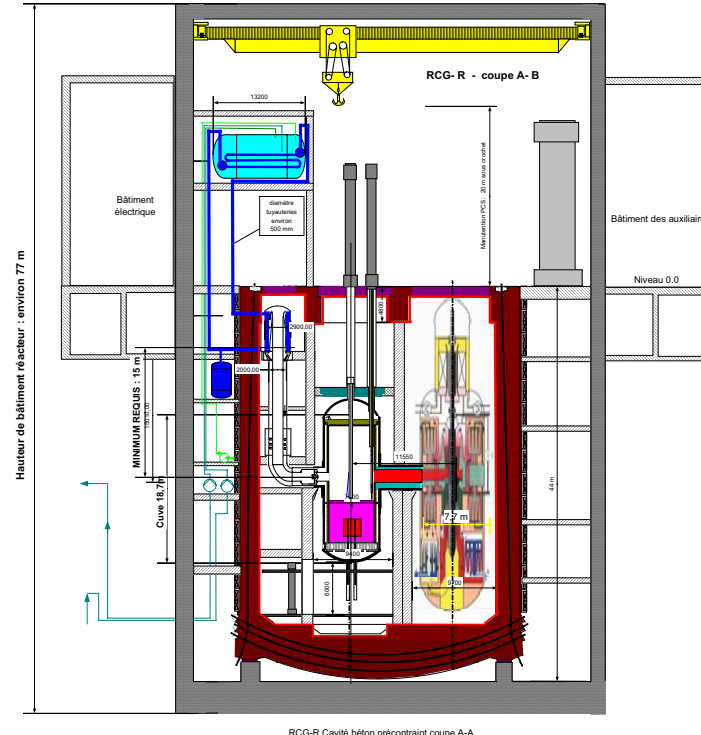


Present and Required Accuracy for Some Specific Data, to Meet Some Preliminary Design Requirements.

ADS Summary of Target Accuracy Requirements

- The required target accuracies on nuclear data can be evaluated in order to meet required target accuracies on integral parameters.
- For example, it is clear that with respect to the present estimated uncertainties, the uncertainty on the fission of Cm-244 should be reduced by an order of magnitude and that the improvement needed on the fission of Am-241 is at least by a factor of two.
- On the contrary, the accuracy announced for the capture of Am-241 looks almost satisfactory.
- Finally, the accuracy required for the inelastic of Fe-56 (~5%), is far from being achieved, and in any case extremely difficult to achieve experimentally.

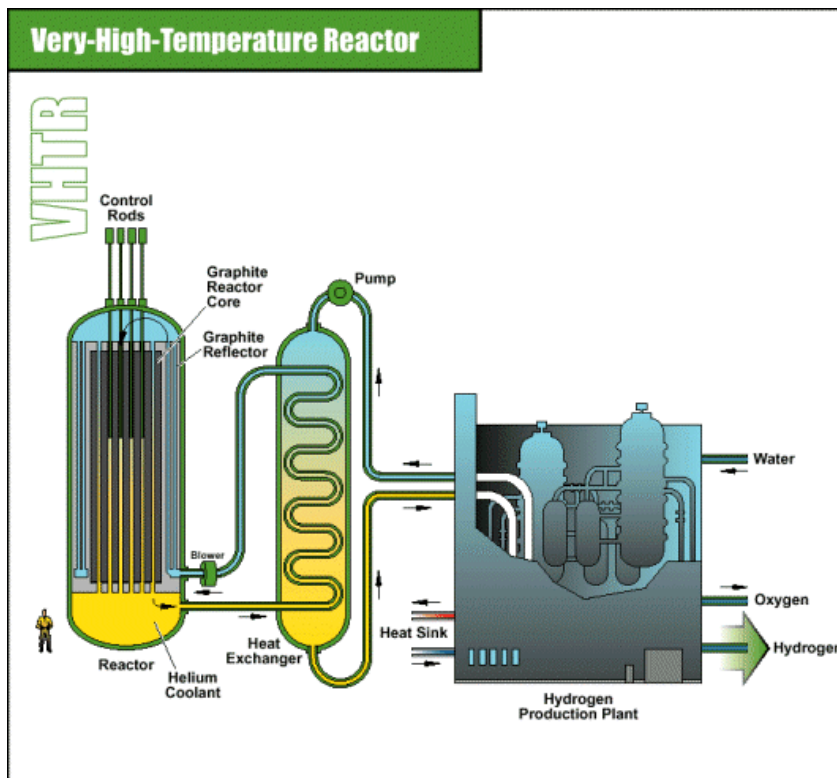
Fast Reactors



Breeder or Burner

**Fuels, structures, and reflectors
might contain new materials
(Zr, Si)**

The Very High Temperature Reactor



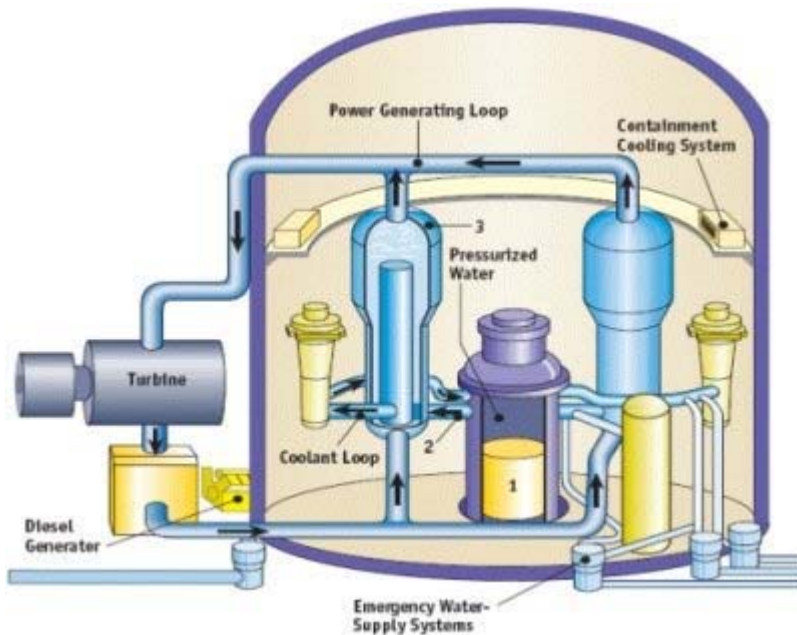
Graphite moderated
U235 enrichment > 10%
Very High Burnup
Very High Thermal Efficiency
High Outlet Temperature



Idaho National Laboratory

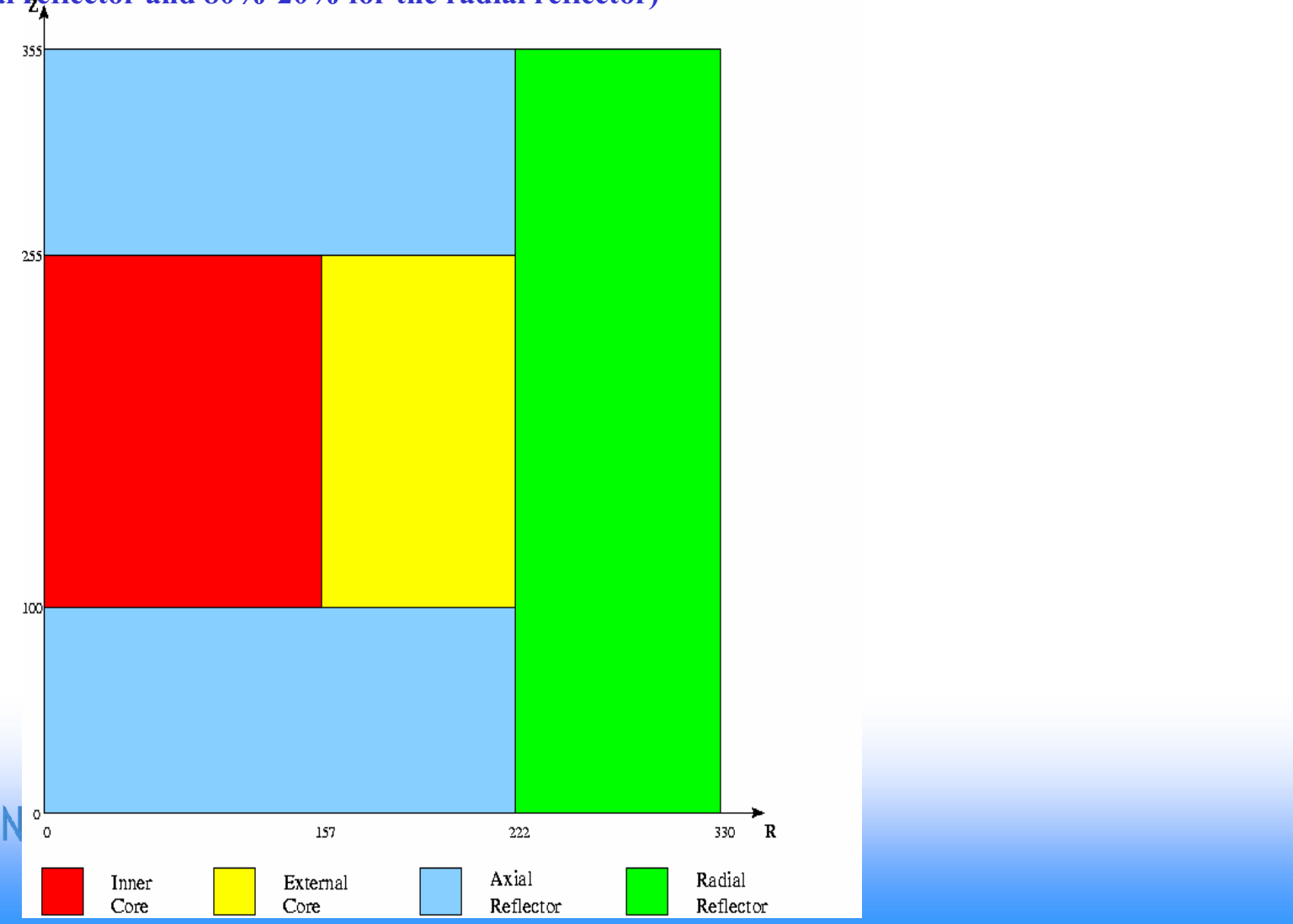
Extended Burnup for LWR's

- Fuel Burnups in LWR's have been slowly increasing in order to reduce costs
- Current plans indicate that burnup might be increased in the [50-100] MWd/ton range
- As burnup increases, the neutronic contributions of transuranics become predominant



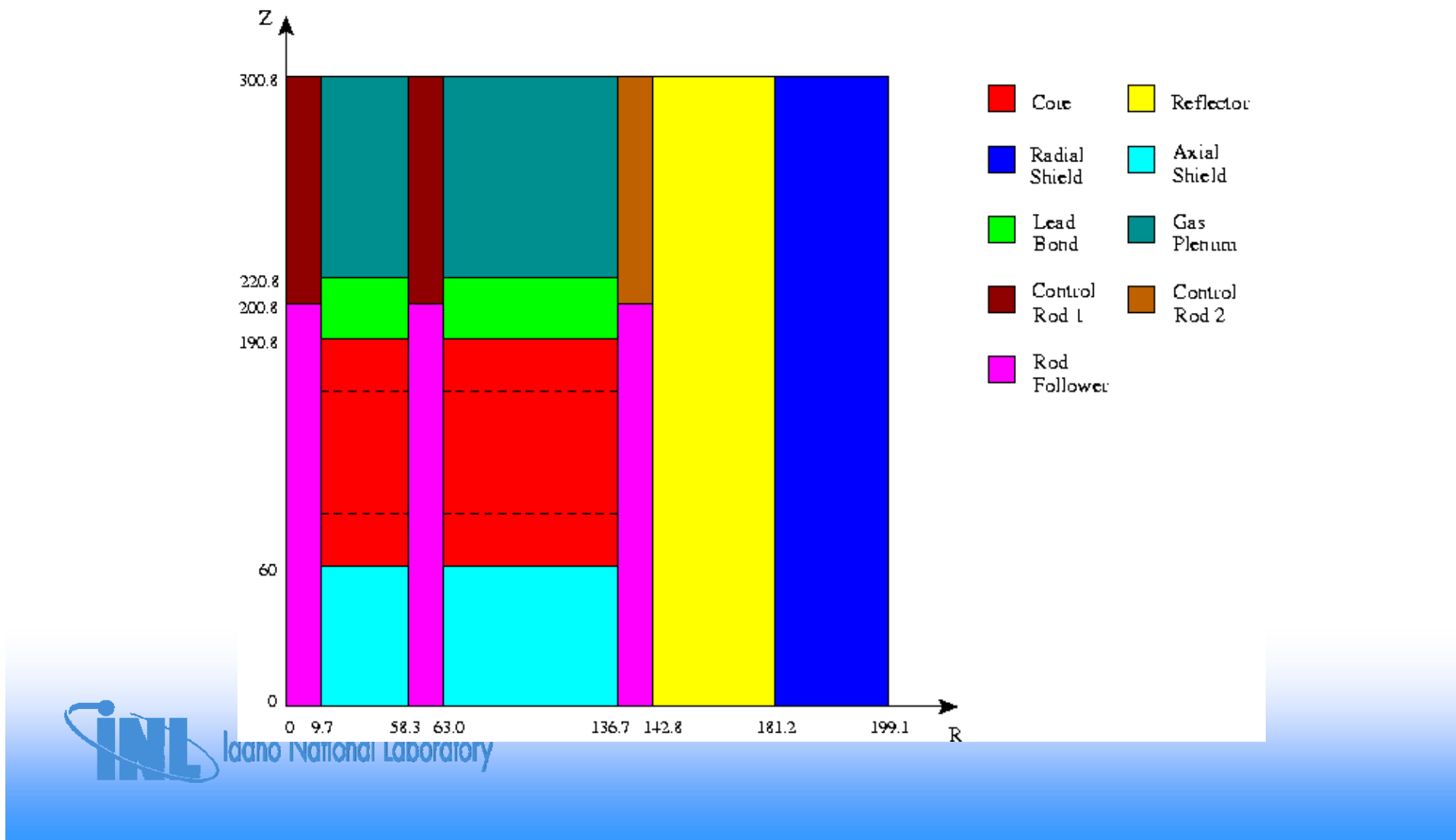
GFR

The gas cooled fast reactor contains CERCER fuel which is a mixture (56%-44%) of a ceramic matrix material SiC and a ceramic heavy metal carbide fuel with 5% of Minor Actinides (MA). The materials of the core region are structure (20%), coolant (40%) and fuel (40%) and the average enrichment (PUC/(UC+PuC)) is 17%. The coolant is helium and the reflector is a mixture of Zr_3Si_2 and coolant (60%-40% for the axial reflector and 80%-20% for the radial reflector)



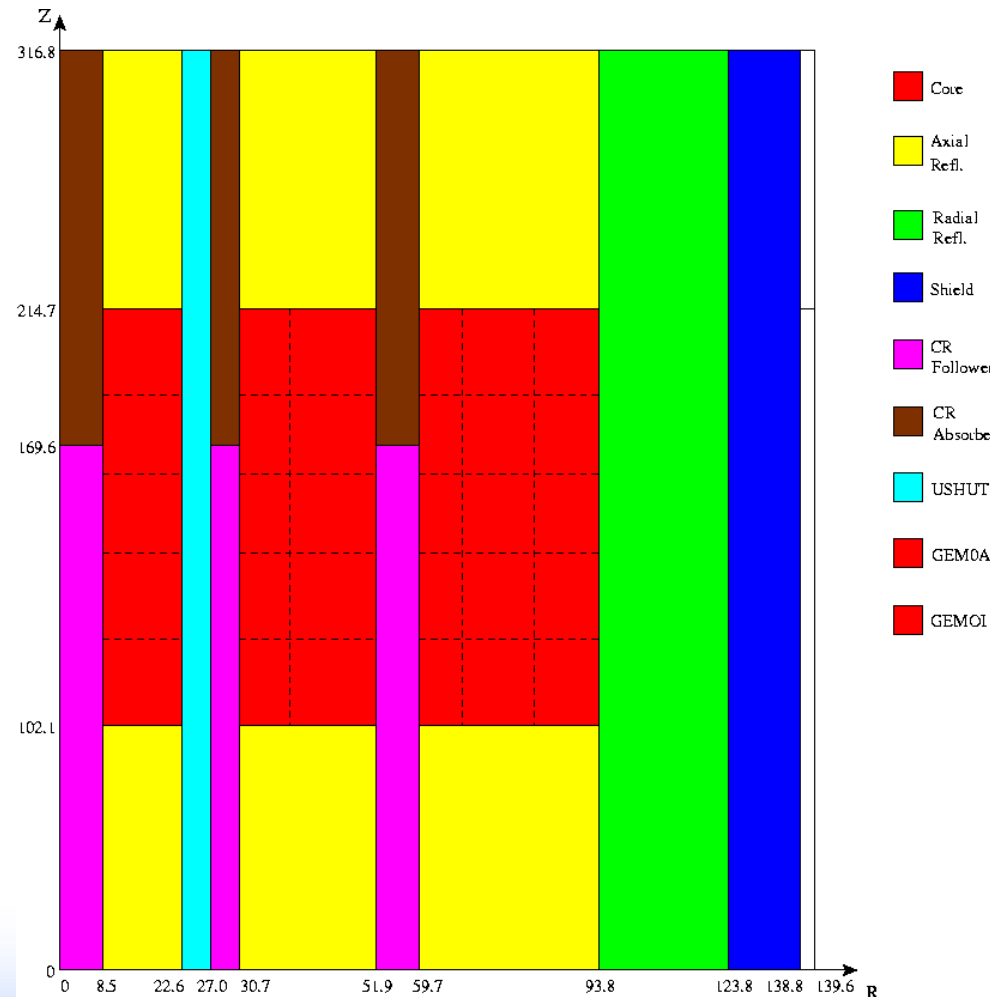
LFR

The lead cooled fast reactor, that is being also investigated in the frame of a benchmark problem prepared by KAERI and also adopted by IAEA, is a 900 MWth reactor loaded with U-TRU-Zr metallic alloy fuels (2% of MA). The core contains 192 hexagonal ductless fuel assemblies and it is surrounded by ducted lead reflector and steel shields.



SFR

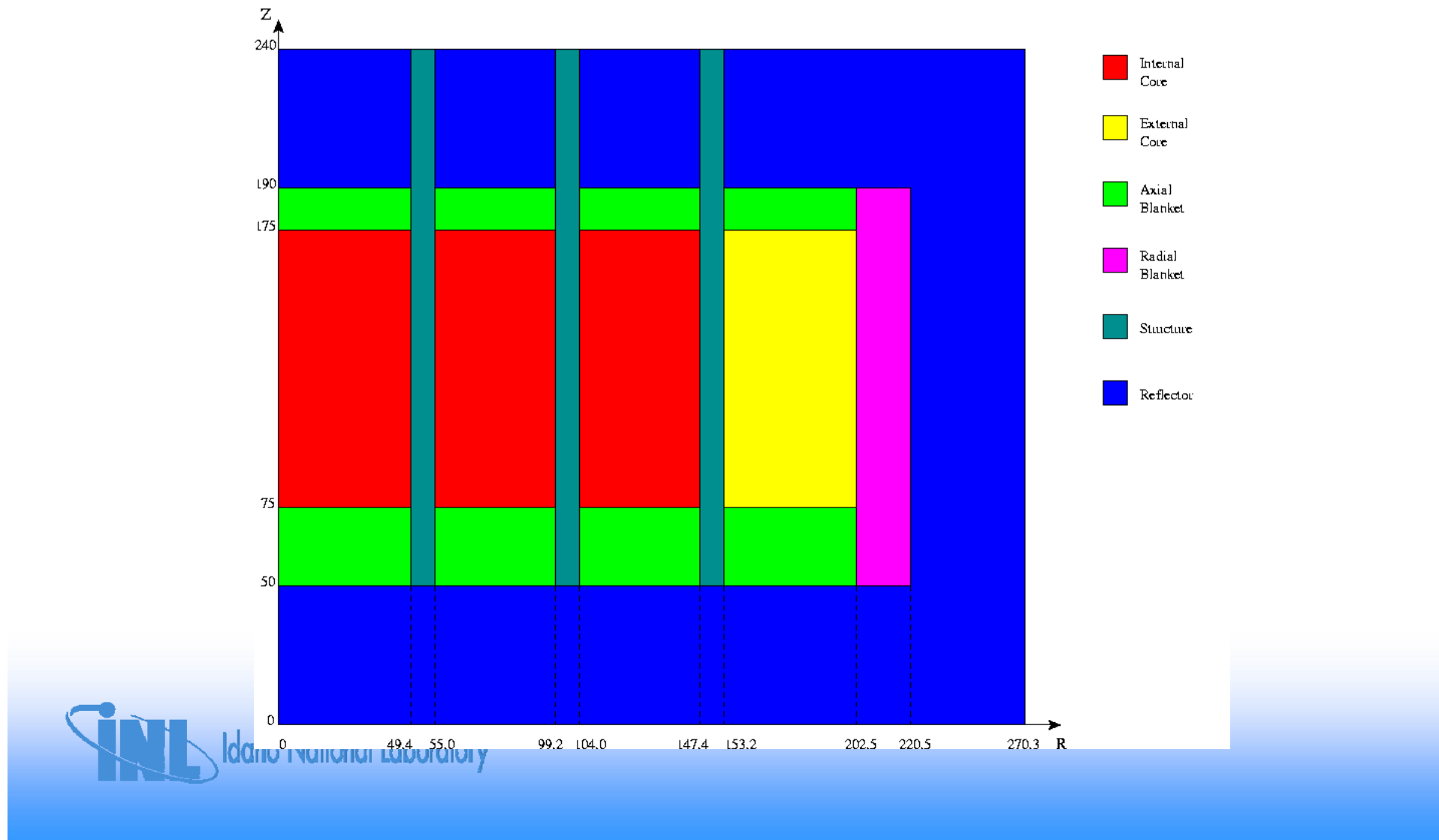
The small size transmuter sodium cooled fast reactor is an 840 MWth reactor loaded with U-TRU-Zr metallic alloy (10% of MA) and very low conversion ratio (<0.25).



Idaho National Laboratory

EFR

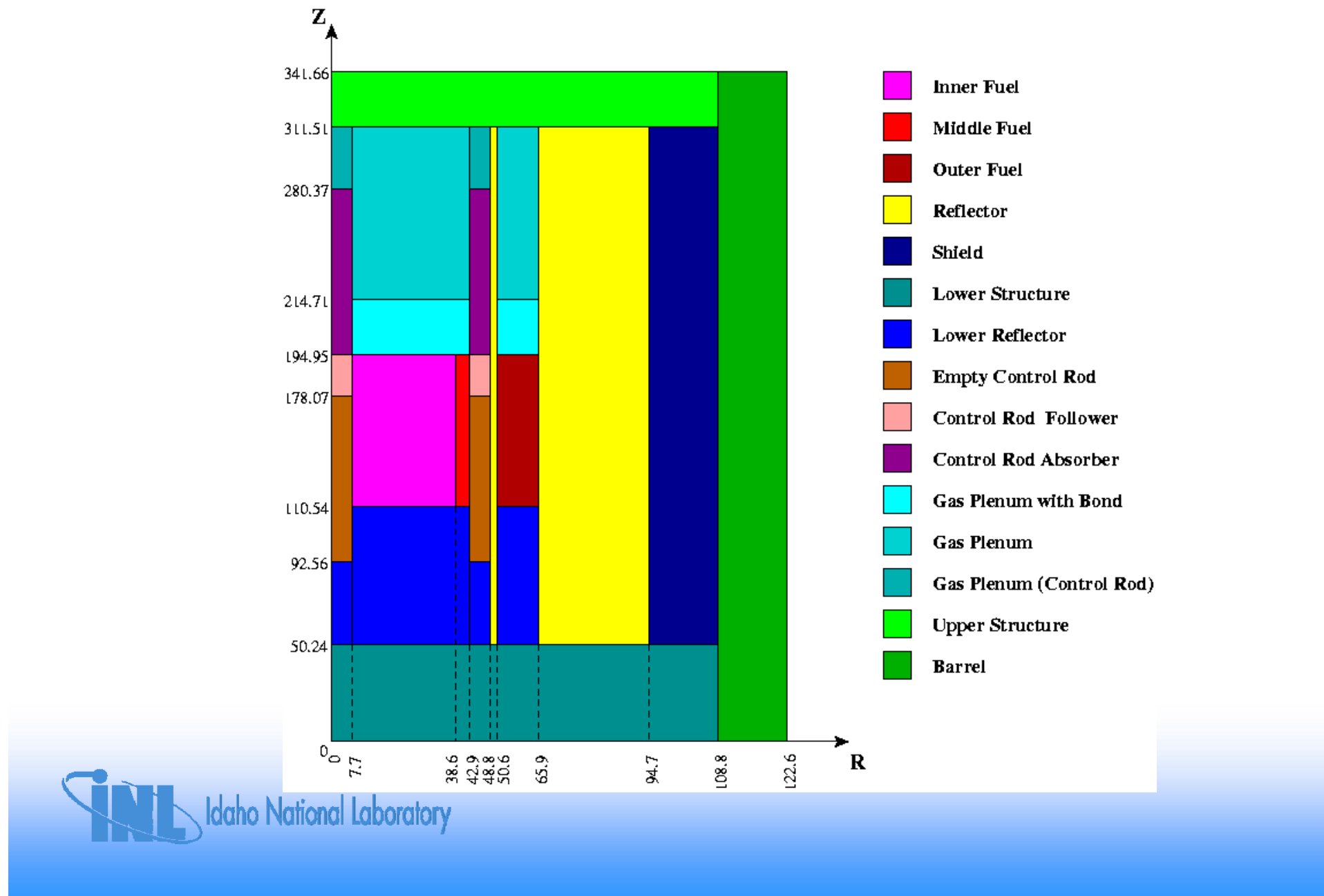
The large size sodium cooled reactor, whose specifications have been provided by the CEA, is a 3600 MWth reactor loaded with U-TRU oxide fuel (1% of MA). The core is surrounded by a blanket.



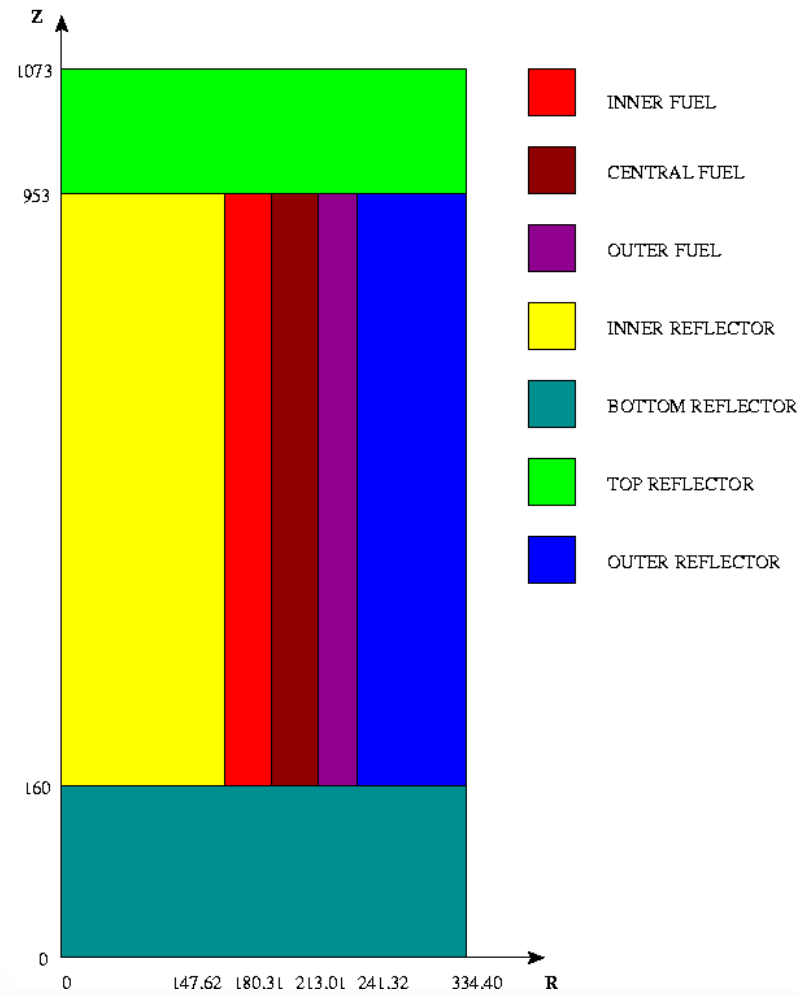
ABTR

- The primary mission of the ABTR (Advanced Burner Test Reactor) is to demonstrate the transmutation of transuramics (TRU) recovered from the LWR spent fuel, and hence the benefits of the fuel cycle closure to nuclear waste management. This requires:
 - to demonstrate reactor-based transmutation of TRU as part of an advanced fuel cycle,
 - to qualify the TRU-containing fuels and advanced structural materials needed for a full-scale ABR,
 - to support the research, development and demonstration required for certification of an ABR standard design by the U.S. Nuclear Regulatory Commission.
- Based on these objectives, core design and fuel cycle studies have been performed to develop ABTR core designs and associated fuel cycle strategies.

ABTR (Metallic Fuel: U,PU, Zr)



VHTR

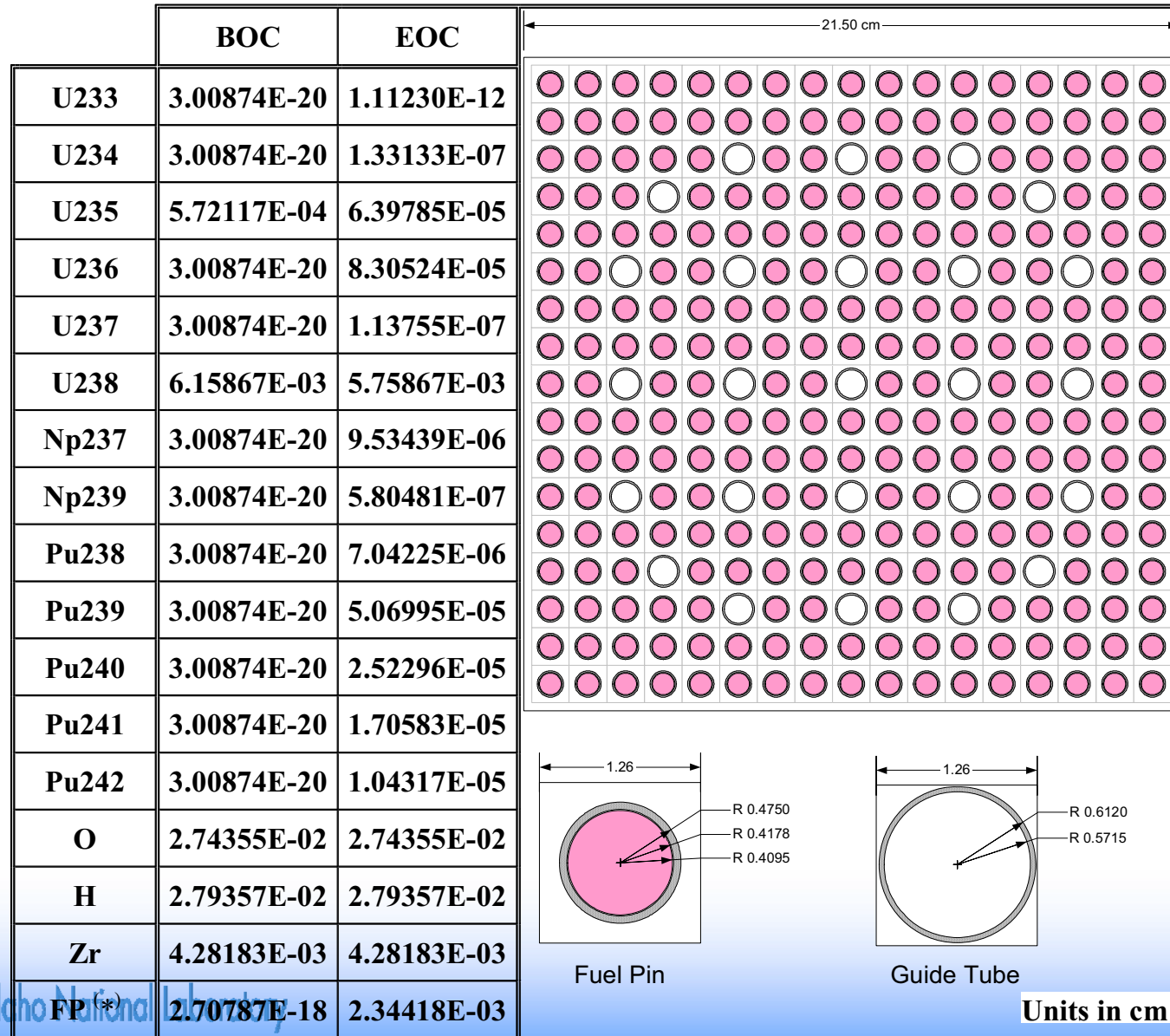


Inner, Central and Outer Fuel		
Isotope	BOC	EOC (90Gwd)
U235	2.49E-05	1.09E-05
U238	1.51E-04	1.41E-04
Np237	-	1.48E-07
Pu238	-	4.86E-08
Pu239	-	2.52E-06
Pu240	-	7.57E-07
Pu241	-	8.91E-07
Pu242	-	2.360E-07
Am241	-	2.07E-08
Am242	-	4.24 E-10
Am243	-	3.38E-08
Cm242	-	7.58E-09
Cm243	-	1.34 E-10
Cm244	-	8.07E-09
Cm245	-	4.30E-10
C	6.40E-02	6.40E-02
O	2.64E-04	2.64E-04
Si	5.23E-04	5.23E-04



Idaho National Laboratory

Extended Burn Up PWR



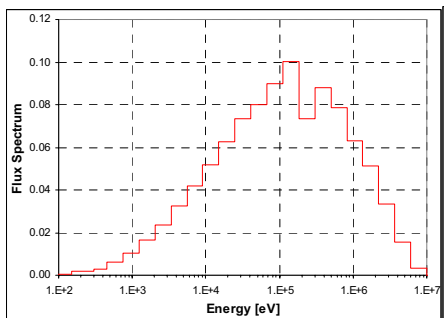
GFR

2400 MWe – He Cooled
SiC – (U-TRU)C Fuel
 Zr_3Si_2 Reflector
Enrichment: 17%
MA: 5%
Irradiation Cycle: 415 d

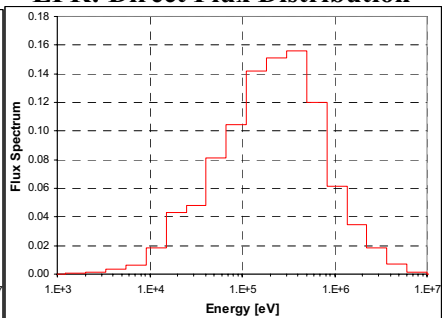
LFR

900 MW_{th} – Pb Cooled
U-TRU-Zr Metallic Alloy
Pb Reflector
Enrichment: 21%
MA: 2%
Irradiation Cycle: 310 d

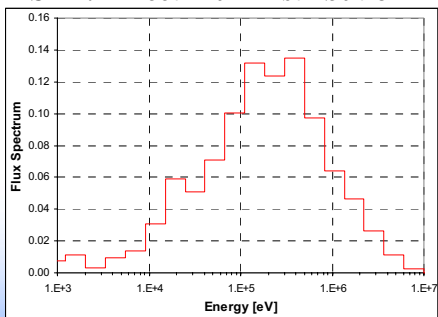
GFR: Direct Flux Distribution



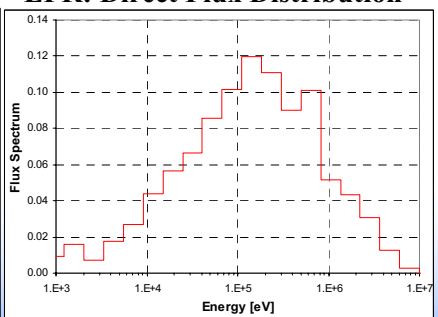
LFR: Direct Flux Distribution



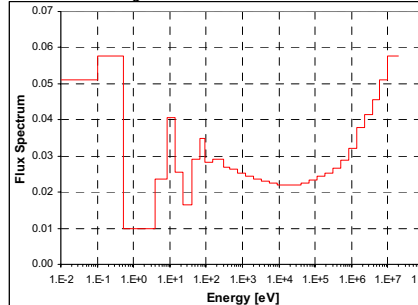
SFR: Direct Flux Distribution



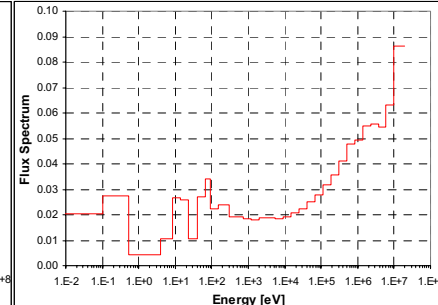
EFR: Direct Flux Distribution



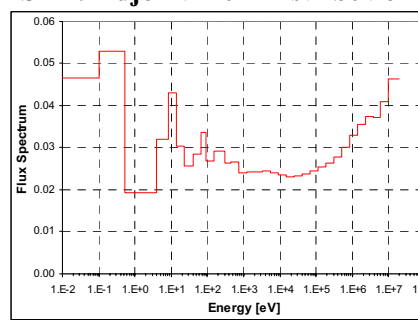
GFR: Adjoint Flux Distribution



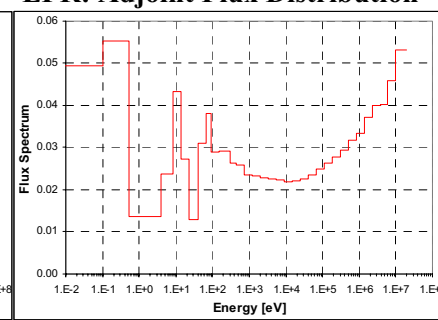
LFR: Adjoint Flux Distribution



SFR: Adjoint Flux Distribution



EFR: Adjoint Flux Distribution



SFR

(Burner: CR = 0.25)

840 MW_{th} – Na Cooled
U-TRU Oxide
U - Blanket
Enrichment: 56%
MA: 10%
Irradiation Cycle: 155 d

EFR

3600 MW_{th} – Na Cooled
U-TRU Oxide
U - Blanket
Enrichment: 22.7%
MA: 1%
Irradiation Cycle: 1700 d



Idaho National Laboratory

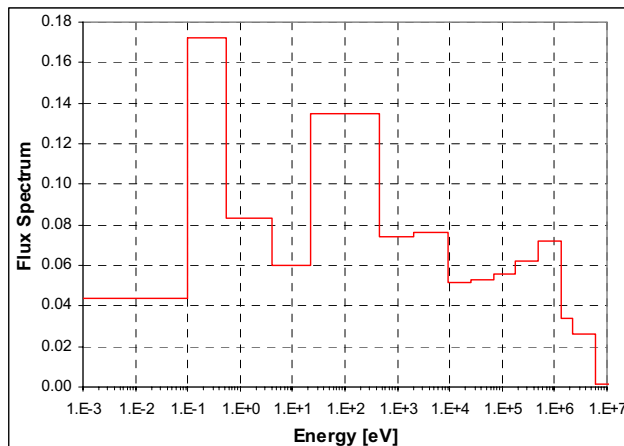
VHTR

TRISO Fuel

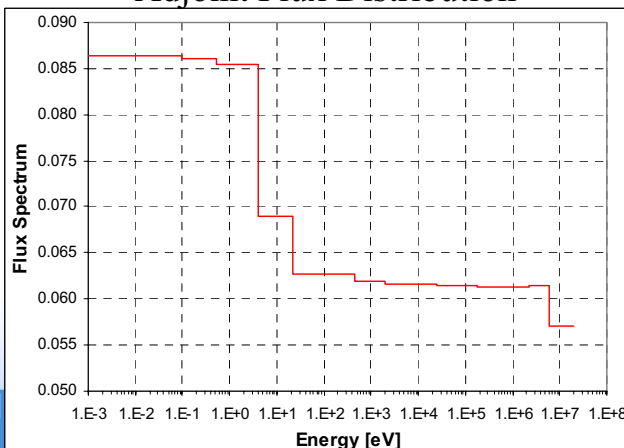
Enrichment: 14%

Burnup: 90 GWd/Kg

Direct Flux Distribution



Adjoint Flux Distribution

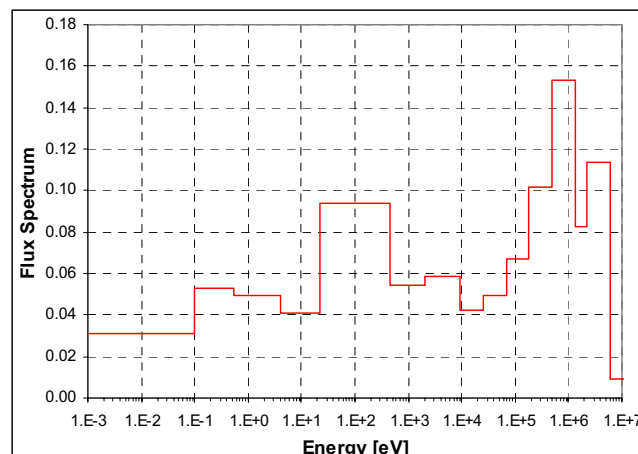


Extended BU PWR

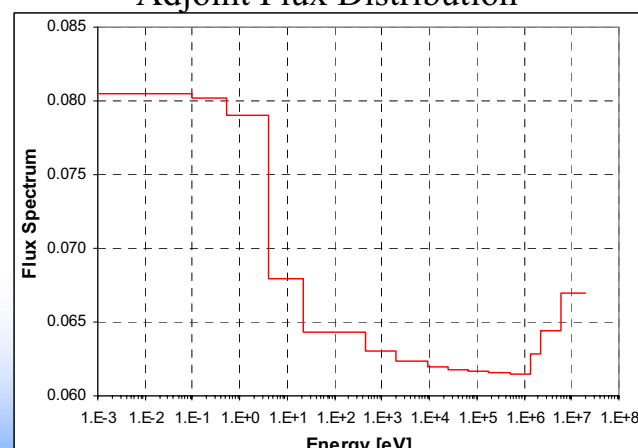
Enrichment: 8.5%

Burnup: 100 GWd/Kg

Direct Flux Distribution



Adjoint Flux Distribution



NUCLEAR DATA UNCERTAINTY IMPACT ON:

Reactor parameters....

- **Criticality (multiplication factor)**
- **Doppler Reactivity Coefficient**
- **Coolant Void Reactivity Coefficient**
- **Reactivity Loss during Irradiation**
- **Transmutation Potential (i.e. nuclide concentration at the end of irradiation)**
- **Peak Power Value**

....and fuel cycle parameters:

- **MA Decay Heat in a Repository (100 years after disposal)**
- **Radiation Source at Fuel Discharge**
- **Radiotoxicity in a Repository (100000 years after disposal)**



Idaho National Laboratory

Thermal Reactor Systems: Total Uncertainties (%)

VHTR

	k_{eff} BOC	k_{eff} EOC	Power Peak BOC	Power Peak EOC	Doppler BOC	Doppler EOC	Burnup [pcm]	Decay Heat	Dose	Neutr. Source
PEC	0.58	1.07	1.9	2.1	3.4	5.6	1574	3.1	2.6	14.3
BOLNA	0.53	0.46	1.0	1.1	1.7	2.0	530	1.4	1.0	5.9

High Burn Up PWR

	k_{eff} BOC	k_{eff} EOC	Doppler BOC	Doppler EOC	Burnup [pcm]	Decay Heat	Dose	Neutron Source
PEC	0.52	1.27	3.1	4.6	2206	3.8	3.1	13.2
BOLNA	0.51	0.74	1.4	1.9	851	1.5	1.0	5.2

Fast Neutron Systems: Total Uncertainties (%)

Reactor		k_{eff}	Power Peak	Doppler	Void	Burnup [pcm]	Decay Heat	Dose	Neutron Source
ABTR	PEC	1.96	0.6	6.4	12.5	97	0.1	0.1	0.5
	BOLNA	0.92	0.3	4.4	6.0	52	0.2	0.1	0.5
SFR	PEC	1.66	0.5	6.0	23.4	234	0.3	0.2	0.9
	BOLNA	1.82	0.4	5.6	17.1	272	0.4	0.3	1.0
EFR	PEC	1.57	1.1	5.1	12.1	989	2.3	1.7	6.0
	BOLNA	1.18	1.2	3.8	7.8	871	2.4	1.2	6.6
GFR	PEC	1.90	1.8	5.5	7.1	384	0.5	0.6	1.8
	BOLNA	1.88	1.7	5.5	7.7	381	0.4	0.5	1.4
LFR	PEC	2.26	1.0	7.8	20.6	258	0.5	0.5	1.1
	BOLNA	1.43	0.6	4.3	7.2	198	0.6	0.4	1.1

ABTR Uncertainties (%) - Breakdown by Isotope

	k_{eff}	Doppler	Power Peak	Void	Burnup [pcm]
U235	0.01	0.04	-	0.06	0.8
U238	0.77	3.40	0.16	3.74	20.1
Pu238	0.02	0.03	0.02	0.04	2.1
Pu239	0.36	1.62	0.11	2.14	30.2
Pu240	0.13	0.32	0.03	0.44	12.1
Pu241	0.12	0.34	0.07	0.27	13.3
Fe56	0.27	1.60	0.18	0.78	9.2
Cr52	0.06	0.45	0.08	0.17	1.0
Ni58	-	0.12	0.01	0.03	0.1
Zr90	0.04	0.13	0.05	0.22	1.0
Na23	0.08	1.51	0.13	4.10	3.1
Total	0.92	4.42	0.34	6.03	51.8

ABTR K_{eff} Uncertainties (%) - Breakdown by Isotope and Reaction

Isotope	σ_{cap}	σ_{fiss}	v	σ_{el}	σ_{inel}	$\sigma_{n.2n}$	Total
U238	0.26	0.04	0.14	0.20	0.69	-	0.77
Pu238	-	0.01	0.01	-	-	-	0.02
Pu239	0.23	0.24	0.13	0.03	0.06	-	0.36
Pu240	0.06	0.09	0.08	-	0.01	-	0.13
Fe56	0.07	-	-	0.08	0.24	-	0.27
Zr90	0.01	-	-	0.01	0.03	-	0.04
Na23	0.02	-	-	0.05	0.07	-	0.08
B10	0.04	-	-	-	-	-	0.04
Total	0.36	0.29	0.20	0.23	0.73	0.01	0.92

ABTR Uncertainties (%) – Energy Breakdown for Selected Isotope/Reaction

Parameter		K _{eff}	K _{eff}	Dopp.	Void	Void	Void	Con. Rod
Gr.	Energy	U238 σ_{inel}	Pu239 σ_{fiss}	Fe56 σ_{inel}	U238 σ_{capt}	Na23 σ_{elas}	Na23 σ_{inel}	B10 $\sigma_{n,\alpha}$
1	19.6 MeV	0.079	0.012	0.20	0.01	0.09	0.75	0.09
2	6.07 MeV	0.479	0.046	0.36	0.02	0.39	1.30	0.35
3	2.23 MeV	0.446	0.053	0.70	0.06	0.58	1.78	0.38
4	1.35 MeV	0.183	0.099	0.81	0.35	0.70	2.79	0.70
5	498 KeV	0.021	0.126	0.00	0.15	1.03	0.15	2.53
6	183 KeV	0.049	0.128	0.00	0.27	1.03	0.00	2.35
7	67.4 KeV	0.014	0.077	0.00	0.46	0.49	0.00	1.38
8	24.8 KeV	0.000	0.059	0.00	3.28	0.48	0.00	1.02
9	9.12 KeV	0.000	0.021	0.00	0.52	0.06	0.00	0.61
10	2.03 KeV	0.000	0.020	0.00	0.59	0.20	0.00	0.05
11	454 eV	0.000	0.009	0.00	0.09	0.03	0.00	0.02
12	22.6 eV	0.000	0.002	0.00	0.01	0.02	0.00	0.01
13	4.00 eV	0.000	0.002	0.00	0.01	0.01	0.00	0.00
14	0.54 eV	0.000	0.000	0.00	0.00	0.00	0.00	0.00
15	0.10 eV	0.000	0.000	0.00	0.00	0.00	0.00	0.00
Total (%)		0.686	0.240	1.14	3.44	1.76	3.63	4.00

SFR Uncertainties (%) - Breakdown by Isotope (Diagonal Values)

	k_{eff}	Power Peak	Doppler	Void	Burnup Total [pcm]
U238	0.16	0.05	0.60	1.65	10.5
Pu238	0.34	0.01	0.86	2.72	45.6
Pu239	0.13	0.02	0.49	1.39	20.6
Pu240	0.38	0.03	0.96	3.83	32.2
Pu241	0.52	0.02	1.70	4.34	89.8
Pu242	0.26	0.02	0.74	2.65	24.4
Np237	0.03	0.01	0.23	0.40	1.2
Am241	0.07	0.01	0.34	0.62	3.4
Am242m	0.37	0.02	1.08	3.06	50.4
Am243	0.05	0.01	0.31	0.53	5.8
Cm242	0.02	-	0.06	0.14	8.6
Cm243	0.01	-	0.02	0.05	2.3
Cm244	0.27	0.01	0.66	2.84	42.6
Cm245	0.19	0.01	0.49	1.28	31.5
Fe56	0.37	0.13	1.89	4.44	31.4
Cr52	0.04	0.01	0.27	0.47	2.2
Zr90	0.03	0.02	0.10	0.24	2.3
Na23	0.23	0.10	1.25	12.29	19.6
B10	0.12	0.24	0.22	1.16	8.7
Total	1.04	0.31	3.62	15.66	152.1



Idaho National Laboratory

SFR Uncertainties (%) - Breakdown by Isotope (With Corr.)

	k_{eff}	Power Peak	Doppler	Void	Burnup Total [pcm]
U238	0.24	0.07	0.94	2.43	16.0
Pu238	0.64	0.02	1.50	3.00	83.2
Pu239	0.19	0.04	0.71	1.75	29.3
Pu240	0.66	0.05	1.60	3.86	56.9
Pu241	0.96	0.02	2.77	4.12	170.2
Pu242	0.41	0.03	1.15	3.37	37.5
Np237	0.06	0.01	0.31	0.51	2.1
Am241	0.11	0.01	0.55	0.91	5.6
Am242m	0.73	0.02	1.84	3.73	100.7
Am243	0.07	0.01	0.49	0.78	8.8
Cm242	0.04	-	0.10	0.13	15.5
Cm243	0.02	-	0.04	0.03	4.5
Cm244	0.40	0.02	1.00	3.01	64.5
Cm245	0.39	0.01	0.95	1.00	62.2
Cm246	0.04	-	0.14	0.28	4.1
Fe56	0.55	0.20	2.48	4.47	47.0
Cr52	0.06	0.01	0.38	0.51	2.9
Zr90	0.03	0.03	0.12	0.29	2.5
Na23	0.25	0.13	1.85	13.53	21.6
B10	0.17	0.36	0.35	1.53	12.8
Total	1.82	0.45	5.57	17.11	271.9

SFR K_{eff} Uncertainties (%) – Energy Breakdown for Selected Isotope/Reaction

Group	Energy	Pu-238 σ_{fission}	Pu-240 σ_{capture}	Pu-241 σ_{fission}	Am-242m σ_{fission}
1	19.6 MeV	0.01	0.00	0.02	0.02
2	6.07 MeV	0.18	0.03	0.10	0.12
3	2.23 MeV	0.23	0.05	0.26	0.15
4	1.35 MeV	0.31	0.11	0.40	0.28
5	498 keV	0.28	0.14	0.47	0.39
6	183 keV	0.12	0.16	0.58	0.39
7	67.4 keV	0.07	0.13	0.29	0.28
8	24.8 keV	0.06	0.13	0.16	0.12
9	9.12 keV	0.03	0.05	0.10	0.08
10	2.03 keV	0.03	0.01	0.08	0.10
11	454 eV	0.00	0.00	0.03	0.02
12-15	22.6 eV	0.00	0.00	0.00	0.00
Total		0.53	0.31	0.96	0.73

GFR Uncertainties (%) - Breakdown by Isotope

	k _{eff}	Power Peak	Doppler	Void	Burnup Total [pcm]
U235	0.07	0.05	0.14	0.17	26.2
U238	1.48	1.57	4.13	5.56	73.9
Pu238	0.25	0.07	0.53	0.32	85.6
Pu239	0.30	0.07	0.86	0.92	150.7
Pu240	0.35	0.12	0.73	0.53	16.3
Pu241	0.82	0.16	2.21	1.66	240.6
Pu242	0.27	0.09	0.68	0.68	18.2
Np237	0.06	0.04	0.24	0.16	10.6
Am241	0.34	0.22	1.37	0.90	57.8
Am242m	0.01	0.01	0.03	0.03	75.4
Am243	0.07	0.05	0.30	0.21	16.4
Cm242	-	-	-	-	85.6
Cm243	0.01	0.01	0.02	0.01	9.5
Cm244	0.13	0.09	0.32	0.27	35.7
Cm245	0.12	0.10	0.28	0.17	25.2
Cm246	-	-	0.01	-	0.5
C	0.31	0.29	1.91	1.65	8.3
He4	0.02	0.01	0.05	4.38	0.3
Si28	0.27	0.27	0.75	0.65	6.3
Zr90	0.02	0.20	0.07	0.07	1.7
Total	1.88	1.68	5.51	7.67	380.7



Idaho National Laboratory

GFR Helium Void Uncertainties (%) - Breakdown by Isotope and Reaction

Isotope	σ_{cap}	σ_{fiss}	ν	σ_{el}	σ_{inel}	Total
U238	1.23	0.03	0.08	0.46	5.40	5.56
Pu239	0.73	0.39	0.24	-	0.31	0.92
Pu240	0.30	0.33	0.27	-	0.10	0.53
Pu241	0.12	1.65	0.09	-	0.04	1.66
Pu242	0.52	0.40	0.10	-	0.16	0.68
Am241	0.82	0.34	0.07	-	0.17	0.90
Am243	0.19	0.06	0.02	-	0.08	0.21
Cm244	0.03	0.27	0.05	-	0.01	0.27
Cm245	0.01	0.17	0.05	-	0.01	0.17
C	-	-	-	1.65	0.05	1.65
He4	-	-	-	4.38	-	4.38
Si28	0.02	-	-	0.22	0.61	0.65
Total	1.78	1.86	0.43	4.71	5.46	7.67

EFR Uncertainties (%) - Breakdown by Isotope

	k _{eff}	Power Peak	Doppler	Void	Burnup Total [pcm]
U238	0.88	0.90	2.79	3.10	82.8
Pu238	0.15	0.04	0.36	0.22	68.1
Pu239	0.32	0.09	1.08	1.49	439.7
Pu240	0.43	0.13	1.02	0.79	109.5
Pu241	0.36	0.07	1.13	1.34	634.0
Pu242	0.09	0.03	0.28	0.13	15.9
Am241	0.06	0.03	0.31	0.24	30.8
Am242m	0.03	0.02	0.06	0.08	30.8
Am243	0.01	0.01	0.08	0.07	19.0
Cm242	-	-	-	-	23.2
Cm243	0.01	0.01	0.02	0.02	11.6
Cm244	0.06	0.02	0.14	0.18	51.5
Cm245	0.06	0.04	0.13	0.10	52.5
Fe56	0.26	0.27	0.86	0.95	64.0
Ni58	0.08	0.05	0.48	0.22	12.1
Na23	0.14	0.25	0.88	6.72	39.8
O16	0.27	0.65	1.05	0.88	93.3
Total	1.18	1.18	3.80	7.83	871.0

EFR Doppler Uncertainties (%) - Breakdown by Isotope and Reaction

Isotope	σ_{cap}	σ_{fiss}	v	σ_{el}	σ_{inel}	Total
U238	0.38	0.08	0.22	0.46	2.71	2.79
Pu238	0.06	0.34	0.11	-	0.01	0.36
Pu239	0.79	0.54	0.22	-	0.45	1.08
Pu240	0.22	0.81	0.55	0.01	0.23	1.02
Pu241	0.11	1.12	-	-	0.02	1.13
Pu242	0.17	0.22	0.04	-	0.03	0.28
Am241	0.30	0.10	0.02	-	0.02	0.31
Cm243	-	0.02	-	-	-	0.02
Cm244	0.02	0.14	0.02	-	0.01	0.14
Cm245	-	0.13	-	-	-	0.13
Fe56	0.14	-	-	0.28	0.80	0.86
Cr52	0.02	-	-	0.11	0.02	0.12
Ni58	0.09	-	-	0.46	0.10	0.48
Na23	0.02	-	-	0.71	0.52	0.88
O16	0.33	-	-	0.99	0.07	1.05
Idaho Total Laboratory	1.05	1.56	0.64	1.41	2.92	3.80



EPR Uncertainty (%) on Pu Isotope Density at End of Cycle

Uncertainty on →		Pu238	Pu239	Pu240	Pu241	Pu242
↓ due to						
U238	capture	-	1.1	0.2	0.1	-
Pu238	capture	1.7	0.1	-	-	-
	fission	4.6	-	-	-	-
Pu239	capture	-	0.8	1.3	0.7	0.1
	fission	-	0.2	-	-	-
Pu240	capture	0.2	-	1.5	6.0	1.0
	fission	-	-	0.8	0.4	-
Pu241	capture	-	-	-	0.8	1.5
	fission	0.2	-	-	5.0	0.7
Pu242	capture	-	-	-	-	3.9
	fission	-	-	-	-	2.2
Am241	capture	1.3	-	-	-	0.2
	fission	0.2	-	-	-	-
Total		5.1	1.3	2.1	7.9	4.9



Idaho National Laboratory

EPR Uncertainty (%) on Selected MA Isotope Density at End of Cycle

Uncertainty on → ↓ due to		Am241	Am242m	Am243	Cm244	Cm245
Pu240	capture	1.6	0.6	0.2	-	-
	fission	0.1	-	-	-	-
Pu241	capture	0.2	0.1	0.4	0.1	-
	fission	1.2	0.4	0.1	-	-
Pu242	capture	-	-	9.3	4.1	1.5
	fission	-	-	0.6	0.2	-
Am241	capture	3.1	2.0	0.1	-	-
	fission	0.9	0.5	-	-	-
Am242m	capture	-	1.6	0.3	0.2	0.1
	fission	-	7.4	0.1	-	-
Am243	capture	-	-	1.9	1.9	1.0
	fission	-	-	0.5	0.2	0.1
Cm244	capture	-	-	-	1.8	7.2
	fission	-	-	-	6.0	2.8
Cm245	capture	-	-	-	-	0.9
	fission	-	-	-	-	15.6
Total		3.8	7.8	9.5	7.8	17.6



Idaho National Laboratory

LFR Uncertainties (%) - Breakdown by Isotope

	k _{eff}	Power Peak	Doppler	Void	Burnup Total [pcm]
U238	0.78	0.08	2.59	4.73	8.5
Pu238	0.42	0.02	0.85	0.60	36.4
Pu239	0.31	0.05	1.35	0.87	106.1
Pu240	0.56	0.03	1.18	0.70	21.9
Pu241	0.61	0.02	1.44	1.37	145.1
Pu242	0.19	0.02	0.68	0.37	5.5
Np237	0.04	0.01	0.17	0.07	1.7
Am241	0.08	0.01	0.31	0.18	4.3
Am242m	0.07	-	0.16	0.16	14.4
Cm242	0.02	-	0.04	0.03	11.4
Cm244	0.16	0.01	0.38	0.12	14.3
Cm245	0.22	0.01	0.49	0.44	33.5
Fe56	0.25	0.08	1.09	1.51	5.4
Pb206	0.20	0.08	0.88	3.10	4.3
Pb207	0.17	0.08	0.86	2.61	3.4
Pb208	0.14	0.22	1.15	2.17	2.3
B10	0.44	0.57	1.02	1.14	6.6
Total	1.43	0.64	4.35	7.18	198.2



Idaho National Laboratory

LFR Pb Void Uncertainties (%) - Breakdown by Isotope and Reaction

Isotope	σ_{cap}	σ_{fiss}	v	σ_{el}	σ_{inel}	$\sigma_{n.2n}$	Total
U238	1.09	0.08	0.37	1.06	4.46	0.01	4.73
Pu238	0.10	0.45	0.39	-	0.02	-	0.60
Pu239	0.53	0.52	0.36	0.13	0.25	-	0.87
Pu240	0.62	0.11	0.30	0.03	0.06	-	0.70
Pu241	0.04	1.37	0.05	-	0.02	-	1.37
Pu242	0.32	0.18	0.04	-	0.04	-	0.37
Am241	0.14	0.11	0.03	-	0.03	-	0.18
Am242m	0.01	0.16	0.01	-	-	-	0.16
Cm244	0.04	0.10	0.06	-	0.01	-	0.12
Cm245	0.01	0.43	0.06	-	-	-	0.44
Fe56	0.16	-	-	0.20	1.49	-	1.51
Zr90	0.02	-	-	0.11	0.61	-	0.62
Pb204	0.42	-	-	0.03	0.17	-	0.46
Pb206	1.31	-	-	0.49	2.77	-	3.10
Pb207	0.77	-	-	0.35	2.47	0.01	2.61
Pb208	0.37	-	-	2.01	0.73	0.02	2.17
B10	1.14	-	-	0.06	0.01	-	1.14
Total	2.43	1.62	0.72	2.37	6.07	0.03	7.18



Idaho National Laboratory

VHTR Uncertainties (%) - Breakdown by Isotope

	k _{eff} EOC	Power Peak EOC	Doppler BOC	Doppler EOC	Burnup Total [pcm]
U235	0.27	0.06	0.74	0.73	235.8
U238	0.19	0.02	0.87	0.67	48.3
Np237	0.01	-	-	0.04	10.2
Pu238	-	-	-	0.01	2.0
Pu239	0.17	0.13	-	0.98	190.8
Pu240	0.06	0.01	-	0.26	215.9
Pu241	0.22	0.10	-	0.93	252.5
Pu242	0.02	-	-	0.05	32.0
Am241	-	-	-	0.02	8.0
Am242m	-	-	-	-	2.2
Am243	-	-	-	0.01	8.5
O	0.01	-	0.01	0.01	1.6
Si	0.01	0.01	0.02	0.03	1.3
C	0.13	1.04	1.26	1.09	38.1
Total	0.46	1.06	1.70	2.01	530.1

VHTR K_{eff} Uncertainties (%) - Breakdown by Isotope and Reaction

BOC

Isotope	σ_{cap}	σ_{fiss}	ν	σ_{el}	σ_{inel}	$\sigma_{n.2n}$	Total
U235	0.13	0.04i	0.47	-	-	-	0.49
U238	0.15	-	-	-	-	-	0.15
Si	0.01	-	-	-	-	-	0.01
C	0.09	-	-	0.04	0.07	-	0.12
Total	0.22	0.04i	0.47	0.04	0.07	-	0.53

EOC

Isotope	σ_{cap}	σ_{fiss}	ν	σ_{el}	σ_{inel}	$\sigma_{n.2n}$	Total
U235	0.05	0.03	0.27	-	-	-	0.27
U238	0.19	-	-	-	-	-	0.19
Np237	0.01	-	-	-	-	-	0.01
Pu239	0.11	0.10	0.07	-	-	-	0.17
Pu240	0.06	-	-	-	-	-	0.06
Pu241	0.13	0.18	0.04	-	-	-	0.22
Pu242	0.02	-	-	-	-	-	0.02
Si	0.01	-	-	-	-	-	0.01
C	0.12	-	-	0.04	0.05	-	0.13
Total	0.29	0.20	0.28	0.04	0.05	-	0.46



Idaho National Laboratory

PWR Uncertainties (%) - Breakdown by Isotope

	k_{eff} BOC	k_{eff} EOC	Doppler BOC	Doppler EOC	Burnup Total [pcm]
U235	0.25	0.11	1.12	0.44	153.0
U238	0.12	0.24	0.95	1.09	139.6
Np237	-	0.02	-	0.04	20.8
Pu238	-	0.01	-	0.04	20.9
Pu239	-	0.25	-	1.08	435.2
Pu240	-	0.09	-	0.34	110.5
Pu241	-	0.29	-	1.06	327.8
Pu242	-	0.04	-	0.03	53.8
Am241	-	0.01	-	0.01	13.4
Am243	-	0.02	-	0.01	41.9
Cm244	-	0.01	-	0.01	15.4
Cm245	-	0.01	-	0.05	13.9
O	0.24	0.43	0.41	0.49	202.2
H	0.01	0.04	0.08	0.11	25.7
Zr	0.01	0.02	0.02	0.03	10.4
Total	0.36	0.64	1.53	2.01	684.6

PWR K_{eff} Uncertainties (%) - Breakdown by Isotope and Reaction

BOC

Isotope	σ_{cap}	σ_{fiss}	v	σ_{el}	σ_{inel}	$\sigma_{n.2n}$	Total
U235	0.15	0.03i	0.39	-	-	-	0.42
U238	0.15	0.01	0.04	-	0.04	-	0.16
O	0.24	-	-	-	0.03	-	0.24
H	0.01	-	-	-	0.02	-	0.02
Zr	0.02	-	-	-	-	-	0.02
Total	0.32	0.03i	0.40	-	0.05	-	0.51

EOC

Isotope	σ_{cap}	σ_{fiss}	v	σ_{el}	σ_{inel}	$\sigma_{n.2n}$	Total
U235	0.03	0.02	0.17	-	-	-	0.17
U238	0.26	0.03	0.10	-	0.17	0.01	0.33
Pu239	0.07	0.18	0.07	-	-	-	0.21
Pu240	0.12	0.01	0.01	-	-	-	0.12
Pu241	0.13	0.34	0.06	-	-	-	0.37
Pu242	0.05	0.01	-	-	-	-	0.05
O	0.43	-	-	-	0.15	-	0.46
H	0.02	-	-	-	0.05	-	0.06
Zr	0.03	-	-	-	0.01	-	0.04
Total	0.55	0.38	0.22	-	0.23	0.01	0.74



Idaho National Laboratory

LESSON DRAWN FROM UNCERTAINTY STUDY

1. A significant result is the strong impact of correlation data (i.e. off-diagonal elements) on the uncertainty assessment. Any credible uncertainty analysis should include the best available covariance data accounting for energy correlations and possibly for cross-correlations among reactions (a typical case would be the inter-relation among total, elastic and inelastic cross-sections) and even for cross-correlation among isotopes, if needed e.g. to account for normalization issues
2. One other important point seems to be the shift of priority from the three major actinide fission data to their inelastic (in particular for U-238) and capture data (for Pu-239, and, to a lesser extent, for U-238; the case of U-235 capture data in the keV region is presently under investigation). The shift of priority is related to the relatively small uncertainty values associated to the fission cross-sections of Pu-239.
3. Higher priority should also be given to higher Pu isotopes (and in particular to their fission data) and to selected coolant/structural material inelastic cross-sections (e.g., Fe-56 and Na-23). Minor actinide data play a significant role only for dedicated burner reactors (ADMAB or SFR) with Conversion Ratio CR=0 and a content of MA in the fuel of 50% or higher. For more conventional burners (Pu/MA~5) and down to CR~0.25, only selected MA data require significant improvements

Fuel Cycle Parameters: SFR

Breakdown

Isotope	Decay Heat	Dose	Neutron Source
Pb210	-	28.01	-
Ra226	-	10.76	-
Ac227	-	0.06	-
Th229	-	2.78	-
Th230	-	7.95	-
Pa231	-	0.05	-
U233	-	0.28	-
U234	0.02	3.20	-
U236	-	0.18	-
Np237	-	1.38	-
Pu238	46.51	-	0.59
Pu239	1.37	34.71	0.01
Pu240	6.82	0.07	0.13
Pu242	0.03	10.52	0.06
Am241	26.61	0.01	0.10
Am242m	0.17	-	-
Am243	0.65	0.02	0.01
Cm242	12.91	-	1.53
Cm243	0.10	-	0.01
Cm244	4.59	-	87.12
Cm245	0.10	0.01	-
Cm246	0.10	-	10.44
Cm248	-	-	0.01
Total	100.00	100.00	100.00

Uncertainty

		Decay	Dose	N.
	capture	0.06	0.04	-
Pu238	fission	0.26	0.23	-
	capture	-	0.02	-
Pu239	fission	-	0.01	-
	capture	0.11	0.01	-
Pu240	fission	0.01	-	-
	capture	0.02	0.01	-
Pu241	fission	0.16	0.02	-
	capture	-	0.02	0.02
Pu242	fission	-	0.03	-
	capture	0.03	0.05	0.02
Am241	fission	0.02	-	-
	capture	0.06	0.03	-
Am242m	fission	0.29	0.18	0.01
	capture	0.01	0.01	0.24
Am243	fission	-	0.01	-
	capture	-	-	-
Cm242	fission	0.02	-	0.01
	capture	0.01	-	0.18
Cm244	fission	0.05	-	0.91
	capture	-	-	0.02
Cm245	fission	-	0.01	-
	capture	-	-	0.03
Cm246	fission	-	-	0.07
Total		0.45	0.31	0.96



Idaho National Laboratory

Fuel Cycle Parameters: EFR

Uncertainty

Breakdown

Isotope	Decay Heat	Dose	Neutron Source
Pb210	-	11.83	-
Ra226	-	4.54	-
Ac227	-	0.13	-
Th229	-	1.90	-
Th230	-	3.36	-
Pa231	-	0.10	-
U233	-	0.19	-
U234	0.02	1.35	-
U235	-	0.01	-
U236	-	0.23	-
U238	-	0.01	-
Np237	-	0.94	-
Pu238	34.15	-	0.67
Pu239	5.58	70.45	0.04
Pu240	14.72	0.08	0.39
Pu241	0.01	-	-
Pu242	0.03	4.87	0.07
Am241	39.38	-	0.14
Am242m	0.03	-	-
Am243	0.39	0.01	-
Cm242	1.96	-	1.95
Cm243	0.21	-	0.02
Cm244	3.42	-	85.82
Cm245	0.05	-	-
Cm246	0.06	-	7.38
Total	100.00	100.00	100.00

		Decay	Dose	N.
	capture	0.50	0.22	0.01
Pu238	fission	1.34	0.71	0.03
	capture	0.37	0.49	0.01
Pu239	fission	0.03	0.16	-
	n,2n	0.01	0.01	-
	capture	1.79	0.23	0.07
Pu240	fission	0.26	0.02	0.01
	capture	-	-	0.10
Pu241	fission	-	0.02	0.05
	capture	0.20	0.04	3.51
Pu242	fission	0.01	0.11	0.15
	capture	0.17	0.24	0.08
Am241	fission	0.21	0.06	0.02
	capture	0.05	0.01	0.12
Am242m	fission	0.26	0.09	0.04
	capture	0.06	0.04	1.60
Am243	fission	0.01	0.01	0.16
	capture	0.07	-	1.50
Cm244	fission	0.23	-	5.11
	capture	-	-	0.16
Cm245	fission	-	-	0.17
	capture	-	-	0.22
Cm246	fission	-	-	0.37
Total		2.40	1.24	6.60



Fuel Cycle Parameters: VHTR

Uncertainty

Breakdown

Isotope	Decay Heat	Dose	Neutron Source
Pb210	-	8.80	-
Ra226	-	3.38	-
Ac227	-	0.74	-
Th229	-	6.17	-
Th230	-	2.50	-
Pa231	-	0.58	-
U233	-	0.62	-
U234	0.01	1.02	-
U235	-	0.05	-
U236	-	0.54	-
U238	-	0.11	-
Np237	0.01	3.04	-
Pu238	18.77	-	1.32
Pu239	3.06	63.00	0.08
Pu240	4.11	0.04	0.38
Pu241	0.02	-	-
Pu242	0.03	9.42	0.30
Am241	72.45	-	0.29
Am243	0.35	0.01	0.01
Cm242	0.09	-	5.23
Cm243	0.03	-	0.01
Cm244	1.06	-	92.14
Cm245	0.01	-	-
Cm246	-	-	0.23
Total	100.00	100.00	100.00

	Decay	Dose	N. Sr
	capture	0.18	0.17
U235	fission	0.03	0.03
	capture	0.07	0.07
U236	fission	-	-
	capture	0.77	0.75
U238	fission	-	-
	n,2n	0.01	0.01
	capture	0.17	0.13
Np237	fission	-	-
	capture	0.03	0.02
Pu238	fission	0.01	0.01
	capture	0.80	0.14
Pu239	fission	0.53	0.40
	capture	0.05	0.03
Pu240	fission	-	-
	capture	0.45	0.45
Pu241	fission	0.28	0.28
	capture	0.05	0.02
Pu242	fission	-	0.01
	capture	0.01	0.02
Am241	fission	-	-
	capture	0.02	0.02
Am243	fission	-	-
	capture	-	-
Cm244	fission	-	0.38
	capture	-	0.03
Total		1.37	1.04
			5.94

Fuel Cycle Parameters: . n_f Uncertainties (%)

	ABTR		SFR		EFR		GFR		LFR		VHTR		PWR	
	Diag.	Full	Diag.	Full	Diag.	Full	Diag.	Full	Diag.	Full	Diag.	Full	Diag.	Full
U235	0.07	0.16	0.31	0.59	2.57	5.14	0.42	0.84	0.36	0.72	0.25	0.44	0.46	0.87
U238	0.01	0.01	0.02	0.02	0.24	0.26	0.04	0.04	0.03	0.03	0.05	0.06	0.04	0.06
Np237	0.25	0.26	0.11	0.22	2.51	3.04	0.25	0.44	0.18	0.33	1.03	1.38	1.05	1.49
Pu238	0.21	0.36	0.42	0.74	2.71	4.91	0.64	1.15	0.56	0.95	1.28	1.55	1.05	1.45
Pu239	0.04	0.05	0.06	0.09	1.13	1.33	0.37	0.41	0.20	0.23	0.96	1.22	0.88	1.22
Pu240	0.13	0.22	0.10	0.19	1.25	2.20	0.31	0.44	0.16	0.31	1.25	1.56	1.11	1.49
Pu241	0.35	0.72	0.62	1.23	3.99	8.01	0.83	1.55	1.19	2.44	2.04	2.33	2.02	2.55
Pu242	0.13	0.22	0.25	0.40	2.75	4.66	0.51	0.84	0.35	0.55	4.75	5.03	3.87	4.47
Am241	0.08	0.13	0.18	0.30	2.12	3.78	0.35	0.60	0.27	0.45	2.13	2.40	2.50	2.94
Am242m	0.47	0.86	0.70	1.40	4.26	8.36	2.17	3.85	1.17	2.22	5.63	7.21	5.41	7.50
Am243	0.35	0.55	0.47	0.76	6.41	10.87	1.07	1.81	0.91	1.46	5.58	5.93	4.48	5.04
Cm242	1.13	1.91	1.38	2.36	1.58	2.87	2.43	4.27	2.49	4.11	1.88	2.15	1.87	2.36
Cm243	1.30	2.53	1.90	3.77	10.59	20.63	3.91	6.51	3.29	6.37	8.37	11.80	5.50	7.56
Cm244	0.38	0.59	0.73	1.10	4.83	7.67	0.91	1.54	0.88	1.28	6.01	6.42	4.77	5.33
Cm245	0.90	1.69	1.47	2.91	9.37	18.15	1.83	3.60	2.35	4.54	8.02	8.76	6.84	7.51
Cm246	0.51	0.89	0.47	0.77	4.48	7.45	1.35	2.56	0.57	0.89	-	-	-	-

Summary Fuel Cycle Performance

- Yucca Mountain repository capacity is dominated by long term heat load (Pu238, Pu239, Am241)
- Neutron source of recycle materials has strong implication for fabrication costs and non-proliferation (Cm244)
- Radiotoxicity is key measure for environmental benefits (Pu239)

Uncertainties on fuel cycle parameters are small:

- Decay heat and dose less than a percent in many cases
- Neutron source a few percents for EFR, VHTR and PWR
- Minor Actinide final density uncertainties significant only in few cases

Target Accuracy Assessment

Fast Systems

Multiplication factor (BOL)	300 pcm
Power peak (BOL)	2%
Burnup reactivity swing	300 pcm
Reactivity coefficients (Coolant void and Doppler - BOL)	7%
Major nuclide density at end of irradiation cycle	2%
Other nuclide density at end of irradiation cycle	10%

VHTR (Source AREVA-NP)

Criticality	300 pcm (operation); 500 pcm (safety)
Local power (in fuel compact)	6% (2% in pin-wise fission rate of fresh fuel; 4% in main fissile isotope conc. of irradiated fuel)
Burnup (cycle length)	1% ($\Rightarrow \sim 500$ MWd/t)
Doppler coefficient	20%
Moderator temperature coefficient	1 pcm/$^{\circ}$C
Nuclide inventories at EOL	
Main fissile isotopes	4%
Fertile isotopes	5%
MA's and FPs	20%

PWR

k_{eff}	Doppler Reactivity Coefficient	Burnup $\Delta\rho$	Transmutation
0.5%	10%	500 pcm	5%



Idaho National Laboratory

Integral parameter Uncertainties Uncertainties (%)

	ABTR	SFR	EFR	GFR	LFR	ADMAB	VHTR	PWR
k_{eff} BOC	0.62	1.04	0.79	1.24	0.88	1.95	0.37	0.36
k_{eff} EOC	-	-	-	-	-	-	0.41	0.64
Power Peak BOC	0.32	0.31	0.81	1.18	0.45	14.22	0.85	-
Power Peak EOC	-	-	-	-	-	-	0.90	-
Doppler BOC	2.86	3.62	2.46	3.62	2.85	-	4.27	1.53
Doppler EOC	-	-	-	-	-	-	2.77	2.01
Void	5.11	15.66	6.68	5.46	4.97	13.11	-	-
Burnup [pcm]	37.4	152.1	584.9	254.2	127.7	602.9	487.0	684.6
$N_{f,U235}$	0.07	0.31	2.57	0.42	0.36	-	0.25	0.46
$N_{f,U238}$	0.01	0.02	0.24	0.04	0.03	-	0.05	0.04
$N_{f,Np237}$	0.25	0.11	2.51	0.25	0.18	0.20	1.03	1.05
$N_{f,Pu238}$	0.21	0.42	2.71	0.64	0.56	1.13	1.28	1.05
$N_{f,Pu239}$	0.04	0.06	1.13	0.37	0.20	0.12	0.96	0.88
$N_{f,Pu240}$	0.13	0.10	1.25	0.31	0.16	0.26	1.25	1.11
$N_{f,Pu241}$	0.35	0.62	3.99	0.83	1.19	0.90	2.04	2.02
$N_{f,Pu242}$	0.13	0.25	2.75	0.51	0.35	0.54	4.75	3.87
$N_{f,Am241}$	0.08	0.18	2.12	0.35	0.27	0.31	2.13	2.50
$N_{f,Am242m}$	0.47	0.70	4.26	2.17	1.17	1.72	5.63	5.41
$N_{f,Am243}$	0.35	0.47	6.41	1.07	0.91	0.27	5.58	4.48
$N_{f,Cm242}$	1.13	1.38	1.58	2.43	2.49	2.78	1.88	1.87
$N_{f,Cm243}$	1.30	1.90	10.59	3.91	3.29	3.04	8.37	5.50
$N_{f,Cm244}$	0.38	0.73	4.83	0.91	0.88	1.07	6.01	4.77
$N_{f,Cm245}$	0.90	1.47	9.37	1.83	2.35	2.48	8.02	6.84
$N_{f,Cm246}$	0.51	0.47	4.48	1.35	0.57	3.12	-	-

Target Accuracy Assessment: VHTR

Isotope	Cross-Section	Energy Range	Uncertainty (%)	
			Initial	Required ($\lambda=1$)
U238	σ_{capt}	454 - 22.6 eV	1.7	1.2
C	σ_{inel}	19.6 - 6.07 MeV	30.0	7.1
C	σ_{capt}	19.6 - 6.07 MeV	20.0	7.1
		4 - 0.54 eV	20.0	5.0
Pu239	σ_{capt}	0.54eV - 0.1eV	1.4	0.9
Pu241	σ_{fiss}	454 - 22.6 eV	19.4	6.4
		4 - 0.54 eV	26.8	9.4
		0.54eV - 0.1eV	2.9	1.5
Pu241	σ_{capt}	0.54eV - 0.1eV	6.8	2.4

Target Accuracy Assessment: PWR

Isotope	Cross-Section	Energy Range	Uncertainty (%)	
			Initial	Required ($\lambda=1$)
O	σ_{capt}	19.6 - 6.07 MeV	100.0	12.1
		6.07 - 2.23 MeV	100.0	9.9
Pu241	σ_{fiss}	454 - 22.6 eV	19.4	4.7
		4 - 0.54 eV	26.8	7.7
		0.54eV - 0.1eV	2.9	1.7
		0.1eV - thermal	3.3	1.9
Pu239	σ_{capt}	0.54eV - 0.1eV	1.4	1.0
U238	σ_{capt}	24.8 - 9.12 keV	9.4	4.6
		454 - 22.6 eV	1.7	1.4
U238	σ_{inel}	6.07 - 2.23 MeV	14.6	5.1
Pu241	σ_{capt}	0.54eV - 0.1eV	6.8	3.0
Pu240	σ_{capt}	0.1eV - thermal	4.8	3.1
O	σ_{inel}	6.07 - 2.23 MeV	54.9	12.6
		19.6 - 6.07 MeV	84.6	15.6

Target Accuracy Assessment: ABTR

Isotope	Cross-Section	Energy Range	Uncertainty (%)		
			Initial	Required	
				$\lambda=1$	$\lambda \neq 1$ case B ^(a)
U238	σ_{inel}	6.07 - 2.23 MeV	19.8	3.3	5.8
		2.23 - 1.35 MeV	20.6	3.6	6.3
		1.35 - 0.498 MeV	11.6	6.5	11.4
U238	σ_{capt}	24.8 - 9.12 keV	9.4	2.9	1.6
Pu239	σ_{capt}	498 - 183 keV	11.6	5.7	3.2
		183 - 67.4 keV	9.0	5.0	2.8
		67.4 - 24.8 keV	10.1	5.8	3.2
		9.12 - 2.04 keV	15.5	7.4	4.1
Pu241	σ_{fiss}	183 - 67.4 keV	19.9	8.8	7.0
Fe56	σ_{inel}	2.23 - 1.35 MeV	25.4	5.6	9.9
		1.35 - 0.498 MeV	16.1	7.5	13.1
Na23	σ_{inel}	1.35 - 0.498 MeV	28.0	10.1	17.7

	$\lambda=1$	$\lambda \neq 1$ case A	$\lambda \neq 1$ case B
$\lambda_{\text{capt,fiss,v}}$ (U235,U238,Pu239)	1	1	1
$\lambda_{\text{capt,fiss,v}}$ (other fissiles)	1	2	2
λ_{capt} (structurals)	1	1	1
λ_{el} (fissiles and structurals)	1	1	1
λ_{inel} (fissiles and structurals)	1	3	10



Idaho National Laboratory

Target Accuracy Assessment: SFR

Isotope	Cross-Section	Energy Range	Uncertainty (%)	
			Initial	Required ($\lambda=1$)
Pu241	σ_{fiss}	1.35 - 0.498 MeV	16.6	3.4
		498 - 183 keV	13.5	2.6
		183 - 67.4 keV	19.9	2.6
		24.8 - 9.12 keV	11.3	3.5
		2.04 - 0.454 keV	12.7	4.4
Fe56	σ_{inel}	2.23 - 1.35 MeV	25.4	3.3
		1.35 - 0.498 MeV	16.1	3.2
Na23	σ_{inel}	1.35 - 0.498 MeV	28.0	4.0
Cm244	σ_{fiss}	1.35 - 0.498 MeV	50.0	5.1
Am242m	σ_{fiss}	1.35 - 0.498 MeV	16.5	4.2
		498 - 183 keV	16.6	3.1
		183 - 67.4 keV	16.6	3.1
		67.4 - 24.8 keV	14.4	4.0
		24.8 - 9.12 keV	11.8	4.2
		2.04 - 0.454 keV	12.2	5.1
Pu240	σ_{fiss}	1.35 - 0.498 MeV	5.8	1.8
Pu240	ν	1.35 - 0.498 MeV	3.7	1.5
Pu238	σ_{fiss}	2.23 - 1.35 MeV	33.8	5.6
		1.35 - 0.498 MeV	17.1	3.3
		498 - 183 keV	17.1	3.6
Pu238	ν	1.35 - 0.498 MeV	7.0	2.7
Pu242	σ_{fiss}	2.23 - 1.35 MeV	21.4	4.9
		1.35 - 0.498 MeV	19.0	3.5
Cm245	σ_{fiss}	183 - 67.4 keV	47.5	6.7
Pu242	σ_{capt}	24.8 - 9.12 keV	38.6	8.4
U238	σ_{capt}	24.8 - 9.12 keV	9.4	4.3
Fe56	σ_{capt}	2.04 - 0.454 keV	11.2	5.3



Idaho National Laboratory

Target Accuracy Assessment: EFR

Isotope	Cross-Section	Energy Range	Uncertainty (%)	
			Initial	Required ($\lambda=1$)
U238	σ_{inel}	6.07 - 2.23 MeV	19.8	3.7
		2.23 - 1.35 MeV	20.6	4.0
		1.35 - 0.498 MeV	11.6	5.0
U238	σ_{capt}	24.8 - 9.12 keV	9.4	2.9
O16	σ_{capt}	19.6 - 6.07 MeV	100.0	14.2
		6.07 - 2.23 MeV	100.0	10.9
Fe56	σ_{inel}	2.23 - 1.35 MeV	25.4	6.6
		1.35 - 0.498 MeV	16.1	8.4
Pu241	σ_{fiss}	1.35 - 0.498 MeV	16.6	8.0
		498 - 183 keV	13.5	6.7
		183 - 67.4 keV	19.9	5.7
		67.4 - 24.8 keV	8.7	6.2
		24.8 - 9.12 keV	11.3	6.8
		9.12 - 2.04 keV	10.4	7.6
		2.04 - 0.454 keV	12.7	6.9
Pu240	σ_{fiss}	1.35 - 0.498 MeV	5.8	3.5
Pu239	σ_{capt}	183 - 67.4 keV	9.0	7.0
		67.4 - 24.8 keV	10.1	6.7
		24.8 - 9.12 keV	7.4	6.1
		9.12 - 2.04 keV	15.5	5.6
Na23	σ_{inel}	1.35 - 0.498 MeV	28.0	7.9
Pu240	σ_{capt}	498 - 183 keV	14.3	8.9
		183 - 67.4 keV	13.8	6.7
		67.4 - 24.8 keV	11.3	6.1
		24.8 - 9.12 keV	10.2	6.5



Idaho National Laboratory

Target Accuracy Assessment: GFR

Isotope	Cross-Section	Energy Range	Uncertainty (%)	
			Initial	Required ($\lambda=1$)
U238	σ_{inel}	6.07 - 2.23 MeV	19.8	1.6
		2.23 - 1.35 MeV	20.6	1.8
		1.35 - 0.498 MeV	11.6	2.4
U238	σ_{capt}	24.8 - 9.12 keV	9.4	1.6
		9.12 - 2.04 keV	3.1	1.4
Pu241	σ_{fiss}	1.35 - 0.498 MeV	16.6	3.5
		498 - 183 keV	13.5	3.1
		183 - 67.4 keV	19.9	2.5
		67.4 - 24.8 keV	8.7	2.5
		24.8 - 9.12 keV	11.3	2.6
		9.12 - 2.04 keV	10.4	2.2
		2.04 - 0.454 keV	12.7	2.8
Pu239	σ_{capt}	9.12 - 2.04 keV	15.5	2.8
Si28	σ_{capt}	19.6 - 6.07 MeV	52.9	5.6
Si28	σ_{inel}	6.07 - 2.23 MeV	13.5	3.0
		2.23 - 1.35 MeV	50.0	5.8
C	σ_{el}	1.35 - 0.498 MeV	5.0	1.7
Pu242	σ_{fiss}	1.35 - 0.498 MeV	19.0	4.0
Pu240	σ_{fiss}	1.35 - 0.498 MeV	5.8	2.2
Am241	σ_{fiss}	6.07 - 2.23 MeV	11.7	3.3

Target Accuracy Assessment: LFR

Isotope	Cross-Section	Energy Range	Uncertainty (%)	
			Initial	Required ($\lambda=1$)
U238	σ_{inel}	6.07 - 2.23 MeV	19.8	2.8
		2.23 - 1.35 MeV	20.6	2.3
		1.35 - 0.498 MeV	11.6	2.1
Pu241	σ_{fiss}	1.35 - 0.498 MeV	16.6	3.7
		498 - 183 keV	13.5	2.6
		183 - 67.4 keV	19.9	2.6
B10	σ_{capt}	498 - 183 keV	15.0	2.4
		183 - 67.4 keV	10.0	2.3
		67.4 - 24.8 keV	10.0	2.7
U238	σ_{capt}	24.8 - 9.12 keV	9.4	2.0
Pu240	σ_{fiss}	1.35 - 0.498 MeV	5.8	1.6
Pu240	ν	1.35 - 0.498 MeV	3.7	1.3
Pu238	σ_{fiss}	1.35 - 0.498 MeV	17.1	3.3
		498 - 183 keV	17.1	3.4
Fe56	σ_{inel}	2.23 - 1.35 MeV	25.4	4.2
		1.35 - 0.498 MeV	16.1	3.6
Pb206	σ_{inel}	2.23 - 1.35 MeV	14.2	3.3
Pb207	σ_{inel}	1.35 - 0.498 MeV	11.3	3.0
Pu242	σ_{fiss}	1.35 - 0.498 MeV	19.0	3.9
Cm244	σ_{fiss}	1.35 - 0.498 MeV	50.0	6.4

Summary on Target Accuracy requirements

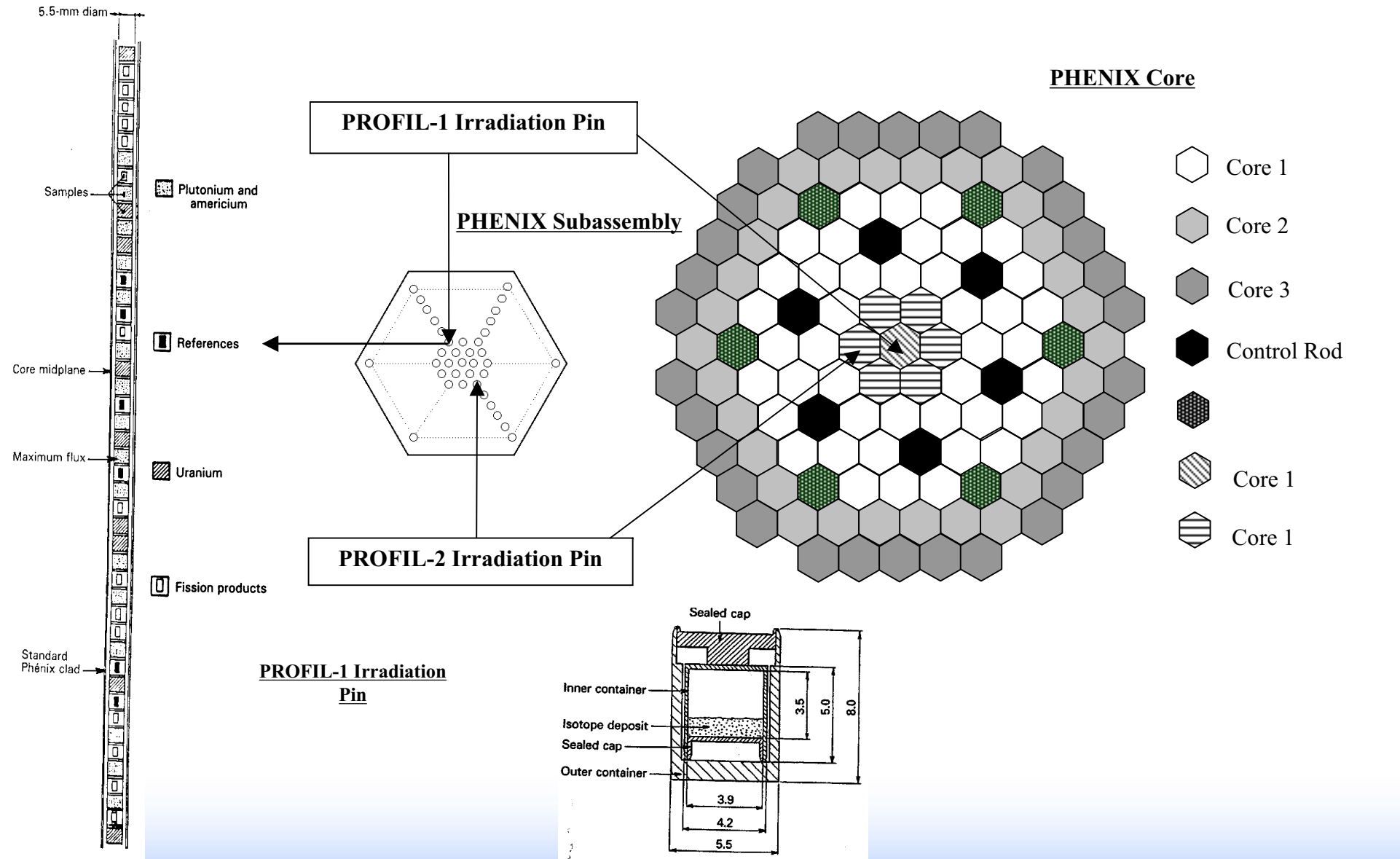
- As expected from the results of the uncertainty analysis, very tight requirements are shown for the σ_{inel} of U-238 (2-3%), Fe-56 (3-6%), Na-23 (4-10%) and even for Pb isotopes. Some of the required accuracies are probably beyond achievable limits with current experimental techniques. There are little margins to relax the requirements on σ_{inel} if one does not want to produce comparably difficult requirements on some Pu isotope σ_{fiss} and σ_{capt} .
- The accuracy requirements for Pu isotopes are very tight (very often <2-3%). As for σ_{capt} , the requirements for U-238 and Pu-239 aim to cut by more than a factor of 2 the current uncertainties. The requirement for improved accuracy of the higher Pu isotopes, and in particular the fission of Pu-241, is more stringent for the EFR, GFR and LFR cases.
- In the case of MA, uncertainties improvements for selected isotopes and reactions in some cases are very significant. However, this is the case when MA play an important role in the critical balance, as for MA dedicated burner with a fuel heavily loaded with MA (SFR). For these very specific cases, the accuracy requirement for σ_{fiss} of selected MA isotopes can range from 3 to 7%.
- A few specific requirements are indicated according to specificities of some cores, e.g., Si data requirements for the GFR and Pb data for the LFR
- The present analysis indicates some important requirements also in the case of the VHTR. For this system it is required to improve Pu-241 σ_{fiss} below ~400 eV. Very tight σ_{capt} requirements for Pu-239 and Pu-241 below ~0.5 eV are also identified, together with C data improvements (both capture and inelastic) with respect to current uncertainty estimates. Finally, for the PWR with extended burn up, the requirements to improve Pu-241 and some O data have been specified.

USE OF INTEGRAL EXPERIMENTS

- The advanced nuclear systems and associated fuel cycles will need good quality cross section data to provide a reliable assessment of their performance. Basic data are available for transuranics (TRU) isotopes (up to Cf) but a validation is needed in order to quantify their reliability. The information that can be gathered on minor actinides (MA) from experiments comes mostly from small sample irradiation, reactivity oscillation, and fission and capture rates measurements. Separate isotope sample and fuel pin irradiation in power reactors provides a unique source of very useful measurements.
- The experimental data of the PROFIL and TRAPU irradiation experiments, performed at the CEA fast reactor PHENIX, provide very clean and useful information on both cross section data and transmutation rates of actinides. These data are essential for the validation of the methods and data to be used by the AFCI program where transmuter systems will be used to reduce the existing inventory of nuclear waste.

PROFIL-1

During the PROFIL-1 experiment performed in 1974 a pin containing 46 samples of pure isotopes, including fission products, major and minor actinides (Uranium, Plutonium, and Americium isotopes) was irradiated in the PHENIX fast reactor for the first three cycles, corresponding to a total of 189.2 full-power days. The experimental pin was located in the central subassembly of the core, and in the third row of pins inside the subassembly. This location is far away from neutronic perturbations allowing clear irradiation conditions. Following the in reactor irradiation, mass spectroscopy was then used, with simple or double isotopic dilution and well-characterized tracers to measure concentrations. The experimental uncertainty obtained with this method was relatively small (maximum of 3%).



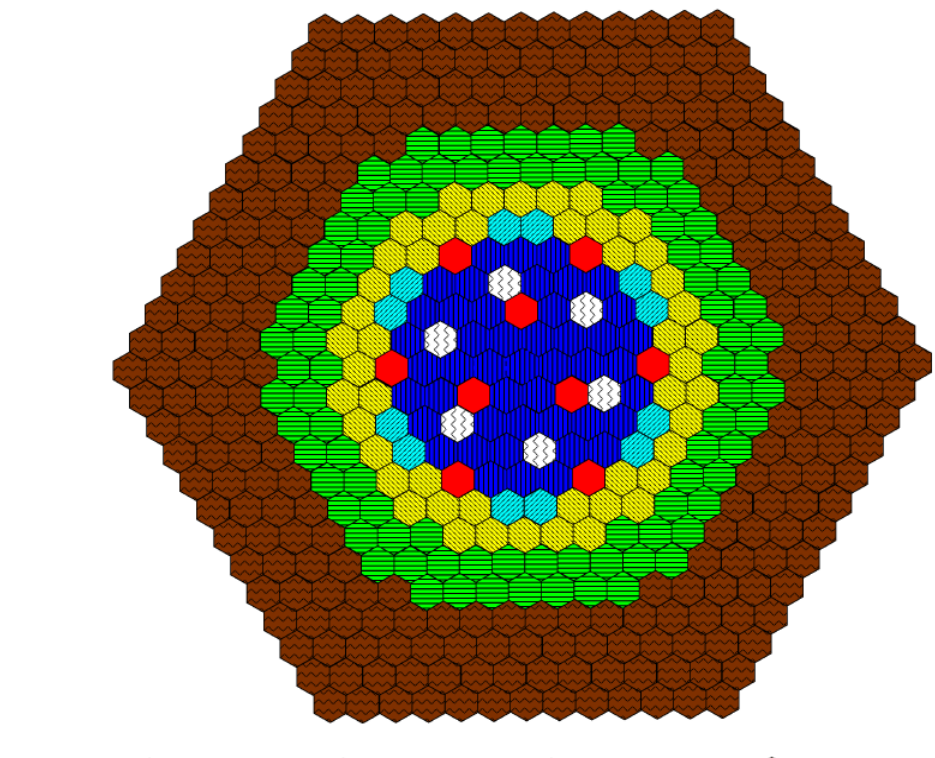
Calculational Scheme

- Cross sections in a 33-group energy structure were generated using the ECCO cell codes (with JEF2.2, JEF3.0, ENDF/B-V, ENDF/B-VI, and ENDF/B-VII data) with a fine description of the experimental subassembly. Three-dimensional transport calculation have been carried out in order to obtain the fluxes at the position of the irradiated pins. With these fluxes, one-group cross sections have been generated by condensing the 33-group structure cross sections coming from the cell calculation.
- In order to correctly normalize the results to the actual value of the flux (and hence eliminate the uncertainty in the total burnup), the production of Nd in the ^{235}U samples has been calculated and compared with the correspondent experimental values. Correcting factors have been obtained and applied to the values of the fluxes used in the time-dependent calculations .
- Time dependent calculations were subsequently performed with the NUTS code in order to obtain isotope concentrations at the end of irradiation.



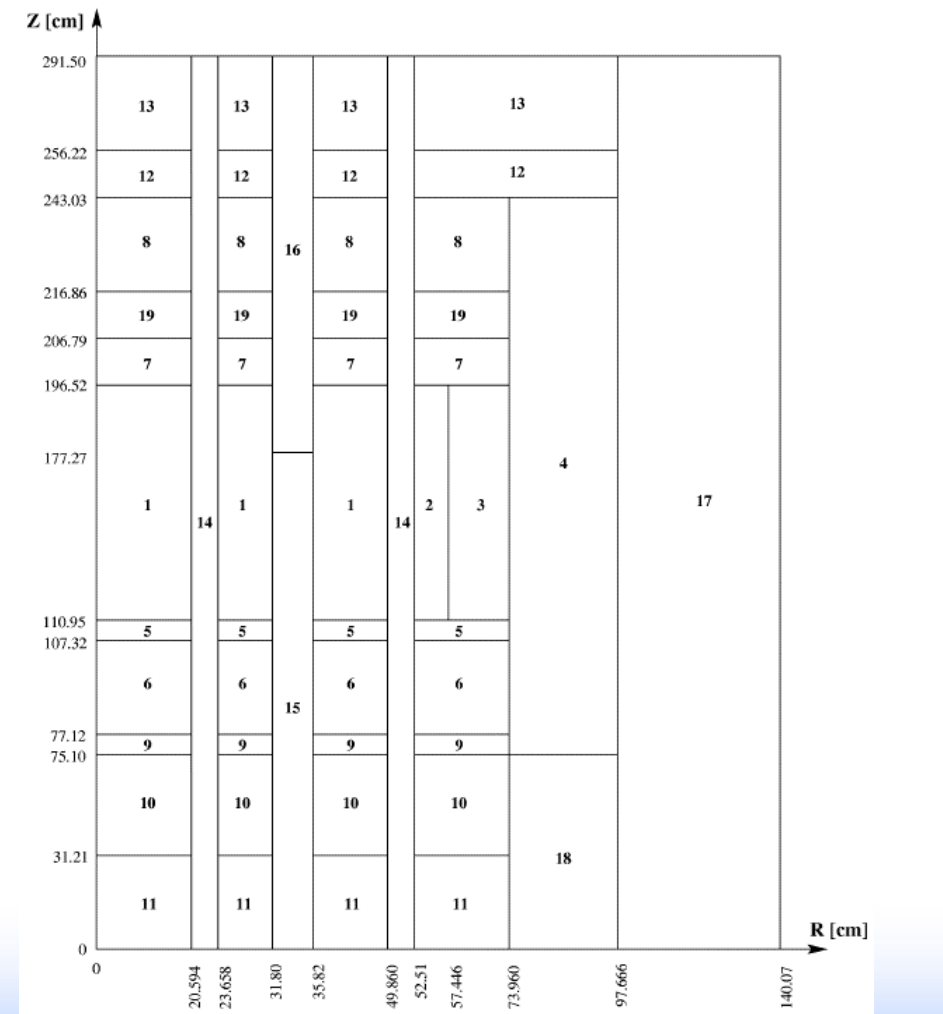
Idaho National Laboratory

PHOENIX Three-dimensional model PROFIL-2



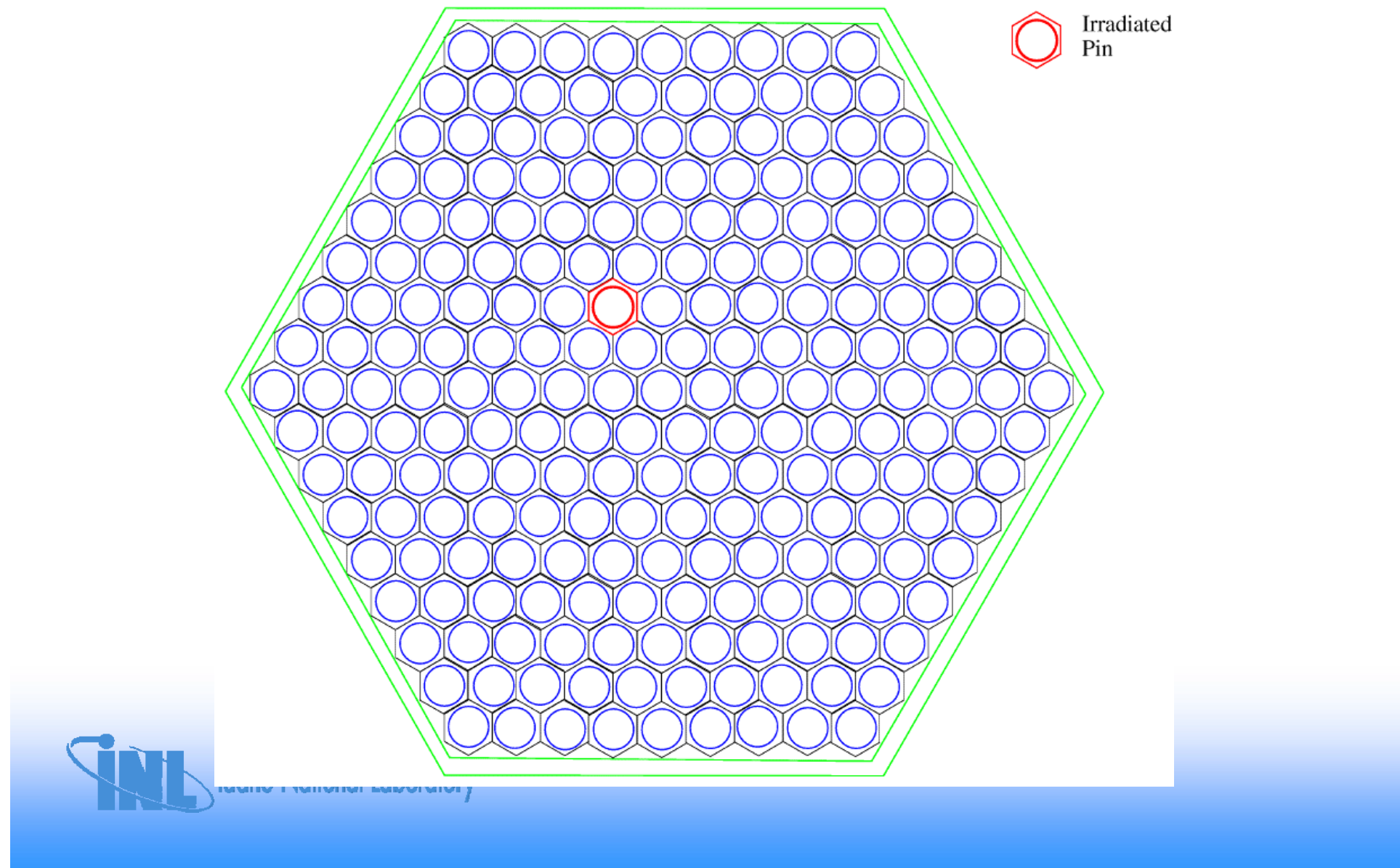
Legend:

	CORE 1		CORE 3		CONTROL ROD		REFLECTOR
	CORE 2		DILUENT MEDIUM		RADIAL		



Idaho National Laboratory

PHOENIX subassembly model PROFIL-1



Calculational Scheme

- A slightly different approach has been applied in order to derive the C/E's. In the past it was used:

$$\sigma_{(c),A} \cdot \tau \cdot f(\tau) \approx \frac{\Delta N_{A+1}}{N_A} = \frac{N_{A+1}(\tau)}{N_A(\tau)} - \frac{N_{A+1}(0)}{N_A(0)}$$

$$f(\tau) = \left[\frac{N_{A+1}^{(\tau)}}{N_A^{(\tau)}} - \frac{N_{A+1}^{(0)}}{N_A^{(0)}} \right] \times \frac{1}{\sigma_{CA} \cdot \tau_{\text{calc.}}}$$

- In the new approach we correct the experimental density variation by a calculated quantity that takes out the variation due to all the phenomena other than the reaction rate that we are considering:

$$\sigma_{(c),A} \cdot \tau \cdot \cong \frac{\overset{\text{corr}}{\Delta N}_{A+1}}{N_A} = \frac{\overset{\text{exp}}{\Delta N}_{A+1}(\tau) - (\overset{\text{calc}}{\Delta N}_{A+1} - N_A^{(0)} e^{-\sigma\tau})}{N_A}$$

PROFIL-1

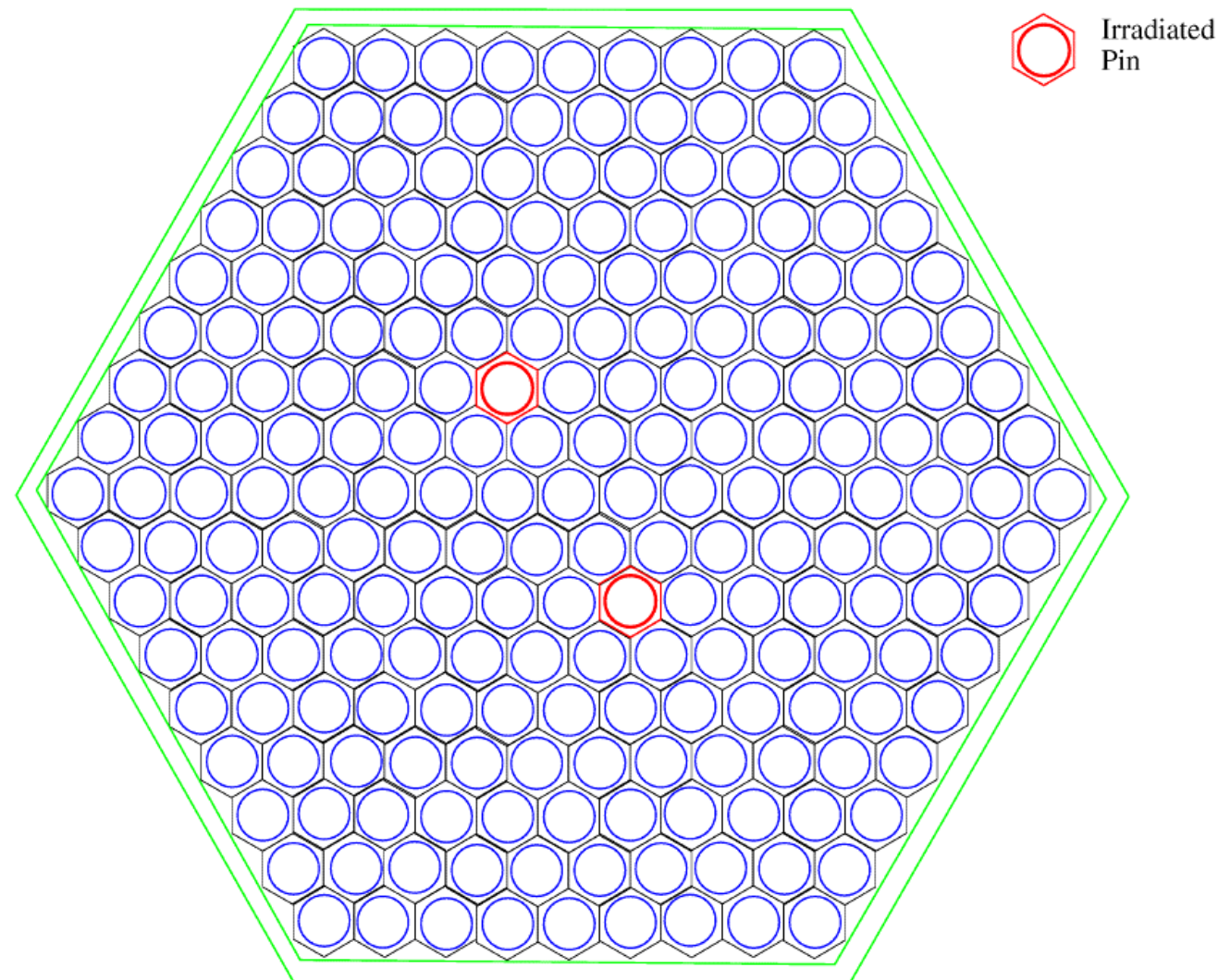
Data Type	C/E					Exp. Unc.
	JEF2.2	JEF3.0	ENDF/B-V	ENDF/B-VI	ENDF/B-VII	
σ_{capt} U-235	0.95	0.98	1.01	0.96	1.02	1.7 %
$\sigma_{n,2n}$ U-235	0.70	0.76	0.47	0.70	0.82	5.0 %
σ_{capt} U-238	0.99	0.99	1.03	0.99	1.02	2.3 %
σ_{capt} Pu-238	0.98	0.96	1.32	1.71		4.0 %
σ_{capt} Pu-239	0.98	0.96	0.97	0.94	0.97	3.0 %
$\sigma_{n,2n}$ Pu-239	0.62	0.97	0.63	1.20	0.80	15.0 %
σ_{capt} Pu-240	1.11	1.00	1.06	0.98		2.2 %
σ_{capt} Pu-241	1.18	1.01	0.98	0.83		4.1 %
σ_{capt} Pu-242	1.18	1.18	1.08	1.07		3.5 %
σ_{capt} Am-241	1.05	1.05	0.94	0.90		1.7 %
σ_{capt} Am-243	0.99	0.99	0.62	0.85		5.0 %
σ_{capt} Mo-95	1.04	1.08	-	2.26		3.8 %
σ_{capt} Mo-97	0.99	1.00	-	1.22		4.4 %
σ_{capt} Ru-101	1.06	1.06	1.13	1.10		3.6 %
σ_{capt} Pd-105	0.87	0.87	0.84	0.82		4.0 %
σ_{capt} Cs-133	0.98	0.95	1.01	0.99		4.7 %
σ_{capt} Nd-145	1.18	1.17	1.02	1.07		3.8 %
σ_{capt} Sm-149	1.11	0.97	1.14	1.14		3.1 %



PROFIL-2

The second part of the PROFIL irradiation campaign took place in 1979. During the experiment two standard pins, each containing 42 separated capsules of fission products, major and minor actinides (Uranium, Plutonium, Americium and Neptunium isotopes), were irradiated for four cycles (from 17th to 20th) in the fast neutron spectrum reactor PHENIX in France. The experimental pins were located in the second row of the core and in the two experimental pins in the third row of the subassembly). Chemical and mass spectrometry analyses have been subsequently performed to determine the post-irradiation isotopic concentrations

PHOENIX subassembly model PROFIL-2

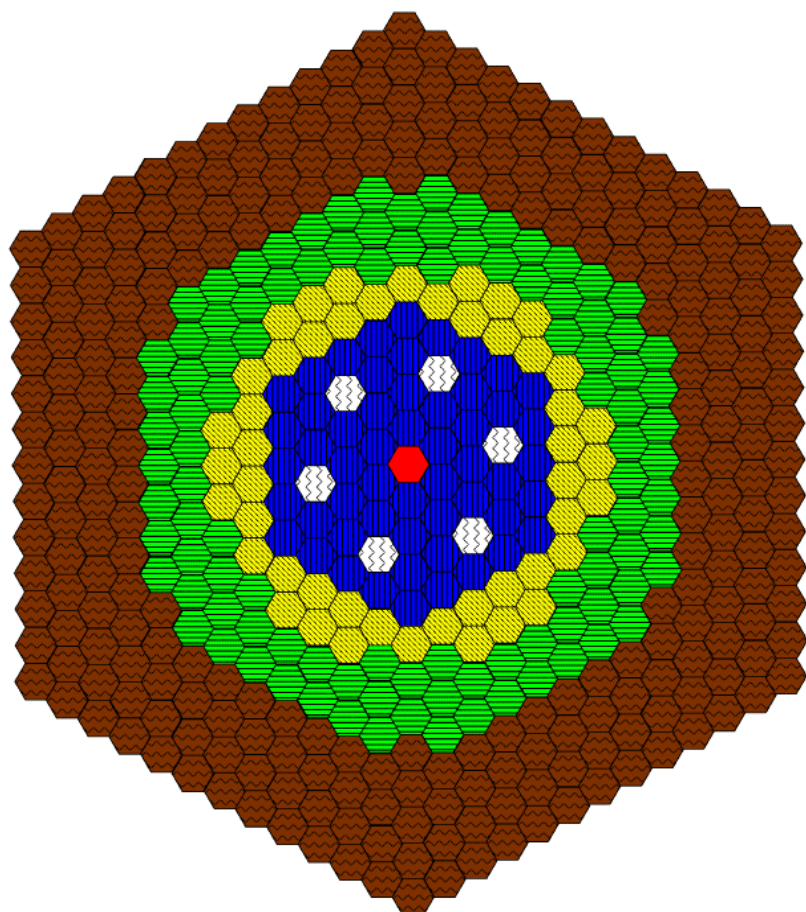


 Irradiated Pin



Idaho National Laboratory

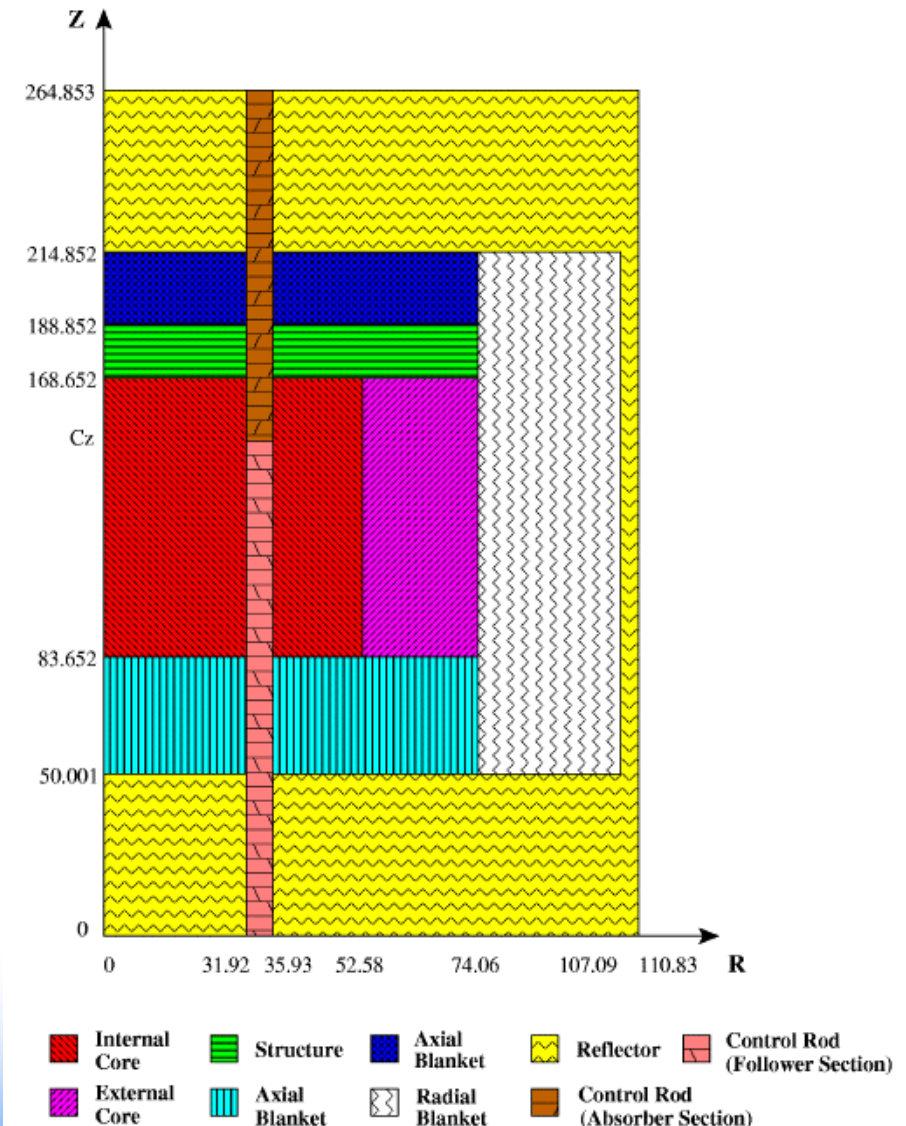
PHOENIX Three-dimensional model PROFIL-2



INTERNAL
CORE
EXTERNAL
CORE

CONTROL
ROD
SAC

REFLECTOR
RADIAL
BLANKET



PROFIL-2

Data Type	C/E					Exp. Unc.
	JEF2.2	JEF3.0	ENDF/B-V	ENDF/B-VI	ENDF/B-VII	
σ_{capt} U-235	0.96	0.99	0.97	0.96	1.01	1.7 %
$\sigma_{n,2n}$ U-235	0.71	0.68	0.41	0.62	0.72	5.0 %
σ_{capt} U-238	1.01	1.01	1.00	1.00	1.03	2.3 %
σ_{capt} Pu-238	0.99	0.98	1.28	1.73		4.0 %
σ_{capt} Pu-239	0.98	0.96	0.92	0.94	0.98	3.0 %
$\sigma_{n,2n}$ Pu-239	0.57	0.74	0.52	0.90	0.60	15.0 %
σ_{capt} Pu-240	1.07	0.97	0.97	0.94		2.2 %
σ_{capt} Am-241	1.05	1.05	0.93	0.93		1.7 %
σ_{capt} Np-237	0.95	0.95	0.97	0.93	0.94	3.6 %



Idaho National Laboratory

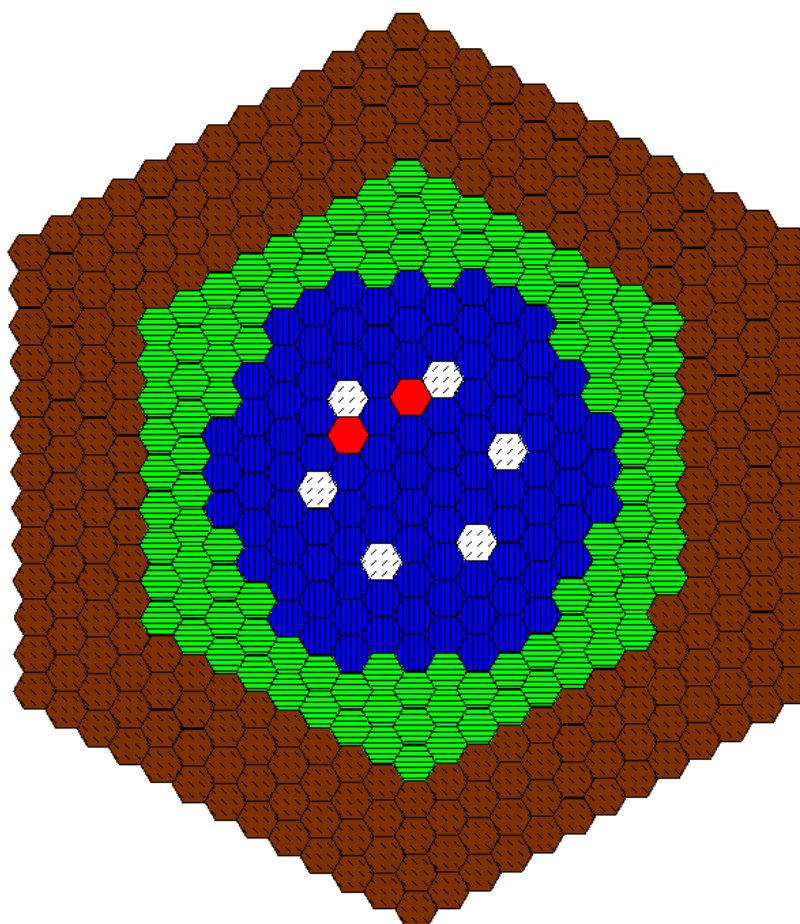
TRAPU

- The TRAPU experiment consisted of a six-cycle irradiation(10th to 15th) of mixed-oxide pins that contained plutonium of different isotopic compositions but heavily charged in the higher isotopes (Pu240, Pu241 and Pu242) compared to typical PHOENIX fuel. Standard pins were placed in regular PHOENIX subassemblies located in the third row of the reactor. Three types of plutonium containing pins were used.
- After irradiation, small samples (20 mm high) were cut from the experimental pins (both fuel and clad) and put into a solution in order to determine the fuel composition by nuclide. Neodymium-148 was used as burnup indicator since it is a stable fission product with a small capture cross section, and it enables determination of the number of fission reactions that have taken place in the sample. Mass spectrometry was then used, with simple or double isotopic dilution and well-characterized tracers.

Plutonium Isotopic Compositions of the Three TRAPU Fuel Pins

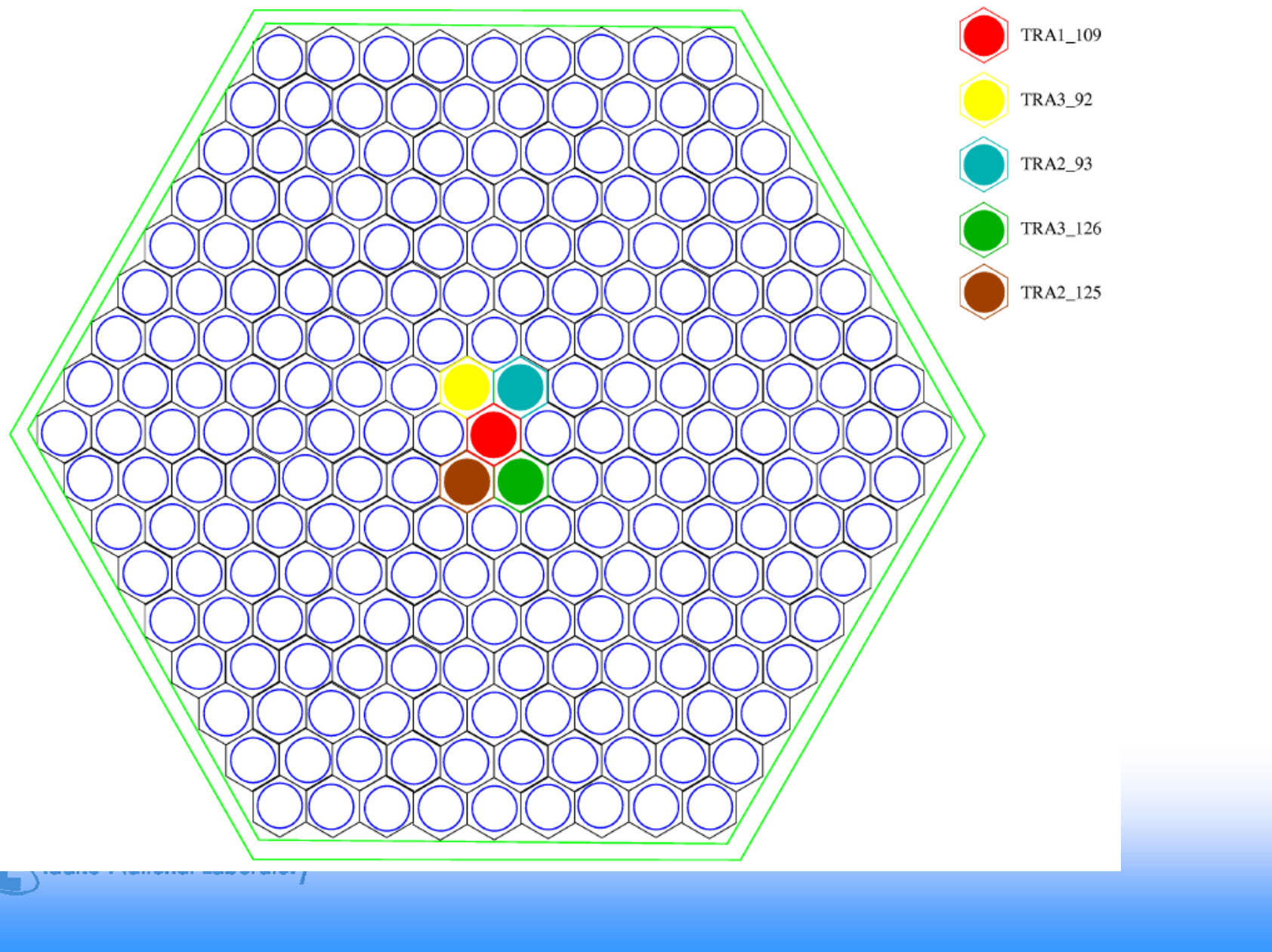
		Isotope Composition [%]				
EXPERIMENT		Pu-238	Pu-239	Pu-240	Pu-241	Pu-242
	TRAPU-I	0.1	73.3	21.9	4.0	0.7
	TRAPU-II	0.8	71.4	18.5	7.4	1.9
	TRAPU-III	0.2	34.0	49.4	10.0	6.4

TRAPU Calculational Model



Idaho National Laboratory

TRAPU Experimental Subassembly



TRAPU-I C/E's

Isotope	JEF 2.2	JEF 3.0	ENDF/B-V	ENDF/B-VI	ENDF/B-VII	Exp. Unc.
U-234	0.98	0.98	0.99	0.97	0.97	± 3.9%
U-235	1.01	1.01	1.01	1.01	1.00	± 0.4%
U-236	0.92	0.96	0.95	0.93	0.97	± 0.8%
Np-237	0.80	0.86	0.83	0.78	0.93	± 6.8%
Pu-238	1.00	1.00	0.94	0.91	0.92	± 1.5%
Pu-239	1.02	1.02	1.03	1.02	1.02	± 0.6%
Pu-240	1.00	1.00	0.99	0.99	1.00	± 0.6%
Pu-241	1.05	1.01	1.03	1.01	1.01	± 0.6%
Pu-242	1.11	1.05	1.04	0.99	0.99	± 0.8%
Am-241	0.97	0.95	0.99	0.99	0.99	± 3.2%
Am-242M	1.03	1.02	0.87	0.85	0.85	± 3.8%
Am-243	1.08	1.04	0.96	0.91	0.92	± 2.6%
Cm-242	1.02	1.01	0.94	0.92	0.92	± 3.9%
Cm-243	-	-	-	-	-	-
Cm-244	1.01	0.98	0.53	0.73	0.73	± 2.1%



Idaho National Laboratory

TRAPU-II C/E's

Isotope	JEF 2.2	JEF 3.0	ENDF/B-V	ENDF/B-VI	ENDF/B-VII	Exp. Unc.
U-234	1.00	1.00	0.99	0.99	0.98	± 3.8%
U-235	1.03	1.03	1.03	1.03	1.02	± 0.4%
U-236	0.94	0.98	0.97	0.95	0.99	± 1.0%
Np-237	0.80	0.85	0.83	0.78	0.92	± 3.3%
Pu-238	1.01	1.00	0.96	0.92	0.92	± 1.0%
Pu-239	1.00	1.00	1.01	1.00	1.01	± 0.5%
Pu-240	0.98	0.98	0.97	0.97	0.98	± 0.6%
Pu-241	1.01	0.99	1.01	1.00	1.01	± 0.6%
Pu-242	1.06	1.01	1.01	0.98	0.98	± 0.6%
Am-241	0.97	0.97	1.00	1.01	1.01	± 3.9%
Am-242M	1.06	1.06	0.90	0.88	0.88	± 4.3%
Am-243	1.04	1.01	0.94	0.90	0.90	± 3.1%
Cm-242	1.00	0.99	0.93	0.91	0.91	± 3.1%
Cm-243	0.75	0.67	0.41	0.42	0.43	± 3.1%
Cm-244	1.12	1.10	0.60	0.82	0.82	± 2.3%

TRAPU-III C/E's

Isotope	JEF 2.2	JEF 3.0	ENDF/B-V	ENDF/B-VI	ENDF/B-VII	Exp. Unc.
U-234	1.05	1.04	1.02	1.02	1.01	± 4.6%
U-235	1.03	1.02	1.03	1.03	1.02	± 0.4%
U-236	0.95	0.98	0.97	0.96	0.99	± 0.9%
Np-237	0.77	0.81	0.79	0.75	0.89	± 3.2%
Pu-238	1.03	1.02	0.95	0.91	0.91	± 1.6%
Pu-239	1.00	1.00	1.01	1.00	1.01	± 0.4 %
Pu-240	0.99	1.00	0.99	1.00	1.00	± 0.6%
Pu-241	1.03	1.00	1.02	1.01	1.01	± 0.6%
Pu-242	1.03	1.01	1.01	0.99	0.99	± 0.6%
Am-241	0.98	0.97	1.01	1.01	1.01	± 2.6%
Am-242M	1.05	1.04	0.89	0.87	0.87	± 3.1%
Am-243	1.07	1.05	0.99	0.96	0.96	± 2.5%
Cm-242	1.00	0.99	0.93	0.91	0.91	± 2.7%
Cm-243	0.75	0.68	0.41	0.43	0.43	± 3.2%
Cm-244	1.14	1.12	0.62	0.85	0.85	± 1.8%

TRAPU-II Sensitivity Coefficients

Basic Data	Isotope build-up						
	234U	235U	236U	237Np	238Pu	239Pu	240Pu
$^{234}\text{U } \sigma_{\text{cap}}$	-10	0.2					
$^{234}\text{U } \sigma_{\text{fis}}$	-6						
$^{235}\text{U } \sigma_{\text{cap}}$		-10.8	90	9.7	0.2		
$^{235}\text{U } \sigma_{\text{fis}}$	-0.2	-36.2	-16.2	-1.2			
$^{236}\text{U } \sigma_{\text{cap}}$			-5.7	10.5	0.2		
$^{238}\text{U } \sigma_{\text{cap}}$				-2.3		26.7	3.9
$^{238}\text{U } \sigma_{(n,2n)}$	0.1			82.5	1.8		
$^{237}\text{Np } \sigma_{\text{cap}}$	0.2			-14.0	1.9		
$^{238}\text{Pu } \sigma_{\text{cap}}$	-1.1				-8.0		
$^{238}\text{Pu } \sigma_{\text{fis}}$	-2.1				-16.9		
$^{239}\text{Pu } \sigma_{\text{cap}}$			0.2			-8.1	26.2
$^{239}\text{Pu } \sigma_{\text{fis}}$						-29.4	-4.3
$^{240}\text{Pu } \sigma_{\text{cap}}$			-0.1	0.1	0.4		-9.3
$^{240}\text{Pu } \sigma_{\text{fis}}$			-0.1				-6.7
$^{241}\text{Am } \sigma_{\text{cap}}$	2.7			-0.7	26.1		



Idaho National Laboratory

TRAPU-II Sensitivity Coefficients

Basic data	Isotope build-up							
	^{241}Pu	^{242}Pu	^{241}Am	^{242}Am	^{243}Am	^{242}Cm	^{243}Cm	^{244}Cm
$^{240}\text{Pu } \sigma_{\text{cap}}$	47.7	10.6	16.5	6.9	4.8	8.6		2.6
$^{241}\text{Pu } \sigma_{\text{cap}}$	-7.7	36.4	-2.7	-1.1	23	-1.4	-0.8	16.6
$^{241}\text{Pu } \sigma_{\text{fis}}$	-35.6	-7.9	-12.3	-5.1	-3.6	-6.4	-3.9	-2
$^{241}\text{Pu } \lambda$	-7.8	-0.9	63.8	50.6		54.5	47.5	0.2
$^{242}\text{Pu } \sigma_{\text{cap}}$		-7.6			94.5		-0.2	96
$^{241}\text{Am } \sigma_{\text{cap}}$		1.8	-26.4	82.4	2.2	78.8	85.5	1.9
$^{242}\text{Am } \sigma_{\text{fis}}$				-26.3	-0.2			-0.1
$^{243}\text{Am } \sigma_{\text{cap}}$					-14.8			89.3
$^{242}\text{Cm } \sigma_{\text{cap}}$						-3.2	97.5	-0.3
$^{242}\text{Cm } \lambda$						-103.4	-52.2	0.2
$^{243}\text{Cm } \sigma_{\text{fis}}$							-20.1	

Summary on Irradiation Experiments Analysis

- The PROFIL-1 results have indicated some large discrepancies in JEF2.2 for some Pu isotopes that in some cases (e. g. Pu240, and Pu241 capture cross sections) have been improved by the JEF3.0 data. The ENDF/B-VI data files show a poor performance for the capture cross section of Pu238, Pu241, Am241, Am243, and Mo95, while the ENDF/B-VII indicated an improvement for the U235 capture cross section. The PROFIL-2 analysis largely confirmed the PROFIL-1 results with a remarkable consistency.
- For the TRAPU analysis, the observed C/E's on the final densities of the measured isotopes for the different basic data files have indicated some large discrepancies that a subsequent sensitivity analysis has attributed to specific cross sections of actinides. This is the case, for instance, of U238 ($n,2n$), capture cross sections of higher plutonium isotopes, Am241, Am243, and Cm242 capture cross sections.



Idaho National Laboratory

Adjustment

- Uncertainty and sensitivity analysis can be used in order to reduce priori uncertainties on performance parameters (like k_{eff} or reactivity coefficients) that characterize a reference design configuration.
- Several approaches (usually called “bias factor” methods) have been attempted. Moreover, statistical “data adjustment” methods have been developed and used (mostly in Europe). E.g. the use of adjusted data did allow to predict the SUPERPHENIX critical mass ($\sim 4\text{t}$ of Pu!) to $<0.3\% \Delta k/k$.
- A general and consistent method can be defined and an application can be performed to show relevant features of the uncertainty reduction process.



Idaho National Laboratory

Summary of the method

The method makes use of:

- “*a priori*” nuclear data covariance information,
- integral experiments analysis to define C/E values
- integral experiment uncertainties

in order to:

- evaluate „*a priori*“ uncertainties on reference design performance parameters
- reduce these uncertainties using integral experiments („*a posteriori*“ uncertainties on performance parameters)
- define „adjusted“ nuclear data and associated „*a posteriori*“ covariances

If we define B_p the “a priori” nuclear data covariance matrix, S_B the sensitivity matrix of the performance parameters B ($B=1.....BTOT$) to the J nuclear data, the “a priori” covariance matrix of the performance parameters is given by:

$$B_B = S_B^T B_p S_B$$

It can be shown that, using a set of I integral experiments A , characterized by a sensitivity matrix S_A , besides a set of **statistically adjusted cross-section data**, a new (“a posteriori”) covariance matrix can be obtained:

$$\tilde{B}_p = B_p - B_p S_A \left(S_A^T B_p S_A + B_A \right)^{-1} S_A^T B_p$$

where B_A is the integral experiment uncertainty matrix.



Idaho National Laboratory

This matrix can then be used to define a new (“*a posteriori*”) covariance matrix for the performance parameters **B**:

$$\begin{aligned}\widetilde{\mathbf{B}}_B &= \mathbf{S}_B^T \widetilde{\mathbf{B}}_p \mathbf{S}_B = \left\{ \mathbf{B}_B - \right. \\ &\quad \left. - \mathbf{S}_B^T \mathbf{B}_p \mathbf{S}_A \left(\mathbf{S}_A^T \mathbf{B}_p \mathbf{S}_A + \mathbf{B}_A \right)^{-1} \mathbf{S}_A^T \mathbf{B}_p \mathbf{S}_B \right\} = \\ &= \mathbf{B}_B \left\{ 1 - (\mathbf{S}_B^T \mathbf{B}_p \mathbf{S}_B)^{-1} (\mathbf{S}_A^T \mathbf{B}_p \mathbf{S}_A + \mathbf{B}_A)^{-1} \times \right. \\ &\quad \left. \times (\mathbf{S}_A^T \mathbf{B}_p \mathbf{S}_B)^2 \right\}\end{aligned}$$

From this expression, it results that in order to reduce the performance parameter „*a priori*“ uncertainties, the most effective integral experiments are those:

- with „representative“ sensitivity profiles ($\mathbf{S}_A \sim \mathbf{S}_B$) and
- small experimental uncertainties ($\mathbf{B}_A \sim 0$).

If we consider only one performance parameter B and only one experiment “i”, and if we put $B_A = 0$, we obtain the expression of the “representativity” of one integral experiment:

$$r_{iB} = \frac{\left(S_i^T B_p S_B \right)}{\left[\left(S_i^T B_p S_i \right) \left(S_B^T B_p S_B \right) \right]^{1/2}}$$

Then, we can consider the previous equation as a generalized expression for the reference parameter uncertainty reduction. This generalized expression accounts for more than one experiment and allows estimating the impact of any new experiment in the reduction of the “a priori” uncertainty of the design performance parameters.

Application and results

The method has been applied to evaluate the potential for reduction of “*a priori*” uncertainties associated to two reference systems:

- an Advanced Burner Reactor (ABR) under study within the GNEP initiative: no MA in the fresh core.
- a TRU burner Sodium-cooled Fast Reactor (SFR): high MA content.

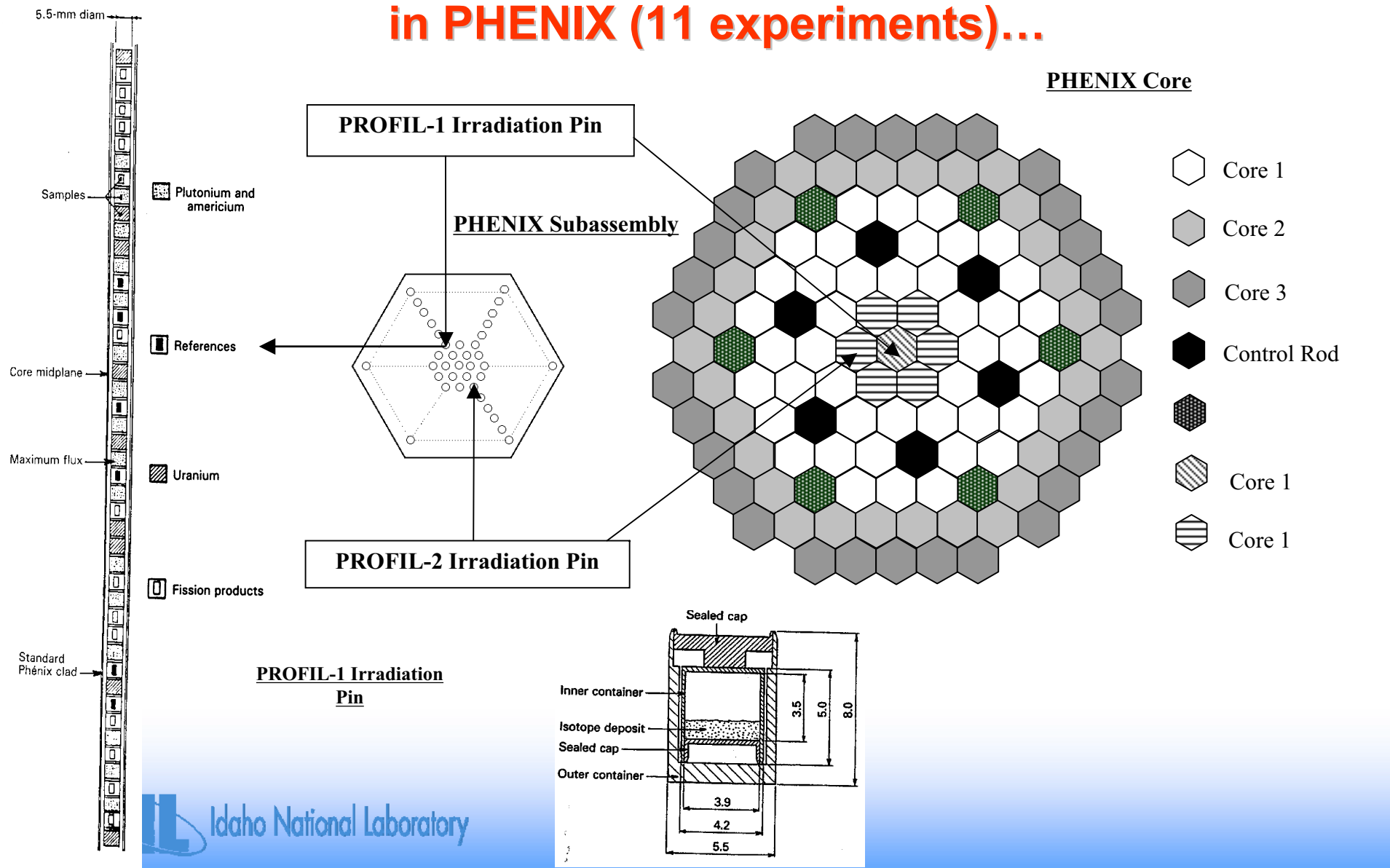
using a set of 42 high accuracy integral experiments.

“*A priori*” uncertainties on selected integral parameters B (k_{eff} and the sodium void reactivity coefficient at core center) have been evaluated for both systems, using a consistent set of basic nuclear data uncertainties and correlations.

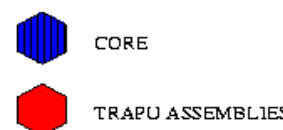
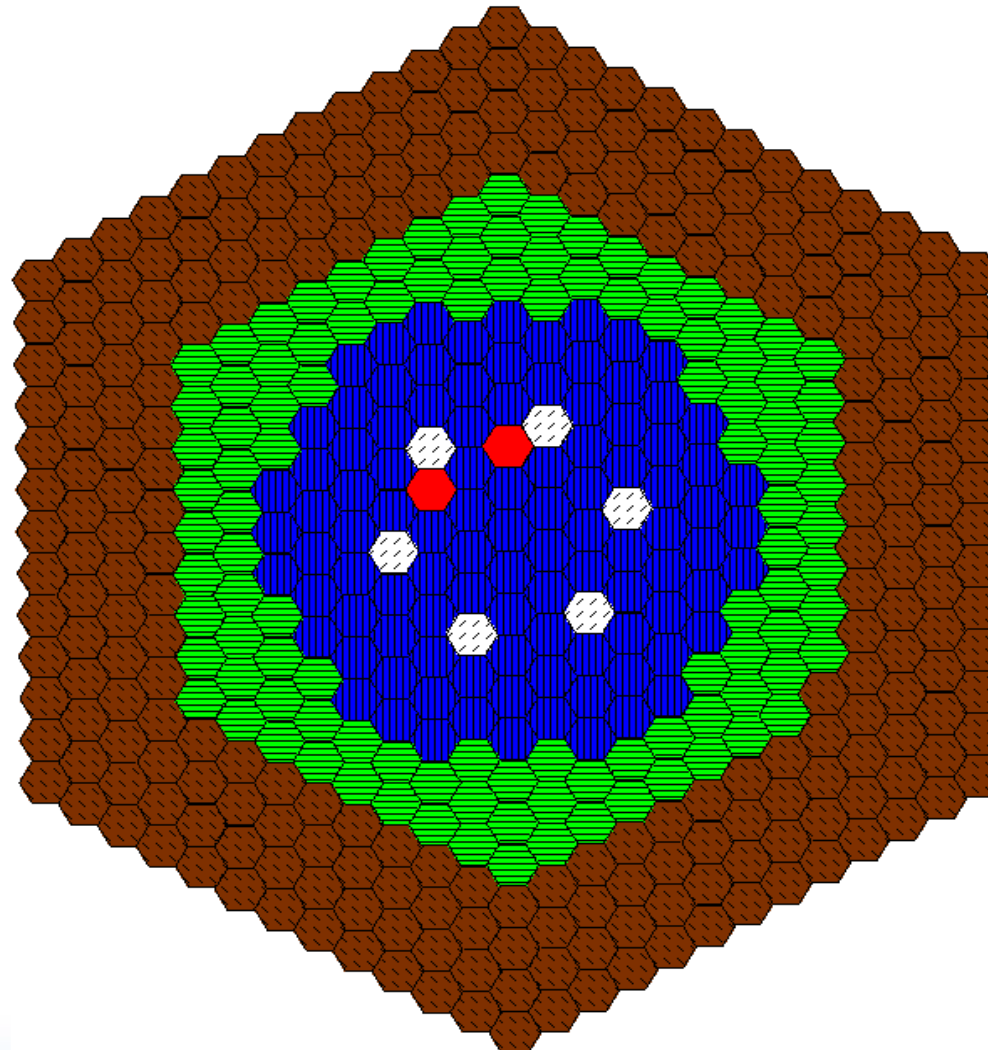


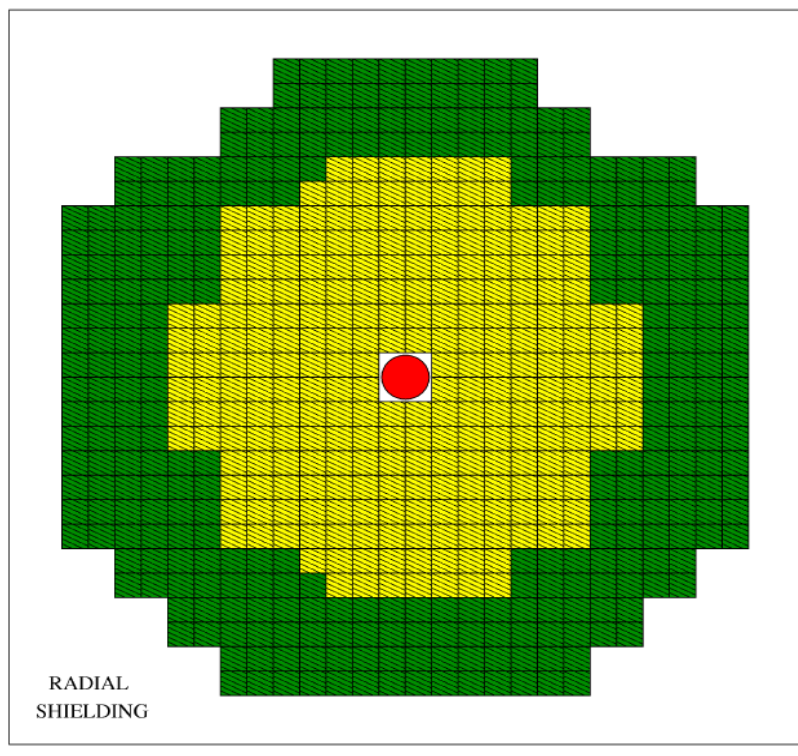
Idaho National Laboratory

Isotope sample irradiation: PROFIL irradiation in PHENIX (11 experiments)...



Fuel pin irradiations: TRAPU Experiment positions in Phénix (13 experiments)...





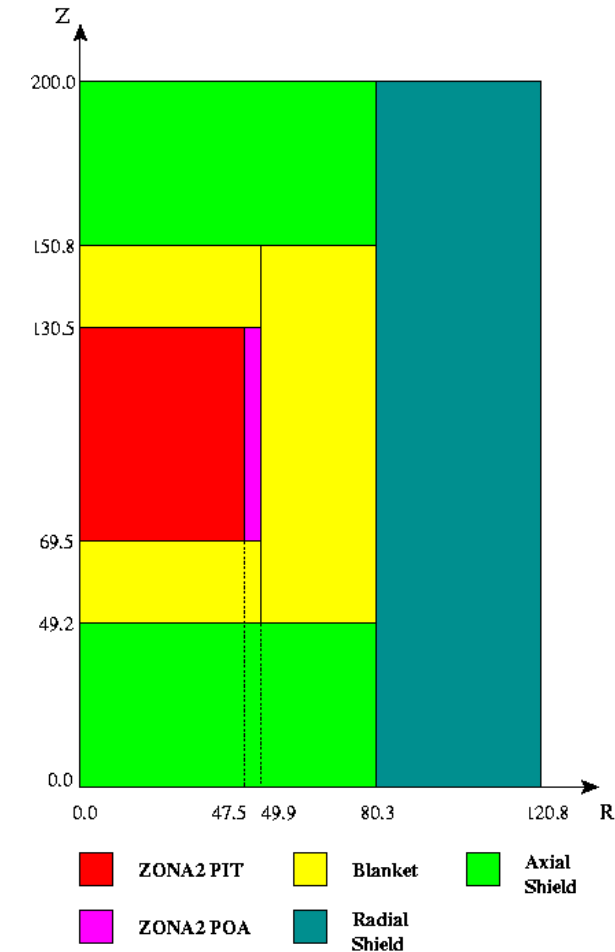
REFLECTOR
Na/SS



FUEL

NEUTRON
GENERATOR

**The MUSE experiment at MASURCA
(critical mass and 9 fission rates)....**



**The CIRANO experiment at
MASURCA (critical mass)...**



Idaho National Laboratory

.....and 7 critical masses from GODIVA, JEZEBEL and Np sphere experiments.

<u>C/E and Associated Uncertainties (ϵ) Before/ After Adjustment</u>				<u>Type of measurement</u>
Pu239/Pu240	atom ratio	0.980 ± 0.030	1.002 ± 0.02	Isotope sample irradiation (PROFIL)
Pu240/Pu241	id	1.131 ± 0.022	1.009 ± 0.017	
Pu241/Pu242	id	1.152 ± 0.041	1.015 ± 0.017	
Pu242/Am243	id	1.120 ± 0.035	0.949 ± 0.02	
Am241/Am242	id	1.061 ± 0.020	0.994 ± 0.014	
Pu239	atom density	1.000 ± 0.010	0.998 ± 0.004	Fuel pin irradiation (TRAPU)
Pu240	id	0.980 ± 0.010	1.001 ± 0.006	
Pu241	id	1.050 ± 0.010	0.994 ± 0.008	
Pu242	id	1.110 ± 0.010	0.984 ± 0.009	
Am241	id	0.970 ± 0.039	1.017 ± 0.006	
Am242	id	1.060 ± 0.031	0.983 ± 0.013	Fission rate in critical exp. (MUSE)
Am243	id	1.080 ± 0.025	1.019 ± 0.02	
Pu239	Fission Rate	0.989 ± 0.020	1.022 ± 0.009	
Pu240	Fission Rate	1.052 ± 0.030	0.978 ± 0.02	
Pu241	Fission Rate	1.011 ± 0.027	0.986 ± 0.022	
Pu242	Fission Rate	1.023 ± 0.030	0.993 ± 0.029	Critical mass
Am241	Fission Rate	1.068 ± 0.030	0.996 ± 0.029	
Am243	Fission Rate	1.056 ± 0.030	0.996 ± 0.029	
Keff MUSE		1.000 ± 0.002	1.002 ± 0.001	
Keff JEZEBEL		1.000 ± 0.002	0.999 ± 0.002	
Keff CIRANO		1.004 ± 0.002	0.998 ± 0.001	



Idaho National Laboratory

Covariance Values Before and After Adjustment for Selected Parameters ^(a)

			Pu-239		Pu-240		Pu-241	
			$\sigma_{\text{fiss}}^{\text{gr.1}}$	$\sigma_{\text{fiss}}^{\text{gr.2}}$	$\sigma_{\text{fiss}}^{\text{gr.1}}$	$\sigma_{\text{fiss}}^{\text{gr.2}}$	$\sigma_{\text{fiss}}^{\text{gr.1}}$	$\sigma_{\text{fiss}}^{\text{gr.2}}$
Pu-239	$\sigma_{\text{fiss}}^{\text{gr.1}}$	before adj.	0.050	-	-	-	-	-
		after adj.	0.007	-0.853	-0.191	0.025	-0.093	0.021
	$\sigma_{\text{fiss}}^{\text{gr.2}}$	before adj.	-	0.050	-	-	-	-
		after adj.	-0.853	0.032	-0.067	-0.006	-0.007	0.002
Pu-240	$\sigma_{\text{fiss}}^{\text{gr.1}}$	before adj.	-	-	0.050	-	-	-
		after adj.	-0.191	-0.067	0.023	-0.127	-0.407	0.109
	$\sigma_{\text{fiss}}^{\text{gr.2}}$	before adj.	-	-	-	0.050	-	-
		after adj.	0.025	-0.006	-0.127	0.050	0.030	-0.005
Pu-241	$\sigma_{\text{fiss}}^{\text{gr.1}}$	before adj.	-	-	-	-	0.150	-
		after adj.	-0.093	-0.007	-0.407	0.030	0.112	-0.419
	$\sigma_{\text{fiss}}^{\text{gr.2}}$	before adj.	-	-	-	-	-	0.100
		after adj.	0.021	0.002	0.109	-0.005	-0.419	0.082

^(a) Diagonal values: variance values. Off-diagonal values: correlation coefficients.

Group 1 (20MeV - 0.5MeV) and group 2 (0.5MeV - 0.067MeV) of the 4 energy group scheme chosen for the present study (group 3: 67KeV - 2KeV; group 4: E<2KeV).



Performance parameter uncertainty reduction: case of k_{eff}

Uncertainty on:	ABR		SFR	
	“a priori”	“a posteriori”	“a priori”	“a posteriori”
K_{eff}	$\pm 2.02 \%$	$\pm 0.36 \%$	$\pm 1.77 \%$	$\pm 1.13 \%$

The “*a posteriori*” uncertainties of the integral experiments are reduced and correlations among experiments that “*a priori*” were equal to zero are now different from zero, and sometimes very significant and well justified on physics ground.

One example is relative to the Pu-239 atom density in the TRAPU2 experiment:

“*a posteriori*” correlation coefficients are observed e.g. with:

- the U-238/Pu-239 and Pu-239/Pu-240 atom ratios in the PROFIL1 experiment (correlation coefficients equal to 0.76 and -0.50 respectively),
- the Pu-240 atom density in the TRAPU1 experiment (0.44),
- the U-238 fission spectrum index in MUSE (0.12), and with the k_{eff} of MUSE and CIRANO (-0.13 and -0.11, respectively).

Summary on adjustment and perspectives

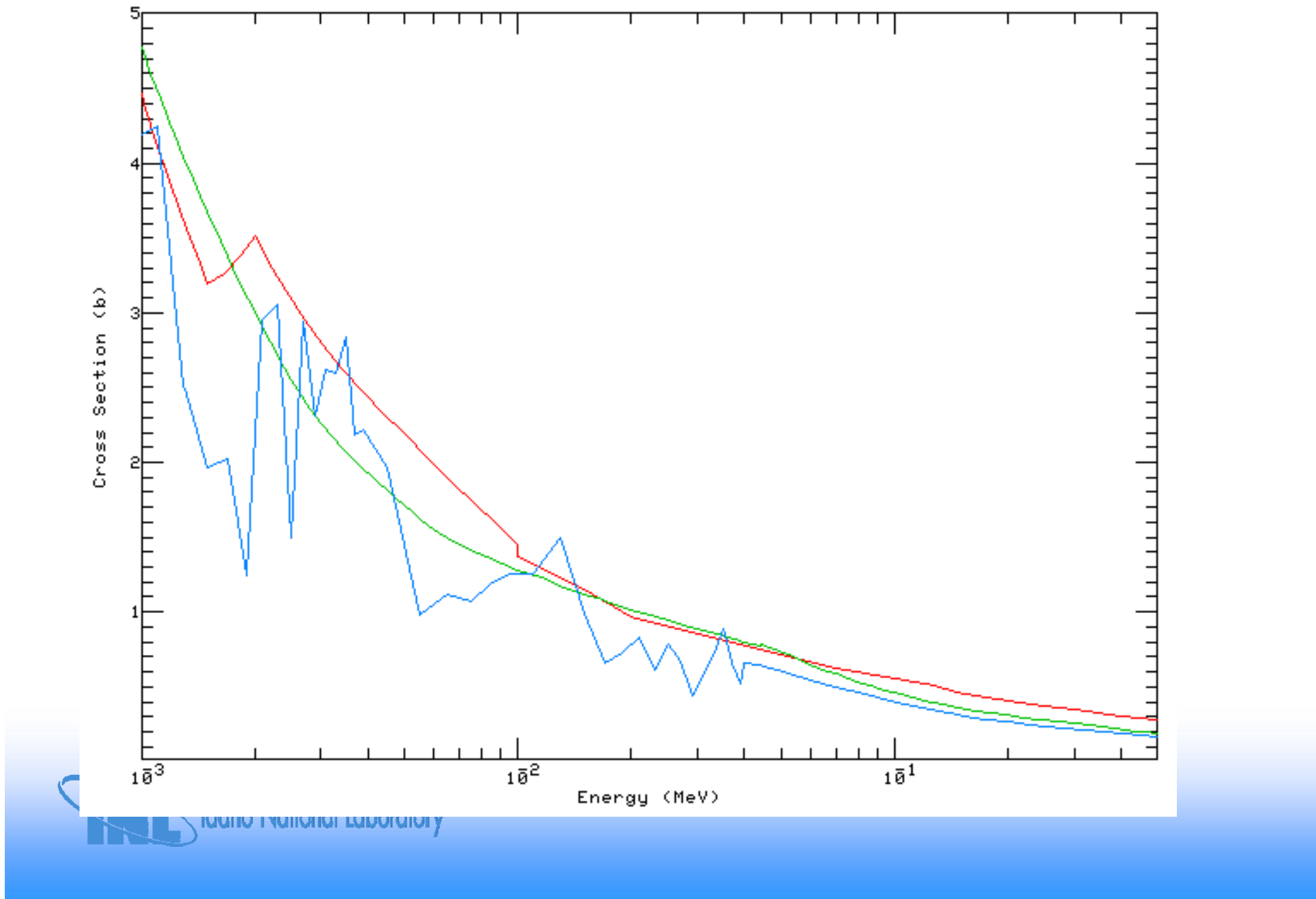
- New and potentially tight uncertainty requirements for innovative systems design and optimization, suggest the complementary use of differential and integral experiments, in order to meet design target accuracies.
- A powerful method has been generalized and applied successfully to Na-cooled fast reactors of interest for both Gen-IV and GNEP.
- This approach will be now applied to a larger set of innovative systems (reactor and associated fuel cycle parameters), using recently developed covariance data and a much wider set of clean integral experiments, both from power reactors and from critical assemblies.

ENDF/B-VII Calculated Adjusted Data Change and Original and Adjusted Standard Deviation (%)

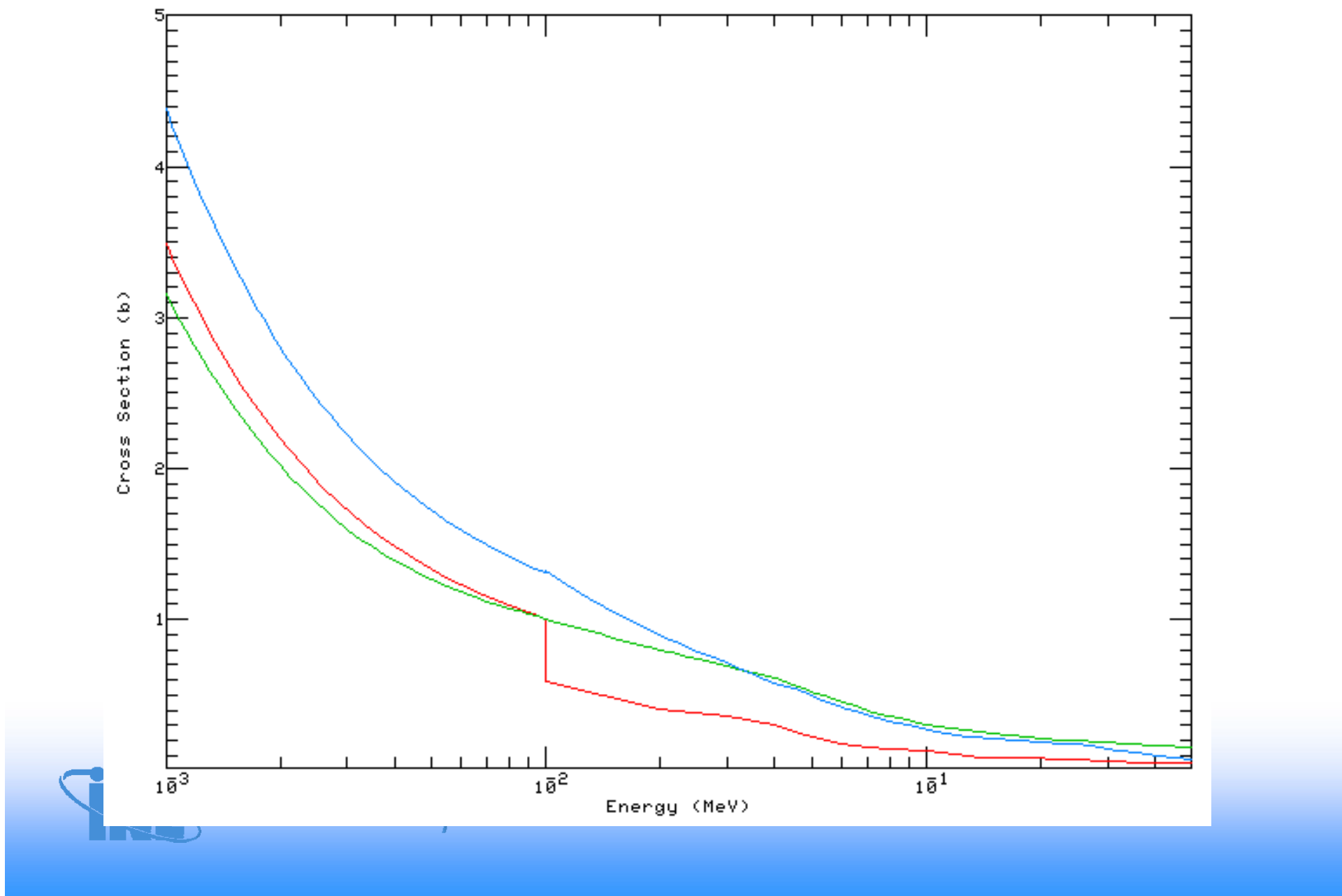
Param.	Adjus. %	Stand. Deviat. %		Param.	Adjus. %	Stand. Deviat. %		Param.	Adjus. %	Stand. Deviat. %	
		Orig.	Adj.			Orig.	Adj.			Orig.	Adj.
U238 σ^{fis} gr. 1	1.1	0.5	0.4	Pu240 σ^{cap} gr. 4	0.0	11.5	11.5	Cm242 σ^{cap} gr. 2	101.5	100.0	70.7
U238 σ^{n2n} gr. 1	9.6	5.0	3.1	Pu240 σ^{fis} gr. 1	-2.6	3.7	1.7	Cm242 σ^{cap} gr. 3	139.5	100.0	24.5
Np237 σ^{cap} gr. 2	-0.1	1.9	1.8	Pu240 σ^{fis} gr. 2	-2.7	4.3	2.9	Cm242 σ^{cap} gr. 4	96.8	100.0	74.3
Np237 σ^{cap} gr. 3	-1.8	5.1	4.2	Pu241 σ^{cap} gr. 2	8.9	14.8	9.3	U238 σ^{inel} gr. 1	3.5	17.1	8.5
Np237 σ^{cap} gr. 4	-1.3	4.3	3.8	Pu241 σ^{cap} gr. 3	3.4	6.4	4.8	Fe56 σ^{inel} gr. 1	-7.9	10.5	8.4
Np237 σ^{fis} gr. 1	1.3	6.3	1.1	Pu241 σ^{cap} gr. 4	3.2	7.2	6.0	Na23 σ^{inel} gr. 1	-3.4	16.7	14.3
Pu238 σ^{cap} gr. 2	-61.9	50.0	22.7	Pu241 σ^{fis} gr. 1	2.9	15.0	6.0	C12 σ^{elas} gr. 1	1.3	5.0	4.2
Pu238 σ^{cap} gr. 3	-67.4	50.0	12.0	Pu241 σ^{fis} gr. 2	2.7	16.9	5.4	C12 σ^{elas} gr. 2	2.8	3.9	2.7
Pu238 σ^{cap} gr. 4	-60.7	50.0	24.3	Pu241 σ^{fis} gr. 3	-0.6	9.1	7.4	C12 σ^{elas} gr. 3	-0.4	3.0	2.7



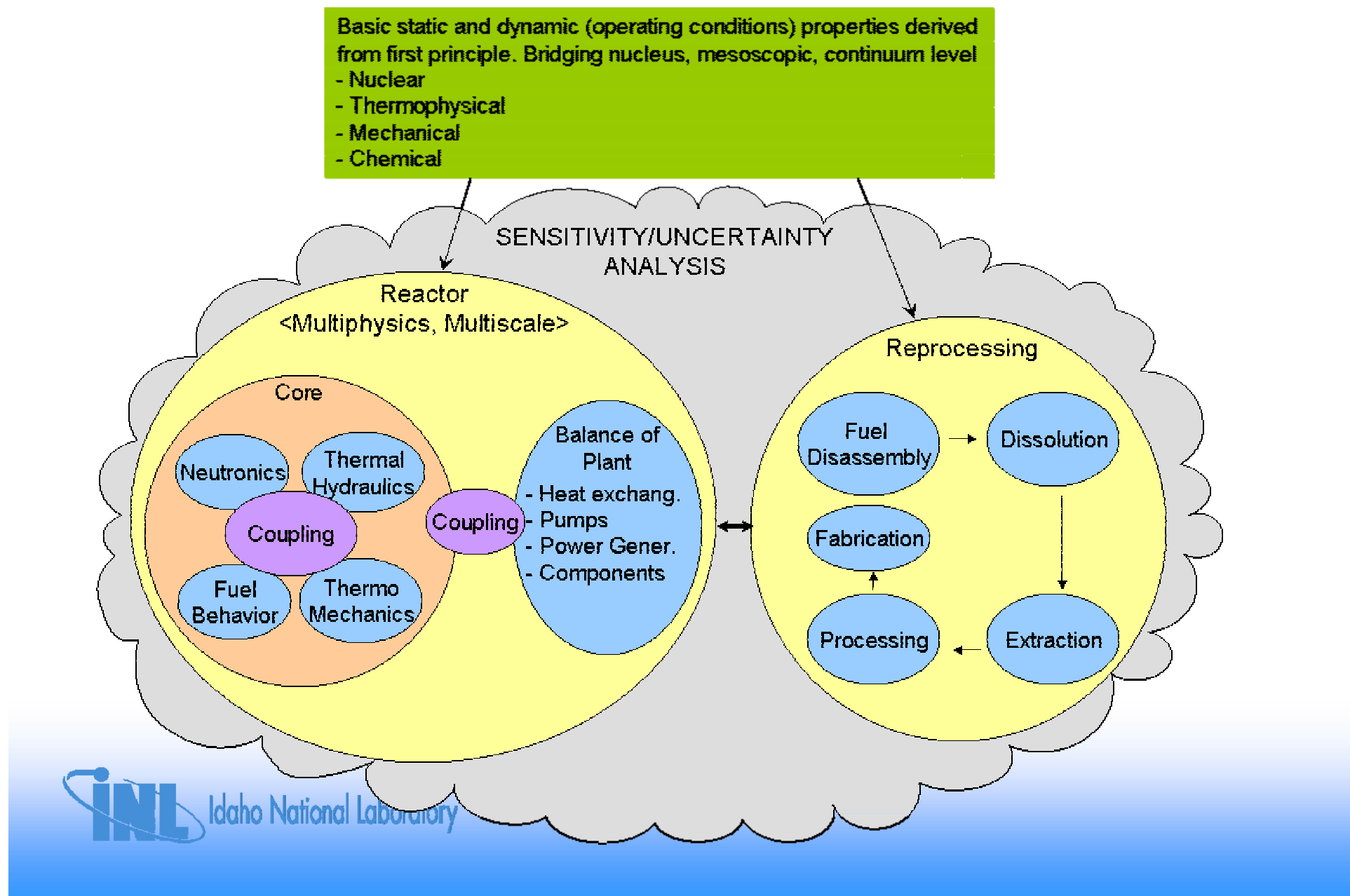
Pu238 Capture cross section. Red: ENDF/B-VII, Green: JENDL 3.3,
Blue: JEF



Cm242 Capture cross section. Red: ENDF/B-VII, Green: JENDL 3.3,
Blue: JEF 2.2



Requirements for Advanced Simulation



Requirements for Advanced Simulation

- An essential attribute of the advanced simulation tool should be the capability to conduct comprehensive sensitivity analyses and uncertainty evaluation.
- This sensitivity capability has to be based on sound theoretical ground using deterministic and/or probabilistic methodologies.
- This capability would achieve several goals, including identifying trends and issues, designing a focused set of validation experiments, quantifying uncertainties, and assessing the quality of data used in the design process.
- Sensitivity analysis allows true system optimization.
- The proper use of sensitivity analysis as an integral part of the simulation can lead to more robust systems that can better withstand transients and off-normal conditions.

Requirements for Advanced Simulation

- The sensitivity analysis capability has to be incorporated from the beginning, in the case of writing of new codes, or added for existing ones that are selected and adopted for the design of new plants as an integral feature of the tool.
- The following domains have to be equipped with sensitivity analysis capability:
 - Neutronics, Fuel Cycle, Decay Heat
 - Thermal-Hydraulics
 - Structural Mechanics
 - Fuel Behavior
 - Balance of Plant
 - Chemical Processing
- When needed (e. g. safety analysis), coupling among the different fields has to be covered by the sensitivity analysis capability:
 - Nonlinear behaviors due to feedback effects need to be taken into account
 - Not only static problems but also time-dependent transient ones have to be treated

Future Approaches

- One promising methodology is a mixture of techniques that leverage very recent advances in computational differentiation and novel mathematical techniques: a combination of stochastic and deterministic techniques.
- In the case where the uncertainty assessment involves average quantities, advanced sampling techniques are adopted. Randomized Quasi Monte Carlo (RQMC) techniques can be used for assessing the uncertainty in cases where there is a large number of uncertain parameters (such as the cross sections) but the effective dimension is low.
- The advantage of RQMC methods is that they need only forward calculations, they are non-intrusive with respect to the various software modules and they exhibit a rate of convergence that is far superior to the classical Monte Carlo method.
- One can use the derivatives of the objectives with respect to the uncertain parameters, provided by the sensitivity analysis, to generate an importance sampling approach. This will results in fewer samples compared to brute force Monte Carlo approaches.

Future Approaches

- P. Turinsky and H. Abdel-Khalik have proposed a new forward method based on random perturbation of input parameters, the Efficient Subspace Method (ESM).
- The method can efficiently approximate the huge sensitivity (Jacobian) matrix, resulting from a large number of input and output parameters, with a limited number of direct calculations.
- The method relies on the singular value decomposition technique in identifying the important subspaces of the domain and range spaces of the Jacobian matrix.
- A major advantage of this method is that no modifications to existing codes are necessary, but only pre- and post-processing of the input and output quantities are needed. It rest to be seen what is the optimal number of direct calculations that is sufficient to characterize the problem.

Future Approaches

- Another recent proposed approach is the stochastic finite element method (SFEM).
- This approach allows to calculate the behavior of the eigenvalue and the eigenvector in the entire parameter range, as opposed to a narrow region around a nominal value which is what classical sensitivity analysis provides.
- This formulation results in solving a nonlinear system of equations, which is N times larger than the original problem, and has N constraints, where N is the number of terms considered in the perturbative expansion of the solution.
- Initial investigation for a small size parameter space indicates that the method has the potential of savings of orders of magnitude over Monte Carlo calculations that attempt to characterize the behavior of the eigenvector and eigenvalue over the entire parameter space.



Idaho National Laboratory

Conclusions

- Sensitivity and uncertainty methodologies have been developed in the past for nuclear reactor applications and applied to a series of different problems: uncertainty analysis, optimization, target accuracy requirements, adjustment, and representativity.
- Most of the methodologies have been developed in the reactor physics field. Extension to other fields is needed: thermal-hydraulics, structural mechanics, fuel behavior, chemical separation, etc.
- A combination of forward and adjoint techniques as well as deterministic and probabilistic will be likely required for evaluating the sensitivity matrix of an integrated simulation tool.
- Credibility of uncertainty evaluation, target accuracy requirements, and adjustment of input parameters is mainly linked to the quality of the covariance information attached to those data.

Backup Slides



Idaho National Laboratory

ERANOS Sensitivity Capabilities (cont.)

ERANOS tools for building the source term of the equations for the importance functions

↳ IMPORTANCE_CALCULATION_SOURCE_CREATION

```
-> edl_source_importance
geometry (edl_geometry) flux (edl_flux)
                           !! value ...
<< response_cross_section 'respname' !!! >>1
                           !! edl ...
! numerator << response_function ... >>1
! numerator << response_function ... >>1 dose
! numerator << response_function ... >>1 denominator
    <<->xnum ->xden>> << response_function ... >>1
<< functional ->functional >> ;
```

the edl in output for each energy group associates to each mesh point the corresponding σ (defined in the 'edl' directory) or value (defined in the 'value' directory) multiplied by the volume of the mesh.

$$\text{creates a source as: } S(r, E) = \frac{\sigma(r, E)dV}{\langle \sigma(r, E)\Phi(r, E) \rangle}$$

$$\text{creates a source as: } S(r, E) = \sigma(r, E)dV$$

creates a source as:

gives the integral over space and energy of the source multiplied by the flux given in 'edl_flux': $\langle S(r, E)\Phi(r, E) \rangle$

```
! set data 1
! set data 2
!! set data 1
!! set data 2
<< set data >>0
<< set data >>1
<< set data >>
```

set data n are exclusive: one and only one must exist;

set data n are optional: they may exist all together and at least one must exist;

set data may be given 0 or n times;

set data may be given 1 or n times;

set data may be given 0 or 1 time.



Idaho National Laboratory

ERANOS Sensitivity Capabilities (cont.)

ERANOS tools for building the source term of the equations for the importance functions

↳ NORME_CALCULATION

it allows to calculate linear integrals, such as $\langle S\Phi \rangle$, where S can be either a cross-section or any source defined on the geometry grid, Φ is a scalar flux, either direct or adjoint.

Can be also used to calculate bilinear integrals, if S is function of the flux.

For instance, if $S_g = [\chi\Phi^*]v_g\Sigma_{f,g}dV$ with $g = 1\dots NG$, NORME_CALCULATION can perform the calculation of $\langle \Phi^*, F\Phi \rangle$.

↳ GENERALIZED_INTEGRAL

it allows to calculate:

linear integrals $\langle S\Phi_1 \rangle$;

bilinear integrals $\langle [S_1\Phi_1][S_2\Phi_2] \rangle$

where S , S_1 and S_2 can be either a cross-section or any source defined on the geometry grid, Φ_1 and Φ_2 are scalar fluxes, either direct or adjoint.



Idaho National Laboratory

ERANOS Sensitivity Capabilities (cont.)

ERANOS procedure for spectral index sensitivity analysis

Adjoint importance function determination

```
importance_calculation_source_creation ->edl_source_ind
  geometry (edl_geometry) flux (edl_flux_dir)
  response_cross_section 'secnum'
    edl (edl_micro) (region_n) (reaction_n) isotope (isotope_n)
  response_cross_section 'secden'
    edl (edl_micro) (region_d) (reaction_d) isotope (isotope_d)
  numerator
    response_function 'secnum' point (point_r_n) (point_z_n)
  denominator ->xnum ->xden
    response_function 'secden' point (point_r_d) (point_z_d)
  functional ->fonic ;
```

Building the source term for the importance function equation:

$$\frac{\sigma_1(E)dV}{\langle \sigma_1 \Phi \rangle} - \frac{\sigma_2(E)dV}{\langle \sigma_2 \Phi \rangle}$$

$$xnum = \langle \sigma_1 \Phi \rangle \quad xden = \langle \sigma_2 \Phi \rangle$$

```
fd_diffusion_matrix_coefficient ->edl_coefficient
  geometry (edl_geometry) macro (edl_macro)
  horizontal_mesh 1. 1. transport anisotropy 1 ;

methode_resolution_diffusion ->edl_method
  coefficient (edl_coefficient) no_print
  plane alternating_direction_implicit calculation ;

direction_cosine_and_weight_creation ->edl_weights_directions
  section_set 'standard' ;

rectangular_sn_transport_iteration ->edl_psi_adj
  angular_flux ->edl_psi_adj_ang
  method (edl_method)
  coefficient (edl_coefficient)
  source (edl_source_ind)
  direction (edl_weights_directions)
  differencing_scheme diamant_pur
  harmonic direct (edl_flux_dir) adjoint (edl_flux_adj)
  calculational_parameter
    outer_iteration maximum_number 50
      integral_convergence 1.e-5
      local_convergence 1.e-5
    inner_iteration maximum_number 25
  no_scale acceleration diffusion diffusion_iteration 20
  variable_spectrum calculation adjoint moment_storage yes ;
```

Adjoint importance calculation:

$$\left(A^* - \frac{1}{K} F^* \right) \Psi^* = \frac{\sigma_1(E)dV}{\langle \sigma_1 \Phi \rangle} - \frac{\sigma_2(E)dV}{\langle \sigma_2 \Phi \rangle}$$

In transport approximation, the method 'diamant_pur' must be used: the method 'diamant_teta 0.9' is not appropriate because the source term could have negative values.

The option 'harmonic' also prevent the use of the method 'diamant_teta 0.9' (fix-ups would be also performed when the sign of the real solution is changing).

Inhomogeneous adjoint calculation:
recommendation 'no scale'.



Idaho National Laboratory

ERANOS Sensitivity Capabilities (cont.)

Indirect term

```
cross_section_variation_creation ->edl_cross_section_variation  
    title      'cross_section_variation'  
    micro     (edl_micro)  
    medium    (edl_medium)  
    section_set full  
    isotope    one_by_one  partial (sensitivity_corp_list) ;
```

standard cross-section variation (100%)
for sensitivity analysis.

```
->dispersion_matrix ;  
pour ->i (rep(sensitivity_corp_list())) ;  
    ->dispersion_matrix (dispersion_matrix) isotope  
sensitivity_corp_list(i)  
    'capture'    rep(ng,1.00)  
    'fission'   rep(ng,1.00)  
    'nu'         rep(ng,1.00)  
    'elastique'  rep(ng,1.00)  
    'inelastique' rep(ng,1.00)  
    'n,xn'       rep(ng,1.00)  
finpour ;
```

```
dispersion_matrix_creation ->edl_dispersion_matrix  
    title 'dispersion matrix for sensitivity analysis'  
    group (ng)  
    deviation_standard (dispersion_matrix) ;
```

Dispersion matrix creation
for sensitivity analysis:
(diagonal terms = 1;
'off-diagonal' terms = 0).

For diffusion calculations add:
'transport' rep(ng,1.00)

```
transport_perturbation_integral ->edl_perturbation_integral  
    angular_flux (edl_flux_dir_ang) (edl_psi_adj_ang)  
    macro        (edl_macro)  
    geometry     (edl_geometry)  
    full ;
```

Calculation of the indirect term in the
sensitivity coefficient formula:

$$\frac{\sigma}{R} \left\langle \Psi^*, \left(\frac{\partial A}{\partial \sigma} - \frac{1}{K} \frac{\partial F}{\partial \sigma} \right) \Phi \right\rangle$$

```
sensitivity_analysis ->edl_indirect_sensitivity  
    dispersion_matrix (edl_dispersion_matrix)  
    variation        (edl_cross_section_variation)  
    integral         (edl_perturbation_integral)  
    transport  
    title ('*** sensitivity index '/(reaction_n)'/ '/(isotope_n)/  
          ' / '(reaction_d)'/ '/(isotope_d) /' ***')  
    diffusion_coefficient_variation approximate  
    normalization_integral input_value 1.00  
    calculational_domain full ;
```

No normalization is performed on the sensitivity
coefficients.

ERANOS Sensitivity Capabilities (cont.)

Direct term: $(\sigma_i \Phi)_{i,g,d} dV / \langle \sigma_i \Phi \rangle$

```
by_group_flux_creation
  flux (edl_flux_dir)  micro (edl_micro)  position (point_r_n) (point_z_n)
  title 'flux by group numerator' ->edl_flux_by_group_n ;
```

$\Phi_g \quad g = 1 \dots NG$
at the point (point_r_n) (point_z_n)

```
sample_macro ->sample_macro_n
  type (reaction_n) section_set_micro (edl_micro) (region_n)
  sample (edl_medium) isotope (isotope_n) proportion value 1.00 ;
by_group_value_creation_with_input_data ->edl_macro_by_group_n
  title 'direct sensitivity numerator'
  by_group_value (sample_macro_n) micro (edl_micro) ;
```

$\sigma_{isotope_n, reaction_n, g} \quad g = 1 \dots NG$
at the point (point_r_n) (point_z_n)

```
by_group_value_operation
  (edl_macro_by_group_n) (edl_flux_by_group_n)
  product ->edl_rate_by_group_n ;
```

$\sigma_{isotope_n, reaction_n, g} \cdot \Phi_g \quad g = 1 \dots NG$

```
(edl_rate_by_group_n) on_valgre group_value ->tpg ;
->total_n somme(tpg) ; ->tpg (tpg/total_n) ;
(edl_rate_by_group_n) on_valgre group_value tpg ;
```

Normalizing:
 $\sigma_{isotope_n, reaction_n, g} \cdot \Phi_g$
 $g = 1 \dots NG$ to sum = 1.

```
sensitivity_edl_changing ->edl_intermediate_sensitivity
  initialization (edl_indirect_sensitivity)
  sommation_valeur_par_groupe (edl_rate_by_group_n)
  domain (region_n) reaction (reaction_n) isotope (isotope_n) ;
```

Adding direct term in correspondence of
reaction_n of isotope_n in the region
region_n.



Idaho National Laboratory

ERANOS Sensitivity Capabilities (cont.)

Direct term: $-(\sigma_2 \Phi)_{i,g,d} dV / \langle \sigma_2 \Phi \rangle$

```
by_group_flux_creation
  flux (edl_flux_dir) micro (edl_micro) position (point_r_d) (point_z_d)
  title 'flux by group denominator' ->edl_flux_by_group_d ;
```

$\Phi_g \quad g = 1 \dots NG$
at the point (point_r_d) (point_z_d)

```
sample_macro ->sample_macro_d
  type (reaction_d) section_set_micro (edl_micro) (region_d)
  sample (edl_medium) isotope (isotope_d) proportion value 1.00 ;
by_group_value_creation_with_input_data ->edl_macro_by_group_d
  title 'direct sensitivity denominator'
  by_group_value (sample_macro_d) micro (edl_micro) ;
```

$\sigma_{isotope_d, reaction_d, g} \quad g = 1 \dots NG$
at the point (point_r_d) (point_z_d)

```
by_group_value_operation
  (edl_macro_by_group_d) (edl_flux_by_group_d)
  produit ->edl_rate_by_group_d ;
```

$\sigma_{isotope_d, reaction_d, g} \cdot \Phi_g \quad g = 1 \dots NG$

```
(edl_rate_by_group_d) on_valgre group_value ->tpg ;
->total_d somme(tpg) ; ->tpg (tpg/total_d) ;
(edl_rate_by_group_d) on_valgre group_value tpg ;
```

Normalizing:
 $\sigma_{isotope_d, reaction_d, g} \cdot \Phi_g$
 $g = 1 \dots NG$ to sum = 1

```
by_group_value_operation
  (edl_rate_by_group_d) (edl_rate_by_group_d)
  linear_combination ->edl_rate_by_group_d -0.5 -0.5 ;
```

In order to add as negative contribution.

```
sensitivity_edl_changing ->edl_total_sensitivity
  initialization (edl_intermediate_sensitivity)
  sommation_valeur_par_groupe (edl_rate_by_group_d)
  domain (region_d) reaction (reaction_d) isotope (isotope_d) ;
sensitivity_edition (edl_total_sensitivity) ;
```

Adding direct term in correspondence of
reaction_d of isotope_d in the region
region_d.



IDAHO NATIONAL LABORATORY

ERANOS Sensitivity Capabilities (cont.)

Additional ERANOS tools for building the source term of the equations for the importance functions

↳ Pointers

(EDL_ADJOINT_FLUX)

ONFINITE_DIFFERENCE ON_REC_FLUX ON_FLUX_AND_SOURCE_POINTER

ONTOTAL_SOURCE(1) SOURCE ->SOURCE;

SOURCE is a vector that contains in each point i of the grid:

(EDL_DIRECT_FLUX)

ONFINITE_DIFFERENCE ON_REC_FLUX ON_FLUX_AND_SOURCE_POINTER

ONTOTAL_SOURCE(1) SOURCE ->SOURCE;

SOURCE is a vector that contains in each point i of the grid: where V_i is the volume of the mesh associated to the point i .

(EDL_FLUX)

ONFINITE_DIFFERENCE ON_REC_FLUX ON_FLUX_AND_SOURCE_POINTER

ON_FLUX(IG,1) FLUX ->FLUX;

FLUX is a vector giving the flux in each point i of the grid for the group IG.

(EDL_IMPORTANCE_CALCULATION_SOURCE_CREATION)

ONFINITE_DIFFERENCE ON_REC_FLUX ON_FLUX_AND_SOURCE_POINTER

ONSOURCE(IG,1,1) SOURCE ->SOURCE;

SOURCE is a vector extrapolated from the EDL obtained with e.g. IMPORTANCE_CALCULATION_SOURCE_CREATION corresponding to the group IG.

ERANOS Sensitivity Capabilities (cont.)

Building the source term for the importance function equation:

$$[\Phi^* \chi] v \Sigma_f(r, E) dV$$

```
importance_calculation_source_creation ->edl_fission_source
geometry (edl_geometry) flux (edl_flux_dir_inh)
response_cross_section 'sigma' edl (edl_macro) 'fuel' 'nu*fission'
    numerator response_function 'sigma' section 'fuel'
dose functional ->fission_source_integrated ;
```

Creating the source term: $v \Sigma_f(r, E) dV$

```
flux_initialization ->edl_flux_nul
with_input_data reperage cylindrique rz
coordinate r 0. 1 142. 60
coordinate z 0. 1 200. 81
number_of_groups (ng) mesh_point centre
scalar_flux 0. external_source 0. total_source 0. ;
```

Creation flux with 0 values everywhere to be used as initialization for 'edl_adjoint_importance_source'.

```
= ->edl_adjoint_importance_source (edl_flux_nul) ;
(edl_flux_adj)
on_finite_difference on_rec_flux on_flux_and_source_pointer
    on_total_source(1) source ->chi_phi ;
pour ->ig (rep(ng)) ;
(edl_fission_source)
on_finite_difference on_rec_flux on_flux_and_source_pointer
    on_source(ig,1,1) source ->nu_sigmaf_dv ;
    ->source_importance_adjointe (chi_phi*nu_sigmaf_dv) ;
(edl_adjoint_importance_source)
on_finite_difference on_rec_flux on_flux_and_source_pointer
    on_source(ig,1,1) source source_importance_adjointe ;
finpour ;
```

Building the term: $[\Phi^* \chi] v \Sigma_f(r, E) dV$

$$\text{chi_phi: } \sum_{g=1}^{NG} \Phi_g^* \chi_g$$

$$\text{nu_sigmaf_dv: } v_g \Sigma_{f,g} dV$$

$$\text{edl_adjoint_importance_source: } \sum_{g=1}^{NG} \Phi_g^* \chi_g \cdot v_g \Sigma_{f,g} dV$$

```
rectangular_sn_transport_iteration ->edl_psi_adj
angular flux ->edl_psi_adj_ang
method (edl_method) coefficient (edl_coefficient)
source (edl_adjoint_importance_source) direction (edl_weights_directions)
differencing_scheme diamant_teta 0.9
calculational_parameter
    outer_iteration maximum_number 30
        integral_convergence 1.e-5
        local_convergence 1.e-5
    inner_iteration maximum_number 30
no_scale acceleration diffusion diffusion_iteration 20
variable_spectrum calculation adjoint moment_storage no ;
```

Adjoint importance function calculation

'diamant_teta 0.9' is used for source terms positive everywhere.

Source-driven problem: no need to use the option 'harmonic'.



Idaho National Laboratory

Sensitivity and Uncertainty Analysis: Liquid Salt VHTR

The gas (helium)-cooled, graphite moderated Very High Temperature Reactor (VHTR) is a leading candidate for the Next Generation Nuclear Power Plant (NGNP).

→ Recently, a liquid salt (molten salt) cooled version of the VHTR, the LS-VHTR, has been proposed to improve the system economy for the NGNP.

A liquid-salt coolant has many favourable properties compared to helium, as lower operating pressure, higher power density, better heat removal properties, reduced shielding requirements for external components.

→ These results leads to an improved system safety and to a potential for cost reduction.

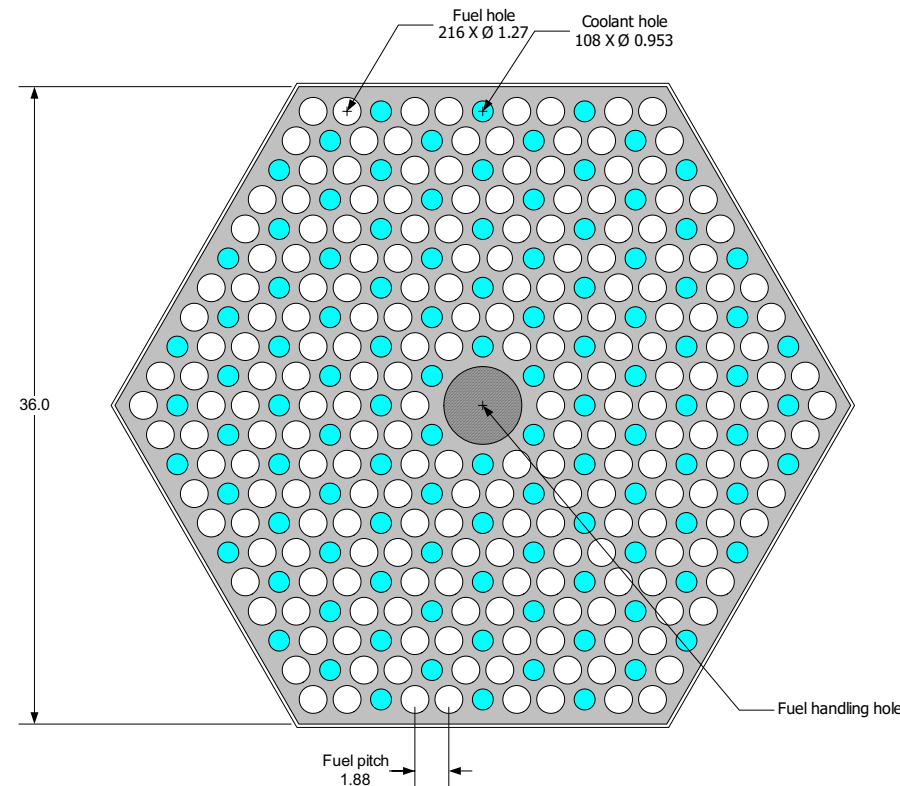
The disadvantages of the LS-VHTR arise from potential material compatibility issues, tritium production, activation of the molten salt, higher corrosion rates, chemical hazard (Be release or HF production from fluoride and tritium), possibility of a positive void reactivity coefficient, and a relative high coolant melting temperature.

Work is ongoing at US national laboratories (ANL, INL, ORNL, SNL) to design a viable LS-VHTR system that could be used for electricity and/or hydrogen production.

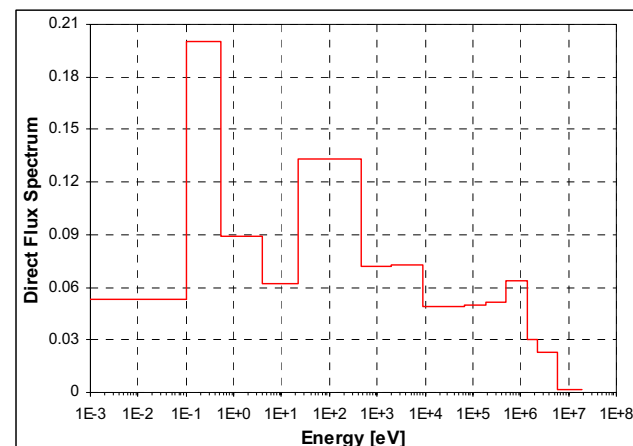
Sensitivity and Uncertainty Analysis: Liquid Salt VHTR

- One of the main issues in the design of the LS-VHTR is the coolant void reactivity coefficient. Contrary to standard VHTR the presence of a liquid salt can lead to a positive reactivity coefficient, in the event of a loss of coolant. As a consequence the safety of the LS-VHTR can be compromised, jeopardizing the viability of the reactor.
- In this study we have performed an analysis of the characteristics of the LS-VHTR coolant void reactivity based on its perturbation components in order to indicate the main contributors in terms of isotopes, reactions, and energy range.
- Subsequently a sensitivity analysis has been carried out for providing information on how the coolant void reactivity coefficient can be improved by modifying composition or spectral characteristics.
- Finally an uncertainty calculation has been performed for evaluating the impact of cross section uncertainties on the value of LS-VHTR coolant void reactivity.

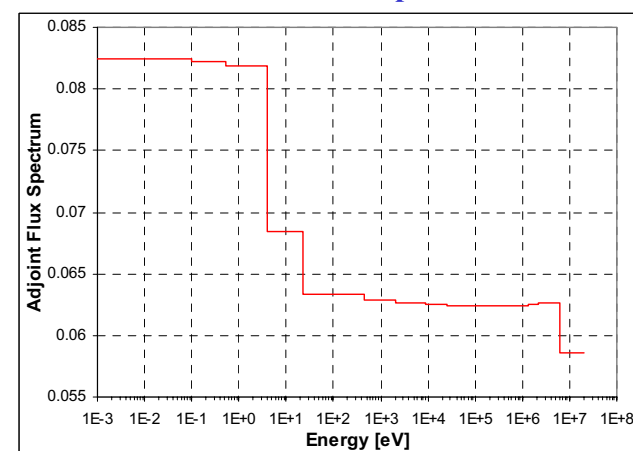
Fuel assembly geometry and compositions:



Average Fuel Compositions [10^{24} at/cm 3]							
U235	2.67056E-5	Si	5.22743E-4	O	2.64187E-4	Li7	1.61951E-3
U238	1.49416E-4	C	7.43196E-2	Li6	9.44526E-8	Be	8.09790E-4
					F	3.23923E-3	



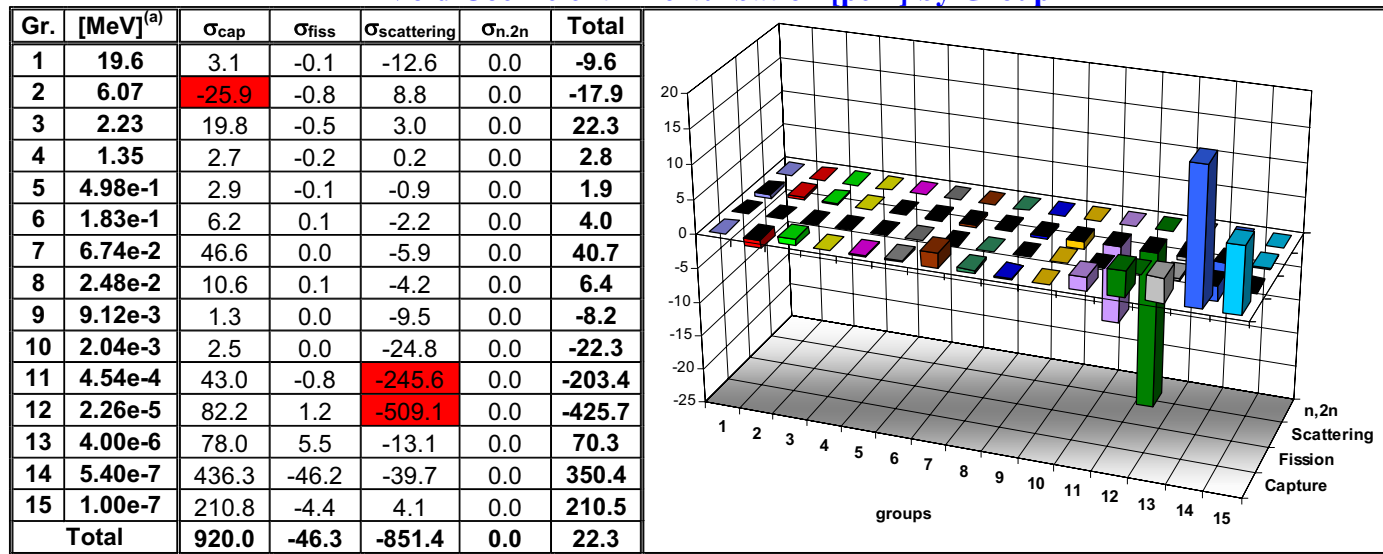
Direct Flux Spectrum



Adjoint Flux Spectrum

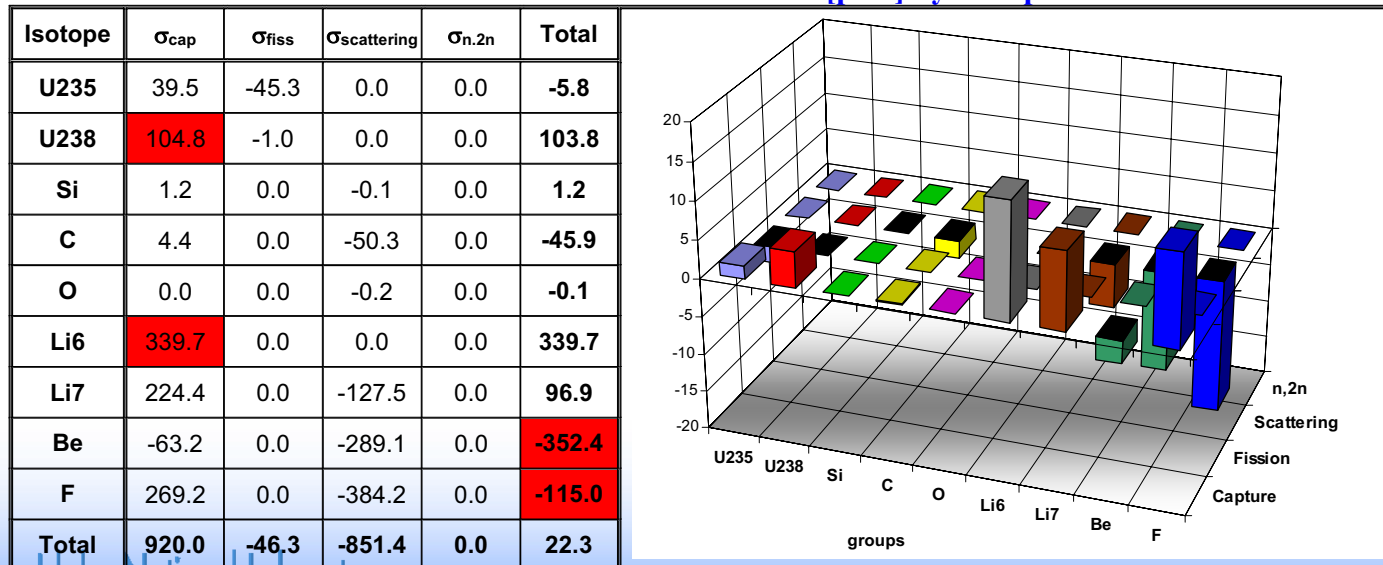
- Cross-sections have been processed with the WIMS code using the JEF2.2 nuclear data library.
- Neutronic flux analysis has been performed with the ERANOS code system, via the S_n BISTRO code.
- Results are reported in a 15-group energy structure although the reference calculations have been done with a 172-group energy structure.

Void Coefficient – Perturbation [pcm] by Group



^(a) High energy group boundary.

Void Coefficient – Perturbation [pcm] by Isotope

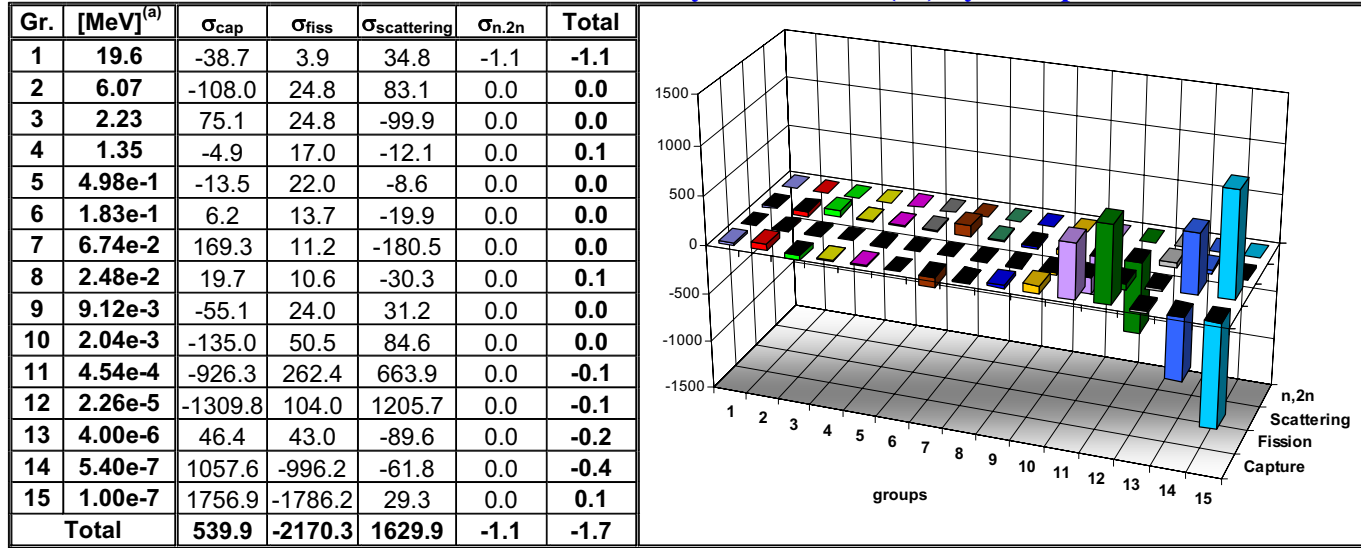


Idaho National Laboratory

Perturbation Analysis

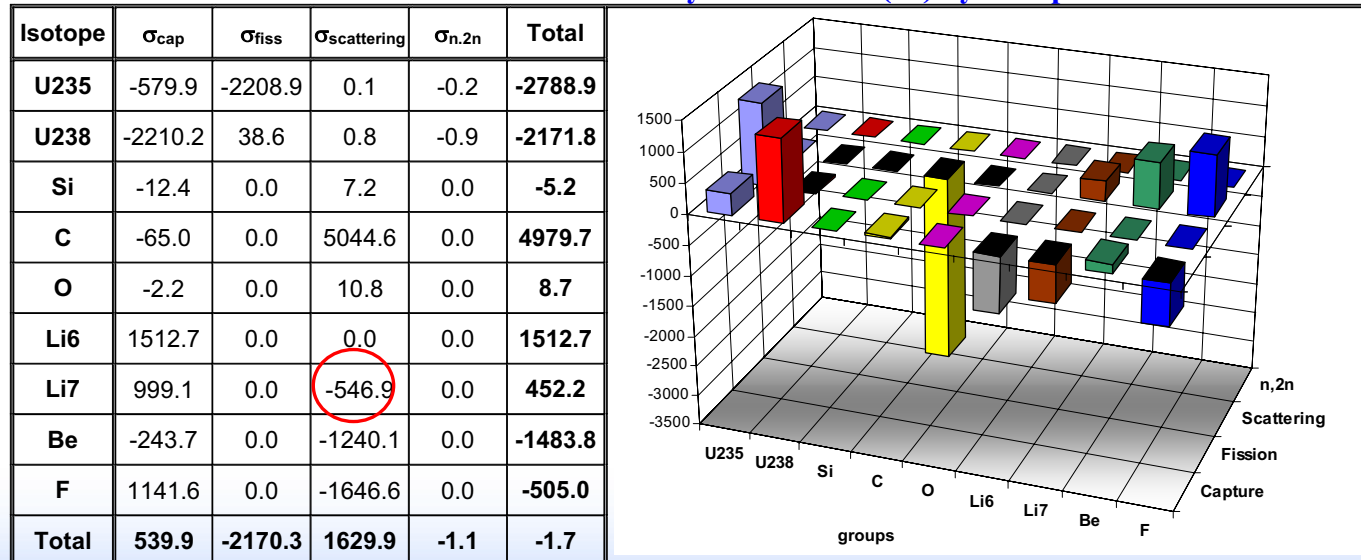
- The small value of the positive reactivity coefficient is the result of the compensation between the capture component (positive) and the scattering one (negative).
- The capture component has the largest values in the thermal energy range where there is the flux peak.
- The scattering component has the largest values in group 11 and 12 (slowing down of neutrons toward a region of spectrum of increased importance).
- Fission component (even if small) give a significant negative contribution.
- U-238 and Li-6 give large positive contributions (capture).
- Be and F give negative contributions (competition between capture and scattering). The opposite happens for Li-7.

Void Coefficient – Sensitivity Coefficients (%) by Group



^(a) High energy group boundary.

Void Coefficient – Sensitivity Coefficients (%) by Isotope

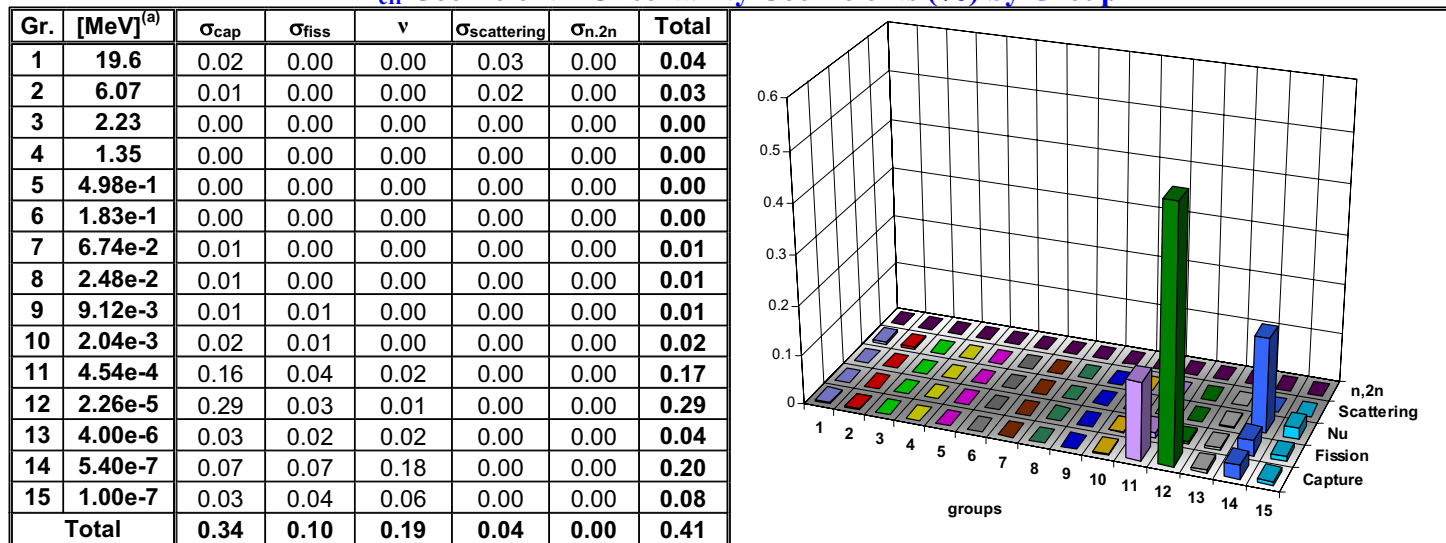


Idaho National Laboratory

Sensitivity Analysis

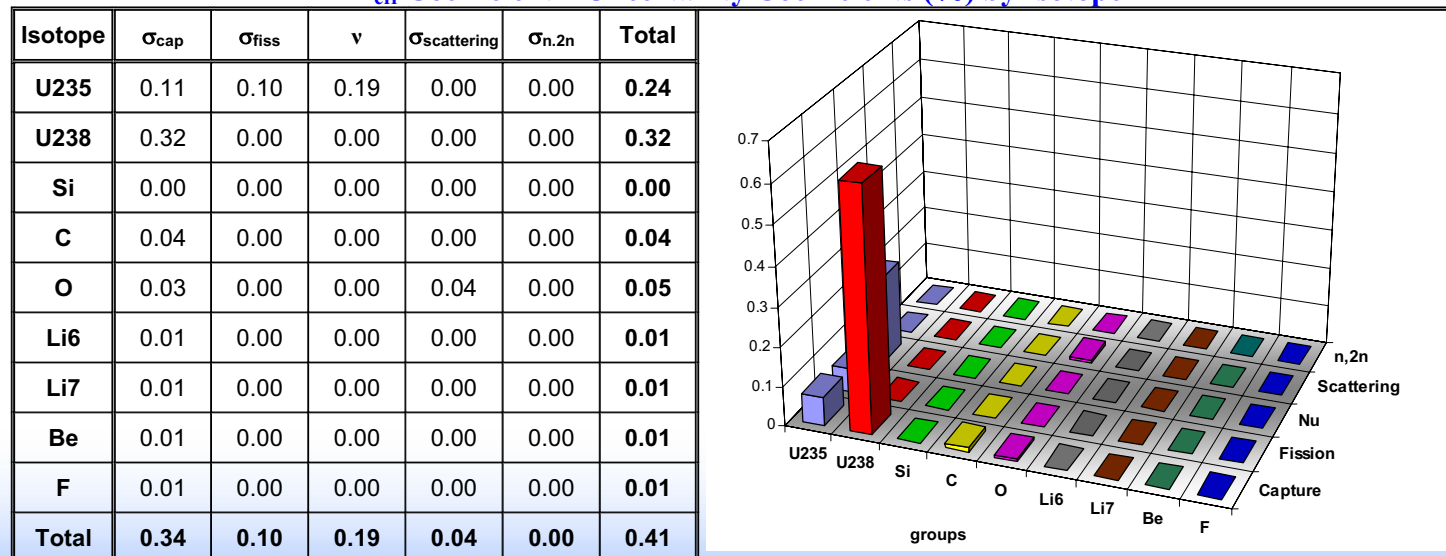
- Large positive sensitivity coefficients of the capture component are present at thermal energy. The increase of capture hardens the spectrum of the reference situation (lower K_{eff}), while in the voided situation the spectrum is already hardened.
- The large negative values in the resonance region (group 11 and 12) indicates that adding an isotope with large capture cross section in that energy range can improve the reactivity coefficient (confirmed in another study using erbium),
- On the contrary, adding a large scatterer in the same energy range will make the coolant void reactivity coefficient more positive.
- Increasing the density of Be and F or reducing the Li-6 content will be beneficial, while increasing graphite or Li-7 will worsen the reactivity coefficient.
- Increasing the enrichment will result in a less positive coefficient thanks to the larger negative contribution of U-235 compared against that of U-238

K_{eff} Coefficient – Uncertainty Coefficients (%) by Group



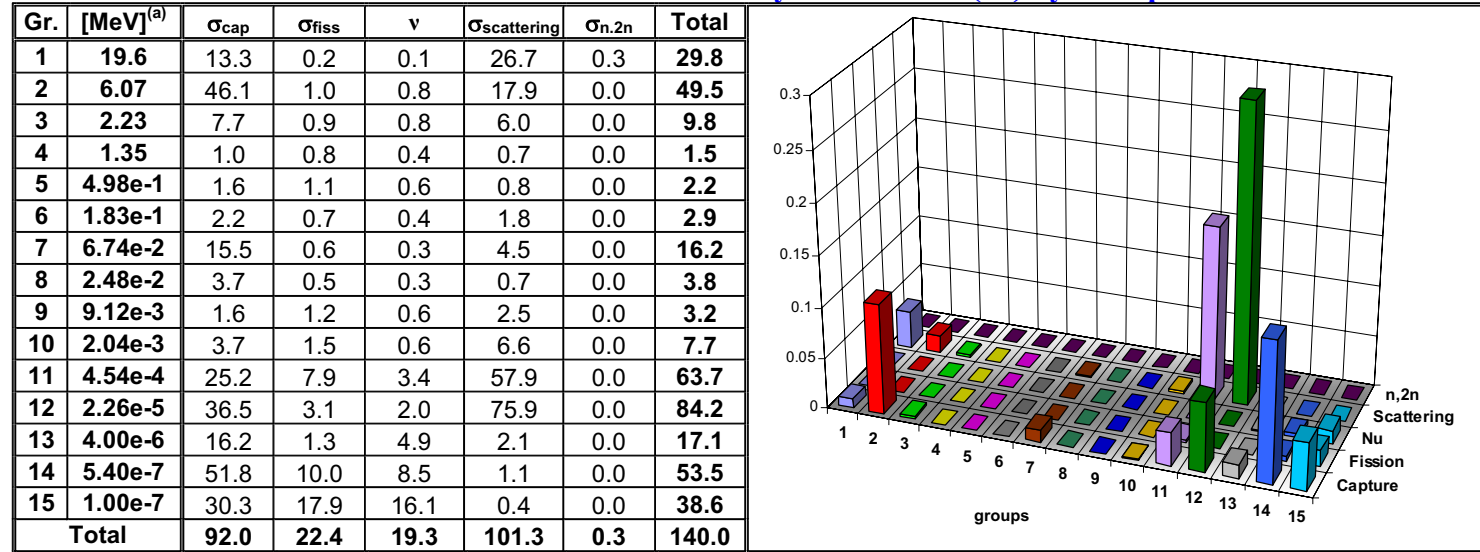
(a) High energy group boundary.

K_{eff} Coefficient – Uncertainty Coefficients (%) by Isotope



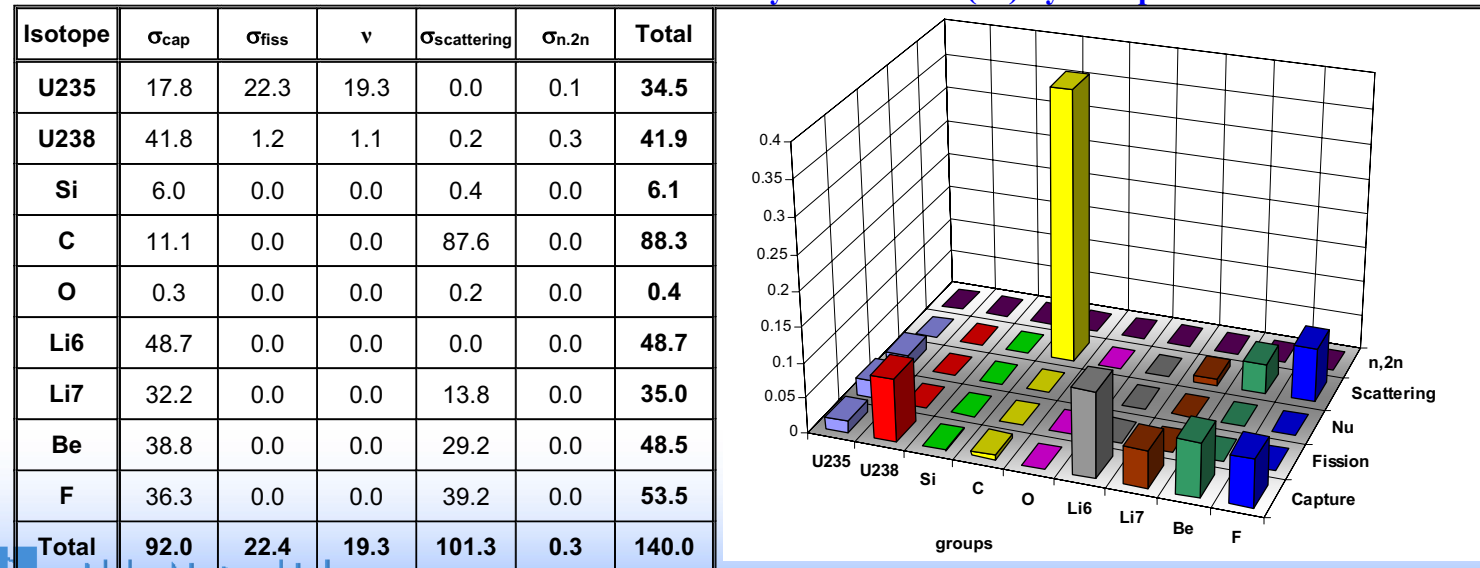
Idaho National Laboratory

Void Coefficient – Uncertainty Coefficients (%) by Group



(a) High energy group boundary.

Void Coefficient – Uncertainty Coefficients (%) by Isotope



Idaho National Laboratory

Uncertainty Evaluation

- Total uncertainty is greater than 100%, meaning that we cannot be sure about the final sign of the reactivity coefficient.
- Large values at high energy related to C scattering cross section (30% of uncertainty), Be ($n,2n$) (10% uncertainty included in the capture).
- The large contributions in group 11 and 12 come from the scattering cross sections of graphite (3% of uncertainty) and Be , F and Li-7 all with 7% of uncertainty.
- In the same energy groups the 5% of uncertainty on U-238 capture leads to a significant contributions
- At thermal energies (group 14 and 15) uncertainties are dominated by the contributions of Li-6 and Li-7 capture cross sections (5% uncertainty).

Summary on LS-VHTR

- A perturbation analysis has provided indications on the major contributors to the LS-VHTR coolant void reactivity coefficient in terms of reactions (competition between capture and scattering), isotopes (U-238, Li-6, Li-7, Be, F), and energy range (resonance, thermal region)
- A sensitivity analysis has suggested how the reactivity coefficient can be improved: adding an isotope with large capture cross section in the resonance region in order to shift the spectrum, increasing the density of Be and Fe, reducing the Li-6 content, increasing enrichment.
- The uncertainty on the void coolant reactivity coefficient has been quantified and the major contributors identified.
- Finally a target accuracy assessment would be very helpful in determining the uncertainty levels to which specific cross section have to be lowered in order to achieve a more reasonable (e. g. 20%) on the LS-VHTR coolant void reactivity coefficient uncertainty